Verification of Tolerance Chains in Micro Manufacturing

Gasparin, Stefania

Publication date:
2012

Document Version
Publisher's PDF, also known as Version of record

Ph.D. Thesis

Verification of Tolerance Chains in Micro Manufacturing

Stefania Gasparin

April 2012

Technical University of Denmark

DTU Mechanical Engineering
Department of Mechanical Engineering

“*La natura*
è immensa e complessa,
ma non è impenetrabile all’intelligenza;
devi girarle intorno,
pungere, sondare,
cercare il varco e fartelo...”

(Primo Levi, *Il sistema periodico*)

Preface

This PhD thesis has been carried out from February 2009 to January 2012 at the Department of Mechanical Engineering - Section of Manufacturing Engineering – Technical University of Denmark (DTU) under the supervision of Professor Hans Nørgaard Hansen, Professor Leonardo De Chiffre and Associate Professor Guido Tosello.

Two weeks from 17^{th} to 28^{th} October 2011 were spent at NPL (National Physical Laboratory) in Teddington (UK) under the supervision of Professor Richard Leach and Mr. Claudiu Giusca.

I would like to express my gratitude to my supervisors: Professor Hans Nørgaard Hansen is gratefully acknowledged for his wide inspirations, his active collaboration and for sharing with me his knowledge in metrology. I would like to thank Professor Leonardo De Chiffre for having introduced me at DTU almost five years ago: I still remember my first day in building 425. Associate Professor Guido Tosello is acknowledged for his patience, constant support and prompt advices during my entire project.

Moreover I would like to thanks Professor Richard Leach for giving me the opportunity to collaborate with his group and Mr. Claudiu Giusca for the fruitful discussions and suggestions on the replica technique investigation.

The work was funded by the Technical University of Denmark and the European project “COTECH-Converging technologies for micro systems manufacturing”. COTECH is a Large Scale Collaborative Project supported by the European Commission in the 7^{th} Framework Programme (CP-IP 214491-2, http://www.fp7-cotech.eu/ . Furthermore parts of the work on process chain validation are relevant for the national Danish project POLYNANO (www.polynano.net).

Kgs. Lyngby, February 2012

Stefania Gasparin

Abstract (English)

The aim of this work is to define methodologies for the tolerance verification of injection moulded components with downscaled dimensions. In micro and nano metrology different challenges can be found: lack of calibration artefacts and available ISO standards, problematic uncertainty budget and tolerance verifications due to no proper measuring instruments.

In connection to the last issue, the characterization of optical components is often difficult to obtain using contact instruments which could damage the surface of the specimen, whereas optical measurements might be inaccurate due to scattered light. In this thesis a replica casting technique is proposed to overcome the problem: the workpiece is replicated and the replica is characterized instead of the part. Different investigations are carried out on roughness specimens and deterministic structures (e.g. grooves) in order to define the replication degree and the replica stability. Moreover a new traceability procedure is studied and proposed when dealing with this methodology. The measuring instrument has to be calibrated on the same replica surface to ensure the traceability. Therefore the aim of the procedure is to perform a replica on a calibrated standard artefact and to measure both in order to assure an unbroken chain of comparisons. The replica technique reveals to be a fast, cost-effective and reliable method.

Regarding the tolerance verification of micro parts and nano-structured surfaces, a systematic approach is discussed based on dimensional and geometrical metrology. If the measurements uncertainty is large compared to the tolerance interval, a small conformance zone is left for process variation. Therefore particular attention has to be paid to the instrument capabilities in order to reduce the measurement uncertainty. Different methods, such as the quality control approach and the measuring indices approach, are investigated in order to optimize and maximize the repeatability of the results. Moreover a useful guideline is proposed to provide a viable method for the uncertainty calculation of measurements in the micro range (0.1 – 200 µm).

Finally, an optical component is investigated with the purpose of suggesting a quality control approach for micro-manufacturing process through a control of the product. It is a useful method to adopt when the aim is to detect and quantify inconsistency or incompatibilities during a process chain. In this way the process parameters can be adjusted in order to fulfil the requirements of the final micro-product.

Abstract (Dansk)

Formålet med dette projekt har været at udvikle metoder til verifikation af tolerancer af sprøjtestøbte miniaturiserede komponenter. Metrologi i mikro- og nanoskala dimensioner er præget af en række udfordringer: mangel på kalibreringsnormaler og ISO standarder, store udfordringer i forhold til usikkerhedsbudgettering og tolerance verifikation samt mangel på anvendelige måleinstrumenter.

Karakterisering af f.eks. optiske komponenter er ofte umulig med instrumenter, der fysisk berører overfladen, og optiske måleprincipper kan være unøjagtige på grund af lysspredningen. I denne afhandling beskrives en replikeringsteknik, der kan anvendes også i disse situationer: der tages et aftryk af overfladen med et plastmateriale, og opmålingen foregår derefter på denne replika. Der er gennemført omfattende undersøgelser på ruhedsnormaler og deterministiske mikrostrukturer (f.eks. kanaler) med henblik på at bestemme replikeringsgrad og stabilitet. Derudover foreslås en metode til at sikre sporbarhed af sådanne målinger. Måleinstrumentet skal kalibreres på det samme replikamateriale for at sikre sporbarhed. Derfor anviser proceduren, at der tages et aftryk af en sporbar normal, og at dette aftryk opmåles og sammenlignes med en opmåling af normalen. Denne replikateknik har vist sig at være hurtig, kosteffektiv og pålidelig også i forbindelse med opmåling af andre mikrokomponenter.

Verifikation af tolerancer på mikrokomponenter og nano-strukturerede overflader er blevet gennemført ved systematisk anvendelse af geometrisk metrologi. Såfremt måleusikkerheden er stor i sammenligning med tolerancezonen, efterlades kun et lille interval til procesvariationer. Derfor er der i denne skala særligt fokus på måleinstrumentets kapabilitet for at reducere måleusikkerheden. Forskellige metoder er blevet anvendt og undersøgt med henblik på at optimere gentagelsesnøjagtigheden. Der foreslås desuden en metode til usikkerhedsvurdering for dimensionsmålinger i området 0.1 – 200 µm.

Endelig foreslås en metode til kvalitetskontrol i mikrodomænet baseret på en opmåling af en optisk komponent. Metoden kan afsløre og kvantificere fejl i procesforløbet gennem

opmålinger af dimensioner og geometri. Igennem resultaterne kan justeringer af de enkelte procestrin foreslås således, at den færdige mikrokomponent lever op til specifikationerne.

Acknowledgements

During these three years I collaborated with several experts in the field of metrology, injection moulding and micro manufacturing. First of all, my appreciation is for Mr. Rene' Sobiecki from DTU Mechanical Engineering: you have always lent me a friendly and helping hand. From you I learnt the most important skills needed in metrology: precision, accuracy and perseverance.

My gratitude is for the technicians at DTU Mechanical Engineering, in particular: Mr. Jakob Rasmussen for his help with the measuring instruments, Mrs. Laila Leth and Mr. Rolf Jensen for the SEM images and the EDS analysis, Mr. Jan F. Pedersen for the realization of the replica device, Mr. Morten Krogsgaard for all the "mounting and dismounting" of the inserts and Mr. Michael Guldager for the injection moulding of the Fresnel lenses.

I would like to acknowledge all the COTECH partners, in particular: Professor Humbert Noll from Fachhochschule Wiener Neustadt Wien (Austria) and DI (FH) Helmut Loibl Msc. from FOTEC Forschungs- und Technologietransfer GmbH (Austria), Dr. Manfred Prantl from Alicona Imaging GmbH (Austria) for performing the 3D-SEM reconstruction and for his prompt advices in using the Infinite Focus instrument. Dr. Igor Di Vora and Dr. Sara Padovani from CRP (Centro Ricerche Plast-Optica, Italy) are thanked for their collaboration and assistance with the characterization of the micro-pyramidal structures on the optical component. Mr. Joseba Esmoris from Tekniker (Spain) is thanked for providing the Fresnel lenses moulds, for making the coating and the relative tribology and nano-indentation hardness tests. Mr. Juan A. Ceña formerly at Grupo GEMA-Ópticos (Spain) is gratefully acknowledged for his collaboration and assistance on optical disc manufacturing technology as well as for providing samples (stampers and discs) and processing data.

I would like to thanks the experts who enhanced fruitful discussions and assistance in connection to the case studies:

- Toggle for hearing aid: Dr. Aminul Islam from DTU Mechanical Engineering - Sonion A/S for providing the samples and the technical drawings;

- Fresnel lenses: Dr. Jose’ A. Albajez from University of Zaragoza (Spain) for making the moulds replica and the optical measurements; Dr. Peter T. Tang from IPU (Denmark) for suggesting the appropriate cleaning of the coated mould;
- Optical discs: Dr. Anders Kühle from Image Metrology A/S (Denmark) and Dr. Francesco Marinello from TeSAF Department (Department of Land, Environment, Agriculture and Forestry), University of Padova, (Italy) for the useful advices in using the Scanning Probe Image Processor (SPIP);
- Micro-pyramidal structures: Dr. Poul Erik Hansen from DFM (Danish Fundamental Metrology A/S, Italy) for the attempt with the optical diffraction microscopy;
- Dr. Kim da Costa Carneiro from DTU Mechanical Engineering for sharing his knowledge in uncertainty budget.

During my stay at NPL (National Physical Laboratory, UK), I received the help and the friendly support from several researchers: Mr. Christopher Jones, Mrs. Lakshmi Nimishakavi, Dr. Wenjuan Sun, Mr. James Claverley and technician Mr. Neil Lockmuller.

I would like to acknowledge the students who contributed to the results of the thesis: M.Sc. Jais A.B. Angel, M.Sc. Martin Hedegaard, B.Sc. Anders Riel and Sture G. Bachmann.

My gratitude is for my colleagues: Giuliano Bissacco, Ugochukwu Chibuzoh Nwaogu, Lukas Pilny, Rasoul Mahshid, Stefano Menotti, Jakob Skov Nielsen, Nikolaj Kjelgaard Vedel-Smith, Finn Paaske Christensen and Flemming Jørgensen for making the life in the office dynamic and lively; in particular Pia Holst Nielsen for showing me the pleasure of running, Yang Zhang for the girlish topics and the ultra-caloric snacks against my steady hunger, David Bue Pedersen for the interesting discussions during lunch time and Matteo Calaon for the long friendship. Special thanks are for the two Arnaud: the master student in Canada and the fish in our office.

A big thank goes to my mum and dad for their constant and continuous support, to my sister Silvia for her countless love-gossip (you don't know, but you are updating me just right now) and to my family and all my friends around Denmark, The Netherlands and Italy.

Finally...grazie Fabio per tutto...you know the many reasons why I have to thank you, hence I decided to mention here only the thesis-related ones: thanks for your help with Matlab and the Fast Fourier Transform, but especially, thanks for spreading your joy and enthusiasm in doing research.

Table of contents

Preface ... iii
Abstract (English) ... v
Abstract (Dansk) ... vii
Acknowledgements ... ix
Table of contents ... xi
1. Background and objectives ... 1
1.1 Introduction ... 1
1.2 Metrology in micro manufacturing ... 2
1.3 Tolerancing in micro manufacturing ... 2
1.4 Problem identification ... 4
1.5 Structure of the work ... 4
1.6 COTECH project ... 5
1.7 References ... 6
2. State of the art for dimensional micro and nano metrology ... 7
2.1 Introduction ... 7
2.2 Solutions for dimensional micro and nano metrology ... 7
2.2.1 Interferometry ... 9
2.2.2 Micro-topography measuring instruments ... 11
2.2.3 Scanning probe and particle beam microscopy ... 14
2.2.4 Coordinate metrology ... 18
2.2.5 Other techniques ... 20
2.2.6 Summary ... 21
2.3 Calibration and traceability ... 21
2.4 Uncertainty evaluation ... 27
2.4.1 Uncertainty budget according to GUM ... 28
2.5 Tolerancing rules ... 32
2.6 Industrial practice (COTECH) ... 35

2.7 Future needs and trends ... 39
2.8 References ... 40
3. Indirect micro/nano metrology based on replication ... 47
3.1 Introduction ... 47
3.2 Replication technique ... 50
3.3 Surface replication ... 52
3.3.1 Surface calibration standard artefact replication ... 53
3.4 Geometries replication ... 74
3.4.1 Geometries calibration standard artefact replication ... 75
3.4.2 Geometries product replication ... 82
3.5 Conclusion ... 89
3.6 References ... 90
4. Process chains for micro-manufacturing ... 95
4.1 Introduction ... 95
4.2 Overview of micro-manufacturing technologies ... 96
4.2.1 Mechanical processes based on material removal ... 97
4.2.2 Energy assisted processes ... 100
4.2.3 Electroforming ... 101
4.2.4 Replication processes ... 102
4.2.5 Summary ... 104
4.3 Tooling fabrication ... 105
4.4 Mould design for micro injection moulding – an example ... 107
4.5 Hybrid tooling ... 110
4.6 Process chain characterization - an example ... 114
4.7 Conclusion ... 120
4.8 References ... 121
5. Surface wear of micro structured tools during injection moulding ... 125
5.1 Introduction ... 125
5.2 Case description ... 126
5.2.1 Tooling ... 127
5.2.2 TiN coating ... 129
5.2.3 Injection moulding ... 130

5.2.4 Replica set-up 130
5.2.5 Micro dimensional geometrical metrology 132
5.3 Replication fidelity results 134
5.4 Dimensional measurements 136
5.5 SEM inspection 141
5.6 EDS inspection 146
5.7 Conclusion 147
5.8 References 148
6. Tolerance chain verification at micro dimensional scale 151
6.1 Introduction 151
6.2 Case description 152
6.3 Measurements using TCMM 154
6.4 Measurements using OCMM 157
6.5 Optical set-up investigation 159
6.6 Quality control approach 163
6.7 Measuring instrument indices approach 165
6.8 Conclusion 168
6.9 References 169
7. Tolerance chain verification at sub-micro dimensional scale 173
7.1 Introduction 173
7.2 Optical discs manufacturing process chain 174
7.2.1 Stamper making 175
7.2.2 Polymer replication 176
7.3 Nano-features dimensional quality control 177
7.3.1 Nano-tolerances of optical disc features 177
7.4 AFM measurements of pit height and track pitch 180
7.4.1 Uncertainty assessment and traceability of measurements 181
7.4.2 Measurements results 182
7.5 SEM measurements of pit width and pit/land length 185
7.5.1 Replication quality 186
7.5.2 Tolerance verification 187
7.6 Conclusion 190

7.7 References 190
8. Process chain validation of 3D micro structured optical surfaces 195
8.1 Introduction 195
8.2 Case description 196
8.2.1 Tooling 196
8.2.2 Injection compression moulding 197
8.3 SEM measurements 198
8.3.1 Results of the SEM measurement on the pitches 200
8.4 3D-SEM measurements 203
8.4.1 Results of the 3D-SEM measurement on the pitches 207
8.4.2 Results of the 3D-SEM measurement on the heights 208
8.4.3 Results of the 3D-SEM measurement on the angles 209
8.5 Optical measurements 210
8.5.1 Results of the optical measurement on the pitches 212
8.5.2 Results of the optical measurement on the heights 213
8.5.3 Results of the optical measurement on the angles 215
8.6 Conclusion 216
8.7 References 217
9. Conclusion 221
9.1 Summary 221
9.2 Discussion and outlook 224
9.3 References 227
10. List of publications 229
10.1 International ISI journal papers 229
10.2 Peer reviewed international conference papers 229
10.3 Research and technical reports 231
11. Appendix 233
11.1 Appendix 1: Measuring instruments at MEK-DTU 233
11.1.1 Stylus profilometer (FTS) 233
11.1.2 Workshop stylus profilometer (Hommel) 242
11.1.3 Atomic force microscope 247
11.1.4 Scanning electron microscope 249

11.1.5 Infinite Focus – Focus Variation 250
11.1.6 Coordinate measuring machine 261
11.1.7 Tactile coordinate measuring machine 265
11.2 Appendix 2: Technical drawing for the volume control of a hearing aid 271
11.3 Glossary 272

1. Background and objectives

1.1 Introduction

Through the last years the demand of micro-products and micro-components has constantly increased in many industrial sectors such as electronics, optics, medical applications, biotechnology and automotive industry. Examples of applications include inject printer nozzles, reading caps for hard discs, pacemakers, medical implants, drug delivery systems, micro-fluidic systems, mobile phones, micro-engines, micro-pumps, micro-connectors and micro-switches [Alting, 2003].

A micro product is characterized by small dimensions, either of the product itself or of the functional features/structures on it. According to this statement, different definitions of "*micro product*" exist [Alting, 2003]:

1. *From a geometrical point of view, three groups can be found*:
   - 2D: two-dimensional structures, e.g. optical gratings;
   - 2½D: two-dimensional structures with a third dimension, e.g. micro-fluidic devices (the structure of the channel system itself is two-dimensional, but since the channels have a finite depth they can be characterised as 2½D);
   - 3D: three dimensional structures, e.g. hearing aids components;
2. *From a philosophical point of view*:
   Some products need to be "small" in order to reach a more compact and portable version, some others achieve their functionality only in virtue of their small dimensions; e.g. fluidic sensors or tools for micro surgery;
3. *From a functionality point of view*:
   A micro product is usually constituted by several components that have to be assembled in order to obtain the desired functionality; therefore a micro product requires reduction in size of the constituting components.

The downscaled dimensions of the micro-parts create challenges in terms of metrology and tolerancing in micro-manufacturing.

1.2 Metrology in micro manufacturing

Metrology in general is traditionally regarded as a key discipline in making possible the industrial manufacture of components. In particular it enables process control on the basis of measurands either defined on the components or on some specific process characteristics. In this way a product is described using absolute values combined with tolerances. Dimensional metrology covers measurement of dimensions and in principle geometries based on distance measurements.

In the traditional manufacturing environment, dimensional metrology is an integral part of all quality assurance systems. The available tools in terms of instrumentation, calibration artefacts, standards and well established procedures support the increasing demands for production in global networks of highly complex components and products.

In the context of Multi-Material Micro Manufacture (4M), metrology has an extremely important role to play because the manufacturing paradigms taken primarily from the macroscopic world are applied to micro or even nano scaled components and functional features. In contrast to semiconductor processing, where each chip location is known to few tens of nanometers at all times during processing, the 4M manufacturing paradigm has to deal with extremely high positioning and alignment accuracies in-between process steps, where each process not originally was intended to deliver such accuracy. Furthermore, many product concepts are based on assemblies of components, usually manufactured in different ways and locations (as seen in macro scale manufacturing). This concept requires detailed knowledge of not only absolute dimensions and geometrical quantities, but also about the uncertainty of measurements. This is a decisive parameter when dealing with mating capability in general.

1.3 Tolerancing in micro manufacturing

In the macro world, the most frequently occurring functions of construction elements are mating capability, sliding and rolling capability, load rating and different surface finishes.

To ensure these functions the specifications are given in terms of maximum deviations from an ideal geometric form. Various ISO standards regulate this field in terms of Geometrical Product Specifications (GPS). Moreover, in conventional machining processes the specifications of the parts as well as the variables for adjusting the dimensions and geometry of the manufactured product are linear dimensions (e.g. the correction to compensate for deflections or tool wear), which means that the primary closed loop control is based on linear dimensions. For the tolerancing in micro manufacturing it looks more straightforward to use the ISO standards of the GPS-series even though some obvious problems occur: for example tolerance grades have not been defined for nominal sizes below 3 mm. In drawings, micro-sizes and tolerances will be preceded by quite some zeros when still expressed in mm. That problem can easily be overcome. More serious is the problem that the ISO-GPS system is set-up with the traditional workshop dimensional metrology in mind. This means that at many places measuring elements are prescribes of mm-size so obvious measuring smaller sizes is not possible when interpreting strictly these standards [Hansen, 2006].

Tolerancing is linked closely together with metrology and it is seen like a bridge between the process chain and the product specification. The quality and the performance of a replicated micro-part depend on the quality and performance of the corresponding micro-mould. One basic requirement of micro-moulds for high throughput micro-replication processes is that the components of the mould (inserts) must be replaceable, so the repeatability of the inserts fabrication processes must be enough to produce inserts which satisfy the required geometric tolerance and ensure parts of acceptable quality. For commercial components, it is usually necessary to combine different tooling technologies which can introduce cumulative repeatability errors. Some attempts to introduce a function-oriented tolerancing concept for monolithic integrated systems (e.g. MEMS) are reported in literature [Weckenmann, 2000] and [Weckenmann, 2001]. This concept is however based on the fact that a layer-by-layer manufacturing methodology is applied. If micro mechanical systems are considered within the usual 4M domain, then a complete lack of guidelines exists.

A growing trend is the production of components and devices with functional micro features and sizes ranging from a few hundred microns to sub-micron, especially those with dimension below 20 µm, together with tolerances in the range of 1 to 10% of the nominal dimensions (in precision engineering < 0.01%) and surface roughness in the range of 10 to 50 nm. Therefore the available technologies appear not sufficient due to this scaling down of the critical dimensions and to an increase of objects geometrical complexity. To answer these challenges, research activities have to include new measuring principles and instrumentation, tolerancing rules and procedures as well as establishment of traceability.

1.4 Problem identification

It is the main objective of this PhD project to develop methodologies in micro manufacturing for tolerancing of components and associated process chains with focus on the micro injection moulding process. This has been achieved by applying a systematic approach based on dimensional and geometrical metrology as well as tooling process chain characteristics related to micro injection moulding.

The project was divided in the following phases:

1. State of the art for dimensional and nano metrology;
2. Calibration and traceability;
3. State of the art for process chains in micro manufacturing;
4. Tolerancing in micro and nano manufacturing;
5. Development of approaches for validation of micro manufacturing process chains.

1.5 Structure of the work

This structure of the thesis reflects the five phases presented in the previous paragraph:

- State of the art for dimensional and nano metrology (*chapter 2*): the chapter presents the available technical solutions for dimensional metrology of micro and nano mechanical parts including the use of ISO GPS standard principles when applied to downscaled dimensions;
- Calibration and traceability (*chapter 3*): reference artefacts and new traceable approaches are proposed in order to ensure traceability of dimensional and geometrical 3D measurements and to allow validation and verification of product

and process tolerances. Focus is given on replica casting techniques, useful when applied to parts difficult to characterize;

- State of the art for process chains in micro manufacturing (*chapter 4*/*chapter 5*): chapter 4 presents available process chains for micro-manufacturing in relation to micro-injection moulding process. In chapter 5, the characterization of two micro-moulds used in an injection moulding machine is performed through a replica casting technique;
- Tolerancing in micro and nano manufacturing (*chapter 6*/*chapter 7*): in order to verify the tolerances of a component, the part has to be measured. If the measurement approach/instrument results in a large measurement uncertainty, then no clear conclusion with respect to compliance can be made. Metrology methods to verify tolerances are developed for a micro part (chapter 6) and for nano structured components (*chapter 7*). A successful verification of a tolerance requires establishment of traceability of the method including the estimation of measurement uncertainty;
- Development of approaches for validation of micro manufacturing process chains (*chapter 8*): the quality control of a manufacturing process for an optical component is performed through a control of the product itself.

The appendix (*chapter 11*) reports a description of the measuring instruments used during the project, focusing on their technical specifications and calibration data. At the end a list of the frequently used abbreviation is given.

1.6 COTECH project

During these three years an intense collaboration with the European project “COTECH-Converging technologies for micro systems manufacturing” has been carried out. COTECH is a Large Scale Collaborative Project supported by the European Commission in the 7th Framework Programme (CP-IP 214491-2, http://www.fp7-cotech.eu/).

The COTECH project was initiated in order to develop manufacturing and process technologies for the production of polymer-based micro-mechanical components and systems.

The main objectives of COTECH are:

- Develop and demonstrate new micro replication techniques supported by emerging tool-making technologies for the manufacturing of polymer-based multi-material components;
- Introduce and demonstrate new micro replication techniques combining capabilities of different processes or techniques based on micro injection moulding;
- Implement global process chains for the manufacturing of polymer-based micro-mechanical components and systems. This will be supported by the use of new advanced simulation models and "in-situ" non destructive testing procedures;
- Demonstrate the capability of producing high added value micro devices with advanced functionalities by means of realizing eight demonstrators coming predominantly from the areas of healthcare technology and automotive industry.

1.7 References

[Alting, 2003] L. Alting, F. Kimura, H.N. Hansen, G. Bissacco, "Micro engineering", Annals of the CIRP, 2003, Volume 52, Issue 2, pp. 635-658.

[Hansen, 2006] H.N. Hansen, K. Carneiro, H. Haitjema, L. De Chiffre, "Dimensional micro and nano metrology", Annals of CIRP, 2006, Volume 55, Issue 2, pp.721-743.

[Weckenmann, 2000] A. Weckenmann, R. Ernst, "Studies on new tolerancing rules for micro- and nanotechnology", 1st EUSPEN Conference, 2000, Volume 1, pp. 214-221.

[Weckenmann, 2001] A. Weckenmann, R. Ernst, R. Hornfeck, "Tolerancing of micromechanical monolithic components", 2nd EUSPEN Conference, 2001, Volume 2, pp. 786-788.

2. State of the art for dimensional micro and nano metrology

2.1 Introduction

Initially a thorough investigation on available technical solutions for metrology of micro and nano mechanical parts was performed. The chapter includes a description of:

- Measuring instruments and their set-ups (*Paragraph 2.2*);
- Available calibration standards and a discussion on the establishment of traceability (*Paragraph 2.3*);
- Uncertainty evaluation (*Paragraph 2.4*);
- Tolerancing issues underlining the use of ISO GPS standard principles when applied to downscaled dimensions (*Paragraph 2.5*).

The chapter deals also with the available measuring instruments among the partners of the European consortium COTECH (COnverging TECHnologies for micro systems manufacturing) and their knowledge about some key-topics of dimensional metrology, such as: measurements, calibration, traceability and uncertainty budget (*Paragraph 2.6*). Finally a discussion on future needs and trends in the metrology field is presented (*Paragraph 2.7*).

2.2 Solutions for dimensional micro and nano metrology

Several technologies are available for carrying out micro and nano dimensional measurements. Their classification is made according to the main measurement principles of the instruments and following the categories proposed in [Hansen, 2006] and [Leach, 2010]:

1. Interferometry;
2. Micro-topography measuring instruments;

3. Scanning probe and particle beam microscopy;
4. Coordinate measuring machine;
5. Other techniques.

Table 2.1 summarizes the measuring instruments discussed in the following paragraphs. Figure 2.1 holds a comparison of the reported techniques: lateral dimensions are plotted in function of vertical dimension; the available instruments are entered according to their capabilities and the boxes represent the measuring range of the considered instrument.

Interferometry	**Micro-topography measuring instruments**	**Scanning probe and particle beam microscopy**	**Coordinate Measuring Machine**	**Other techniques**
- Homodyne - Heterodyne	- Stylus profilometers - Optical instruments: *Scanning* • Triangulation • Confocal microscopes • Optical profilometers • Interferometers *Other optical techniques* • Focus variation	- SPM: • STM • AFM • SNOM - Electron Microscopy: • SEM • TEM	µCMM	Computer tomography

Table 2.1 - Classification of the available technologies for carrying out micro and nano dimensional measurements.

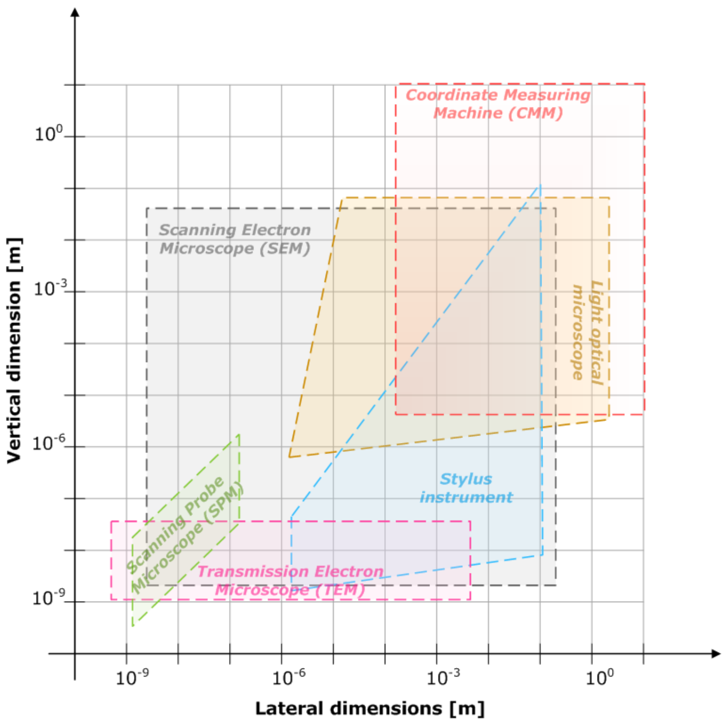

Figure 2.1 - Measurement instruments for dimensional micro and nano metrology [Hansen, 2006].

2.2.1 Interferometry

Interferometry is based on analysis of the interference pattern created by the superposition of two or more waves. Different interferometric principles exist, however displacement (i.e. change in length) interferometry is usually based on the Michelson configuration or some variants of that basic design.

Michelson interferometer operate with a point source, *S*, as it is shown on the left of Figure 2.2. *A* represents the beam splitter, *B* the detector of the interference fringes, *C* is the compensator, while *M1*, *M2* are the mirrors. The *Twyman-Green* principle is a modification of the Michelson interferometer: the source is replaced by a point source at the focus of a well-corrected concave lens (on the right of Figure 2.2). An advantage is that the paths in both beams can be made equal in order to obtain white light interference. However this technique is sensitive to turbulence and vibration. In both cases, the displacement measurements are carried out by counting the number of fringes as the object being measured is displaced. Photodetectors and digital electronics are used to count the fringes and the fraction is determined electronically sub-dividing the fringe [Leach, 2010].

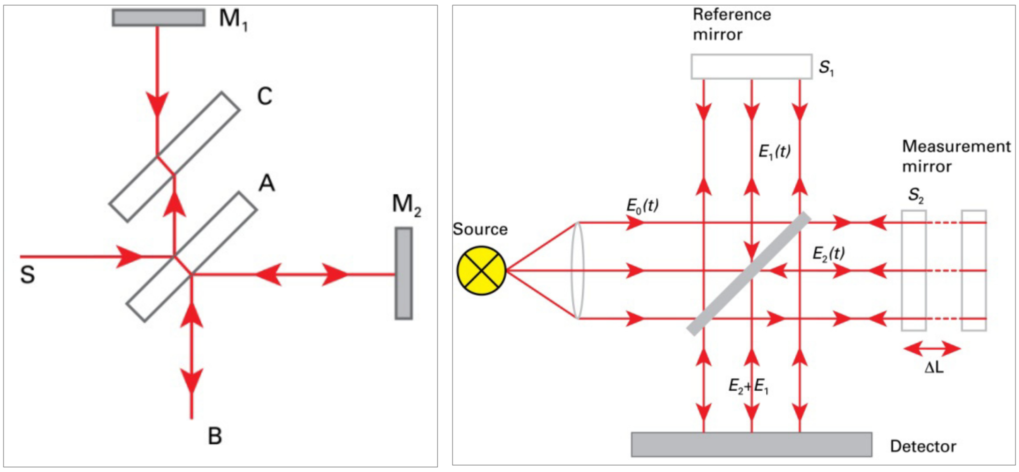

Figure 2.2 - Left: schema of the original Michelson interferometer. Right: schema of a Twyman-Green interferometer [Leach, 2010].

The most common interferometers are *homodynes* which use a single laser beam f1 (on the left of Figure 2.3) and *heterodynes* which use a dual-frequency laser source containing two orthogonal polarizations, one with a frequency *f1* and the other with a frequency *f2*, (on the right of Figure 2.3). In the homodyne system, the reference and the measurement beams are split at the interferometer and not inside the laser; therefore the light can be delivered to the interferometer via a standard fibre optical cable [Leach, 2010].

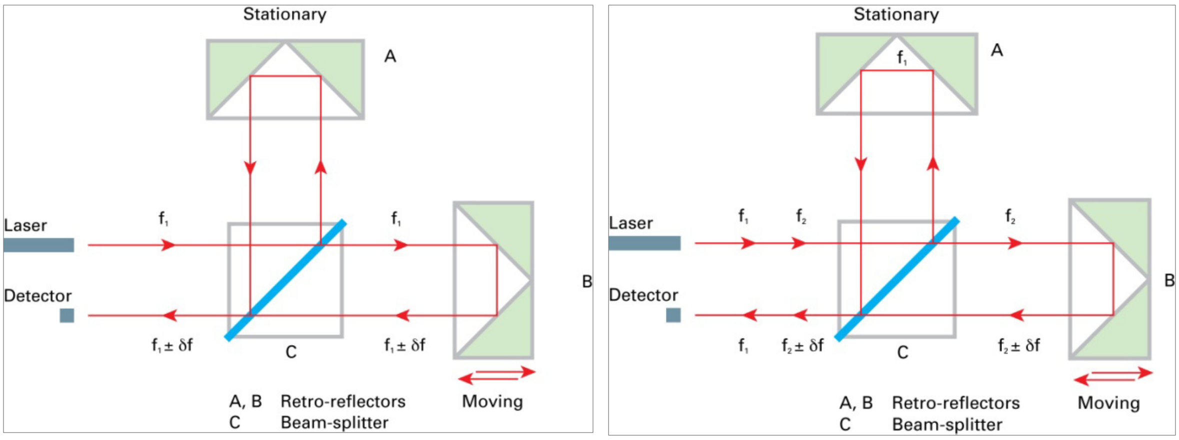

Figure 2.3 - Left: homodyne interferometer configuration. Right: heterodyne interferometer configuration [Leach, 2010].

The resolution is in the range of 0.1 and 10 nm, obtained in the direction of the beam propagation. This means that interferometers are 1-D technique. The measurements range depends on the coherence length of the source: 300 nm for white light, centimetres for spectral lamps and 1 - 10 m for commercially available laser interferometers [Hansen, 2006].

The error sources which are proportional to the displacement being measured are called cumulative errors; otherwise non-cumulative errors if they are independent from the length being measured. Typical errors are [Leach, 2010]:

- Thermal expansion of the metrology frame, proportional to the displacement;
- Dead-path length: distance in air between the reference, the measurement reflectors and the beam-splitter;
- Cosine error: despite how perfectly aligned the system appears to be, there will be always a small, residual error that will cause a shorter measurement;
- Non-linearity in the relationship between the measured phase difference and the displacement [Cosijns, 2002], [Peggs, 2002];
- Random error sources, such as acoustic vibration, air turbulence and electronic noise, which are described in [Leach, 2010].

The interferometers are used for calibration of 1-D scales, in chip production for wafer-steppers and scanners, as direct traceability when detecting the displacement of the axes in micro and nano coordinate metrology and as link to the primary standards for laser interferometer systems [Hansen, 2006].

2.2.2 Micro-topography measuring instruments

The principal methods used for the characterization of surface topography are: stylus profilometers, optical scanning techniques and scanning probe microscopy. These methods scan point by point the surface giving quantitative information of the profile heights with respect to the position.
In the following paragraphs a description of the different methods is presented.

2.2.2.1 Stylus profilometers

The stylus profilometers physically contact the measured surface using a tip; in the meanwhile a transducer converts the vertical movement of the tip into an electrical signal.
The stylus is typically provided with a diamond tip with a cone angle of 60° or 90° and a tip radius in the range of 1 - 10 µm [Hansen, 2006], [De Chiffre, 2011]. Due to their shape, some styli do not penetrate into the valleys of the surface texture. Moreover the force applied by the stylus can generate plastic deformation; therefore they are systems not suitable for the characterization of soft or polished surfaces [Whitehouse, 2011]. Another disadvantage regards the time required to achieve an areal measurement: one scan could last up to 2 hours [Leach, 2010].

2.2.2.2 Optical instruments

The optical instruments guarantee no risk of damaging the specimen surface because no physical contact is needed during the measurements. The other main advantage is the time required for measuring: a measurement is relatively fast and can be in the range of minutes. However they have some limitations: the optical resolution is affected by the numerical aperture of the optical system which determines the largest slope angle on the surface that can be measured. Moreover the optical resolution of the object and the optical scan size depend on the spot size which influences the area of the measured surface while the instrument is scanning [Leach, 2010].

There are many types of optical instruments; the ones covered in this section are based on scanning optical technique and other techniques, such as the areal optical system.

<u>*Scanning optical techniques*</u>:

The characterization of the surface is achieved by scanning physically a light spot across the surface [Wilson, 1984]. The instruments which use this technique are:

- ***Triangulation instruments***:

  They measure the relative distance to an object or surface as it is shown in Figure 2.4 on the left. The typical height resolution is 100 nm over several mm of vertical range. For this reason, they are used for measuring surfaces with relatively large structure such as paper fabric [Xu, 1998], structured plastic [Shiou, 2008] and road surfaces [Laurent, 1997]. When measuring small features, limitations are due to the laser beam which varies throughout the vertical range acting as averaging filter.

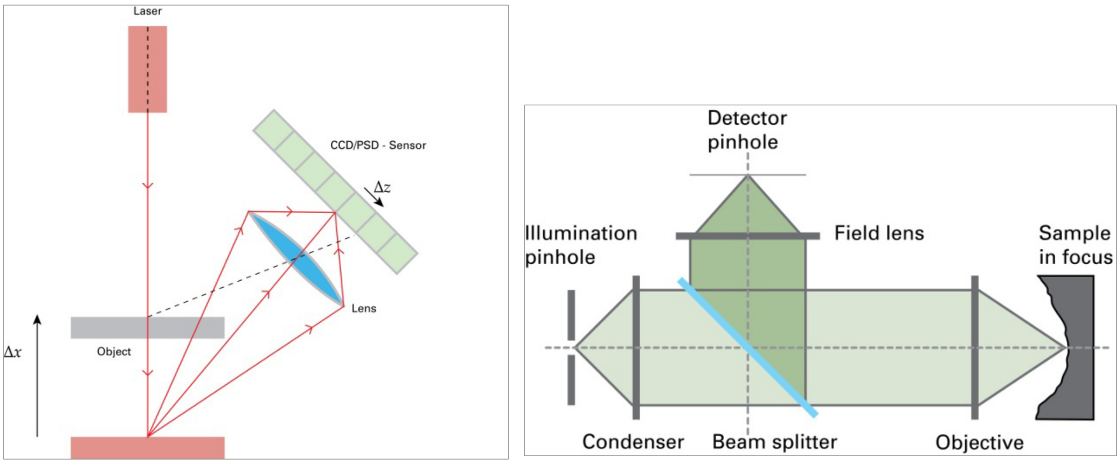

Figure 2.4 – Left: Principle of a laser triangulation sensor [Leach, 2010]. Right: Confocal set-up with an object in focus [Leach, 2010].

- ***Confocal microscopes***:

  They are based on focus detection principles, where one surface picture element (pixel) is imaged at time, Figure 2.4 on the right. They are characterized by a maximum detectable slope up to 75° [Wilson, 1990], [Diaspro, 2002].

- ***Optical profilometers***:

  They are based on the autofocusing signal of a laser beam detector, Figure 2.5. The beam has a spot diameter of about 1 µm with a vertical resolution of approximately 5 nm. The maximum detectable slope is 15° [Hansen, 2006], [Leach, 2010].

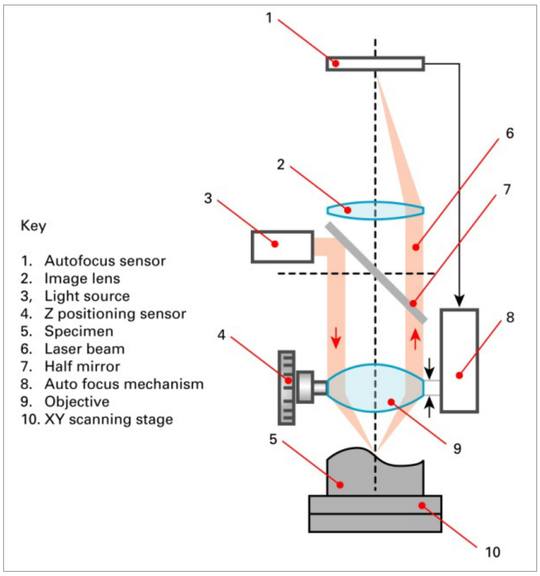

Figure 2.5 - Schema of a point autofocus instrument [Leach, 2010].

– ***Interferometers***:

  They combine an optical microscope and an interferometer object into a single instrument. The measurements of flat surfaces are fast. For surfaces with average roughness down to 0.1 nm and peak-to-valley heights up to several µm (depending on the objectives) the vertical resolution is in the range of sub-nanometer. Limitations are on surfaces slope (max 30°) and on the lateral resolution [Bariani, 2005].

<u>*Other optical techniques*</u>:

– ***Focus variation instruments***:

  The focus variation instruments combine the small depth of focus of an optical system with vertical scanning to provide topographical and colour information from the variation of focus, see Figure 2.6. The vertical resolution depends on the chosen objective and it can reach 10 nm. The maximum detectable slope is not dependent on the numerical aperture of the objective; therefore measurements of slope angle exceeding 80° can be achieved. This technique is applied only for measuring surfaces where the focus varies sufficiently during the vertical scanning process: transparent specimens or components with only a small local roughness cannot be characterized [Danzl, 2008].

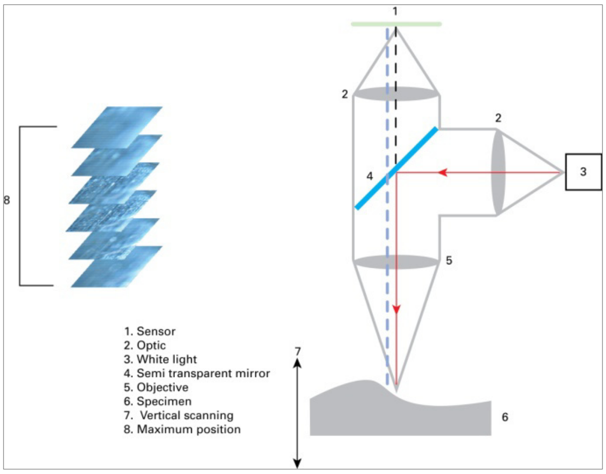

Figure 2.6 - Schema of a focus variation instrument [Leach, 2010].

2.2.3 Scanning probe and particle beam microscopy

This group includes the principal methods that have been developed to measure properties at the sub-nanometre range, as Scanning Probe Microscopy (*SPM*) and electron microscopy.

2.2.3.1 Scanning probe microscopy

SPM is a non-destructive technique that works equally well on metals, semiconductors and even on biological specimens. A very sharp tip, with a radius of a few nanometres, is scanned in close proximity to a surface using a piezoelectric scanner. Depending on the physical interaction of the tip with the surface, the system can be:

- ***Scanning Tunneling Microscopes (STM)***:
  Based on the quantum-mechanical tunnelling effect;
- ***Atomic Force Microscope (AFM)***:
  Based on intermolecular forces, see Figure 2.7;
- ***Scanning Near-field Optical Microscope (SNOM)***:
  Based on near-field optics to scan the surface.

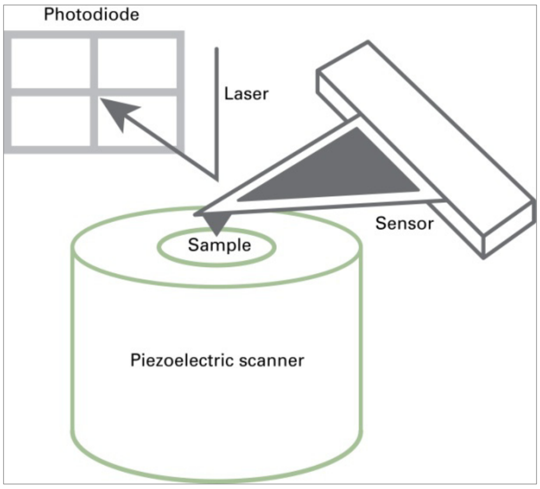

Figure 2.7 - Schematic image of an Atomic Force Microscope (*AFM*) [Leach, 2010].

The measurements on the surface cover an area up to 100 µm x 100 µm and height less than 10 µm. The vertical resolution is about 0.1 nm, while the horizontal resolution for most AFMs is typically 2 nm to 10 nm [Hansen, 2006].

A new AFM, Metrological Large Range Atomic Force Microscope (*Met. LR-AFM*), was developed at the Physikalisch-Technische Bundesanstalt (*PTB*) [Dai, 2010]. This new equipment scans direct large area within a measurement volume of 25 mm x 25 mm x 5 mm. Versatile scanning functions have been implemented to allow the choice of different application, e.g. step height, lateral pitch, nano-roughness and other parameters of nano structures.

In a recent work [Marinello, 2009] a *SPM* was implemented as system for coordinate metrology. Using a new non-raster measurement approach, the probe is moved to sense points along free paths on the sample surface, with no loss of accuracy and with scan time reduction. Moreover new probes with long tips and innovative geometries, see Figure 2.8, were developed in order to characterize structures normally not accessible using standard probe.

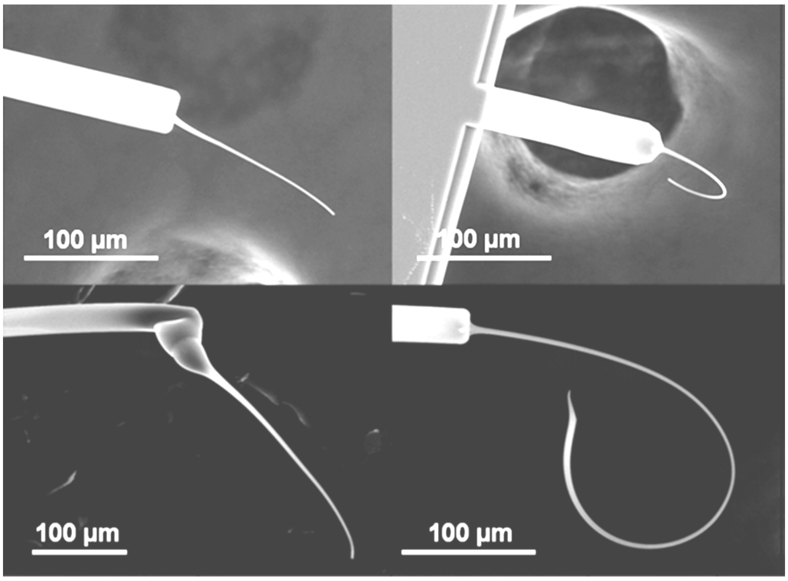

Figure 2.8 - Four different probes realized with different tip geometries [Marinello, 2009].

2.2.3.2 Electron microscopy

The instruments described in this section are:

- ***Scanning Electron Microscope (SEM)***:

  It is based on scanning an electron beam on the specimen. This interaction leads to several emissions, which can be detected and used to characterize physical and chemical properties of the sample, see Figure 2.9. In particular, characteristic x-rays are produced when electrons hit the specimen. These x-rays have energies that characterize specific elements contained in the upper layers of the surface. The instrument which can effectively be used to measure these energies is the energy dispersive x-ray spectrometer (EDS) which is fitted to the SEM. Its detector orientation to the axis of the x-ray beam is located in one of the SEM ports [Whitehouse, 2011].

  Typical SEMs can achieve image magnifications in the range of 100x - 100000x, resolution down to 2 nm, large depth of field, long working distance, elemental analysis capability and minimum diffraction effects [Rai-Choudhury, 1997]. Some disadvantages compared to optical microscopy include usually high vacuum requirement, relatively low throughput and potential for sample charging [Goodhew, 2001]. This technique can also be used for qualitative surface topography analysis, primarily based on the fact that SEM allows an excellent visualisation through the very high depth of focus [Hansen, 2006]. The achieved information is inherently 2D and no height information can be extracted. Reconstruction from stereo pairs or triplets of SEM images can be used for creating 3D information of the sample; as described in e.g. [Bariani, 2005] and [Carli, 2010].

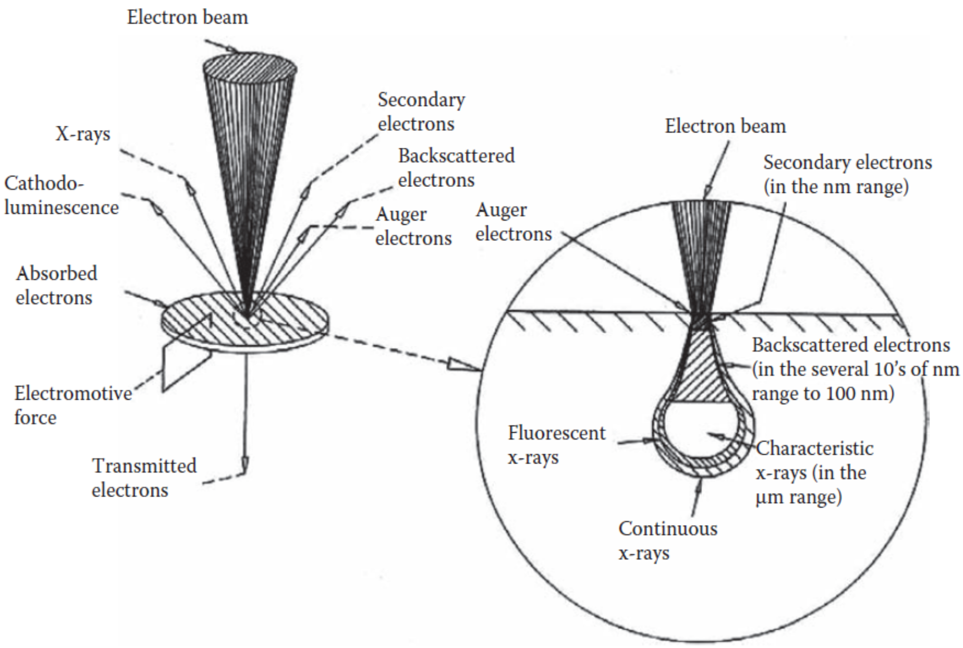

Figure 2.9 - Close up of the contact point of the electron beam [Whitehouse, 2011].

- ***Transmission Electron Microscope (TEM)***:

  It operates on the same basic principle as a light microscope, but it uses electron instead of light. Unlike the SEM in which only one spot is illuminated at a time and the image built up sequentially, TEM spreads the illumination over the sample. The illumination lens consists of a series of lenses which can provide various illumination modes to get high resolution and diffraction while the imaging lens provide high magnification, rotation free imaging, and angular correlation between the image and its diffraction pattern [Whitehouse, 2011]. The resolution is in the range of 0.05 nm with aberration-corrected instruments. In general the specimen itself causes loss of definition in the image due to chromatic aberration of the electrons, which have lost energy in transit through it [Leach, 2010].

2.2.4 Coordinate metrology

A Coordinate Measuring Machine (*CMM*) measures single points on the specimen surface or scans a selected surface in order to collect the data continuously as the stylus tip is dragged across the part.

The stylus tip in contact with the surface is usually a synthetic ruby ball and typical diameter dimensions are in the range of 0.5 mm - 10 mm.

In recent years smaller CMMs have been developed to enable 3D measurements of nanometre features; typically with ranges of tens of mm and tens of nm accuracy in *x*, *y* and *z* directions. Different micro-nano CMMs are described in [Hansen, 2006]:

- *Vermeulens Machine*: Abbe principle (*the displacement measuring system should be in line with the functional point whose displacement is to be measured. If this is not possible, either the slideways that transfer the displacement must be used to calculate the consequences of the offset* [Bryan, 1979]) is fulfilled in two axis, the use of linear scales is enabled by using an intermediate body and air bearings are involved. The measuring volume is 100 mm x 100 mm x 100 mm [Vermeulen, 1998], [Vermeulen, 1999];
- *NPL Machine*: uses the movement scales of a conventional CMM with a retrofitted high-accuracy probe with six degree of freedom. The working volume is 50 mm x 50 mm x 50 mm with a volumetric accuracy of 50 nm [Peggs, 1999];
- *Ruyls Machine*: Abbe principle is fulfilled in three axes, the measurement reference is a solid zerodur block that moves with the workpiece in 3 directions, while being measured by 3 flat-mirror laser interferometer systems. The measuring volume is 100 mm x 100 mm x 40 mm [Ruijl, 2001];
- *Van Seggelens Machine (Eindhoven University)*: it is a further improvement and miniaturization of the Vermeulens Machine. The measuring volume is 50 mm x 50 mm x 4 mm [Seggelen, 2005];
- *Ilmenau Machine*: it is equipped with 3 laser interferometers like the Ruyls Machine [Jaeger, 2002], [Hüser, 2005];
- *PTB Machine*: it allows coordinate measurements on microstructures to be carried out with an uncertainty < 100 nm. The measuring volume is 25 mm x 40 mm x 25 mm. It is available on the market [Brand, 2002];

- *University of Tokyo*: this device uses an optical scale to achieve high stability. It has a measuring range of 10 mm x 10 mm x 10 mm and a resolution of 10 nm [Fujiwara, 2003].

Most miniature CMMs usually have standard probe tips with a diameter of 0.3 mm, which is too large to measure MEMS structures or micro holes. Therefore smaller probes have been developed. Silicon flexures, meshes or membranes are used to suspend the probe shaft in order to reduce the probing force. Probes consisting of multiple layers of electrical connections, strain gauges flexures, meshes or membranes are made using chemical etching or vapour deposition processes [Leach, 2010].

Probes equipped with piezoelectric strain sensors have been developed at the Eindhoven University of Technology (TUE) and at PTB, see Figure 2.10 on the left. If this type of probes makes contact with the measured surface, a voltage signal is produced when a membrane deformation occurs. Due to inertia, they must be moved at very slow speed in order to avoid false readings [Haitjema, 2001], [Brand, 2000].

In a further attempt, probes which take optical measurements from illuminated glass fibres have been developed in order to reduce the surface damage caused by probe interactions, see Figure 2.10 on the right. However, due to the surface forces, the probe tends to hold the head on the surface, even while the CMM head is retracting [Schwenke, 2001].

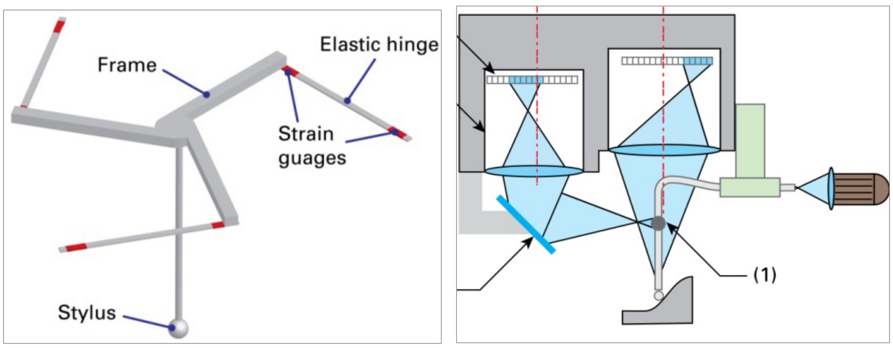

Figure 2.10 – Left: Silicon micro-scale probe [Leach, 2010]. Right: A fibre probe [Leach, 2010].

Other probes, the vibrating probes, are forced to vibrate at a specific frequency: any contact made with the measured surface will result in a change in the frequency, detected by a piezoelectric sensor, see Figure 2.11, [Weckenmann, 2004].

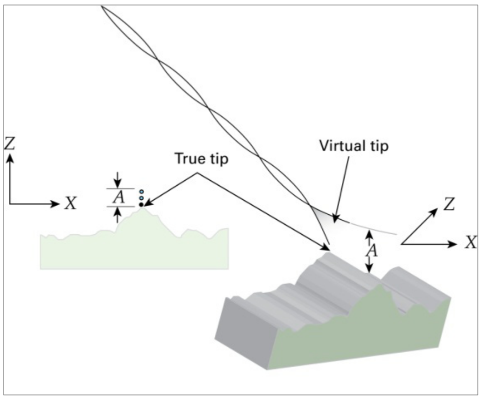

Figure 2.11 - A vibrating fibre probe [Leach, 2010].

Further investigations were carried out by:

- The National Physical Laboratory (NPL), proposing a 3 axis vibrating probe with isotropic probing forces [Claverley, 2010];
- PTB, a high resolution, self sensing and self actuated probe was suggested for CMM and scanning force microscopy [Illers, 2010];
- Ilmenau University of Technology, proposing a 3D tactile microscope with an optical detection system [Balzer, 2010].

2.2.5 Other techniques

Another technique is called micro Computer Tomography (*CT*). A micro-focused x-ray source illuminates the object; during the image acquisition, the sample is rotated stepwise through 180° and images are recorded at each position, see Figure 2.12. Resolution down to 0.15 μm can be reached. Recently, new metrological CT systems have been developed to be used in substitution to classical CMMs or integrated on multisensory CMMs [Carmignato, 2007]. Measurement uncertainties have not yet been completely quantified due to its complexity, while some measurement uncertainties contributions have been assessed in [Carmignato, 2007] and [Weckenmann, 2009].

The attractiveness of these technologies lies in the fact that they give precise quantitative information on the whole structure of a body without destroying it within a short period of time [Kak, 1988]. This is what has made CT very interesting for testing and inspecting manufactured workpieces like engine blocks, gear boxes or even injection nozzles [Bartscher, 2007]. Hence, they have been in use for non destructive testing and for dimensional measurements [Schwenke, 2002]. New applications of industrial CT are the analysis of fluid flows or fat content determination of meat or the analysis of the germination capacity of crops in the food industry [Bartscher, 2004].

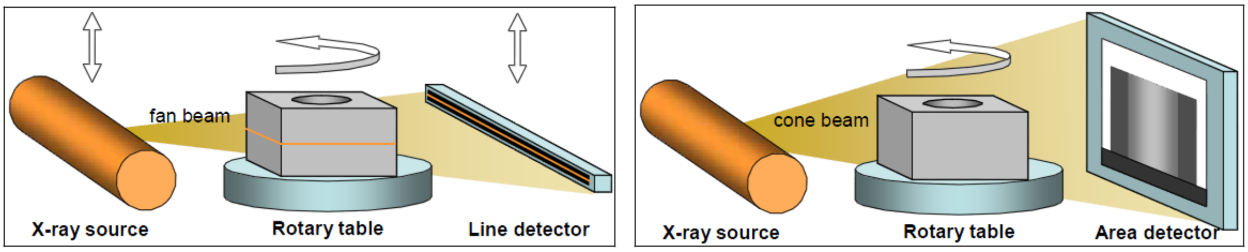

Figure 2.12 - Schematic representation of industrial CT systems. Left: 2D CT using line detector. Right: 3D CT with flat panel detector [Carmignato, 2007].

2.2.6 Summary

Measuring techniques relevant for this thesis are: micro topography measuring instruments, scanning electron microscope and coordinate measuring machines. In particular, for the characterization of surface topography on roughness calibrated artefacts and replica specimens the used instruments were: stylus profilometer, confocal microscope and InfiniteFocus. When dealing with dimensional measurements of step artefacts and micro products, such as Fresnel lenses, record stampers and optical components, the used instruments were: stylus profilometer, InfiniteFocus, white light interferometer and SEM-EDS. Dimensional verification of micro parts, e.g. toggle for hearing aids components, was performed using tactile and optical coordinate measuring machines.

2.3 Calibration and traceability

Calibration and traceability are two important steps in order to verify and assure the consistency and the accuracy of a measurement.

Calibration is the operation that, under specified conditions, establishes, in a first step, a relation between the quantity values *with measurement uncertainties* provided by measurement standards and corresponding indications *with associated measurements* *uncertainties*. In a second step, this information is used to establish a relation for obtaining a measurement result from an indication [VIM, 2008]. The measurement uncertainty, described in paragraph 2.4, plays a fundamental role and it is the information that differentiates “calibration” from “adjustment”. The adjustment could be related to a mechanical adjustment of the instrument itself or to a software change. It consists in tuning some parameters in order to provide an indication that is closer to a known value [Leach, 2010]. A calibration may be expressed by a statement, a calibration function, a calibration diagram, a calibration curve or a calibration table. In some cases, it may consist of an additive or multiplicative correction of the indication with associated measurement uncertainty [VIM, 2008].

In the macro world different kinds of calibration artefacts are available: scales, step gauges, ball plates, optical flats, etc. These calibration artefacts are available in a range of forms for both profile and areal calibration, but they must be calibrated by a primary instrument.

The profile measuring instruments are calibrated following ISO 5436-part 1 [ISO 5436-1, 2000]; the ISO describes five types of artefacts to use (Type A, Type B, Type C, Type D and Type E). ISO 12179 [ISO 12179, 2000] describes the methodologies to be applied for calibration of a surface texture measuring instrument such as the need for repeated measurements, general instrument set-up and what to include on a calibration certificate. Optical instruments are not covered in ISO 5436 [ISO 5436], but many of the described artefacts can be adapted to calibrate the profile in optical mode. Other available artefacts for profile calibration are presented in [Wilkening, 2005].

ISO 25178 part 701 [ISO 25178-701, 2010] describes five types of artefacts (Type ER, Type ES, Type CS, Type CG and Type DT) for calibration of areal surface texture measuring instruments, which can be adapted for optical instruments.

The verification of large CMMs is carried out using gauge blocks and following ISO 10360 part 2 [ISO 10360-2, 2009]. For verification of micro-nano CMMs, miniaturized ball bars have been developed for one-dimensional verification. Arrays of balls or holes and 2D/3D calotte plate/cube have been made for two-dimensional verification, see Figure 2.13.

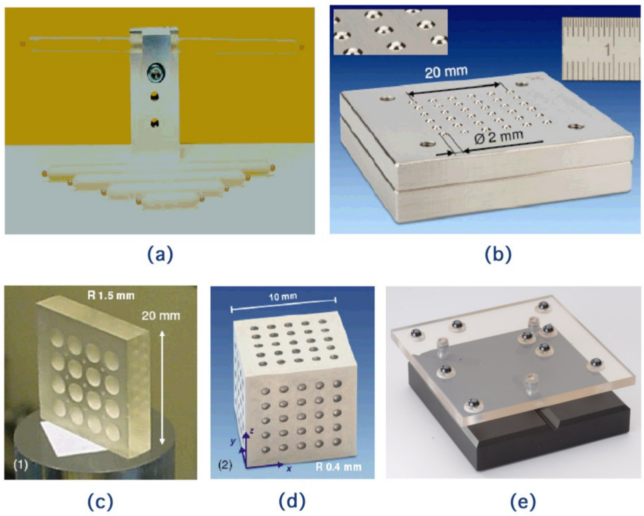

Figure 2.13 - Miniature CMM performance verification artefacts. (a) METAS miniature ball bar, (b) PTB calotte plate, (d) PTB calotte cube, (e) Zeiss half-sphere plate [Leach, 2010].

In the micro world fewer standards are in use: step heights, scales, 2D scales and crystalline or silicone surfaces, see Figure 2.14. The problems related to the micro world are due to the fact that the artefacts cannot be handled so easy or can hardly be prepared; moreover standards of organic materials are needed for nanotechnology in all kind of processes (manufacture, monitoring and measurement).

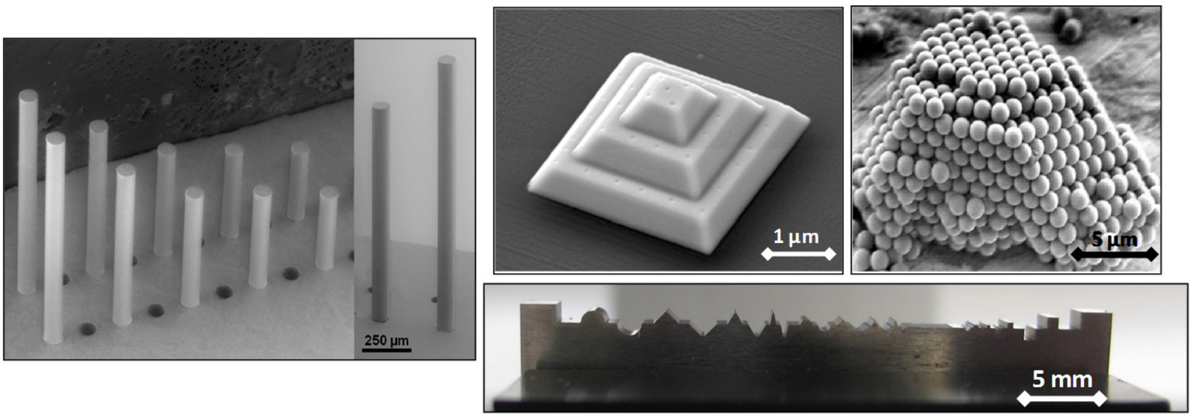

Figure 2.14 - Some available artefacts for micro-scale: fibre gauges [Marinello, 2008], a micro-pyramid [Ritter, 2004], silica beads [Microparticles, 2011] and micro-contour [PTB, 2005].

Figure 2.15 shows the available calibration artefacts for dimensional micro and nano metrology. Looking at the graph, relatively large areas of the diagram are uncovered indicating the need for calibration artefacts. In particular all standards seem to represent low aspect ratio hence no real 3D standards are available in this regime [Hansen, 2006].

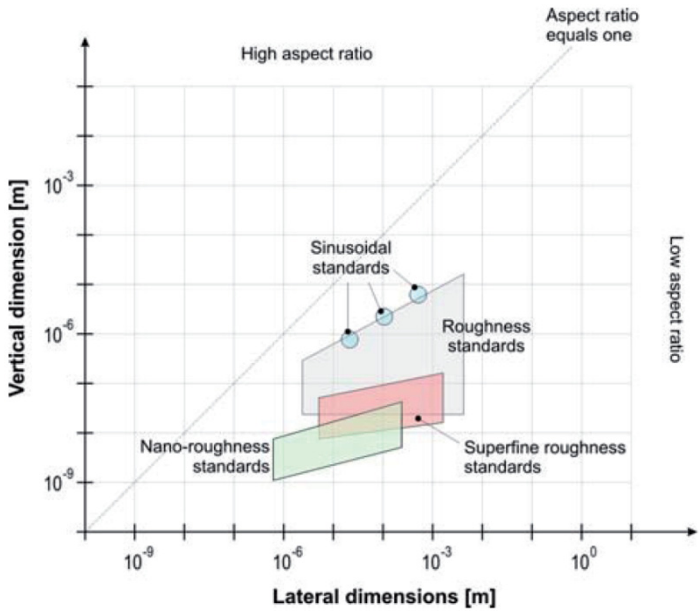

Figure 2.15 – Calibration artefacts for dimensional micro and nano metrology [Hansen, 2006].

A new concept of micro artefact called “The fiber gauge” is described in [Marinello, 2008], see Figure 2.14. It consists of a set of optical fibres sticking out from a flat surface. The fibres are arranged as a regular array of different height cylinders with aspect ratio up to 20:1. The artefact can be applied to calibrate most of contact or non-contact instruments for characterization of surface topographies and 3D micro geometries, such as micro or nano CMMs and optical instruments.

Another reference standard is proposed in [Carmignato, 2010], called “Olympic gauge”. It has been fabricated with five borosilicate glass cylindrical tubes supported by a carbon fibre frame for metrological performance verification of x-ray micro-tomography systems.

Traceability is the result of a measurement whereby it can be related to stated references, usually national or international standards, through a documented unbroken chain of comparisons all having stated uncertainties [VIM, 2008]. “*All having stated uncertainty*” is an essential concept for ensuring traceability. For example, in order to verify that the measurement of a micrometer is “correct”, the instrument must be checked or calibrated against a more accurate displacement system or must be compared to a calibrated transfer artefact, see Figure 2.16.

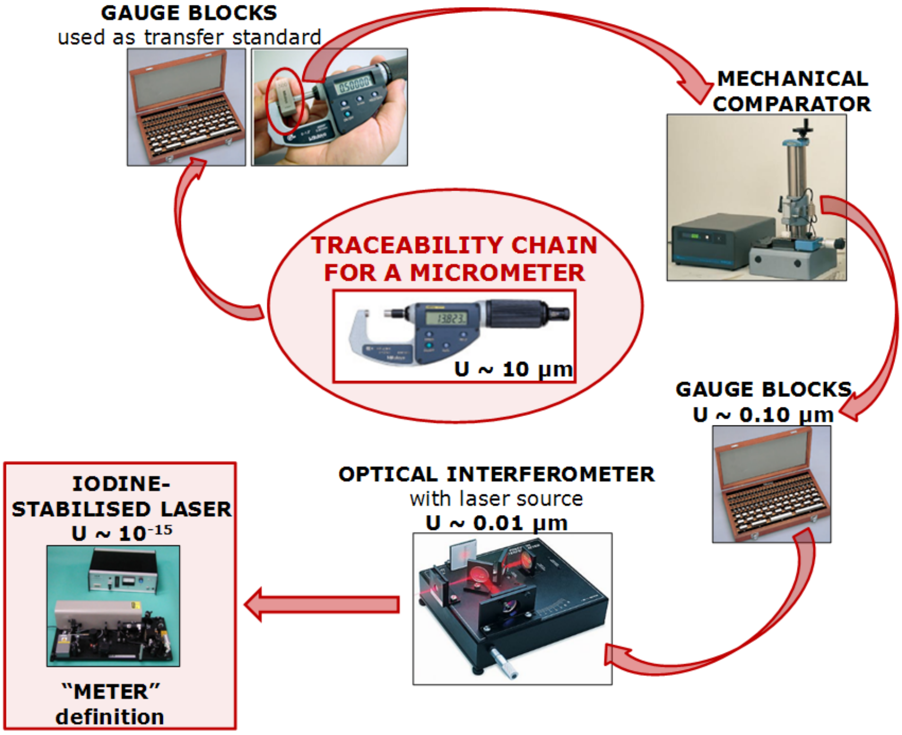

Figure 2.16 - Traceability chain for a micrometer through primary meter, primary gauge block and workshop gauge block.

Therefore the traceability chain for a micrometer consists in the following steps: the micrometer has to be calibrated using a gauge block, which was previously calibrated by a mechanical length comparator. This comparator would be calibrated by a more accurate gauge block which has been calibrated using an optical interferometer with a laser source. This laser source is calibrated against the iodine-stabilised laser that realises the definition of the meter [Leach, 2011], [De Chiffre, 2011]. These steps assure an unbroken chain of comparisons.

The standards currently available for the traceability and the verification of an instrument are the following:

- *for CMMs (Coordinate Measuring Machines):*
    1. ISO 10360 [ISO 10360] describes a number of widely accepted tests covering the most common aspects for the performance verification of CMMs;
    2. ISO 15530 [ISO 15530] provides a full traceability of CMMs measurements.

- *for stylus instruments:*
  1. ISO 5436 [ISO 5436] describes the calibration artefacts to use for the traceability of profile measurements using a stylus instrument;
  2. ISO 25178-701 [ISO 25178-701, 2010] describes the calibration artefacts to use for the traceability of areal measurements using a stylus instrument.
- *for optical instruments-3D scanners:*
  1. Currently there is only a draft of the ISO specification standard (likely ISO 25178-702) which is expected covering all optical instruments that use areal topography analysis [Leach, 2011].

This kind of instruments can perform very numerous and different measurement tasks involving a large number of uncertainty contributors. Therefore the correct approach is the so called "*task related*" uncertainty evaluation [Wilhelm, 2001] which establishes traceability for individual measurement tasks, where measurements strategy and conditions are specified [De Chiffre, 2011].
In the case of dimensional nano-metrology, there are many examples when it is not always possible to ensure traceability because there is a break in the chain. There may not be national or international specifications standards available and the necessary measurement infrastructure may not have been developed, e.g. complex three-dimensional micro-nano technology measurements. Where there are no guidelines or where there is a new measurement instrument or technique to be used, the metrologist must apply good practise and should consult other experts in the field [Leach, 2010].

In relation to these problems, chapter 3 of the present work proposes an alternative way for verification and calibration. A replica casting method is useful when dealing with parts difficult to characterize using the available measuring techniques. The idea is to replicate the part and, afterwards, characterize the replica instead of the part. A traceable procedure is achieved applying the replica technique to a calibrated artefact.

2.4 Uncertainty evaluation

Several approaches are available for the calculation of the measuring uncertainty with different degree of rigorousness and easiness of implementation [De Chiffre, 2011]:

1. GUM: Guide to the expression of Uncertainty in Measurement – described in [GUM, 2008]
   - Rigorous metrological approach;
   - “conventional true uncertainty” – “GUM uncertainty”;
   - Complex and, sometimes, time consuming;
   - EA-4/02: Expression of the Uncertainty of Measurement in Calibration;
   - Intended for calibration laboratories.
2. PUMA: Procedure for Uncertainty Management – described in ISO 14253 part 2 [ISO 14253-2, 1998]
   - Simplified, iterative procedure based on GUM principles;
   - Upper bound strategy – overestimation;
   - “approximated uncertainty”;
   - Intended for industrial users.
3. Substitution approach (Comparator method) – described in ISO 15530 part 3 [ISO 15530-3, 2004][a]
   - Repeated measurements on calibrated workpieces with same conditions as actual measurands (alignament, handling, etc);
   - Calculation of uncertainty by simple formula;
   - Intended for industrial users;
   - Requires a calibrated workpiece or a number of calibrated reference artefacts.
4. Other approaches – described in ISO 15530 Series (under development)
   a. Expert Judgment;
   b. Statistical estimation from measurement history;
   c. Computer simulation;
   d. Measurements after multi-positioning.
5. Proficiency Test
   a. Using En values to access usable values for U.

[a] A revised version is available (ISO15530-3:2011).

For a practical introduction to uncertainty of measurements, see [Bell, 2001].
In the following paragraph, the important steps of the GUM are described since most of the uncertainty budgets calculated in the present work are based on it (*chapter 3*, *5*, *6*, *7*, *8*).

2.4.1 Uncertainty budget according to GUM

The primary guide in metrology on uncertainty evaluation is the GUM [GUM, 2008]. It presents a framework for uncertainty evaluation based on the use of the law of propagation uncertainty and the central limit theorem.
According to the GUM, the ideal method for evaluating and expressing the uncertainty of a measurement result should be:

- *Universal*: the method should be applicable to all kinds of measurements and to all types of input data used in measurements;
- *Internally consistent*: the uncertainty should be directly derivable from the components that contribute to it, as well as independent of how these components are grouped and of the decomposition of the components into subcomponents;
- *Transferable*: it should be possible to use directly the uncertainty evaluated for one result as a component in evaluating the uncertainty of another measurement in which the first result is used.

This method involves the identification of all sources of uncertainty, which has to be estimated and combined in order to give an overall figure. Therefore, the measurement has to be represented by a model of the generic form:

$$Y = f(X_1,...,X_n) \qquad (2.1)$$

Where Y is the measurand and X_i are the input quantities.
There are clear rules for assessing the contribution of each source of uncertainty. Two approaches are available:

1. *Type A evaluation*: estimated by statistical analysis of observations (usually from repeated readings).
   The mean value $\underline{x}$ of a number n of measurement results x_i is an estimate of the true value of the mean μ of the distribution.

$$\underline{x} = \frac{1}{n}\sum_{i}^{n} x_i \qquad (2.2)$$

The experimental standard deviation of the distribution based on *n* measurement values u_x is an estimate of the standard deviation of the distribution *σ*.

$$u_x = \sqrt{\frac{\sum_1^n (\underline{x} - x_i)^2}{(n-1)}} \tag{2.3}$$

The standard deviation of the mean value $u_{\underline{x}}$ is equal to the standard deviation of the distribution divided by the square root of the number of measurements *n*.

$$u_{\underline{x}} = \sqrt{\frac{\sum_1^n (\underline{x} - x_i)^2}{n \cdot (n-1)}} = \frac{u_x}{\sqrt{n}} \tag{2.4}$$

The standard deviation of the distribution is used in the uncertainty budget when the measurement result is obtained using single readings of the interested component. Meanwhile, the standard deviation of the mean value is used in the uncertainty budget when the measurement result is obtained using the mean of several readings of the interested component.

2. *Type B evaluation*: calculated from assigned probability distributions (see Table 2.2): from past measurements experience, from calibrated certificates, manufacture's specifications, from calculations, from published information and, finally, from common sense.

Once the different sources of uncertainty are estimated, the *combined standard uncertainty* is calculated as the estimated standard deviation associated with the result. It is equal to the positive square root of the combined variance obtained from all variance-covariance components, however evaluated, using the law of propagation of uncertainty.

Combined standard uncertainty for uncorrelated (independent) input quantities:

$$u_c(y) = \sqrt{\sum_{i=1}^{n} \left(\frac{\partial f}{\partial x_i} \right)^2 u^2(x_i)} \tag{2.5}$$

Combined standard uncertainty for correlated input quantities:

$$u_c^2(y) = \sum_{i=1}^{N} \sum_{j=1}^{N} \frac{\partial f}{\partial x_i} \frac{\partial f}{\partial x_j} u(x_i, x_j) = \sum_{i=1}^{N} \left(\frac{\partial f}{\partial x_i} \right)^2 u^2(x_i) + 2 \sum_{i=1}^{N-1} \sum_{j=i+1}^{N} \frac{\partial f}{\partial x_i} \frac{\partial f}{\partial x_j} u(x_i, x_j) \tag{2.6}$$

Type	Diagram	Equivalent standard deviation	Use
Normal	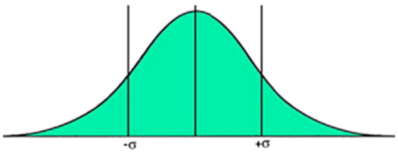	$s = \sigma$	When type A evaluations can be shown to follow this distribution
Triangular	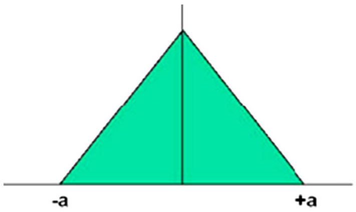	$s = \frac{a}{\sqrt{6}} \approx 0.4 \cdot a$	When “hard” limits can be estimated easier than σ, e.g. noise and vibration
Rectangular	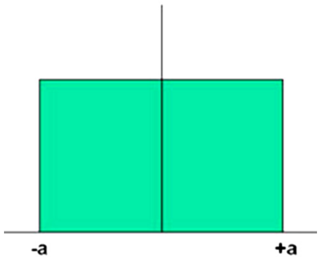	$s = \frac{a}{\sqrt{3}} \approx 0.6 \cdot a$	When only the variations limits are known, e.g. calibration certificates, specification by the manufacturer
U-shaped	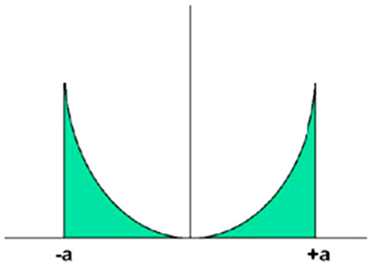	$s = \frac{a}{\sqrt{2}} \approx 0.7 \cdot a$	For cyclic influences, e.g. temperature variation
Step	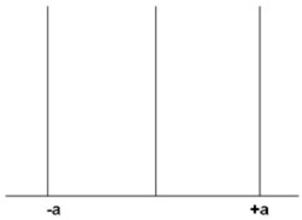	$s = \frac{a}{2\sqrt{3}} \approx 0.3 \cdot a$	When resolution is limited, e.g. digital readout, Verniers, scale read by operator.

Table 2.2 - Probably density function used for type B standard uncertainty evaluation [EA, 1999].

The *expanded uncertainty U* is obtained by multiplying the combined standard uncertainty u_c by a coverage factor *k*. The intended purpose of *U* is to provide an interval for result of a measurement that may be expected to encompass a large fraction of the distribution of values, that could be reasonably be attributed to the measurand. The complete statement of the result of measurement requires the statement of the estimate *y* for the measurand *Y* and its expanded u_n certainty *U*. The units of *y* and *U*, which are the same, should always be given. The approximate level of confidence to be associated with the interval (-*U*; +*U*) should be given as well.

Expanded uncertainty *U*:

$$y \pm U = y \pm (k \cdot u_c) \qquad (2.7)$$

The *coverage factor k* is a numerical factor used as multiplier of the combined standard uncertainty in order to obtain an expanded uncertainty. The coverage factor is chosen on the basis of the desired level of confidence, see Table 2.3.

Level of confidence *p* (%)	68.27	90	95	95.45	99	99.73
Coverage factor *k*	1	1.645	1.960	2	2.576	3

Table 2.3 - Coverage factor k values corresponding to the different levels of confidence.

A common uncertainty budget for all uncorrelated uncertainty components may result in an equation as follows:

$$u_c = \sqrt{u_1^2 + u_2^2 + \ldots + u_n^2} \qquad (2.8)$$

where u_1 .. u_n = standard uncertainty components;

$$U = k \cdot u_c \qquad (2.9)$$

Most commonly with a coverage factor *k* = 2. Consequently, a general expression for dimensional measurements can be as follows:

$$U = k\sqrt{u_r^2 + u_m^2 + u_w^2 + u_e^2 + u_p^2} \qquad (2.10)$$

Where:

- *U* = expanded uncertainty;
- *k* = coverage factor;
- u_r = standard uncertainty from calibrated artefact;
- u_m = standard uncertainty from measuring instrument;
- u_w = standard uncertainty from workpiece;
- u_e = standard uncertainty from environment (temperature, vibrations, dirt, ..);

- u_p = standard uncertainty from procedure (standard deviations of the measurements).

2.5 Tolerancing rules

In the macro world the tolerancing rules play a fundamental role in optimizing and protecting the functional behaviour of manufacturing processes and mechanical parts. Specifically the most encountered functions which have to be ensured are: the assembly between two elements, the sliding and the rolling capabilities (e.g. for shafts and holes), the load rating and different surfaces finishing [Weckenmann, 2000].

These functions are represented in the technical drawings by “tolerances” or “specifications” which are given in terms of maximum deviations from an ideal geometric form and they are regulated by the international standards called GPS. They have the aim to be a common language between design, manufacture and tolerance verification; and are characterized by [De Chiffre, 2011]:

- A new classification called Masterplan which summarizes and groups all the geometrical standards - ISO 14638 [ISO 14638, 1995];
- A new approach based on functionality which gives a detailed description of geometrical features linked to functional properties;
- A new philosophy called the Skin Model, based on the idea that no perfect geometry can be achieved in reality, but from a large number of points it is possible to give a realistic picture of the geometry of an object - ISO 14660 [ISO 14660, 1999];
- A new rule of taking measuring uncertainty into account in tolerance verification – ISO 14253 [ISO 14253, 1998] – which replaces the Golden Rule of Metrology. According to the Golden Rule, the measuring instrument should have a resolution which is one tenth of the tolerance to verify and the uncertainty of measurement should be 10 - 20% of the tolerance range.

In the micro and nano world it seems straightforward to use and adapt the ISO from GPS; however some problems may occur [Hansen, 2006], [Weckenmann, 2005]:

- The absolute dimensions are small and so are the tolerances. These facts result in at least two challenges: (a) finding a suitable measurement method to actually measure the components; (b) ensuring that the measurement uncertainty is sufficiently small to actually be able to verify the tolerance. The consequence in all cases usually is that the measurement uncertainty becomes larger compared to the tolerance interval leaving a much smaller conformance zone for process variations (see Figure 2.17);

- Tolerance grades are not defined for nominal sizes below 3 mm;
- Quite some zeros are needed to express the tolerances in the technical drawings;
- ISO-GPS system was created having in mind mm-size; therefore, as example, how to define straightness on nanometre scale or the characterization of atomic structured surfaces?
- Available calibration artefacts are not good enough in order to ensure the traceability of measurements on micro-nano parts. This limitation is underlined by the approach proposed in [Schobel, 2005] for the development of tolerance systems for micro-nano features obtained using micro milling and sputtering.

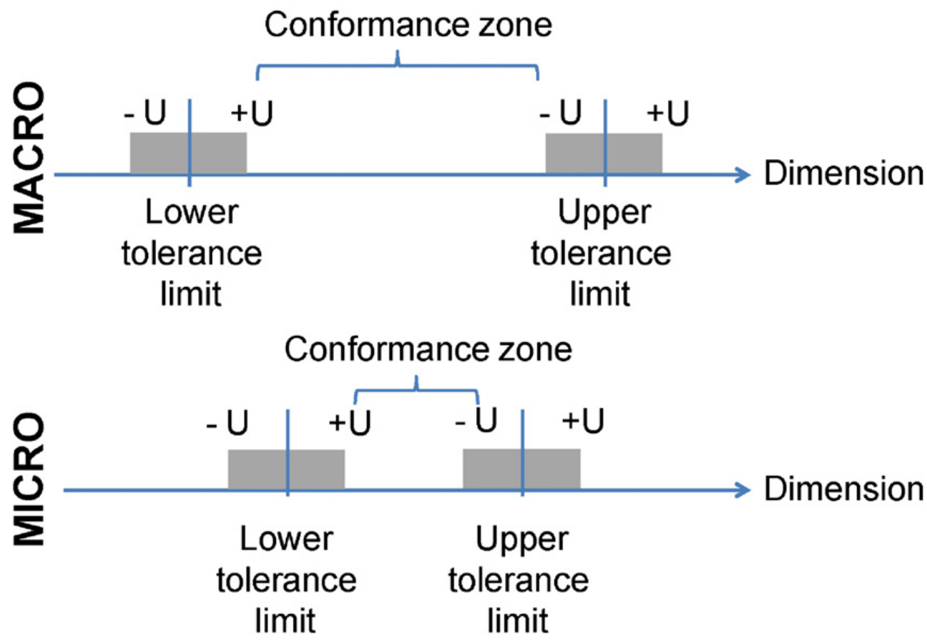

Figure 2.17 - Illustration of relationship between tolerance and measurement uncertainty. In this representation the measurement uncertainty was kept constant and the tolerance zone decreased [Tosello, 2009].

In [Weckenmann, 2005], it is proposed to adapt the traditional GPS approach when applied to nano metrology. In particular this involves fundamental studies regarding single atoms of the surface which may become dominant when assumptions based on continuum mechanics are no longer valid.

Other problems may occur when considering manufacturing processes: the technologies used for manufacturing micro components are quite different than those for macro components and the integration of parts in assemblies is obtained in different ways [Alting, 2003], [Hansen, 2006]. For this reason and according to [Weckenmann, 2000], three different integration techniques may be distinguished in micro and nano technology:

1. *Hetero integration*: geometric tolerances are required to achieve the functionality of the assembly, as for the macro mechanical parts;
2. *Hybrid integration*: the positional accuracy of a micro component on a substrate is the most important parameter; in fact the micro part is placed, fixed and assembled resulting a fully functioning micro system;
3. *Monolithic integration*: geometric measurements are not of primary importance; all the process steps of the micro component are integrated in a single substrate. For example in the case of etching processes, the most important variables to be taken into account are the parameters of the process itself, as for instance the etching time, and not the geometrical dimensions of the component. In [Weckenmann, 2001] a function-oriented tolerancing concept is proposed. According to this concept, a tolerance is associated to the overall function of the micro component. If the calculated performance deviations during the various process steps are larger than the product tolerances, the parameters of the currently active manufacturing step will be corrected, so that the final product is situated within the expected product tolerances as defined by the functional behaviour.

In relation to this topic, two different case studies for dimensional verification of micro-nano injection moulded components are presented in chapters 6 and 7: a toggle for hearing aid application and CD/DVD/HD-DVD. The two investigations focus on the fact that combined uncertainties of the measurements and production process determine boundaries of achievable manufacturing results and, therefore, they create challenges for the verification of the tolerances.

The first case study, chapter 6, identifies the problems related to the tolerance verification when the absolute dimensions are scaled down to the micrometer range; in particular the

measurement uncertainty becomes relatively large compared to the tolerance interval, leaving a smaller conformance zone for process variations.
The second case study, chapter 7, involves optical disc features: the requirement that has to be satisfied is the correct data transfer. For this reason the crucial phase of the process is the data encoding which has to be controlled by the process parameters 'time' and 'scanning velocity': it is an example of monolithic integration.

2.6 Industrial practice (COTECH)

A metrology questionnaire was created by DTU and distributed among all the partners of the European consortium COTECH between December 2008 and April 2009. The aim was to become acquainted with the available metrology equipment inside the consortium and to be aware of their knowledge about some key-topics of dimensional metrology.
The questionnaire was divided into three parts:

1. General information of the partner;
2. Overview and instruction regarding the questionnaire;
3. Description of the instrument:
    - *Equipment*: in this section it was required to fill tables regarding the environment where the measurements were normally carried out and the equipment specifications, e.g. the instrument designation, a picture of the instrument, the used probe/tip, the stage type and the software used for the analyses;
    - *Calibration*: questions concerning, for examples, the used calibration standards, how frequent a calibration of the instrument is performed, ... ;
    - *Measurements*: information about the measured workpieces and the followed ISO standards;
    - *Uncertainty*: questions regarding the calculation of the uncertainty budget.

Table 2.4 summarizes the available instruments and their beneficiary. They have been grouped in seven categories according to the measurement principles described in paragraph 2.2. The number of instruments available for each category is grouped and summarize in Figure 2.18, inspired by Figure 2.1.

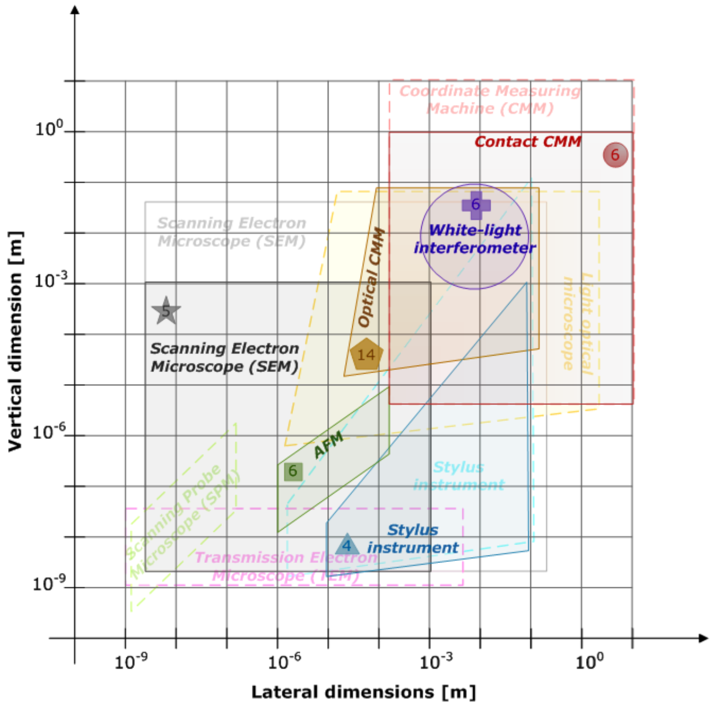

Figure 2.18 - Instruments available inside COTECH consortium and Figure 2.1 as background.

The questionnaire showed that forty-four instruments are present in the COTECH consortium covering every single category listed above. In particular, the optical CMMs seem to be the most familiar: fourteen instruments are available (31% of the total), see Figure 2.19.

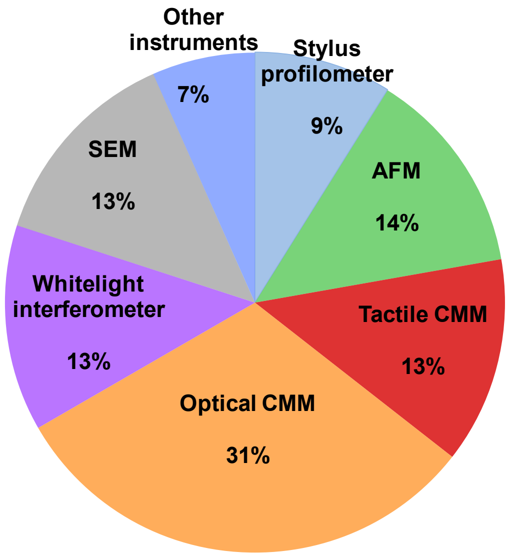

Figure 2.19 – Instruments available inside COTECH consortium.

Instruments		Beneficiary (*country*)
Stylus profilometers	Dektak 3ST	IT, company
	FTS 50 Inductive	DK, university
	Profilometer Tencor P2	DE, research organization
	Dektak 8	ES, research organization
Atomic Force Microscopes	PSI Thermomicroscopes M5 AP500	IT, company
	XE-100 from Park Systems	UK, university
	DME DualScope 95-200 mounted on CMM	DK, university
	Nanosurf easy scan 2	AT, university
	AFM Multimode	DE, research organization
	NT-MDT AFM SOLVER PRO	ES, research organization
Contact CMMs	ZEISS UPMC 850 CARAT	DK, university
	VideoCheck IP 250	AT, research organization
	VideoCheck IP 400	DE, company
	Werth VideoCheck HA 400	DE, institute
	SARIX SX-100-HPM 3D µEDM Milling	CH, company
	UPMC-850 CARAT	ES, research organization
Optical CMMs	InfiniteFocus	AT, company/ DK, un
	Quick Vision Accel Pro from Mitutoyo	UK, university
	DeMeet 220	DK, university
	Ubm Microfocus 1080	DK, university
	Nikon MM-60	ES, company
	VideoCheck IP 250	AT, research organization
	Leitz UWM SKI	DE, research organization
	VideoCheck IP 400	DE, company
	Werth VideoCheck HA 400	DE, institute
	Nikon MM-40	CH, company/ DK, company /ES, research org
	Nikon ME 600P	ES, research organization
Whitelight interferometer	WYKO NT 1100	UK, university / ES, research org
	MicroXam from ADE Phase Shift	UK, university
	MicroProf 100	AT, research organization
	SARIX SX-100-HPM 3D µEDM Milling	CH, company
	Sensorfar PLµ 2300	NL, research organization
Scanning electron microscopes	Philips XL30	FR, company/ res org
	FP 2012/11 Quanta 200-FEI	IT, company
	JEOL JSM-6600	DE, research organization
	ZEISS ULTRAPLUS	ES, research organization
Other instruments	Prometeus MT-136/Biref 126	ES, company
	NanoCalc-2000-UV-VIS	AT, university
	0.001/12 mm Mitutoyo	DK, company

Table 2.4 - Instruments available in COTECH consortium and their beneficiary.

From the answers collected on the '*Calibration*' part, it is clear that the instrument calibration is performed at least every year by more or less all the COTECH partners and very few do not perform it on their instrument. The involved reference standards are: height steps, gauge blocks, hole plates, ball bars, spheres and glass plates.
Problems encountered during the calibration are: "*for height measurements, the calibration of the instrument relies on one point calibration method and it has limitations when the measured artefacts have dimensions that lies far from the values of the step height used for calibration*" and "*normally the measurements are out of acceptance criteria, due to chuck problems (leads to unstable measure), vibrations or dirty into the calibration disc*".
From the '*Measurements*' part, the micro- and nano- components measured daily are: micro-lenses, inserts for moulds, polymer films, wafer substrates, gold structures for x-ray masks, nano imprint lithography templates in quartz, micro injection moulding inserts in silicon, nickel electroformed components, moulds, cavities, tools with details in the micrometer range, micromechanics parts on steel and hard alloys, watch industry components, car injectors holes (80 µm in diameter), shaped pieces with structures down to 10 µm, surface roughness with Ra values larger than 10 nm, steep slopes (up to 88°), micro moulds and plastic parts for medical applications, cavities and geometries typically 1 - 5 mm total size with features ~ 500 µm to 1 µm and replicated CD, DVD, HD.
After the measurements, the tolerances are sometimes verified and the measurement results are calculated automatically by the software for the analysis.
The last part is the '*Uncertainty*' part. It reveals to be the most critical and crucial one: very few answers and the measurements uncertainty is often confused with the measurements repeatability, which is only a contribution of the total uncertainty.
As result of the survey, in Europe the trend in metrology concerns:

- Measurements and verifications of micro components which require quite challenging measuring procedures, as for micro-lenses or specimens with steep slopes;
- The traceability of the equipment is performed, especially because every year the instrument manufacturer offers calibration service;
- The uncertainty budget usually requires time and good knowledge; therefore its evaluation procedure is often reduced to the only measurement repeatability calculation.

2.7 Future needs and trends

In the metrology field, future trends and new application are [Weckenmann, 2007]:

- *Holistic measurements*:
  Fusion of inhomogeneous data from different sensors is the future challenge in multi sensor metrology, together with the combination of the advantages of different technologies (multi sensor CMM with tactile, optical and tomographic inspection methods) in order to have faster, more robust and more reliable measurement results;
- *Micro-nano metrology*:
  Scanning force microscopes are undergoing further development in several directions. True 3D measurement of nanostructures, development of 3D probes, novel measurements strategies and data fusion models are the first needs. The second relates to the measurements on samples with special materials. SEM and TEM require 3D measurements on nano-particles and internal structures. Better imaging and improvement algorithms are the key requirements for high-quality reconstructions of 3D nanostructures [Danzebrink, 2010].
- *Calibration artefacts*:
  Recently, the development of new artefacts has been focused on SPMs; therefore standards with high lateral resolution and low aspect ratios (such as silicon grids, height steps) are available. On the other hand a general lack is present for 3D real reference artefacts. Physical standards for surface roughness, subsurface properties, form (flatness, sphericity, aspheriticy) glass, ceramics and metals are needed, as well as standards made of inorganic materials.
- *Cost reduction of standard measurements*:
  Conditioning of the measuring environment is more important for micro-nano measurements than for the macro ones. This is very expensive and feasible only to a certain degree. Computer based non-linear correction or compensation methods will help in future to reduce this effort and to improve stability of measuring results.

The real challenge is improving the ease of instrument use in order to obtain valid results with small uncertainty even from unskilled personnel.

2.8 References

[Alting, 2003] L. Alting, F. Kimura, H.N. Hansen, G. Bissacco, “Micro engineering”, Annals of the CIRP, 2003, Volume 52, Issue 2, pp. 635-658.

[Balzer, 2010] F.G. Balzer, N. Dorozhovets, N. Hofmann, T. Hausotte, E. Manske, G. Jäger, S. Büttgenbach, “3-D microprobe with optical detection system”, 10th International Conference of EUSPEN, 2010, Volume 1, pp. 104-107.

[Bariani, 2005] P. Bariani, “Dimensional metrology for microtechnology”, PhD thesis, Department of Manufacturing Engineering and Management, Technical University of Denmark, 2005.

[Bartscher, 2004] M. Bartscher, U. Neuschaefer-Rube, F. Waldele, “Computed tomography a highly potential tool for industrial quality control and production near measurements”, VDI Berichte, 2004, Volume 1860, pp. 477-482.

[Bartscher, 2007] M. Bartscher, U. Hilpert, J. Goebbels, G. Weidemann, “Enhancement and proof of accuracy of industrial computed tomography (CT) measurements”, Annals of CIRP, 2007, Volume 56, Issue 1, pp. 495-498.

[Bell, 2001] S. Bell, “A beginner’s guide to uncertainty of measurement”, Measurement good practice guide No. 11, Issue 2, 2001, NPL.

[Brand, 2000] U. Brand, T. Kleine-Besten, H. Schwenke, “Development of a special CMM for dimensional metrology on microsystem components”, Proc. 15th ASPE, 2000, pp. 542-546.

[Brand, 2002] U.Brand, T. Kleine-Besten, H. Schwenke, “Development of a special CMM for dimensional metrology on microsystem components”, Proc. ASPE Conference, 2000, pp. 542-546.

[Bryan, 1979] J.B. Bryan, “The Abbe principle revisited: an updated interpretation”, Precision Engineering, 1979, Volume 1, pp.129-132.

[Carli, 2010] L. Carli, “3D-SEM metrology for coordinate measurements at the nanometer scale”, PhD thesis, Department of Manufacturing Engineering and Management, Technical University of Denmark, 2010.

[Carmignato, 2007] S. Carmignato, “Traceability of dimensional measurements in computed tomography”, Proceedings of 8th A.I.Te.M. Conference, 2007.

[Carmignato, 2010] S. Carmignato, A. Pierobon, F. Marinello, E. Savio, "Olympic gauge: a new reference standard for testing x-ray microtomography systems", 10th International Conference of EUSPEN, 2010, Volume 1, pp. 217-220.

[Claverley, 2010] J.D. Claverley, R.K. Leach, "A novel three-axis vibrating micro-CMM probe with isotropic probing forces", 10th International Conference of EUSPEN, 2010, Volume 1, pp. 59-62.

[Cosijns, 2002] S.J.A.G. Cosijns, H. Haitjema, P.H.J. Schellekens, "Modeling and verifying non-linearities in heterodyne displacement Interferometry", Precision Engineering, 2002, Volume 26, pp. 448-455.

[Dai, 2010] G. Dai, H. Wolff, F. Pohlenz, H.U. Danzebrink, "Further improvements of the measurement capability of a metrological large range AFM" 10th International Conference of EUSPEN, 2010, Volume 1, pp. 55-58.

[Danzebrink, 2010] H.U. Danzebrink, T. Dziomba, M. Xu, "Scanning probe microscopy, scanning electron microscopy and critical dimension: nanometrology status and future needs within Europe", Nanometrology, Discussion papers 2010; Co-Nanomet.

[Danzl, 2008] R. Danzl, F. Helmli, P. Rubert, M. Prantl, "Optical roughness measurements on specially designed roughness standards", Proceedings of the SPIE - The International Society for Optical Engineering, 2008, Volume 7102, pp. 71020M.

[De Chiffre, 2011] L. De Chiffre, "Geometrical metrology and machine testing", DTU Mechanical Engineering, Course 41731, 2011.

[Diaspro, 2002] A. Diaspro, "Confocal and two-photon microscopy: foundations, applications and advances", Wiley Blackwell, 2002.

[EA, 1999] EA (European co-operation for Accreditation), "Expression of the uncertainty of measurement in calibration", EA-4/02, 1999.

[Fujiwara, 2003] M. Fujiwara, K. Takamasu, S. Ozono, "Evaluation of properties of nano-CMM by thermal drift and tilt angle", Proc. XVII IMEKO World Congress, 2003, pp. 1794-1797.

[Goodhew, 2001] P.J. Goodhew, J. Humphreys, R. Beanland, "Electron microscopy and analysis", Taylor and Francis, 2001.

[GUM, 2008] Joint Committee for Guides in Metrology (JCGM). JCGM 100:2008, Guide to the Expression of Uncertainty in Measurement (GUM), 2008, pp. i–viii, 1–132.

[Haitjema, 2001] H. Haitjema, W.O. Pril, P.H.J. Schellekens, “Development of a Silicon-based Nanoprobe System for 3-D Measurements”, Annals of CIRP, 2001, Volume 50, Issue 1, pp. 365-368.

[Hansen, 2006] H.N. Hansen, K. Carneiro, H. Haitjema, L. De Chiffre, “Dimensional micro and nano metrology”, Annals of CIRP, 2006, Volume 55, Issue 2, pp.721-743.

[Hüser, 2005] D. Hüser, R. Petersen, H. Rothe, “Coordinate measurements in Microsystems by using AFM-probing: problems and solutions”, In: Nanoscale calibration standards and methods: dimensional and related measurements in the micro- and nanometer range, Wilkening G., Koenders L. eds., Wiley-VCH, 2005, pp. 60-72.

[Illers, 2010] H. Illers, N. Ishikawa, A. Saito, K. Hidaka, H.U. Danzebrink, “A high-resolution, self-sensing and self-actuated probe for micro and nano coordinate metrology and scanning force microscopy”, 10th International Conference of EUSPEN, 2010, Volume 1, pp. 63-66.

[ISO 10360] ISO 10360 - Geometrical Product Specifications (GPS) - Acceptance and reverification tests for coordinate measuring machine (CMM).

[ISO 10360-2, 2009] ISO 10360 part 2: 2009 Geometrical Product Specifications (GPS) - Acceptance and reverification tests for coordinate measuring machine (CMM) - Part 2: CMMs used for measuring size.

[ISO 12179, 2000] ISO 12179: 2000 Geometrical Product Specification (GPS) - Surface texture: Profile method - Calibration of contact (stylus) instruments.

[ISO 14253, 1998] ISO 14253:1998 Geometrical Product Specification (GPS) - Inspection by measurement of workpieces and measuring equipment.

[ISO 14253-2, 1998] ISO 14253 part 2:1998 - Geometrical Product Specifications (GPS) – Inspection by measurement of workpieces and measuring equipment – Part 2: Guide to the estimation of uncertainty in GPS measurement, in calibration of measuring equipment and in product verification.

[ISO 14638, 1995] ISO/TR 14638:1995 Geometrical Product Specification (GPS) - Masterplan.

[ISO 14660, 1999] ISO 14660:1999 Geometrical Product Specification (GPS) - Geometrical features.

[ISO 15530] ISO 15530 - Geometrical Product Specifications (GPS) - Coordinate Measuring Machine (CMM): techniques for determining the uncertainty of measurement.

[ISO 15530-3, 2004] ISO 15530 part 3: 2004 - Geometrical Product Specifications (GPS) - Coordinate Measuring Machine (CMM): techniques for determining the uncertainty of measurement – Part 3: Use of calibrated workpieces or standards.

[ISO 25178-701, 2010] ISO 25178 part 701:2010 - Geometrical Product Specifications (GPS) - Surface texture: areal - Part 701: calibration and measurement standards for contact (stylus) instruments.

[ISO 5436] ISO 5436 - Geometrical Product Specifications (GPS) - Surface texture: profile methods; measurement standards.

[ISO 5436-1, 2000] ISO 5436 part 1: 2000 Geometrical Product Specification (GPS) - Surface texture: Profile method - Measurements standards - Part 1 Material measures.

[Jaeger, 2002] G. Jaeger, E. Manske, T. Hausotte, W. Schott, “Operation and analysis of a Nanopositioning and nanomeasuring machine”, Proc. ASPE 17th annual meeting, 2002, pp. 299–304.

[Kak, 1988] A.C. Kak, M. Slaney, “Principles of computerized tomographic imaging, IEEE Press, 1988.

[Laurent, 1997] J. Laurent, M. Talbot, M. Doucet, “Road surface inspection using laser scanners adapted for the high precision 3D measurements of large flat surfaces”, Proceedings International Conference on Recent Advances in 3-D Digital Imaging and Modeling, 1997.

[Leach, 2010] R. Leach, “Fundamental principles of engineering nanometrology”, Elsevier, 2010.

[Leach, 2011] R. Leach, “Optical measurement of surface topography”, Springer, 2011.

[Marinello, 2008] F. Marinello, E. Savio, S. Carmignato, L. De Chiffre, “Calibration artefact for the microscale with high aspect ratio: The fiber gauge”, CIRP Annals - Manufacturing Technology, 2008, Volume 57, pp. 497-500.

[Marinello, 2009] F. Marinello, E. Savio, P. Bariani, S. Carmignato, “Coordinate metrology using scanning probe microscopes”, Measurement science and technology 20 084002, 2009.

[Microparticles, 2011] www.microparticles.de, 2011.

[Peggs, 1999] N.G. Peggs, A. J. Lewis, S. Oldfield, “Design for a compact high-accuracy CMM”, Annals of CIRP, 1999, Volume 48, pp.417-420.

[Peggs, 2002] N.G. Peggs, A. Yacoot, “A review of recent work in sub-nanometre displacement measurement using optical and x-ray Interferometry”, Phil. Trans. R. Soc. Lond. A, 2002, Volume 360, pp. 953-968.

[PTB, 2005] Calibration certificate - Micro-contour standard, reference number: PTB-05.4021640, 2005.

[Rai-Choudhury, 1997] P. Rai-Choudhury, “Handbook of microlithography, micromachining and microfabrication, Volume 1: Microlithography”, SPIE Optical Engineering Press, 1997.

[Ritter, 2004] M. Ritter, M. Hemmleb, O. Sinram, J. Albertz, H. Hohenberg, “A versatile 3D calibration object for various micro-range measurement methods”, XXth ISPRS Congress, 2004, Proceedings of Commission V, pp. 696-701.

[Ruijl, 2001] T. Ruijl, “Ultra Precision Coordinate Measuring Machine; Design, Calibration and Error Compensation”, PhD thesis, Delft University of Technology, 2001.

[Schobel, 2005] J. Schobel, E. Westkamper, “An approach to the development of tolerance systems for micro and nanotechnology”, Nanoscale calibration standards and methods: dimensional and related measurements in the micro- and nanometer range, 2005, pp. 230-240.

[Schwenke, 2001] H. Schwenke, F. Wäldele, C. Weiskirch, H. Kunzmann, “Opto-tactile sensor for 2D and 3D measurement of small structures on coordinate measuring machines”, Annals of CIRP, Volume 50, Issue 1, pp. 361–364.

[Schwenke, 2002] H. Schwenke, U. Neuschaefer-Rube, H. Kunzmann, T. Pfeifer, “Optical methods for dimensional metrology in production engineering”, Annals of CIRP, 2002, Volume 51, Issue 2, pp. 685-699.

[Seggelen, 2005] J.K.V. Seggelen, P.C.J.N. Rosielle, P.H.J. Schellekens, H.A.M. Spaan, R.H. Bergmans, G.J.W.L. Kotte, "An Elastically Guided Machine axis with nanometer Repeatability", Annals of the CIRP, 2005, Volume 54, Issue1, pp 487-490.

[Shiou, 2008] F.J. Shiou, Y.W. Deng, "Simultaneous flatness and surface roughness measurement of a plastic sheet using a fan-shaped laser beam scanning system", Key engineering materials, 2008, Volume 734, Issue 381, pp. 233.

[Tosello, 2009] G. Tosello, H.N. Hansen, S. Gasparin, "Applications of dimensional micro metrology to the product and process quality control in manufacturing of precision polymer micro components", Annals of the CIRP, 2009, Volume 58, Issue 1, pp. 467-472.

[Vermeulen, 1998] M.M.P.A. Vermeulen, P.C.J.N. Rosielle, P.H.J. Schellekens, "Design of a high-precision 3D-Coordinate Measuring Machine", Annals of the CIRP, 1998, Volume 47, Issue 1, pp. 447-450.

[Vermeulen, 1999] M.M.P.A. Vermeulen, "High-Precision 3D-Coordinate Measuring Machine", PhD Thesis, Eindhoven University of Technology1999.

[VIM, 2008] Joint Committee for Guides in Metrology (JCGM). JCGM 200:2008, International vocabulary of metrology - Basic and general concepts and associated terms, 2008, pp. i–xiv, 1–104.

[Weckenmann, 2000] A. Weckenmann, R. Ernst, "Studies on new tolerancing rules for micro- and nanotechnology", 1st EUSPEN Conference, 2000, Volume 1, pp. 214-221.

[Weckenmann, 2001] A. Weckenmann, R. Ernst, R. Hornfeck, "Tolerancing of micromechanical monolithic components", 2nd EUSPEN Conference, 2001, Volume 2, pp. 786-788.

[Weckenmann, 2004] A. Weckenmann, T. Estler, G. Peggs, D. McMurtry, "Probing systems in dimensional metrology", Annals of CIRP, Volume 53, Issue 2, 2004, pp. 657–684.

[Weckenmann, 2005] A. Weckenmann, Th. Wiedenhoefer, "The use of the GPS-standard in nanometrology", 5th Euspen conference, 2005, pp. 169-172.

[Weckenmann, 2007] A. Weckenmann, P. Kraemer, J. Hoffmann, "Manufacturing metrology - State of the art and prospects", 9th International symposium on measurement and quality control (9th ISMQC), mADRAS, 2007.

[Weckenmann, 2009] A. Weckenmann, P. Kramer, “Predetermination of measurement uncertainty in the application of computed tomography”, 11th CIRP Int. Conf. Computer Aided Tolerancing, 2009.

[Whitehouse, 2011] D.J. Whitehouse, “Handbook of Surface and Nanometrology”, CRC Press, Second Edition.

[Wilhelm, 2001] R. G., Wilhelm, R. Hockena, H. Schwenkeb, “Task specific uncertainty in coordinate metrology”, Annals of CIRP, 2001, Volume 50, Issue 2, pp 553-563.

[Wilkening, 2005] G. Wilkening, L. Koenders, “Nanoscales calibration standards and methods”, WILEY-VCH Verlag GmbH & Co. KGaA, 2005.

[Wilson, 1984] T. Wilson, “Theory and practice of scanning optical microscopy”, Academic Press, 1984.

[Wilson, 1990] T. Wilson, “Confocal microscopy”, Academic Press, 1990.

[Xu, 1998] B. Xu, D.F. Cuminato, N.M. Keyes, “Evaluating Fabric Smoothness Appearance with a Laser Profilometer”, Textile research journal, 1998, Volume 68, Issue 12, pp. 900-906.

3. Indirect micro/nano metrology based on replication

3.1 Introduction

New techniques for surface characterization are emerging. The need comes from difficulties in measurement or when the definition of new sound procedures are required [Lonardo, 2002]. For example, quality control of optical surface structures is a challenging task in terms of characterization using tactile or optical instruments. Tactile measuring machines could damage the surface, while optical ones could lead to wrong measurements due to bad reflections of the light. A way to overcome these challenges is to replicate the optical components through polymer casting methods using PDMS (polydimethylsiloxane) and epoxy (polyepoxide) resins.

The polymer casting technique is usually employed for surface quality control in two main areas [Hansen, 2011]:

1. Surface inspection (e.g. metallographical inspection);
2. Quantitative topographical measurements (e.g. surface roughness measurements).

This method has been used for different topography purposes and several examples can be found in literature:

- When there is risk of damaging the surface during its preparation for inspection (e.g. when polishing is needed on brittle glass surfaces [Mecholsky, 1992]);
- To study the effect of medical treatments on human skin [Efsen, 1995];
- In the medical field of dermatology in order to investigate the effect of repeated exposure to actinic radiation at high altitudes [Mazzarello, 2001];
- For machined parts as steel sheets, a cylinder line, a crankshaft and a face-ground surface [Nilsson, 2001];
- When the instrument (e.g. microscope) cannot be placed on the specimen to be inspected (e.g. in the case of dental wear characterization [Scott, 2006]);
- For studying biological structures [Koch, 2008];

- During the characterization of highly finished (e.g. optical) surfaces using tactile instruments such as roughness tester [Gasparin, 2011(1)];
- To reproduce roughness standard for optical instruments calibration. Optical instruments need to be calibrated on the same type of surface as the surface replica and this is achieved by producing soft replicas of the calibrated standards. Such standards are used to obtain traceable measurements on specimens having the similar surface characteristics [Gasparin, 2011(2)];
- For the characterization of a mould for polymer optics application mounted in an injection moulding machine [Tosello, 2012] and [Gasparin, 2012].

The replica casting technique is a fast and cost effective method that could also be used for producing reference artefacts. Usually the master geometries may be produced by electroformed nickel, e.g. [Rubert, 2011], wire-cut EDM, die-sinking EDM or diamond turning. In some cases, the surfaces have to be structured, e.g. by laser processing, to achieve metrologically suitable artefacts [PTB website, 2011]. During the 1990s a European funded research project called CALISURF was carried out in order to investigate capabilities of polymer replication technologies to produce low cost and reliable reference artefacts. The project focused on the development of different tools to enable their reliable use in an industrial environment. The project was successful from a technological point of view; however, polymer based surface roughness calibration standards are still not commercially available [Hansen, 2011].

This chapter presents several investigations on the replica method with the aim of:

1. Defining the replication degree;
2. Estimating the stability of the replica process;
3. Ensuring a traceable procedure.

The *replication degree* is closely linked to the type of specimen being replicated; therefore its definition is given according to the artefact used as master for the replica technique:

a. <u>Surface specimen</u>: typically described in terms of surface roughness parameters [Hansen, 2011]. In this case, the replication degree is defined as the ratio between the replica roughness and the standard ("*master*") roughness. For this study 2 artefacts for calibration purposes were taken into account (see Table 3.1):
   - A periodic roughness artefact with Ra equal to 500 nm;

   – A random roughness artefact with Ra equal to 500 nm.

b. Geometry specimen: typically characterized by well-defined geometries (e.g. grooves, holes, pillars, etc.). The replication degree is given as the ratio between the measured feature on the replica and the measured feature on the specimen ("*master*"). For this study two artefacts were taken into account (see Table 3.1):
   – A contour calibrated profile characterized by steps and grooves;
   – An optical component characterized by micro-pyramidal structures.

For all definitions it should be noted that the replication process involves a mirroring of the structure in such a way that an indent on the master is seen as a protrusion on the replicated part [Hansen, 2011].

The *stability* investigations were carried out in order to ensure reliability of the replicas over different periods of time. The selected specimens were (see Table 3.1):

a. Surface specimen: a periodic roughness standard with Ra equal to 500 nm;
b. Geometry specimen: one mould used for the injection moulding of Fresnel lenses.

SPECIMENS USED AS MASTER		**INVESTIGATIONS**		
		Replication degree	Stability	Traceable procedure
Surface specimens (*Paragraph 3.3*)	Calibration standards	Roughness standards: • Periodic profile, Ra equal to 500 nm • Random profile, Ra equal to 500 nm	Roughness standard: • Periodic profile, Ra 500 nm	Roughness standard: • Random profile, Ra equal to 200 nm
Geometries specimens (*Paragraph 3.4*)	Calibration standards	• Contour profile		• Step height standard
	Product	• Optical component	• Fresnel lenses	

Table 3.1 – Specimens used as master for the replica casting investigations of this chapter.

Finally, the chapter proposes a new procedure for the *traceability of the replica method*. According to GUM [GUM, 2008], the measuring equipment has to be calibrated through the measurements on a calibrated standard in order to obtain traceable results of a workpiece, see Figure 3.1a. If the replica casting technique is used, the new proposed procedure is to replicate the standard artefact and measure both: standard and replica. The reason is that the measuring instrument needs to be calibrated on the same type of the surface replica. In this way a traceable procedure is achieved. Afterwards, the workpiece can be replicated and the replica itself is measured in order to characterize the workpiece, see Figure 3.1b.

For this purposes the investigated artefacts were (see Table 3.1):

a. Surface specimen: a random roughness standard with Ra equal to 200 nm;
b. Geometry specimen: a height calibration artefact.

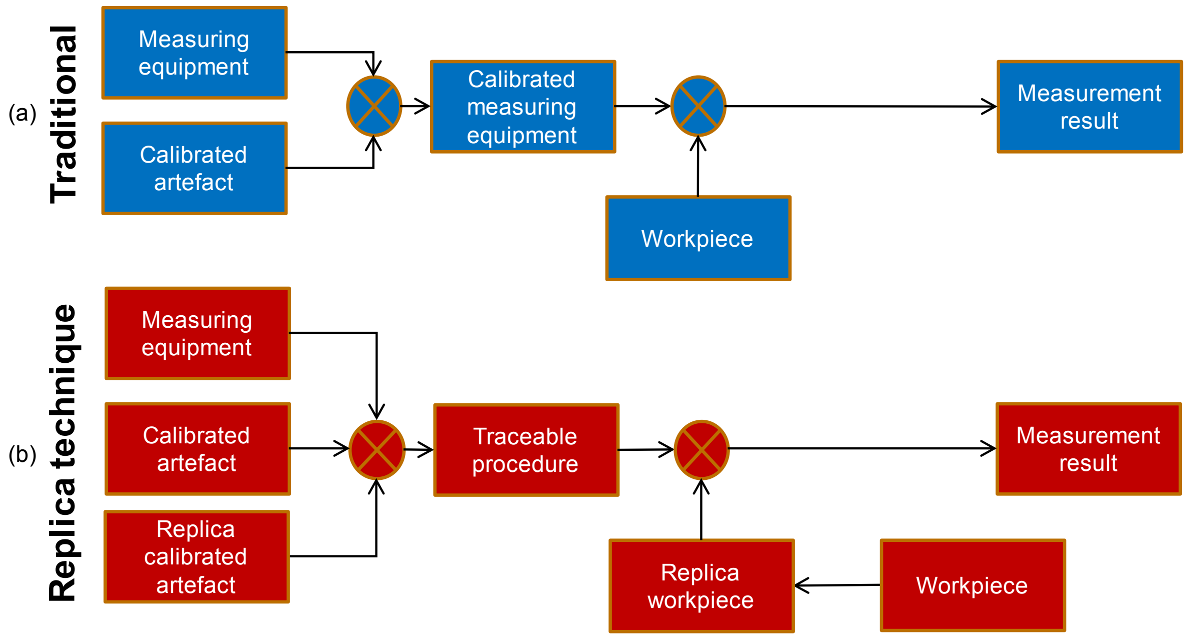

Figure 3.1 – In blue (a): traditional approach, according to [GUM, 2008]; in red (b): the traceability approach proposed in this chapter for the replica casting technique.

3.2 Replication technique

The replica casting technique was performed using a compound supplied in cartridges containing both the polymer and the curing agent, which were automatically mixed in a disposable static-mixing nozzle, see Figure 3.2. During the replica process the nozzle-end of the gun was pointed downwards as close as possible to the surface in order to avoid trapping air in the replica and to force the material into the surface features. Another way of avoiding air trapping was to manually spread a little amount of compound on the surface. Afterward a load was applied and the compound was left drying for the curing time suggested by the manufacturer. At the end the replica was removed carefully.

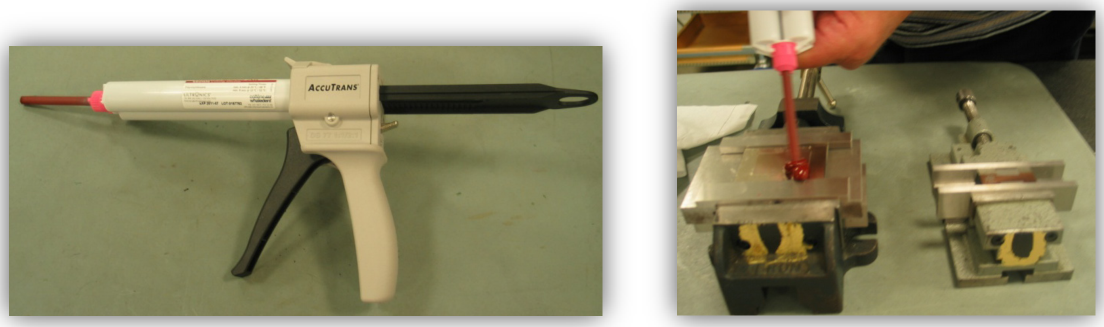

Figure 3.2 – Left: dispensing gun and cartridge; right: application of the compound on the surface.

Three different compounds were used for the replica investigation:

1. LuxaBite: mainly made by acrylic resin, glass powder and silica. The compound is hard (Barcol hardness = 25 after 1 hour), characterized by a blue colour (Figure 3.3). The application time is 4 minutes at 20°C. It is mainly used for medical purposes as human teeth replication [LuxaBite].
2. RepliSet: a two-part silicone rubber compound. It is a soft material with a grey colour (Figure 3.3). The application time is 20 min at 20°C. It is used in case of flexible high-resolution replica of 3D structures for comparator macroscopy or metrology [RepliSet].
3. AccuTrans Casting Silicone: a low-viscosity compound used for producing accurate impressions on smooth, textured or rough surfaces. It is a soft material with a red colour (Figure 3.3). The application time is 10 minutes at 20°C. It is mainly used for forensic investigation [AccuTrans].

The blue material (LuxaBite) and its stability were previously investigated for dimensions in the 2 - 4 mm range. Optical measurements of grooves and pitches were compared with tactile measurements. Results demonstrated a good stability of the replicated artefact over a period of eight months [De Chiffre, 2009] and [Cantatore, 2010].

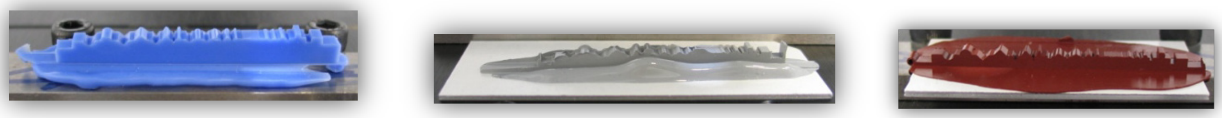

Figure 3.3 – The three different compounds used for the replica technique investigation. The same specimen was replicated with: LuxaBite (*blue*) on the left; RepliSet (*grey*) in the centre; AccuTrans Casting Silicone (*red*) on the right.

3.3 Surface replication

For the surface replica investigation, five specimens were chosen for three studies:

1. *Replication degree study*: 2 roughness artefacts were selected: one with a periodic profile and one with a random profile, both characterized by a nominal Ra equal to 500 nm (*Paragraph 3.3.1.1*). The two artefacts were chosen with the same roughness in order to see if the different nature of the surface texture could have any influence on the replica results. At the same time, the aim was to evaluate the replication degree of the three replica materials described in the previous paragraph. Results showed that no difference was seen as a function of the type of roughness profile and that the most suitable material for the replication study was the soft red compound;
2. *Stability case study*: since no difference was observed as function of the roughness profile, the selected artefact for the present investigation was a roughness standard characterized by a periodic profile and a nominal Ra of 500 nm (*Paragraph 3.3.1.2*). Results showed a good replica stability of the red soft compound;
3. *Traceable procedure*: the traceable procedure was investigated using one roughness artefact characterized by a random profile and a nominal Ra equal to 200 nm (*Paragraph 3.3.1.3*).

Table 3.2 summarizes the investigations and the used abbreviations.

Investigations	Surface specimens – Calibration standard (*Abbreviation*)	Compound	Paragraph
Replication degree	Roughness standards: 1. Periodic profile, Ra equal to 500 nm (*P1165*)	• LuxaBite (*Blue*) • RepliSet (*Grey*) • AccuTrans Casting Silicone (*Red*)	3.3.1.1
	Roughness standards: 2. Random profile, Ra equal to 500 nm (*PTB625*)	• LuxaBite (*Blue*) • RepliSet (*Grey*) • AccuTrans Casting Silicone (*Red*)	
Stability	Roughness standard: 3. Periodic profile, Ra 500 nm (*IF500*)	• AccuTrans Casting Silicone (*Red*)	3.3.1.2
Traceable procedure	Roughness standards: 4. Random profile, Ra equal to 200 nm (*PTB619*)	• AccuTrans Casting Silicone (*Red*)	3.3.1.3

Table 3.2 – Investigations carried out for the surface specimens. The abbreviations used in the paragraph 3.3 are underlined and written in italic.

3.3.1 Surface calibration standard artefact replication

Two roughness artefacts were used for the *replication degree* case study: P1165 and PTB625. For surface specimens typically described in terms of surface roughness parameters, the replication degree was defined as the ratio between the replica roughness and the standard roughness (e.g. *Sa,replica/Sa,reference•100*).

P1165 presents a periodic sinusoidal profile with a Ra equal to 504 ± 13 nm (expanded uncertainty, k = 2, confidence level = 95%) [P1165, 2006], see Figure 3.4a.

PTB625 has a random profile repeated every 4 mm with a Ra equal to 481 ± 12 nm (expanded uncertainty, k = 2, confidence level=95%) [PTB 625, 2001], see Figure 3.4b.

(a)

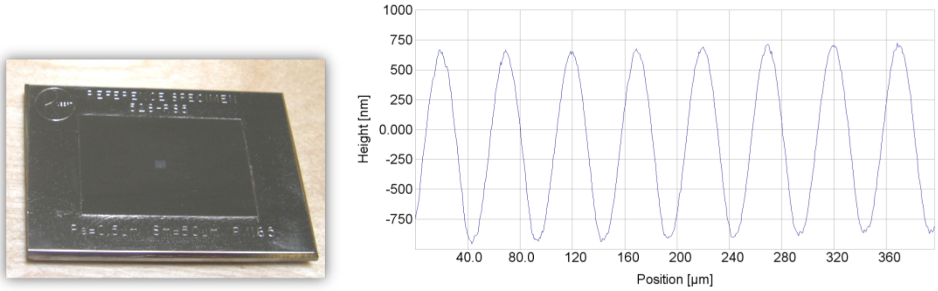

(b)

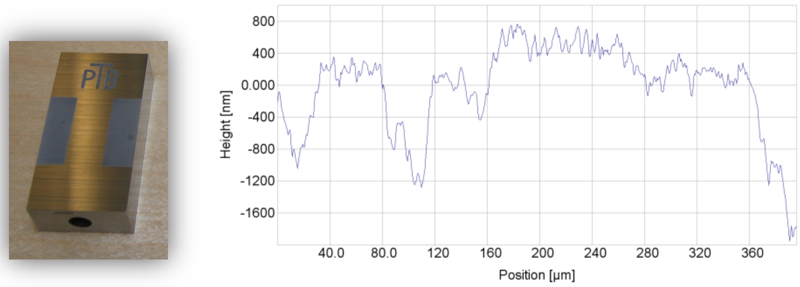

Figure 3.4 - (a) Roughness standard with a periodic triangular profile (P1165); (b) Roughness standard with a random profile (PTB 625).

These two artefacts were replicated using the three different compounds described in paragraph 3.2 in order to evaluate the replication degree of the three replica materials.

The two reference standards and the corresponding two blue replicas were measured using the contact profilometer described in appendix 11.1.1. The two grey and two red replicas are soft; therefore they were measured using the InfiniteFocus instrument described in appendix 11.1.5. In both cases 3D measurements of 300 x 300 μm^2 have been carried out in 5 defined spots of the specimens chosen in order to cover different zones of the measuring area. In each area, 5 equally distributed profiles were taken into account for the measurement analysis, see Table 3.3.

P1165 – PTB625	Measuring instrument	Measurement set-up	Analysis set-up
Standard	Contact profilometer	• 5 Areas: 300 x 300 μm^2	5 profiles for each area: • Profile alignment
Blue replica	Contact profilometer	• 5 Areas: 300 x 300 μm^2	5 profiles for each area: • Profile alignment
Grey replica	InfiniteFocus	• Lens: 50x • 5 Areas: 286 x 218μm^2 • *z*-res: 50 nm	5 profiles for each area: • Profile alignment
Red replica	InfiniteFocus	• Lens: 50x • 5 Areas: 286 x 218μm^2 • *z*-res: 50 nm	5 profiles for each area: • Profile alignment

Table 3.3 – Replication degree study: measurement and analysis set-up for the roughness artefacts P1165, PTB625 and their replicas.

For the *stability* investigation the selected roughness artefact was IF500. It was developed by Alicona Imaging GmbH with the aim of verifying roughness measurements performed using an InfiniteFocus instrument. The specimen is characterized by an etched region which allows both optical and stylus measurements, see Figure 3.5.

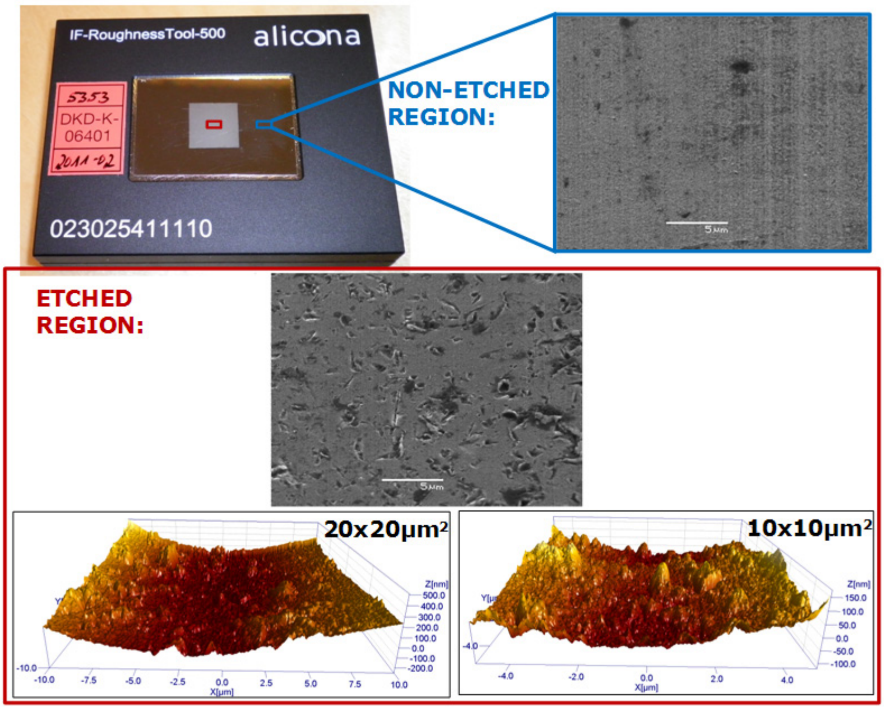

Figure 3.5 - SEM and AFM measurements on the etched and non-etched region of the roughness tool IF500.

The profile is periodic, see Figure 3.6, with a Ra equal to 503 ± 35 nm (expanded uncertainty, k = 2, confidence level = 95%) [IF500, 2011].

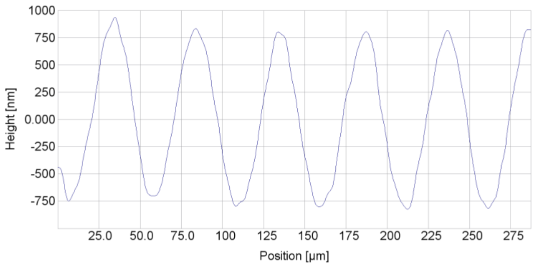

Figure 3.6 - Profile of the roughness standard IF500 measured with the InfiniteFocus instrument.

IF500 was replicated using the red-soft compound described in paragraph 3.2 in order to evaluate the long term stability during a period of 28 days. The measurements were carried out in the spot defined in the certificate [IF500, 2011] using the instrument InfiniteFocus described in appendix 11.1.5. The measurements were performed using the area and the stitching technique in different days, see Table 3.4.

IF500	Measurement set-up of the InfiniteFocus	N° days of measurements	Repeatability	Evaluated roughness parameters
Standard	*Area (50x lens)*: 286µm x 218 µm *z*-res: 20 nm	5	5 consecutive measurements without repositioning the sample	Sa
	Stitching: 1.55 mm x 220 µm *z*-res: 20 nm	10		Ra
Red replica	*Area (50x lens)*: 286µm x 218 µm *z*-res: 20 nm	28	5 consecutive measurements without repositioning the sample	Sa
	Stitching: 1.55 mm x 220 µm *z*-res: 20 nm			Ra

Table 3.4 – Stability study: measurement and analysis set-up for the artefact IF500 and its replica.

The last selected artefact, PTB619, has a random profile repeated every 4 mm with a Ra equal to 207 ± 9 nm (expanded uncertainty, k = 2, confidence level = 95%) [PTB 619, 2003], see Figure 3.7. The investigation was carried out in collaboration with the national measurement institute NPL (National Physical Laboratory, UK) in October 2011. This specimen was replicated 5 times using the red-soft compound described in paragraph 3.2 in order to investigate and document a *traceable measuring procedure*.

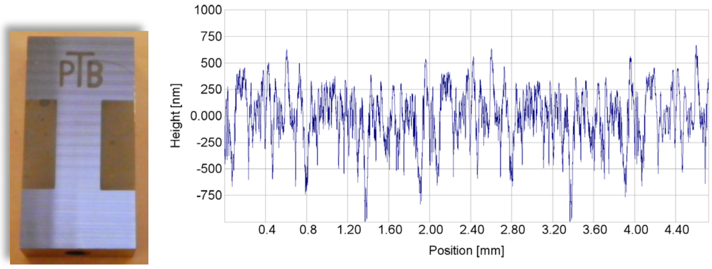

Figure 3.7 - Roughness standard with a random profile [PTB 619, 2003].

Measurements and analysis set-up for the roughness artefact PTB619 are shown in Table 3.5. The standard was measured using a contact profilometer from Taylor Hobson [PGI, 2011]: 5 profiles were traced in the centre of the measuring area of the specimen and a profile analysis was carried out. The standard was also measured using an InfiniteFocus, as the one described in appendix 11.1.5, and a confocal microscope from Olympus [LEXT, 2011]. The 5 red replicas were measured using the two optical instruments to avoid damages on the polymer surface. The optical measurements were carried out in 5 defined spots of the specimens chosen in order to cover different zones of the measuring area. An area analysis was performed and, in the same area of the contact measurements, 5 equally distributed profiles were taken into account for a profile analysis.

PTB619	Measuring instrument	Measurement set-up	Analysis set-up
Standard	Contact profilometer	• 5 profiles, length =4mm	Profile analysis: • Profile alignment • λs = 2.5μm, λc = 500μm
	InfiniteFocus	• Lens: 20x, *z*-res: 50 nm • 5 Areas: 715 x 544 μm^2	5 profiles for each area and area analysis: • Profile alignment • λs = 2.5μm, λc = 500μm
	Confocal	• Lens: 20x, *z*-res: 10 nm • 5 Areas: 64 x 64 μm^2	
5 Red replicas	InfiniteFocus	• Lens: 20x, *z*-res: 50 nm • 5 Areas: 715 x 544 μm^2	5 profiles for each area and area analysis: • Profile alignment • λs = 2.5μm, λc = 500μm
	Confocal	• Lens: 20x, *z*-res: 10 nm • 5 Areas: 64 x 64 μm^2	

Table 3.5 – Traceable procedure: measurement and analysis set-up for the artefact PTB619 and its replicas.

3.3.1.1 Replication degree results

P1165 and PTB625 were used as masters in order to evaluate the replication degree of three replica compounds: blue (hard), grey and red (soft).

The analysis was carried out evaluating:

- *Sa*: areal roughness parameter chosen because it is an arithmetic average parameter;
- *Rpk, Rk, Rvk*: functional roughness parameters chosen because they consider respectively the peaks, the core and the valleys of a profile [ISO 13565-2, 1996].
- *Power spectrum investigation*: to quantify the discrepancy between two profiles as an alternative to the direct comparison of the roughness values;
- *Uncertainty budget*.

For all definitions it should be noted that the replication process involves a mirroring of the structure in such a way that an indent on the master is seen as a protrusion on the replicated part [Hansen, 2011]. Please note that in all the investigations the replica profiles were inverted before starting the analyses.

The parameter Sa for the two roughness reference standards and their replicas was analyzed. The results are shown in Figure 3.8.

The replication degree (*Sa,replica/Sa,reference•100*) achieved was 95% to 96%. As a consequence, the resulting deviations with their standard deviations fell inside the uncertainty range of the reference standard (29 nm for P1165 and 57 nm for PTB625).

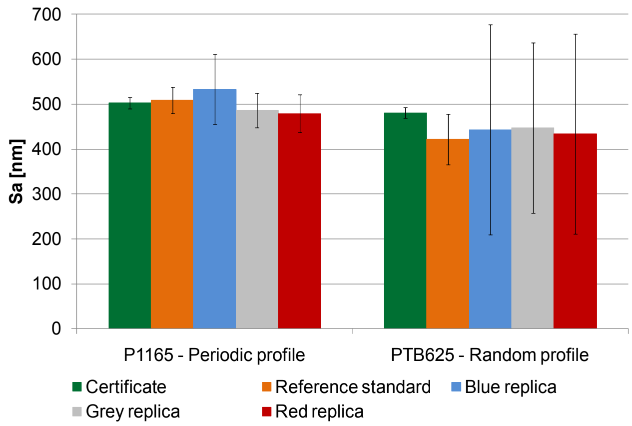

Figure 3.8 - Sa values obtained from the periodic (P1165) and the random (PTB625) profile carried out using different instruments [Gasparin, 2011(2)].

The parameters related to the Abbott curve (Rpk, Rk and Rvk) were analyzed on the replicas and compared with the reference standards values. Considering the results of the soft replicas (i.e. grey and red) for the periodic standard P1165 (see Figure 3.9a), a good replication of the core of the profile was achieved and proved by the parameter Rk. According to ISO 13565 part 2 [ISO 13565-2, 1996], Rk is the core roughness depth: the roughness profile excluding the protruding peaks and deep valleys. On the other hand, the results for the hard replica (i.e. blue) showed an average deviation of 250 nm from the Rk reference standard value. This was due to the blue replica material characteristic to have limited replication performance, especially in following the profile slopes. For the parameter Rvk (*reduced valleys depth*, i.e. *the average depth of the profile valleys projecting through the roughness core profile*) and Rpk (*reduced peak height*, i.e. *the average height of the protruding peaks above the roughness core profile*), deviations of approximately 200 nm from the reference values were obtained for all three materials. This led to the conclusion that both hard (i.e. blue) and soft (i.e. grey and red) materials had difficulties to fill completely the valleys of the profile, giving as output a smaller depth of the valleys (i.e. *Rvk,replica<Rvk,reference*) and also to replicate the peaks, as indicated by the Rpk parameter (i.e. *Rpk,replica>Rpk,reference*, even if the peaks were replicated correctly, as it is shown in Figure 3.10a). These effects changed the final region of the Abbott curve and therefore it modified the slope of the secant whose gradient was used for the calculation of Rpk, Rk and Rvk parameters (Figure 3.10b).

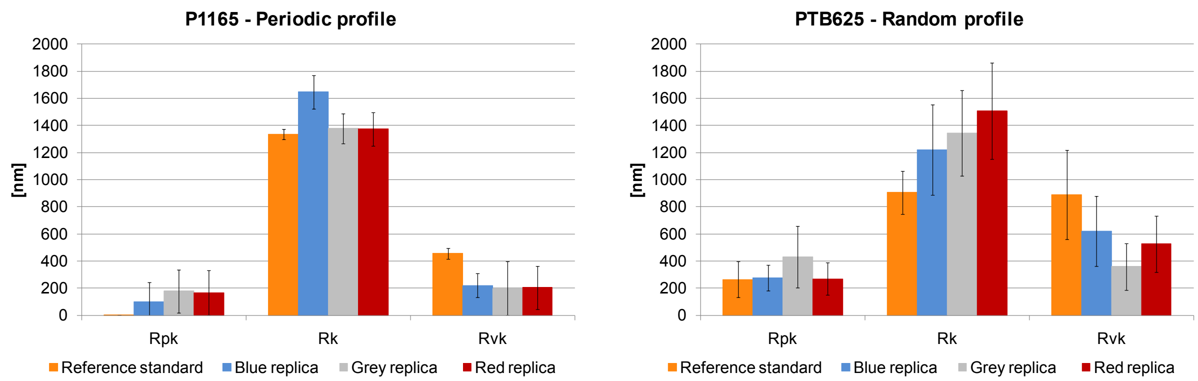

(a) (b)

Figure 3.9 - Rpk, Rk and Rvk values obtained from the periodic (P1165) and the random (PTB625) profile carried out using different instruments [Gasparin, 2011(2)].

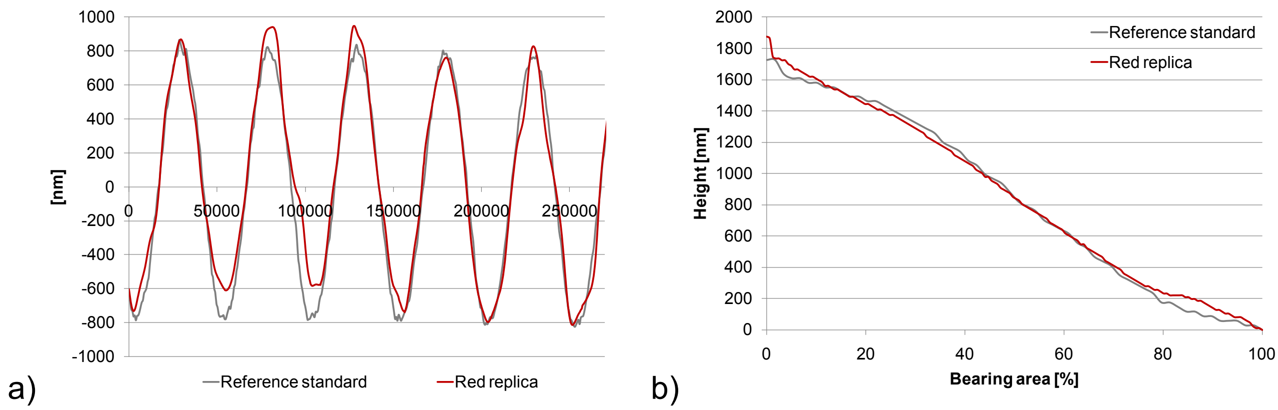

Figure 3.10 - Poor replication of the profile valleys which led to a larger final region on the Abbott curve [Gasparin, 2011(2)].

Considering the results of the soft replicas (i.e. grey and red) for the standard with a random profile PTB625 (see Figure 3.9b), the core of the profile (i.e. Rk parameter) seemed to be poorly replicated. However, large standard deviations were observed in all measurements. This was due to the fact that the sampling length (300 µm) was much shorter than the actual pitch of the random profile (4 mm), clearly causing a relatively large relocation error. In fact, since five different areas were measured on the specimens' surfaces, different regions of the profile were considered and therefore different values were obtained.

The power spectrum was estimated for the two standards and their replicas using the Fast Fourier Transform algorithm (FFT). As in [George, 1979] and [Narayanasamy, 1979], the power spectrum can be used to quantify the discrepancy between two profiles as an alternative to the direct comparison of the roughness values [Gasparin, 2008].
Figure 3.11 shows the power spectrum of the periodic standard P1165 and its replicas of 5 different profiles (P1, ... , P5) in a defined area "*A*". The same is illustrated for the random specimens PTB625 in Figure 3.12. It was chosen to show the spectrum of only one area since there was no difference in results between the spectrums of the 5 measured areas.

The periodic profile of the standard P1165 is a sine wave, characterized by a wavelength of 50 µm; therefore in its power spectrum it was expected to find a unique peak at the wavelength of 50 µm. Looking at the spectrums of Figure 3.11, the peak of the standard and its replicas is at the wavelength of 50 µm. This means that all the three replicas presented the principal characteristic of the master. The only difference was in its amplitude. Moreover the short wavelengths show the noise of the instrument. In the spectrums the short wavelengths were more well-defined in the standard and in the blue replica. On the other hand, for longer wavelengths there were several smaller peaks which were smoother in the soft replicas (i.e. grey and red).

Regarding these observations, it is important to underline that the standard artefact and the blue replica were measured using a contact profilometer, while the grey and the red replica were measured using an optical instrument. The difference in the short and long wavelengths could be due to the use of the different instruments. Moreover the colour wavelength of the replica material, grey and red, was not influencing the optical measurements since no difference in the grey and red spectrum was observed.

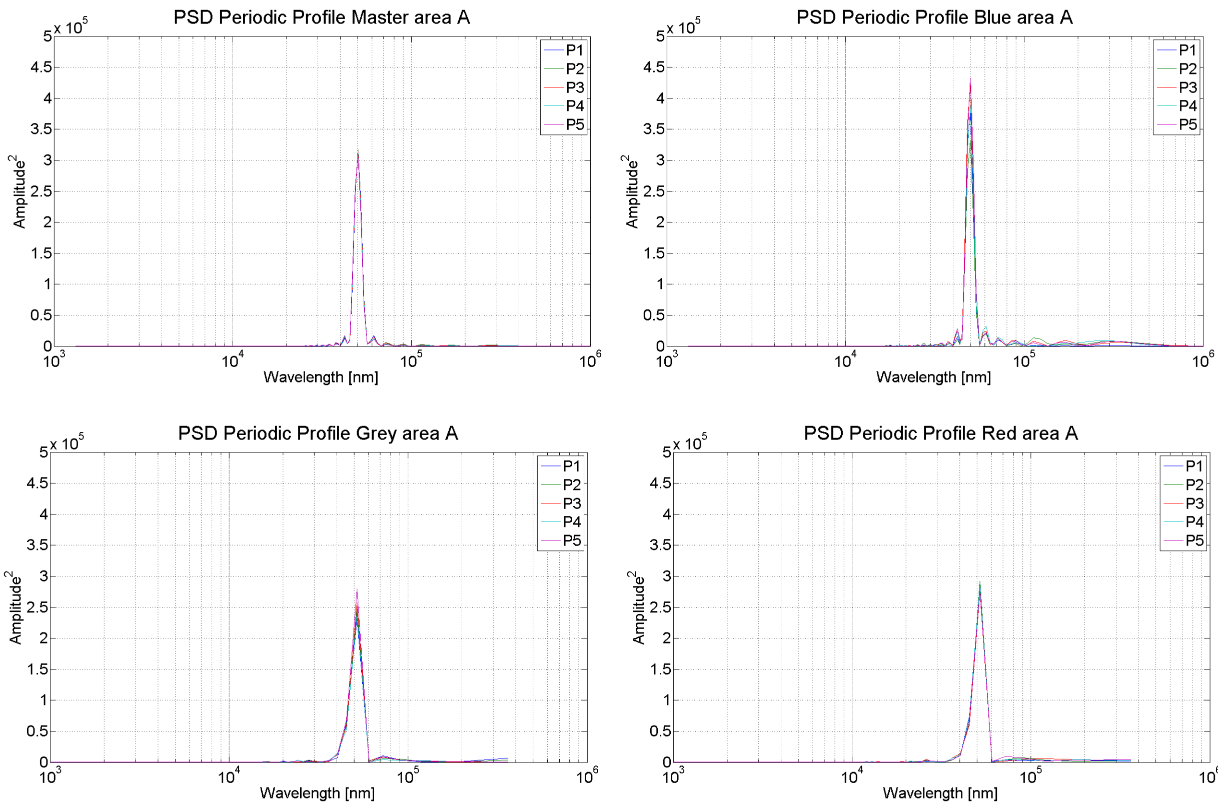

Figure 3.11 – Power spectrum of 5 different profiles (P1, ..., P5) for the periodic standard P1165 and its replicas: blue, grey and red in a defined area “*A*”.

The standard PTB625 is characterized by a random profile which is repeated every 4 mm. If a profile is perfectly random, the spectrum is expected to be characterized by a line with the same amplitude for all the wavelengths. Since the measurements were taken in a length of 300 µm, the single profiles could be considered random, but not perfectly random. In fact looking at the power spectrums in Figure 3.12, several peaks are present, but no one can be identified as the dominant peak and the overall shape of the replicas is similar to the master one. For this observation, it is important to underline that, as in the previous case, the standard and the blue replica were measured using a contact profilometer, while the grey and the red replica were measured using an optical instrument. Again no difference was observed between the grey and red spectrum and therefore there was no influence of the colour wavelength on the optical measurements.

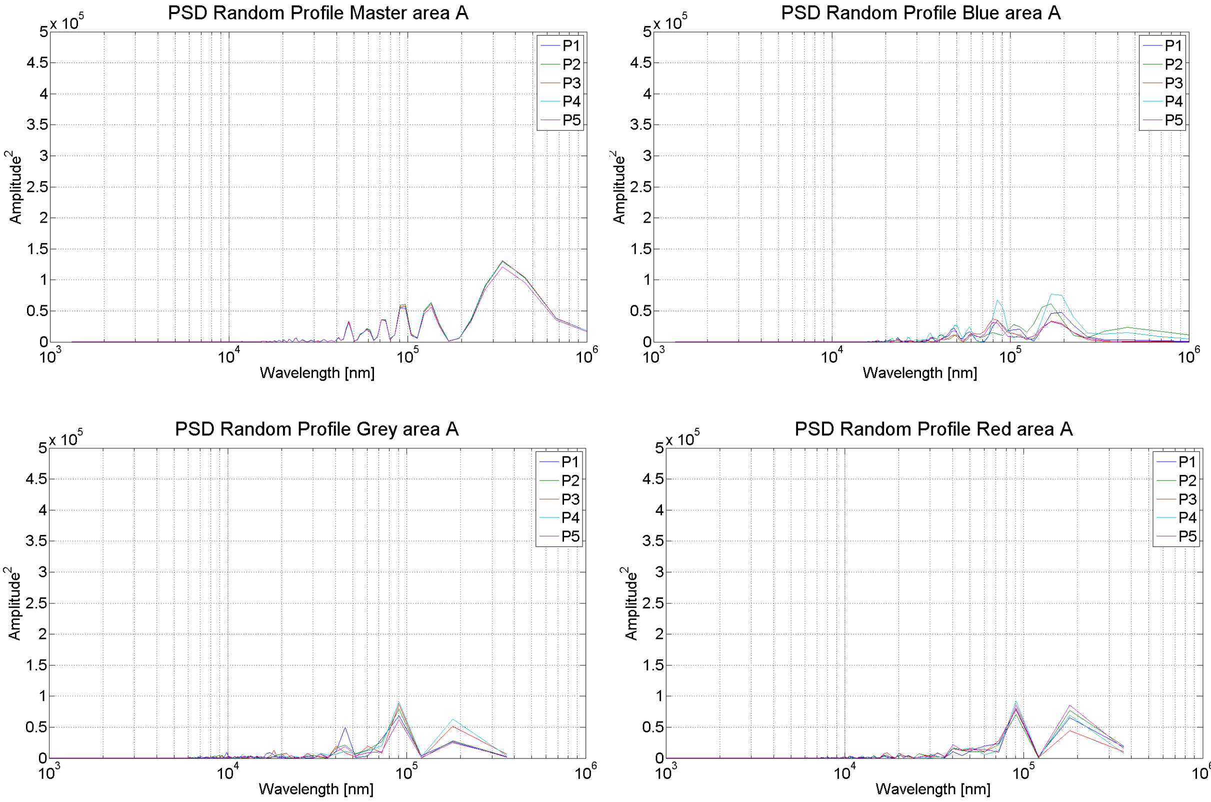

Figure 3.12 - Power spectrum of 5 different profiles (P1, ..., P5) for the random standard PTB625 and its replicas: blue, grey and red in a defined area "*A*".

The uncertainty budget of the roughness measurements on P1165 and on PTB625 was estimated following GUM [GUM, 2008] and the results are summarized in Table 3.7. The expanded uncertainty was calculated with a confidence level of 95% (k = 2) considering four contributors (see equations (3.1, 3.2)) among the following:

- u_{cal} = calibration uncertainty given by the calibration certificate if the measurements are performed using the tactile instrument (on the reference standard and on the blue replica). In case of optical instruments (on the grey and on the red replica), the calibration values were given by the uncertainty calculated from measurements carried out on the reference specimen and on the replicas using an atomic force microscope;

- u_{res} = resolution uncertainty equal to the *z*-vertical resolution applied during the optical measurements;
- u_{instr} = resolution uncertainty of the contact profilometer;
- u_{rep} = repeatability of the measuring process equal to the standard deviation of the measurements on five defined areas of the specimens.

$$U_{contact} = k \cdot \sqrt{u_{cal}^2 + u_{instr}^2 + u_{rep}^2} \qquad (3.1)$$

$$U_{optical} = k \cdot \sqrt{u_{cal}^2 + u_{res}^2 + u_{rep}^2} \qquad (3.2)$$

In the uncertainty budget the effect of the temperature was not taken into account. The reason was that the standard artefacts and their replicas were kept in a clean environment with a constant temperature of 20 ± 1°C for the entire investigation. The deviation of 1°C from the reference temperature (20°C) led to a contribution in the range of 10^{-6} µm (see Table 3.6) and therefore it could be considered negligible.

Material	**α [$10^{-6}K^{-1}$]**	**L [µm]**	**ΔT [°C]**	**u_w [µm]**
Blue (*Luxabite*)	94[a]	0.23 -1000	1	$2.0 \cdot 10^{-6}$ – $9.0 \cdot 10^{-2}$
Grey/red (*Silicone rubber*)	8.1[b]			$1.8 \cdot 10^{-6}$ – $1.0 \cdot 10^{-2}$

Table 3.6 – Temperature related standard uncertainty (u_w) for the roughness and the dimensional measurements covered in this chapter ([a] [DeChiffre, 2009]; [b] [Matbase, 2011]).

Looking at the results for P1165, larger uncertainties were obtained for the blue replica, mainly due to the low repeatability of the measurements. Summing up, the hard material (i.e. blue) was less suitable for roughness replication, confirmed also by the replication degree which was in the order of 95%. The uncertainties obtained for the other specimens proved that the optical measurements were adequate: the roughness random artefact could be verified even if the measurements were focussed only on a measuring range of

300 μm instead of 4 mm (length defined in ISO 4288 [ISO 4288, 1996]). This explained the considerable uncertainties which came from the measurements performed in 5 different areas of the random profile specimen.

Sa [nm]	**P1165 - Periodic profile**				**PTB625 - Random profile**			
	Reference	Blue	Grey	Red	Reference	Blue	Grey	Red
U (k=2)	29	78	38	43	57	234	190	223

Table 3.7 - Standard uncertainty contributors for the roughness measurements on the periodic P1165 and random PTB625 artefacts [Gasparin, 2011(2)].

As conclusion, for both case studies the most suitable material for replication was the soft one (i.e. grey and red) due to its high replication fidelity on every kind of surface. On the other hand its soft nature does not permit contact measurements. The hard material is useful for verification using profilometers or contact instruments as CMM, however the replication technique is more difficult and time consuming. For these reasons, the following surface investigations consider replicas made using the soft compound, in particular the red one. This choice is also recommended by the manufacturer of the InfiniteFocus as the most suitable material for the instrument [IFM, 2009].

3.3.1.2 Stability results

The specimen IF500 was used as master for the investigation on the red replica stability. Both the master and the replica were measured using the InfiniteFocus described in appendix 11.1.5 and the measurements were analyzed using three different approaches:

1. *Sa-area*: a well defined area of 286 x 218 μm^2 (matching the field of view of the 50x lens) was studied and characterized by evaluating the Sa roughness parameter;
2. *Sa-stitching*: a well defined image field, made by 6 of the previous areas, was studied and characterized by evaluating the Sa roughness parameter;
3. *Ra-stitching*: a well defined image field, the same of the previous point, was studied and characterized by evaluating the Ra roughness parameter, according to the calibration certificate of the standard [IF500, 2011].

A first investigation was performed in order to estimate the repeatability and the stability of the three approaches previously described. The involved specimen was the standard artefact. For the repeatability evaluation, the specimen was measured 5 times without repositioning. The results are shown in Figure 3.13.

For the stability evaluation, the standard artefact was measured in 5 and 10 different days. The results are shown respectively in Figure 3.14 and Figure 3.15.

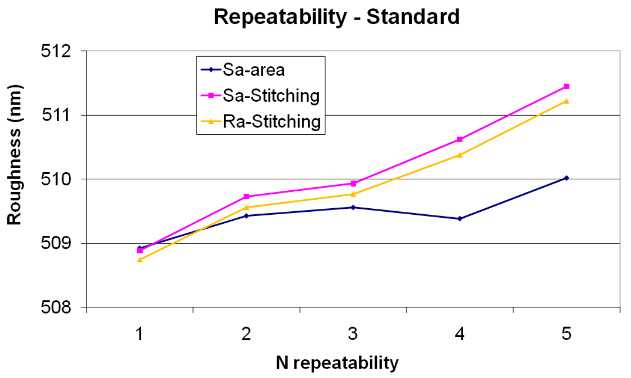

Figure 3.13 - 5 consecutive measurements on IF500 without repositioning the specimen.

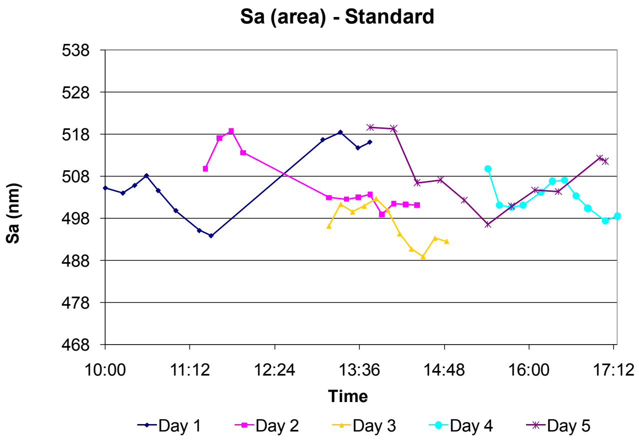

Figure 3.14 - Measurements performed in the IF500 at different times on 5 different days and using the approach *Sa-area*. *Sa-stitching* and *Ra-stitching* have same results.

From the analysis, the conclusions drawn are:

- 5 nm of measurement variation were observed between the two stitching approaches results and the area method results during periods of time shorter than 2 hours, see Figure 3.13;
- 15 nm of measurement variation was seen between different periods of time. During these periods, the sample was not removed from the measuring instrument and the InfiniteFocus was left on with light off, see Figure 3.14;

– *Sa-area* approach presented greater variations than *Sa-stitching* and *Ra-stitching* since it was covering a smaller area, see Figure 3.15. It should also be noted that *Sa-area* was affected by the repositioning of the measuring table after every single capture.

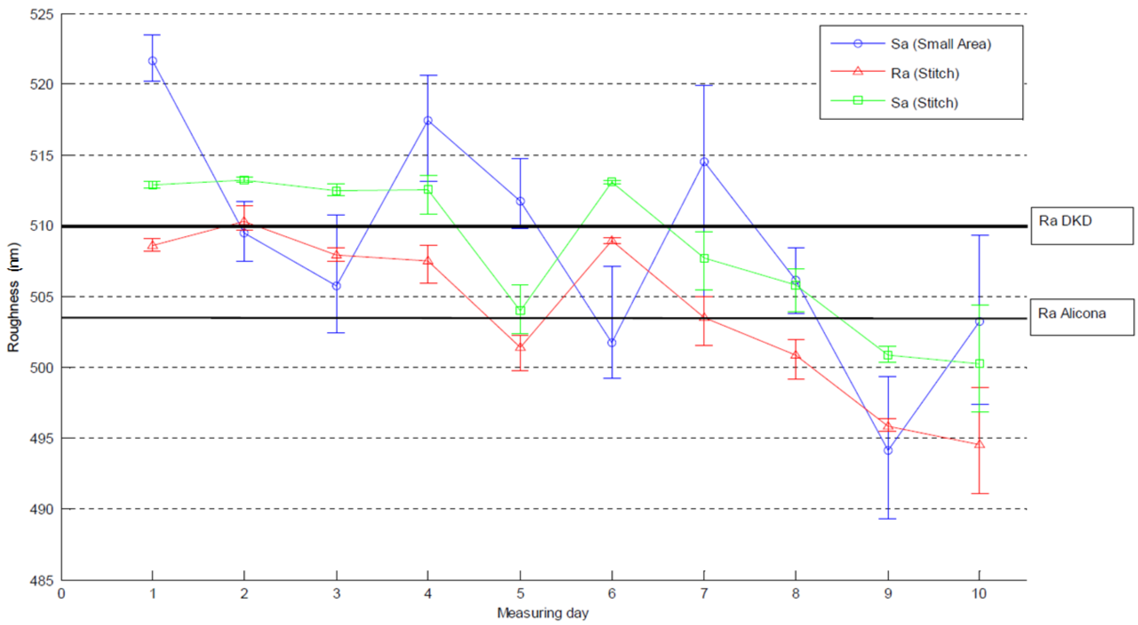

Figure 3.15 - Measurements performed in the IF500 on 10 different days and using 3 different approaches (*Sa-area*, *Sa-stitching*, *Ra-stitching*). *Ra DKD* is the Ra value given from a DKD certificate [IF500, 2011]. *Ra Alicona* is the Ra value given from the Alicona certificate [IF500, 2011].

A second investigation concerns the measurements repeatability and the long term stability of the red-soft replica made from the IF500 specimen.

For the repeatability evaluation, 5 measurements were carried out without repositioning the replica. The results are shown in Table 3.8. The approaches were repeatable inside a range of 2 nm; but the difference between their values was equal to 14 nm.

[nm]	Ra (Stitch)	Sa (Stitch)	Sa (Area)
Average	494	500	507
Standard deviation	0.40	0.28	0.28

Table 3.8 – Results of 5 consecutive measurements obtained without repositioning the IF500 replica.

The long term replica stability was estimated during a period of 28 days. The results are shown in Figure 3.16. The standard deviation of the measurements was in the order of 10 nm, whereas the measurement range was around 30 nm which corresponded to 2 - 6% of the average measured value. The replica revealed to be stable if kept in a clean environment with a constant temperature of 20°C.

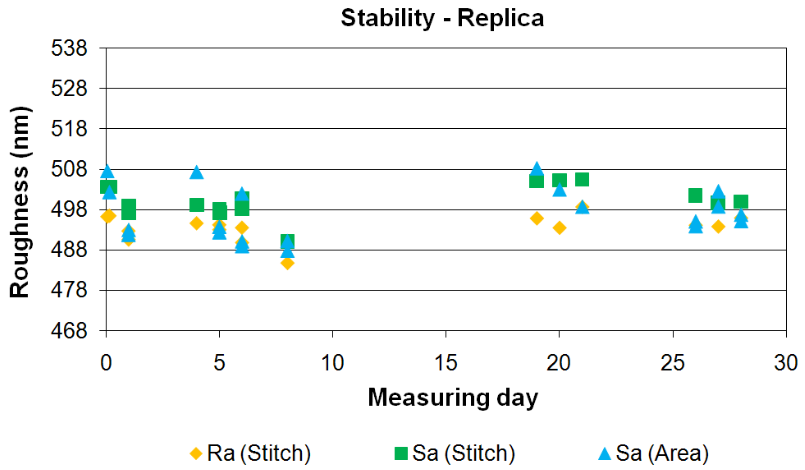

[nm]	Ra (Stitch)	Sa (Stitch)	Sa (Area)
Average	497	503	499
Standard deviation	9.4	8.5	8.0
Range	33.5	30.7	31.2

Figure 3.16 - Long term stability of the IF500 replica during a period of 28 days.

3.3.1.3 Traceable procedure

The specimen PTB619 was chosen as master in order to define a traceable measuring procedure of its 5 replicas.

The traceable measuring procedure was established following three steps:

1. The centre spot of the measuring area was measured on the standard using a traceable stylus profilometer. A 2D analysis was carried out and 4 roughness parameters were calculated: Ra, Rpk, Rk and Rvk ("*Traditional*", blue boxes of Figure 3.17);
2. The same well defined spot was measured on the standard and on the replicas using an optical instrument. A 2D analysis was carried out and 4 roughness parameters were calculated: Ra, Rpk, Rk and Rvk ("*Replica*", green boxes of Figure 3.17);
3. The optical results were compared with the contact ones in order to estimate the uncertainty of the optical measurements ("*Traceable procedure*", red boxes of Figure 3.17).

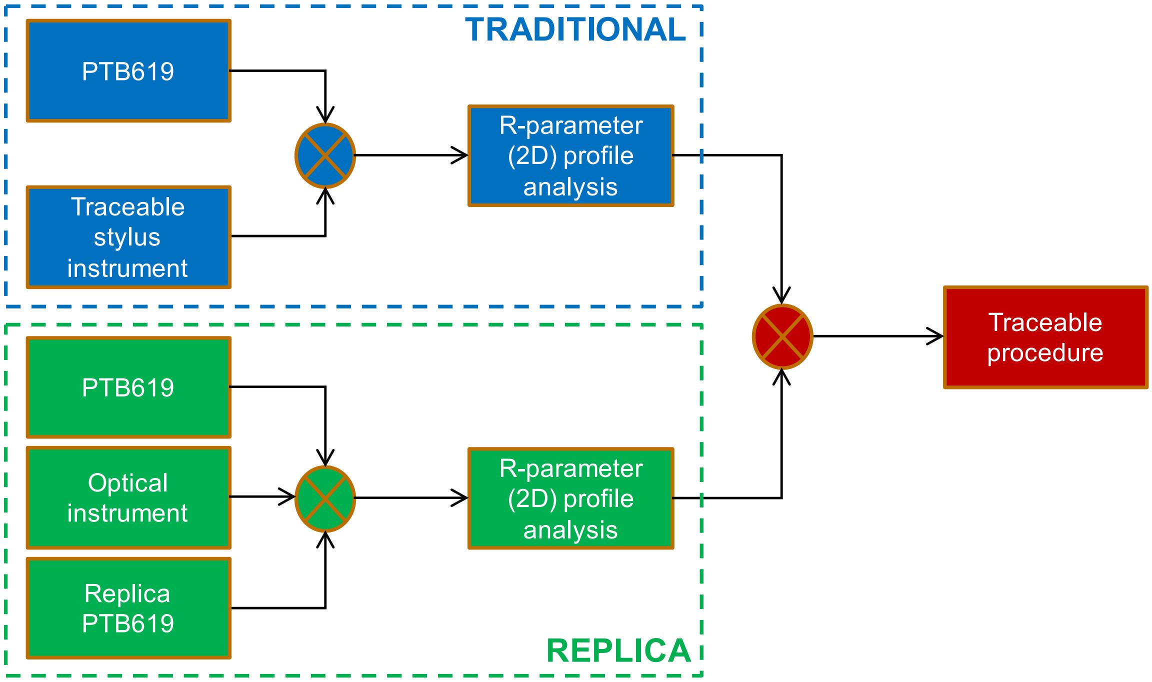

Figure 3.17 - Traceable measuring procedure for the PTB619 replicas.

The results of Ra, Rpk, Rk and Rvk parameters are shown in Figure 3.18. As listed in Table 3.5, two optical instruments were used: an InfiniteFocus instrument and a confocal microscope. Please note that the replica profiles were inverted before starting the analysis.

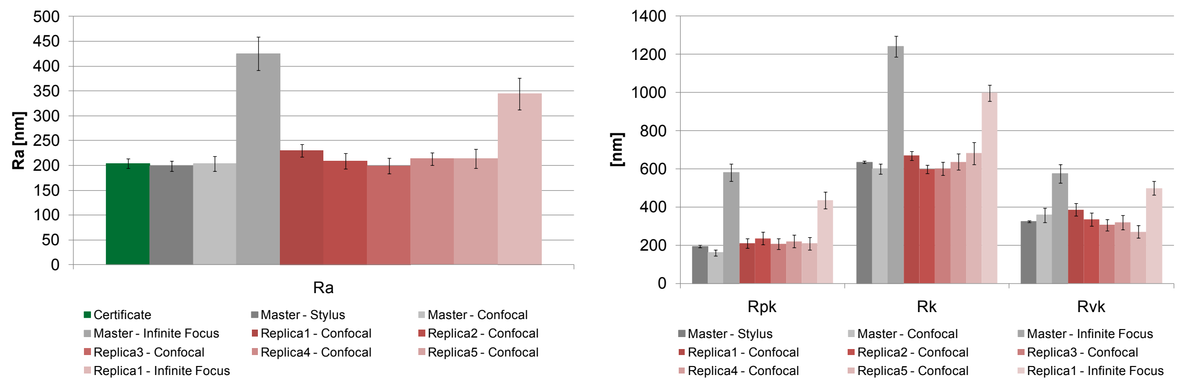

Figure 3.18 – Ra, Rpk, Rk and Rvk parameters for the standard PTB619 (*master*) and its 5 replicas obtained using a stylus profilometer (*Stylus*), an InfiniteFocus instrument (*InfiniteFocus*) and a Confocal microscope (*Confocal*).

Comparing the standard artefact results achieved using the contact and the optical instruments it was found out that the larger deviation was obtained using the InfiniteFocus instrument. The achieved difference was more than 200 nm, which meant that the results were 50% larger than the certificate value (207 nm). This significant variation was due to the standard artefact characteristics which are not suitable for the working principle of the instrument. The areas between the peaks and the valleys of the standard are too smooth for FocusVariation; the surface has to exhibit local contrast in order to get reasonable measurements [IFM, 2009]. The profiles from the contact measurement (a) and from the optical measurement (b) are shown in Figure 3.19. The optical profile is undoubtedly rougher than the contact one.

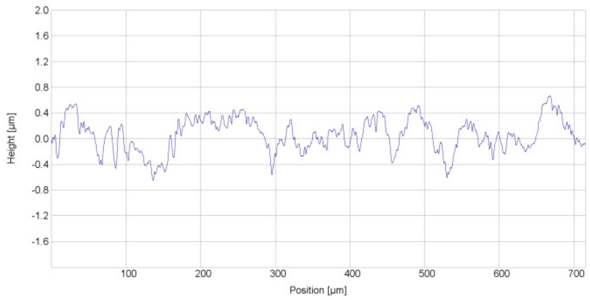

(a)

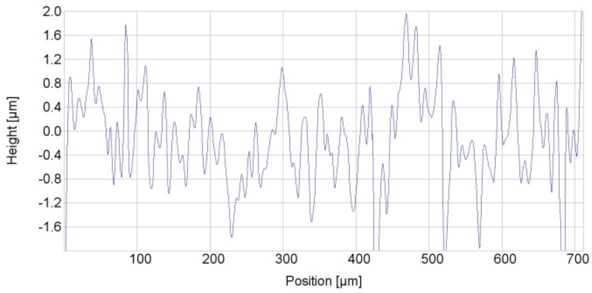

(b)

Figure 3.19 – Profiles of the standard artefact PTB619 measured using a stylus profilometer (a) and an InfiniteFocus instrument (b).

The same conclusions can be drawn for the optical results of the red-soft replica: a considerable deviation in the range of 100 nm was achieved. The replica variation (100 nm) was smaller than the standard variation (200 nm) because the characteristic of the replica itself, i.e. its red colour and the silicon material, created a pattern on the surface suitable for optical measurements.

As conclusion the results were not acceptable, therefore the optical measurements from the InfiniteFocus instrument were not considered anymore in the investigation. Further comments with the word "*optical*" are related to the confocal instrument.

The roughness results obtained using the confocal instrument on the standard differed 10 - 30 nm from the contact values. The same results were achieved for the 5 replicas, which showed also a repeatability of the replica process within 10 nm. Larger variations were instead obtained for the parameters Rk and Rvk. As it was discussed in paragraph 3.3.1.1, it was related to some difficulties of the material in filling completely the valleys of the profile. This led to have as output a smaller depth of the valleys (i.e.

Rvk,replica<Rvk,reference). These effects changed the final region of the Abbott curve and therefore it modified the slope of the secant whose gradient was used for the calculation of Rpk, Rk and Rvk.

The power spectrum was calculated for the standard and its 5 replicas as in the replication degree case study, paragraph 3.3.1.1.

Figure 3.20 shows the power spectrum of the standard measured using a stylus profilometer in a defined area "*C1*". The standard PTB619 is characterized by a random profile which is repeated every 4 mm. Since the measurements were taken in a length of 700 µm, the single profiles could be considered random. If a profile is perfectly random, as explained in paragraph 3.3.1.1, the spectrum is expected to be characterized by a line with the same amplitude for all the wavelengths. The spectrum of the standard presented several peaks of a relatively small amplitude spread between wavelengths from 50 µm to 500 µm. Before and after such limits the spectrum had negligible power. These observations could be related to several phenomena:

- The specimen is not a "natural" artefact but it was made by grinding [Halle, 2011]. This means that the mechanical process itself could filter the signal of the profile and limited the "randomness" of the profile;
- The single profiles were filtered using a Gaussian filter λs equal to 2.5 µm and a Gaussian filter λc equal to 500 µm. These filters had, therefore, "created" a new profile which was not random any more by nature.

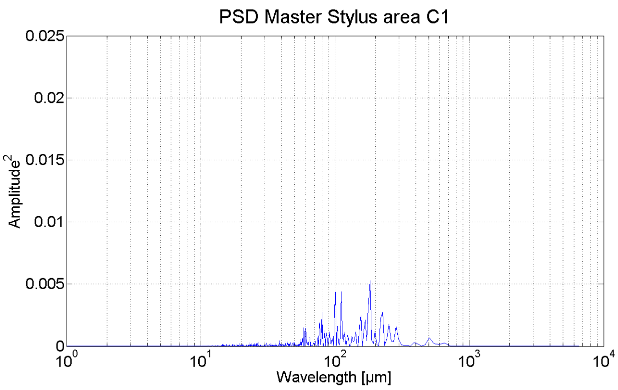

Figure 3.20 - Power spectrum of the standard PTB619 measured using a stylus profilometer in a defined area "*C1*".

Figure 3.21 shows the power spectrum of the standard and its 5 replicas measured using a confocal instrument in a well defined area "*C1*".

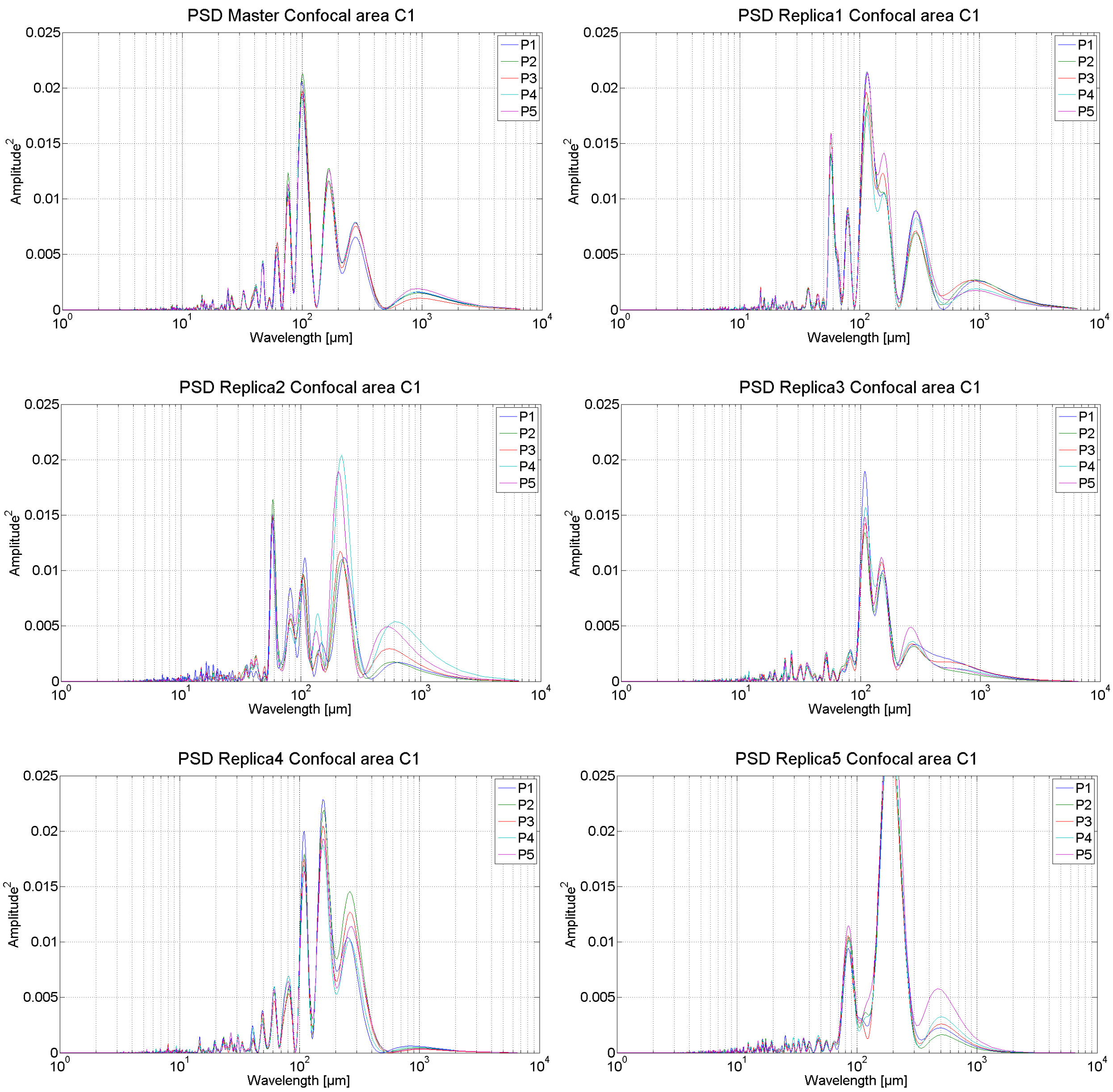

Figure 3.21 - Power spectrum of the standard PTB619, "*Master*", and its 5 replicas measured using a confocal instrument in a defined area "*C1*" in 5 different profiles (P1, ..., P5).

Looking at the power spectrums of the optical measurements, the bandwidth was still between 50 µm and 500 µm, but the amplitude of the signal was 5 times larger than the one obtained from the contact measurements. The difference was most probably related to the measuring technique: the optical instrument characterized the artefact as having a larger "energy" on its signal.

In both the artefact and its replicas the spectrum was limited by the same bandwidth and presented 3 well defined peaks. The amplitudes of the replicas peaks were distant, in average, 11 µm from the amplitudes of the master peaks. This led to the conclusion that the fundamental characteristic of the specimen was well replicated according to the optical measurements. Moreover the replica process was stable: the 3 peaks were visible in all 5 replicas and, at the same time, the bandwidth could be easily identified.

The uncertainty budget of the roughness measurements on PTB619 and its replicas was estimated following GUM [GUM, 2008] and the results are summarized in Table 3.9. The expanded uncertainty was calculated with a confidence level of 95% (k = 2) considering three contributors (see equations (3.3, 3.4)) among the following:

- u_{cal} = calibration uncertainty given from the calibration certificate [PTB619, 2003];
- u_{res} = resolution uncertainty equal to the *z*-vertical resolution applied during the optical measurements;
- u_{instr} = resolution uncertainty of the contact profilometer;
- u_{rep} = repeatability of the measuring process equal to the standard deviation of the measurements on five defined areas of the specimens.

$$U_{contact} = k \cdot \sqrt{u_{cal}^2 + u_{instr}^2 + u_{rep}^2} \qquad (3.3)$$

$$U_{optical} = k \cdot \sqrt{u_{contact}^2 + u_{res}^2 + u_{rep}^2} \qquad (3.4)$$

In this case the uncertainty of the contact instrument, $u_{contact}$, was considered as contributor of the uncertainty of the optical instrument, $U_{optical}$, instead of u_{cal}. The reason is that u_{cal} was defined applying a Gaussian filter λc equal to 800 µm; while the actual measurements were analyzed applying a λc equal to 500 µm. Therefore the contact instrument results were considered as reference.

In the uncertainty budget the effect of the temperature was not taken into account. The reason was that the standard artefacts and their replicas were kept in a clean environment with a constant temperature of 20 ± 1°C for the entire investigation. The deviation of 1°C

from the reference temperature (20°C) led to a contribution in the range of 10^{-6} µm (see Table 3.6) and therefore it could be considered negligible.
The obtained uncertainties were in average equal to 12 nm, a value comparable to the uncertainty of the calibration certificate, which is equal to 9 nm.

Ra [nm]	**Standard**		**Optical**				
	Contact	Optical	Replica 1	Replica 2	Replica 3	Replica 4	Replica 5
U (k=2)	10	15	12	16	16	13	19

Table 3.9 - Standard uncertainty contributors for the roughness measurements on the standard PTB619 and its 5 replicas measured with a contact profilometer ("*Contact*") and a Confocal instrument ("*Optical*").

This investigation showed that it is possible to ensure a traceable procedure for a replica casting method. In particular if the replica technique is applied for surfaces characterized by a Ra equal to 200 nm, the process is repeatable within 10 nm and the measurement uncertainty is in the range of 12 nm for confocal measurements.

Once the traceability of the replica procedure was ensured, the 2D analysis was compared with a 3D analysis: the optical profile roughness parameters were compared with the optical areal roughness parameters, as it is shown in Figure 3.22.
It is important to underline that the profiles taken into account in the previous investigation were extracted from the area, called "*C*", considered also in the present study.

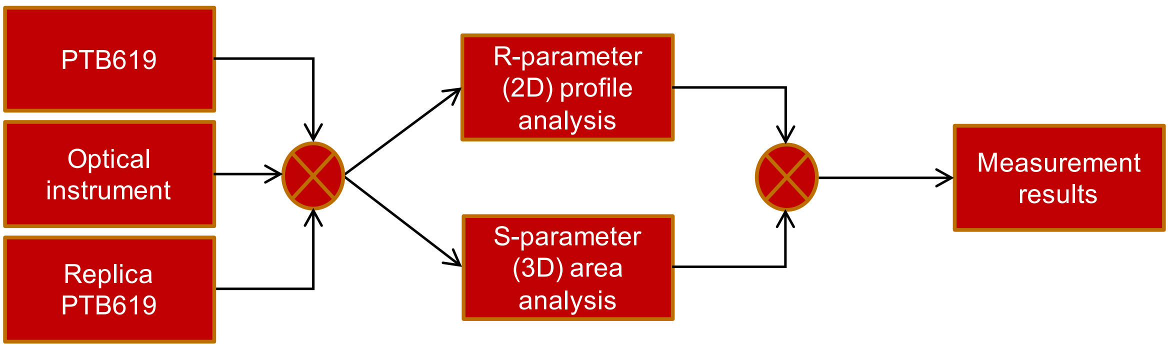

Figure 3.22 – 3D analysis compared with the traceable 2D analysis of PTB619.

The roughness results are shown in Figure 3.23. The difference between the profile and the areal parameters was, in average, equal to 10 nm. In general, the 3D values presented larger results compared to the 2D values. The reason was that the calculation of the areal parameters involved the entire measured area; while the calculation of the profile parameters involved the single extracted profile.

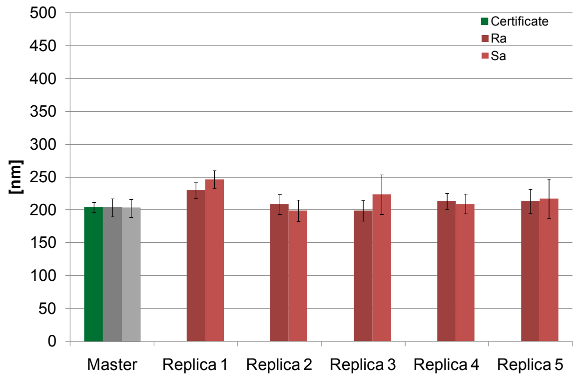

Figure 3.23 – Comparison between the profile roughness parameter Ra with the areal roughness parameters Sa. The profiles taken into account for the 2D analysis were extracted from the area interested in the 3D analysis. The results were obtained measuring the standard, “*Master*”, and its 5 replicas using a confocal instrument.

Finally, the 3D results obtained in the “*C*” area were compared with the 3D results obtained in other 4 well defined areas, “*A*”, “*B*”, “*D*” and “*E*”. The results are shown in Figure 3.24. It is shown that the repeatability of the replica process was approximately 10 - 15 nm. Moreover the deviation between the master values and the optical values did not exceed 20 nm. Note that replica 2 in area “*A*” and replica 3 in area “*B*” were affected by deformation and therefore larger variations were detected.

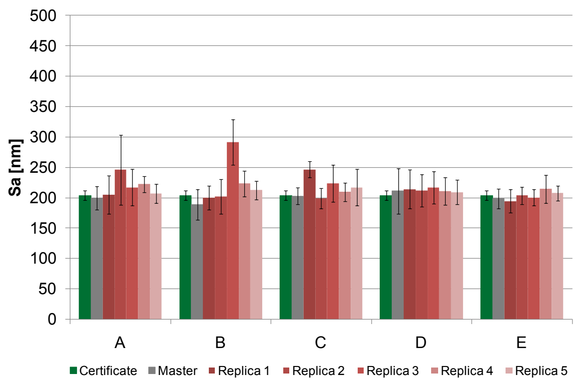

Figure 3.24 - Comparison of the roughness parameters Sa between 5 different areas: “*A*”, “*B*”, “*C*”, “*D*” and “*E*”. The results were obtained measuring the standard, “*Master*”, and its 5 replicas using a confocal instrument.

3.4 Geometries replication

For the geometries replica investigation, four specimens were chosen for three studies:

1. *Replication degree study*: one contour profile was investigated in order to evaluate the replication degree of the replica materials described in paragraph 3.2. The specimen was chosen because of the grooves which cover a range of 250 µm – 1000 µm (*Paragraph 3.4.1.1*). Results showed that the most suitable material for replication is the soft red compound. The replica process was also applied in a real optical component in order to compare the achieved results (*Paragraph 3.4.2.1*);
2. *Stability study*: a mould for injection moulding of Fresnel lenses was selected for the stability study of the red soft compound (*Paragraph 3.4.2.2*). Results showed a good replica stability;
3. *Traceable procedure*: The traceable procedure was investigated using a step height artefact characterized by grooves of 0.2 µm – 10 µm (*Paragraph 3.4.1.2*).

Table 3.10 summarizes the different investigations and shows the abbreviations used in the present section.

Investigations	Geometrical specimens – Calibration standard (*Abbreviation*)	Compound	Paragraph
Replication degree	Calibration standards: 1. Contour profile (*Contour profile*)	• LuxaBite (*Blue*) • RepliSet (*Grey*) • AccuTrans Casting Silicone (*Red*)	3.4.1.1
Traceable procedure	Calibration standards: 2. Step height standard (*TypeA2*)	• AccuTrans Casting Silicone (*Red*)	3.4.1.2
Investigations	**Geometrical specimens - Product**	**Compound**	**Paragraph**
Replication degree	3. Optical component (*Optical component*)	• LuxaBite (*Blue*)	3.4.2.1
Stability	4. Fresnel lenses (*Fresnel lenses*)	• AccuTrans Casting Silicone (*Red*)	3.4.2.2

Table 3.10 – Investigations carried out for the geometries replica investigation. The abbreviations used in the paragraph 3.4 are underlined and written in italic.

3.4.1 Geometries calibration standard artefact replication

The first standard artefact chosen for the *replication degree* study is a contour profile developed by PTB [PTB, 2005] characterized by several different geometries, such as cylinders, wedges, height steps or grooves, see Figure 3.25. For the geometry specimens, typically characterized by well-defined geometries (e.g. grooves, holes, pillars, etc.), the replication degree was defined as ratio between the measured feature on the replica and the measured feature on the specimen.

The investigated section is underlined by the red circle in Figure 3.25. The section is characterized by 6 regions: 3 steps (S2, S4, S6) and 3 grooves (S1, S3, S5) with nominal vertical dimensions of 250 µm, 500 µm, 1000 µm and an uncertainty equal to 0.75 µm (expanded uncertainty, k = 2, confidence level = 95%).

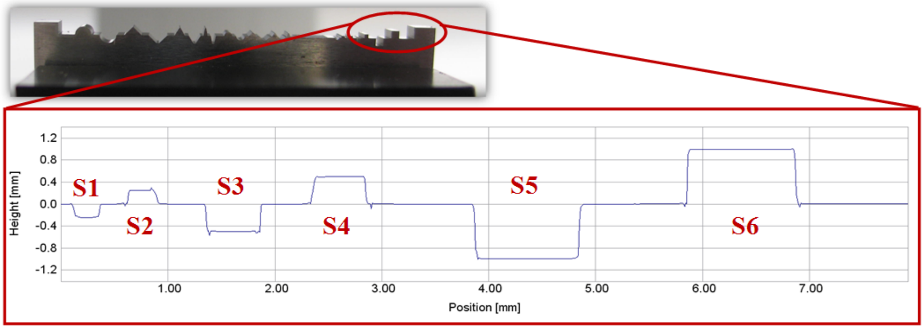

Figure 3.25 – PTB Contour profile. The red circle highlights the profile section where the investigation is focusing [Gasparin, 2011(2)].

The artefact was replicated using the three different compounds described in paragraph 3.2 in order to evaluate the replication degree of the three replica materials. The 6 regions of the specimens were measured five times using the InfiniteFocus instrument described in appendix 11.1.5 and analyzed following ISO 5436 [ISO 5436], see Table 3.11.

Contour profile	Measuring instruments	Measurement set-up	Analysis set-up
Standard Blue Replica Grey Replica Red Replica	InfiniteFocus	• Lens: 5x • Stitching • *z*-res: 2 µm	• Profile analysis following ISO 5436 [ISO 5436]

Table 3.11 – Replication degree study: measurement and analysis set-up for the contour profile and its replicas.

The second selected standard is a Type A2 artefact characterized by 6 grooves, see Figure 3.26, with step heights (expanded uncertainty, k = 2, confidence level = 95%) [Halle, 2004] equal to:

Groove 1: 0.230 ± 0.029 µm;

Groove 2: 0.464 ± 0.030 µm;

Groove 3: 1.173 ± 0.030 µm;

Groove 4: 2.571 ± 0.032 µm;

Groove 5: 5.603 ± 0.038 µm;

Groove 6: 9.263 ± 0.048 µm.

The investigation was carried out in collaboration with the national measurement institute NPL (National Physical Laboratory, UK) in October 2011. 5 red replicas were made with the aim of ensuring a *traceable measuring procedure*.

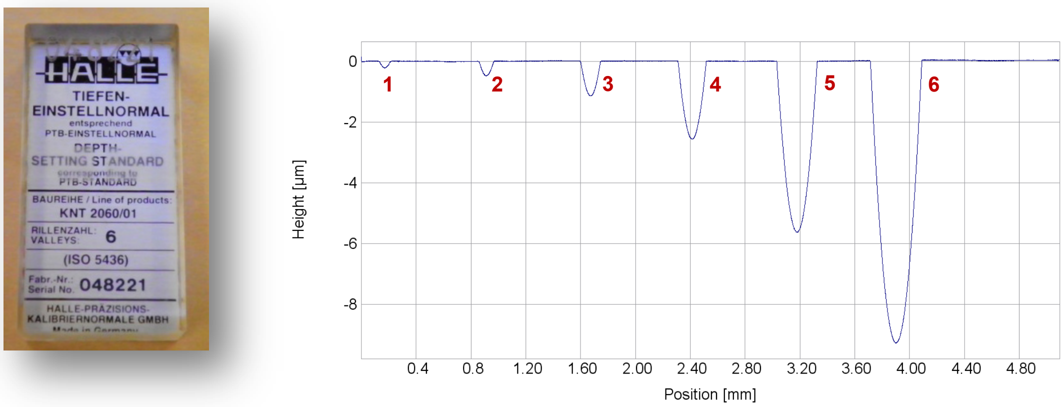

Figure 3.26 – 6 grooves of the TypeA2 standard.

The measurements and analysis set-up are summarized in Table 3.12.

The standard was measured using a contact profilometer from Taylor Hobson [PGI, 2011]: 5 profiles were traced along the measuring area according to [Halle, 2004]. Both the standard and the replicas were measured using a whitelight interferometer from Taylor Hobson [CCI, 2011]. The results were calculated taking into account 5 profiles distributed over the measuring area.

TypeA2	Measuring instrument	Measurement set-up	Analysis set-up
Standard	Contact profilometer	• 5 profiles, length =5mm	• Profile analysis following ISO 5436 [ISO 5436]
	Whitelight interferometer	• Lens: 50x/20x • z-res: 0.1 nm	• Profile analysis following ISO 5436 [ISO 5436]
5 Red replicas	Whitelight interferometer	• Lens: 50x/20x • z-res: 0.1 nm	• Profile analysis following ISO 5436 [ISO 5436]

Table 3.12 – Traceable procedure: measurement and analysis set-up for the TypeA2 artefact and its replicas.

3.4.1.1 Replication degree results

The results for the contour profile artefact and its replica are shown in Figure 3.27.

The replication degree achieved was different from material to material: for the blue-hard replica it was approximately 91%; for the grey-soft replica 92% and for the red-soft replica 99%. Moreover it seemed that using the blue and the grey material, the valleys and the grooves were shallow compared to the reference ones. The most suitable material for geometry replication was again the soft one (i.e. grey and red), even if promising results were obtained with the hard compound (i.e. blue).

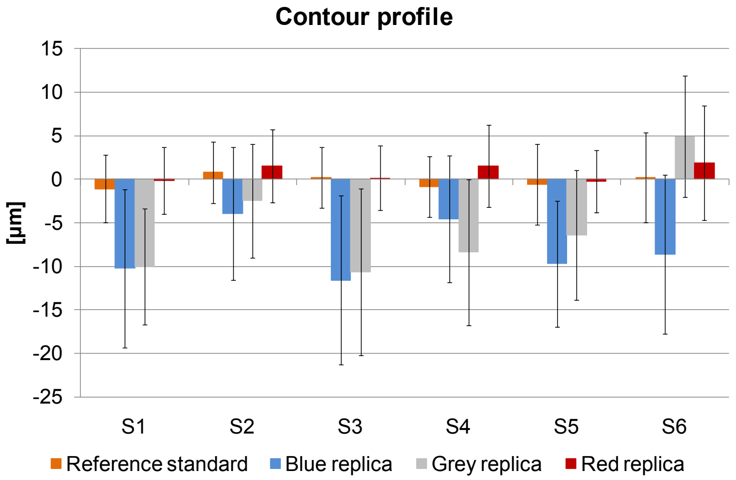

Figure 3.27 - Deviation of the measurement values from the nominal ones of the heights (S2, S4, S6) and the grooves (S1, S3, S5) [Gasparin, 2011(2)].

The uncertainty budget for the dimensional measurements was estimated following GUM [GUM, 2008] and ISO 15530 part 3 [ISO 15530-3, 2004]. The results are summarized in Table 3.13. The expanded uncertainty was calculated with a confidence level of 95% (k = 2) considering three contributors (see equation (3.5)) among the following:

- u_{cal} = calibration uncertainty given in the calibration certificate of the PTB contour profile [PTB, 2005];
- u_{res} = resolution uncertainty equal to the *z*-vertical resolution applied during the optical measurements;
- u_{rep} = repeatability of the measuring process equal to the standard deviation of five measurements performed on the specimen.

$$U_{optical} = k \cdot \sqrt{u_{cal}^2 + u_{res}^2 + u_{rep}^2} \qquad (3.5)$$

In the uncertainty budget the effect of the temperature was not taken into account. The reason was that the standard artefacts and their replicas were kept in a clean environment with a constant temperature of 20 ± 1°C for the entire investigation. The deviation of 1°C from the reference temperature (20°C) led to a contribution in the range of 10^{-2} - 10^{-1} µm (see Table 3.6) and therefore it could be considered negligible.

Looking at the results, the specimen having values compatible with the reference ones was the red-soft replica. The blue-hard replica showed the largest uncertainty. The main contributor of the uncertainty was the repeatability of the measurements: approximately 4 µm, half of the combined expanded uncertainty.

[µm]	**S1**				**S2**				**S3**			
	Reference	Blue	Grey	Red	Reference	Blue	Grey	Red	Reference	Blue	Grey	Red
U (k=2)	3.9	9.1	6.6	3.8	3.5	7.7	6.5	4.2	3.5	9.7	9.6	3.7
[µm]	**S4**				**S5**				**S6**			
	Reference	Blue	Grey	Red	Reference	Blue	Grey	Red	Reference	Blue	Grey	Red
U (k=2)	3.5	7.3	8.4	4.7	4.6	7.2	7.4	3.6	5.2	9.1	7.0	6.6

Table 3.13 - Standard uncertainty contributors for the measurements on the contour profile [Gasparin, 2011(2)].

3.4.1.2 Traceable procedure

The specimen TypeA2 was chosen as master in order to define a traceable measuring procedure of its 5 replicas.

The traceable measuring procedure was established following three steps:

1. 5 profiles distributed over the measuring area were chosen on the standard and measured using a calibrated stylus profilometer. A profile analysis was carried out and the heights of the 6 grooves were calculated following ISO 5436 [ISO 5436] ("*Traditional*", blue boxes of Figure 3.28);
2. The standard and its replicas were measured using an optical instrument and 5 profiles were selected over the measuring area and a profile analysis was carried out following ISO 5436 [ISO 5436] ("*Replica*", green boxes of Figure 3.28);
3. The optical results were compared with the contact ones to estimate the uncertainty of the optical measurements ("*Traceable procedure*", red boxes of Figure 3.28).

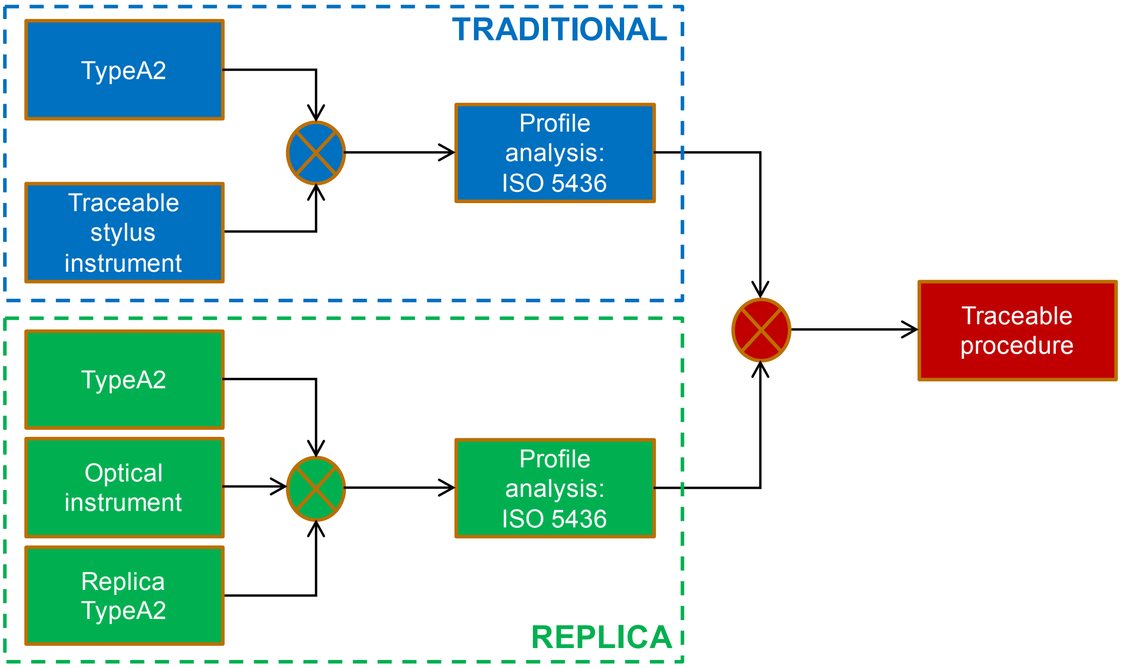

Figure 3.28 - Traceable measuring procedure for the TypeA2 replicas.

The results are shown in Figure 3.29.

The optical values obtained for the standard artefact differed of 0.2 - 4% from the contact values. This proved that both the used measuring technique and the implemented analysis set-up led to traceable results with small deviations from the reference values.

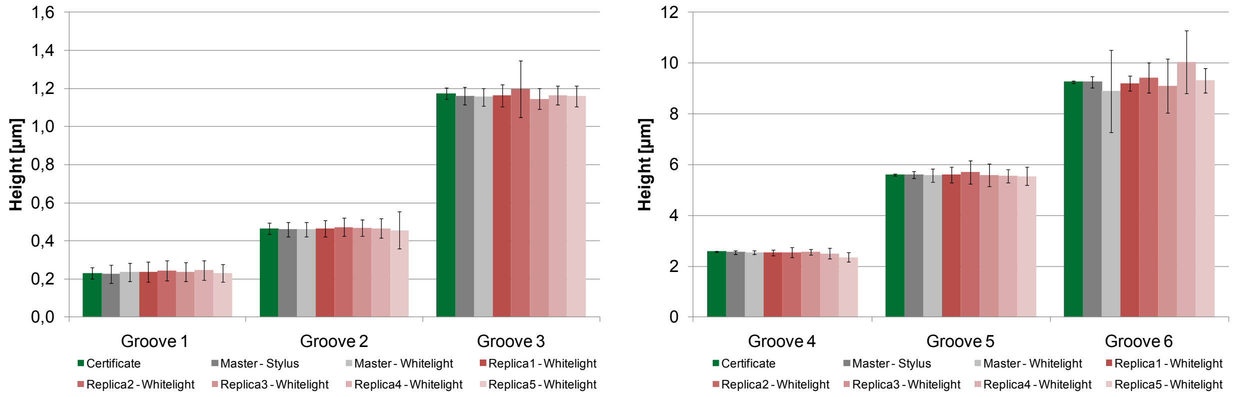

Figure 3.29 – 6 grooves height values of the certificate, of the TypeA2 standard measured with the stylus profilometer (*Master – Stylus*), of the standard measured with the whitelight interferometer (*Master – Whitelight*) and of the 5 replicas measured with the whitelight interferometer (*Replica# – Whitelight*).

The optical values obtained for the standard artefact differed of 0.2 - 4% from the contact values. This proved that both the used measuring technique and the implemented analysis set-up led to traceable results with small deviations from the reference values.

The same variation was obtained when comparing the replica values with the master ones: 0.4 – 5%. Moreover the replica repeatability had a standard deviation of 1.2 - 4% which was included in the deviations from the master results.

It is important to underline that some macro deformations were observed in groove 1 and 2. These defects were produced during the replica process under the form of "weld lines". They were visible by eyes and led to a lower replication of the groove, see Figure 3.30. For this reason it was not possible to apply a suitable correction/alignment to the measured area without modifying the original shape of the groove, therefore no results could be calculated for some measurements of grooves 1 and 2.

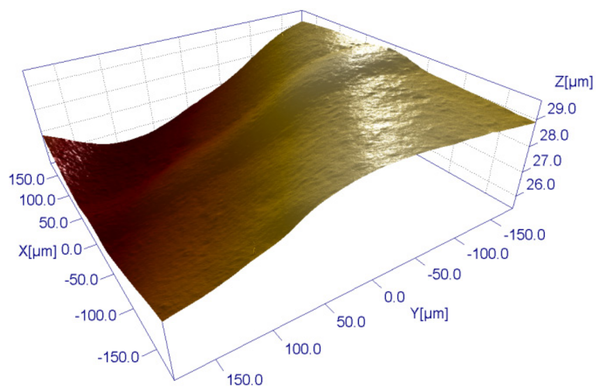

Figure 3.30 – Macro deformation in groove 1.

The uncertainty budget of the roughness measurements on TypeA2 and its replicas was estimated following GUM [GUM, 2008] and the substitution method [ISO 15530-3, 2004][b]. The results are summarized in Table 3.14. The expanded uncertainty was calculated with a confidence level of 95% (k = 2) considering four contributors among the following:

- u_{cal} = calibration uncertainty given in the calibration certificate [Halle, 2004];
- u_{res} = *z*-vertical resolution applied during the optical measurements;
- u_{instr} = resolution uncertainty of the contact profilometer;
- u_{rep} = repeatability of the measuring process equal to the standard deviation of the measurements on five defined areas of the specimens.

$$U_{contact} = k \cdot \sqrt{u_{cal}^2 + u_{instr}^2 + u_{rep}^2} \qquad (3.6)$$

$$U_{optical} = k \cdot \sqrt{u_{contact}^2 + u_{res}^2 + u_{rep}^2} \qquad (3.7)$$

In the uncertainty budget the effect of the temperature was not taken into account. The reason was that the standard artefacts and their replicas were kept in a clean environment with a constant temperature of 20 ± 1°C for the entire investigation. The deviation of 1°C from the reference temperature (20°C) led to a contribution in the range of 10^{-6} – 10^{-4} µm (see Table 3.6) and therefore it could be considered negligible.

The obtained uncertainties were in average equal to 5 – 20% of the measured value. The larger uncertainty were obtained for groove 1 (20%) and for groove 2 (11%) due to macro deformations which led to difficulties on the measurement analysis. For the same reason the uncertainty on the replicas of groove 6 differed largely (up to 400%).

U (k=2) [µm]	**Stylus**	**Optical**					
	Master	Master	Replica 1	Replica 2	Replica 3	Replica 4	Replica 5
Groove 1	0.046	0.048	0.053	0.052	0.050	0.051	0.046
Groove 2	0.037	0.038	0.042	0.048	0.044	0.051	0.098
Groove 3	0.046	0.046	0.057	0.149	0.053	0.050	0.055
Groove 4	0.070	0.071	0.115	0.190	0.115	0.205	0.179
Groove 5	0.139	0.257	0.306	0.455	0.444	0.250	0.359
Groove 6	0.222	1.619	0.300	0.599	1.067	1.228	0.483

Table 3.14 - Standard uncertainty contributors for the step height measurements on the TypeA2 standard and its 5 replicas measured with a contact profilometer ("*Stylus*") and a Whitelight interferometer ("*Optical*").

[b] A revised version is available (ISO15530-3:2011).

This investigation showed that it is possible to ensure a traceable measuring procedure for a replica casting method. In particular if the replica technique is applied for step heights between 1 and 9 µm, the process is repeatable within 98% and the measurement uncertainty is in the range of 0.05 and 0.5 µm respectively. When the replica process is applied for step heights around 0.2 – 0.5 µm it is important to adopt a fixture that ensures a unique flow of the material in order to minimize the “weld lines”.

3.4.2 Geometries product replication

An optical component was chosen in order to analyze and evaluate the feasibility of the replication technique. For this optical component two samples were taken into account: a micro-structured optical component and its mould, both characterized by micro-pyramidal structures as shown in Figure 3.31. The mould is in nickel (Ni) made through an electroforming process; while the optical part was produced through an injection compression moulding process using polymethyl-methacrylate (PMMA, ALTUGLASS V 825 T grade) as polymer material.
Both the mould and the polymer part were replicated using the blue-hard material described in paragraph 3.2.

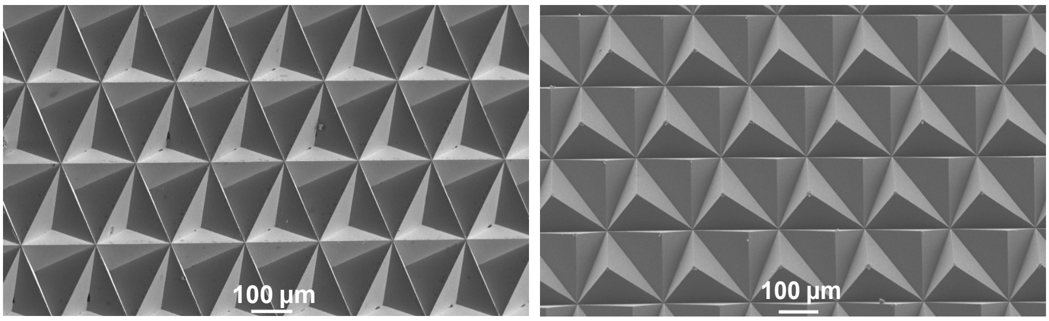

Figure 3.31 - Left: SEM images of the nickel mould; right: SEM images of the PMMA polymer part [Gasparin, 2011(1)].

The micro-pyramidal structures of the mould, the polymer part and the replicas were characterized through the analysis of SEM (Scanning Electron Microscope) images. The SEM instrument is described in appendix 11.1.4. The measurements of the specimens were carried out on ten different areas (A, B, … , L), represented in Figure 3.32. On each area three different features were taken into account and analyzed using an image processor software.

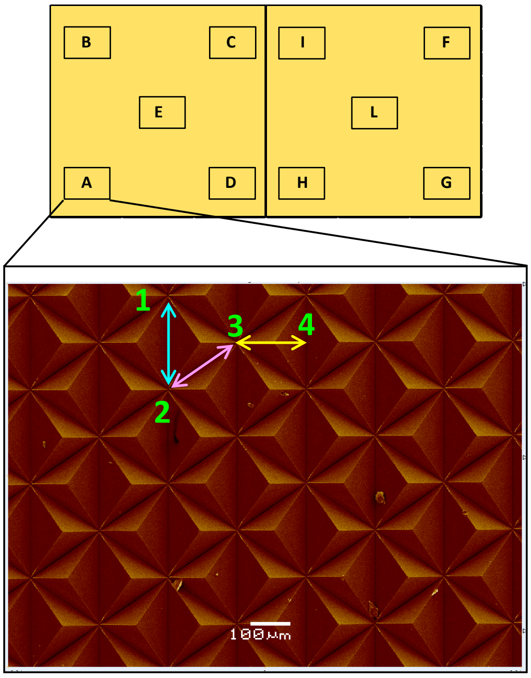

Figure 3.32 - Ten areas (A, B, ..., L) investigated on the optical component and the three measured pitches: vertical (1-2), diagonal (2-3) and horizontal (3-4) [Gasparin, 2011(1)].

Referring to Figure 3.32, the three investigated features were:

a) Vertical pitch (1-2): 21 vertical pitch measurements were carried out for each area and the average was calculated;
b) Diagonal pitch (2-3): 24 diagonal pitch measurements were carried out for each area and the average was calculated;
c) Horizontal pitch (3-4): 42 horizontal pitch measurements were carried out for each area and the average was calculated.

The second investigation dealt with the replica material stability (short and long term stability) and with the measurements repeatability. The components were two moulds used for the injection moulding of Fresnel lenses. Both moulds are in nickel, but one with titanium nitride (TiN) as coating, see Figure 3.33.

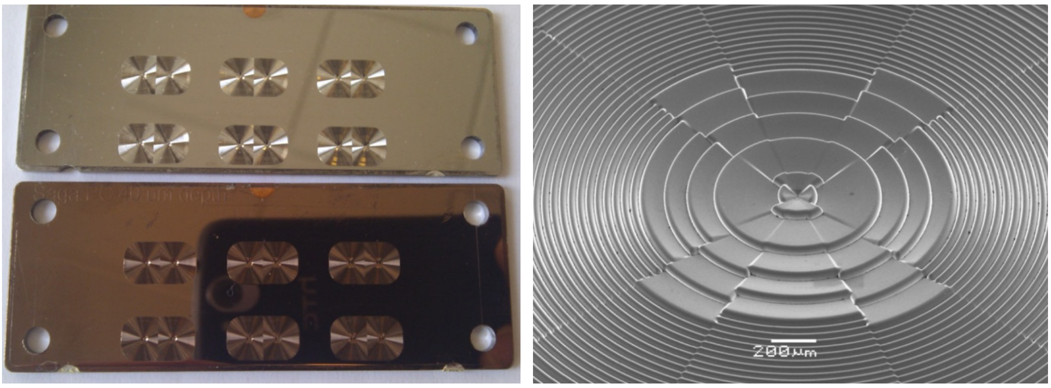

Figure 3.33 – Left upper: Ni mould; Left lower: Ni mould with TiN as coating; Right: SEM picture of a Fresnel lens.

A red-soft replica of one mould was prepared and during the first three hours the measurements were carried out every 30 minutes in order to evaluate the short term stability. The measurements interested two areas: 10 small ribs, 3 large ribs and centre geometry, see Figure 3.34, with the aim of calculating the ribs height. The replica was characterized using the optical instrument described in appendix 11.1.5.

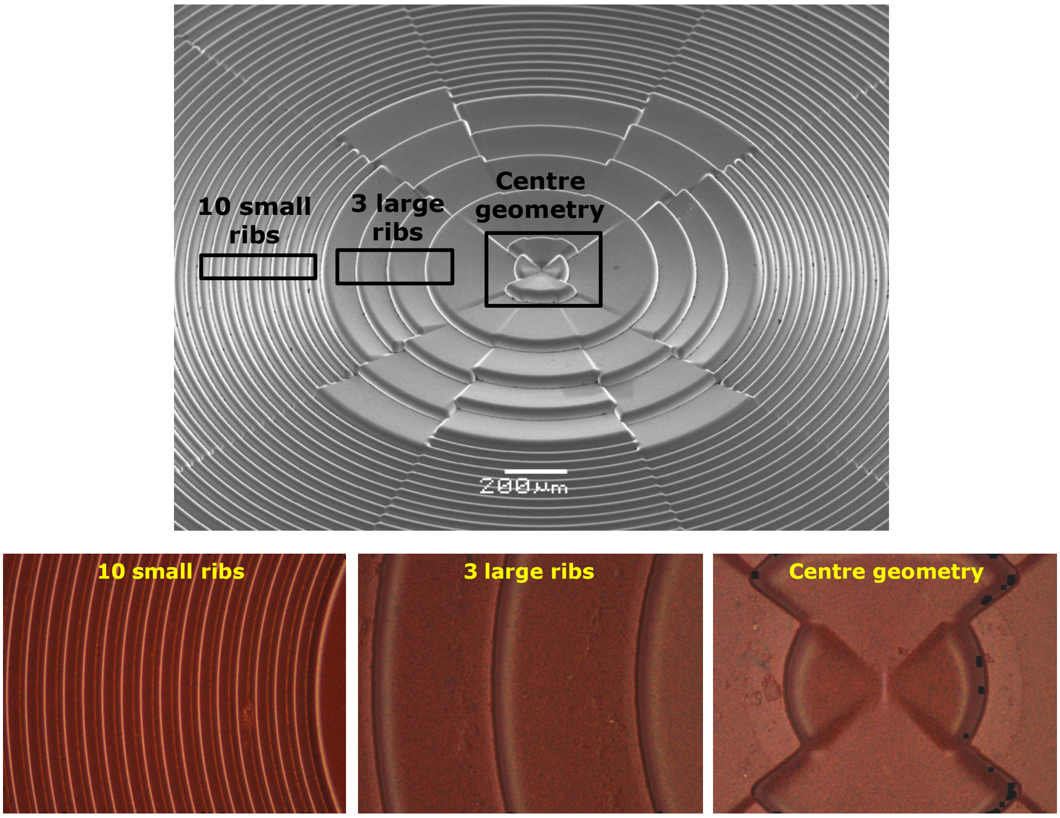

Figure 3.34 – Upper: overview of a lens and the three areas investigated during the optical measurements. Lower: The three areas measured by the optical instrument: 10 small ribs, 3 large ribs and centre geometry.

3.4.2.1 Replication degree results

The replica casting technique was performed on the mould and on its optical component in order to investigate the quality control of the replication method. The measurements on both replicas were taken and analyzed as described in paragraph 3.4. The results were compared and are graphically represented in Figure 3.35 and Figure 3.36.

The results achieved on the replica mould (red columns on Figure 3.36) were spread equally on the same area of the different pitches and they were equal to 236 µm (vertical pitch, 1-2), 207 µm (diagonal pitch, 2-3) and 171 µm (horizontal pitch, 3-4). These values were 95% of the ones obtained from the mould measurements (see chapter 8) as shown in Table 3.15. A better quality replication (99%) was achieved for the replica part as it is shown in Table 3.16. It was probably due to the fact that the pyramids were peaks on the part, therefore easy to be replicated, and valleys on the mould, therefore difficult to be filled in. The results proved that this kind of replication technique represents a promising method to evaluate and characterize surfaces that are difficult to measure.

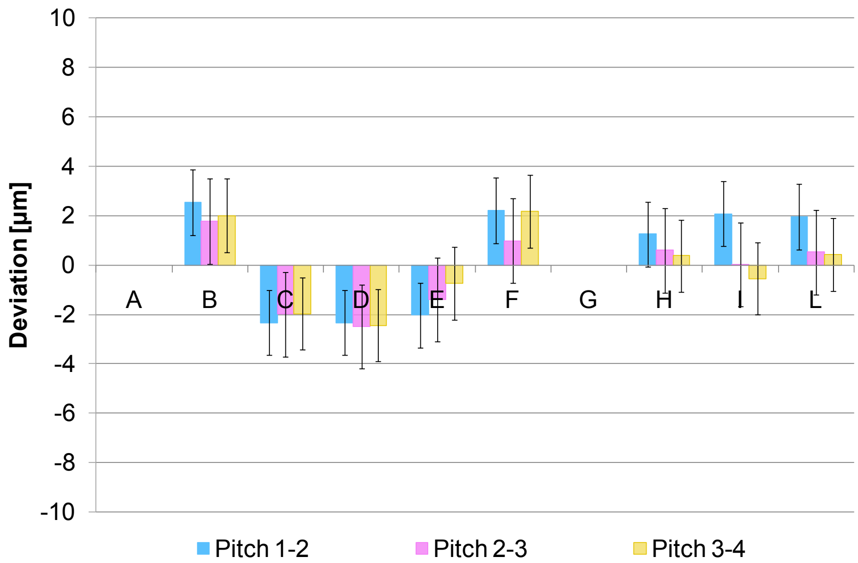

Figure 3.35 - Deviation of the measured pitches on the replica of the optical component with respect to the measured pitches on the mould replica: vertical pitch (1-2); diagonal pitch (2-3) and horizontal pitch (3-4) [Gasparin, 2011(1)]. The results were obtained from SEM calibrated images.

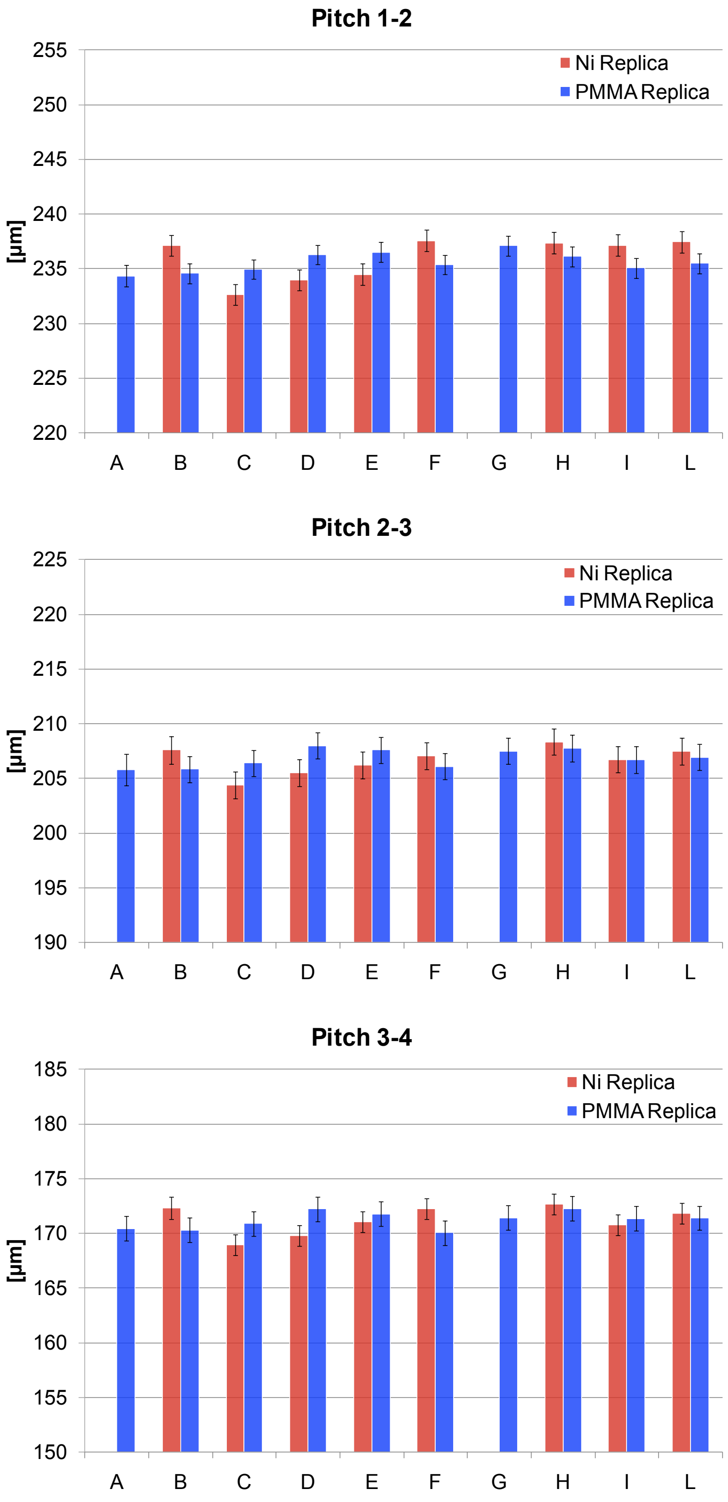

Figure 3.36 - Comparison between the measured pitches on the replica mould (red columns) and on the replica of the optical component (blue columns): vertical pitch (1-2); diagonal pitch (2-3) and horizontal pitch (3-4). A and G areas were not measured. The results were obtained from SEM calibrated images [Gasparin, 2011(1)].

	Pitch 1-2	Pitch 2-3	Pitch 3-4
Mould [µm]	250	220	180
Replica mould [µm]	236	207	171
%	94.4	94.1	95.0

Table 3.15 - Comparison between the pitches measured on the mould (see chapter 8) and on the replica mould [Gasparin, 2011(1)].

	Pitch 1-2	Pitch 2-3	Pitch 3-4
Part [µm]	237	210	173
Replica part [µm]	236	207	171
%	99.6	98.6	98.8

Table 3.16 - Comparison between the pitches measured on the polymer part (see chapter 8) and on the replica part [Gasparin, 2011(1)].

The uncertainty budget for width and length (equation (3.8)) was calculated following the Guide to the Expression of Uncertainty in Measurements [GUM, 2008] and the substitution method applied to CMM [ISO 15530-3, 2004].

$$U_i = k \cdot \sqrt{u_{res}^2 + u_{cal}^2 + u_{SEM,i}^2 + u_{magn}^2} \qquad (3.8)$$

With:

$$u_{SEM,i} = \max(u_{rep}; u_{area}) \qquad (3.9)$$

Where:

- *U* = expanded combined uncertainty;
- *i* = *x*, *y* depending on the measurand (*x* for horizontal pitch; *y* for vertical pitch; *xy* for diagonal pitch);
- *k* = 2 in order to obtain a confidence level of approximately 95%;
- u_{res} = instrument resolution;
- u_{cal} = calibration uncertainty;
- u_{rep} = repeatability (equation (3.9)) = standard deviation of three measurements carried out on the same five pitches;
- u_{area} = standard deviation of all the pitches measured in the same area (equation (3.9));

- u_{magn} = deviation between the nominal pixel size and the measured one according to [Bariani, 2005], see appendix 11.1.4.

Measurements on the same pitches as well as on different pitches of the components were affected by instrument repeatability. Therefore, the maximum value among the uncertainty contributors (u_{rep}, u_{area}) was selected to not overestimate the repeatability.

For each measurement performed on the replica mould and on the replica part, the uncertainty budget was calculated according to equation (3.8) and the average of the different uncertainties is listed in Table 3.17. The uncertainties calculated for the replica mould and the replica part were 0.6% of the measured pitches.

U (k=2) [µm]	Pitch 1-2	Pitch 2-3	Pitch 3-4
Replica mould	1.0	1.2	1.0
Replica part	0.9	1.2	1.1

Table 3.17 - Average of the uncertainty budgets calculated for the different pitches measured on the ten areas of the corresponding component [Gasparin, 2011(1)].

3.4.2.1 Stability results

Stability studies were performed in order to ensure the reliability of the replica over different periods of time. The replica of one mould was measured after 180 minutes, 24 hours and 14 days from its realization. The optical measurements were carried out in the same area every time. The selected features were: 10 small ribs, 3 large ribs and centre geometry with, respectively, an average height of 23 µm, 34 µm and 35 µm. The measurement analyses were performed applying an automatic procedure consisting in the height distribution method to exclude the influence of the ribs sidewalls. During the entire experiment, the replica was kept in a clean environment with a constant temperature of 20 ± 1 °C. The results are summarized in Table 3.18 and showed a stability of the replica ribs within a range of 0.1 µm during 180 minutes; 0.3 µm during 24 hours and 0.4 µm during 14 days.

Time period	180 min	24 h	14 days
Stability range	0.1 µm	0.3 µm	0.4 µm

Table 3.18 - Replica stability over different periods of time. The stability range is equal to the standard deviation of the measurements performed during the time period.

Based on the results of the presented investigation, the optimal way to measure the replicas would be waiting for at least one hour before measuring. Moreover if the replica is kept in a clean environment with a constant temperature of 20°C, reliable results can be obtained even after one week.

3.5 Conclusion

The replica casting process is becoming important in a wide range of applications, e.g. the characterization of specimens difficult to measure such as optical components. This chapter reported and discussed a deep investigation of the whole methodology in order to determine limits and properties of the process.

The replica method revealed to be a fast, cost-effective and reliable technique. Different polymer materials can be used, but the silicone compound showed the best replication fidelity on several surface types. The dimensional range covered by the study was 200 - 500 nm for roughness measurements and 0.2 µm - 1000 µm for step heights. The major problem was encountered in dimensional replication of 0.2 – 0.5 µm step heights because macro deformation obtained during the replica process caused a less replication of the grooves. The process showed a good short term (three hours) and long term (1 month) stability. This can be achieved by keeping the replica in a clean environment with a constant temperature, preferably around 20°C.

A traceable procedure can be established in case the replica method has to be applied for the characterization of a workpiece. This has been demonstrated through different case studies, discussed in relation to roughness and step heights measurements.

To overcome the limits of traceability on measurements at the micro dimensional scale, e.g. availability of calibration artefacts, future works should aim at developing artefacts specifically designed for the replica technique. Such objects would act as reference standards for the replica process and should be characterized by features similar to the workpiece to be measured. In particular they should include regions with different roughness surfaces and different dimensional features. A challenge could be represented by the aspect ratio of the structures. The aspect ratio is the ratio between width and height of a feature: high aspect ratios are usually difficult to replicate and complicate to identify.

As a consequence, by having specific designed artefacts, the limitations of the replica technique could be understood more deeply.

3.6 References

[AccuTrans] AccuTrans - Automix Casting Silicone, manual instruction (info@coltenewhaledent.ch).

[Bariani, 2005] P. Bariani, "Dimensional metrology for microtechnology", PhD thesis, Department of Manufacturing Engineering and Management, Technical University of Denmark, 2005.

[Cantatore, 2010] A. Cantatore, L. De Chiffre, S. Carmignato, "Investigation on a replica step gauge for optical 3D scanning of micro parts", Proceedings of the Euspen International Conference, 2010, Volume 1, pp. 200-203.

[CCI, 2011] Talysurf CCI by Taylor Hobson, http://www.taylor-hobson.com

[De Chiffre, 2009] L. De Chiffre, S. Carmignato, A. Cantatore, J. D. Jensen, "Replica calibration artefacts for optical 3D scanning of micro parts", Proceedings of the Euspen International Conference, 2009, Volume 2, pp. 352-355.

[Efsen, 1995] J. Efsen, H.N. Hansen, S. Christiansen, "Laser profilometry", Handbook of Non-Invasive Methods and the Skin, 1995, 3:97–105 (Chapter 5).

[Gasparin, 2008] S. Gasparin, "Traceability of optical roughness measurements on polymer", Master thesis - Technical University of Denmark, 2008.

[Gasparin, 2011(1)] S. Gasparin, G. Tosello, H.N. Hansen, I. Di Vora, S. Priante, S. Sinesi, "Replication quality control of metal and polymer micro structured optical surfaces", 4th Swedish symposium, 2011, pp. 533-539.

[Gasparin, 2011(2)] S. Gasparin, H.N. Hansen, G. Tosello, "Traceable surface characterization using replica moulding technology", 13th International conference on metrology and properties of engineering surfaces, 2011, pp. 310-315.

[Gasparin, 2012] S. Gasparin, G. Tosello, H.N. Hansen, J.A. Albajez, "Replica casting technique for micro Fresnel lenses characterization", Proceeding of 12th International Euspen Conference 2012, pp. 319-322.

[George, 1979] A.F. George, “A comparative study of surface replicas”, Proceedings Conference on metrology and properties of surfaces, 1979, pp. 51-61.

[GUM, 2008] Joint Committee for Guides in Metrology (JCGM). JCGM 100:2008, Guide to the Expression of Uncertainty in Measurement (GUM), 2008, pp. i–viii, 1–132.

[Halle, 2004] Halle TypeA2, serial number 048221, “Calibration certificate”, CGM (Center for Geometrisk Metrologi”, 19th July 2004.

[Halle, 2011] http://www.halle-normale.de/, December 2011.

[Hansen, 2011] H.N. Hansen, R.J. Hocken, G. Tosello, “Replication of micro and nano surface geometries”, Annals of the CIRP, 2011, Volume 60, pp.695-714.

[IF500, 2011] IF-RoughnessTool-500, “Calibration certificate and technical description”, Alicona Imaging GmbH, Version C, 15th September 2010.

[IFM, 2009] IFM Manual, IFM 3.1.1.2 EN, Alicona Imaging GmbH, 26th February 2009.

[ISO 13565-2, 1996] ISO 13565-2: "Geometrical Product Specifications (GPS) - Surface texture: Profile method; Surfaces having stratified functional properties - Part 2: Height characterization using the linear material ratio curve", 1996.

[ISO 15530-3, 2004] ISO 15530 part 3: 2004 - Geometrical Product Specifications (GPS) - Coordinate Measuring Machine (CMM): techniques for determining the uncertainty of measurement – Part 3: Use of calibrated workpieces or standards.

[ISO 4288, 1996] ISO 4288: “Geometrical Product Specifications (GPS) – Surface texture: Profile method – Rules and procedures for the assessment of surface texture”, 1996.

[ISO 5436] ISO 5436 - Geometrical Product Specifications (GPS) - Surface texture: profile methods; measurement standards.

[Koch, 2008] K. Koch, A.J. Schulte, A. Fischer, S.N. Gorb, W. Barthlott, “A fast, precise and low-cost replication technique for nano- and high-aspect-ratio structures of biological and artificial surfaces”, Journal of Bioinspiration & Biomimetics, 2008, 3 046002.

[LEXT, 2011] LEXT OLS4000: 3D Measuring Laser Microscope by Olympus, http://www.olympus.co.uk/microscopy/26_LEXT_OLS4000.htm.

[Lonardo, 2002] P.M. Lonardo, D.A. Lucca, L. De Chiffre, "Emerging Trends in Surface Metrology", Annals of the CIRP, 2002, Volume 51, Issue 2, pp. 701-723.

[LuxaBite] LuxaBite – manual instruction by DMG (www.dmg-hamburg.de).

[Matbase, 2011] http://www.matbase.com/material/polymers/elastomers/silicone-rubber/properties, December 2011.

[Mazzarello, 2001] V. Mazzarello, M. Cametti, G. Leone, P. Iacovelli, P. Ena. G. Leigheb, "Analysis of the microtopography of the skin by silicone replicas after repeated exposure to actinic radiation at high altitudes", Journal of the European Academy of Dermatology and Venereology, 2011, Volume 15, pp. 224- 228.

[Mecholsky, 1992] J.J. Mecholsky, J.R. Plaia, "Fractal analysis on fracture surfaces of glass using replication techniques", Journal of Non-Crystalline Solids, 1992, Volume 146, pp. 249–255.

[Narayanasamy, 1979] K. Narayanasamy, V. Radhakrishnan, R.G. Narayanamurthi, "Analysis of surface reproduction characteristics of different replica materials", Conference on metrology and properties of surfaces, 1979, pp. 63-69.

[Nilsson, 2001] L. Nilsson, R. Ohlsson, "Accuracy of replica materials when measuring engineering surfaces", International Journal of Machine Tool and Manufacture, 2001, Volume 41, pp. 2139-2145.

[P1165, 2006] P1165, "Calibration certificate", CGM (Center for Geometrisk Metrologi), 13th June 2006.

[PGI, 2011] Form Talysurf PGI by Taylor Hobson, http://www.taylor-hobson.com/ultra-precision-pgi-range.html.

[PTB 619, 2003] PTB 619, "Calibration certificate", CGM (Center for Geometrisk Metrologi", 29th October 2003.

[PTB 625, 2001] PTB 625, "Calibration certificate", CGM (Center for Geometrisk Metrologi", 16th July 2001.

[PTB, 2005] Calibration certificate - Micro-contour standard, reference number: PTB-05.4021640, 2005.

[PTB website, 2011] http://www.ptb.de/index_en.html, December 2011.

[RepliSet] RepliSet – Users guide and applications by Struers A/S (www.struers.com).

[Rubert, 2011] http://www.rubert.co.uk/, December 2011.

[Scott, 2006] R.S. Scott, P.S. Ungar, T.S. Bergstrom, C.A. Brown, B. Childs, M.F. Teaford, A. Walker, "Dental microwear texture analysis", Journal of Human Evolution, 2006, Volume 51, pp. 339–349.

[Tosello, 2012] G. Tosello, H.N. Hansen, S. Gasparin, J.A. Albajez, J.I. Esmoris, "Surface wear of micro structured TiN coated nickel tool during the injection moulding of polymer micro Fresnel lenses", Annals of the CIRP, 2012, Volume 61, Issue 1, pp. 535-538.

4. Process chains for micro-manufacturing

4.1 Introduction

A process chain describes the development and the manufacture of a product through a physical flow which starts with the image or concept of the product and ends with its realization. The "*material*" is processed into "*part/component*" and the parts are assembled into a "*product*". The "*image of the product*" is given by the "*design*" and introduced into the physical flow through the "*control and measurements*", see Figure 4.1 [Masuzawa, 2000].

One of the main challenges related to the manufacturing of a micro product is to connect the previous individual steps into a continuous flow. In fact micro and nano manufacturing needs competences in different fields such as physics, biology, medicine and engineering and, at the same time, several technologies are required for the production of a micro component [Alting, 2003], [Qin, 2010] and [Brousseau, 2010]. These tasks create difficulties in establishing a continuous and coherent micro process chain. Therefore, special considerations are given in this chapter with respect to design, tool fabrication and quality assurance. In particular, the relationship between *required functionality* - *specifications* - *final tolerancing* is a key step in the micro product development. To ensure the required functions, the specifications are given in terms of maximum deviations from an ideal geometric form and are described by absolute values combined with tolerances [Hansen, 2006].

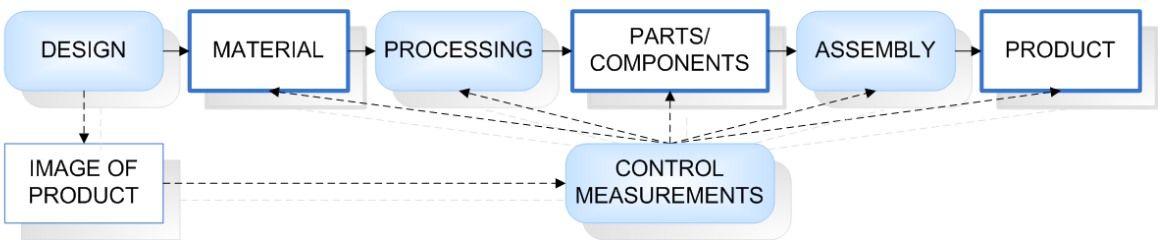

Figure 4.1 - Relationship among technologies (*design*, *processing*, *assembly* and *control measurements*) and objects (*material*, *parts/components* and *product*) in production [Masuzawa, 2000].

The tooling process chains are described and analyzed in relation to the micro injection moulding process. An overview of the most common process technologies is introduced focusing on micro milling, polishing, micro EDM, die sinking EDM, wire EDM, electroforming, injection moulding and direct/indirect tooling approaches (*Paragraphs 4.2* and *4.3*).

Finally, three case studies are investigated in a specific step of their process chain:

1. <u>Design</u>: design principles of a mould for a hearing aid volume control (*Paragraph 4.4*);
2. <u>Processing</u>: strategies for the realization of a micro-milling/micro-EDM milling hybrid tooling experiment (*Paragraph 4.5*);
3. <u>Process control</u>: characterization of a hearing aid speaker, its mould and electrode (*Paragraph 4.6*).

4.2 Overview of micro-manufacturing technologies

The machining of precision parts and microstructures can be subdivided into two general types of technologies: MicroSystem Technologies (*MST*) and Micro-Engineering Technologies (*MET*) [Brinksmeier, 2001], as shown in Figure 4.2.

MST are qualified for the manufacture of products of Micro Electro Mechanical System (*MEMS*) and Micro Opto Electro Mechanical Systems (*MOEMS*) including UV-lithography, silicon-micromachining and LIGA (Lithography, Electroplating and Moulding). *MET* comprise the production of highly precise mechanical components, moulds and micro structured surfaces. Typical mechanical processes employed in this field are diamond machining (e.g. turning, milling and precision grinding), as well as micro engraving.

Furthermore, energy assisted processes include manufacturing processes, such as Laser Beam Machining, Focused Ion Beam Machining, Electron Beam Machining and Micro Electro Discharge Machining (micro EDM).

The categories can overlap between each other and, moreover, the products can either be manufactured individually or as mass products using moulds in micro-replication techniques, such as forming, injection moulding and casting.

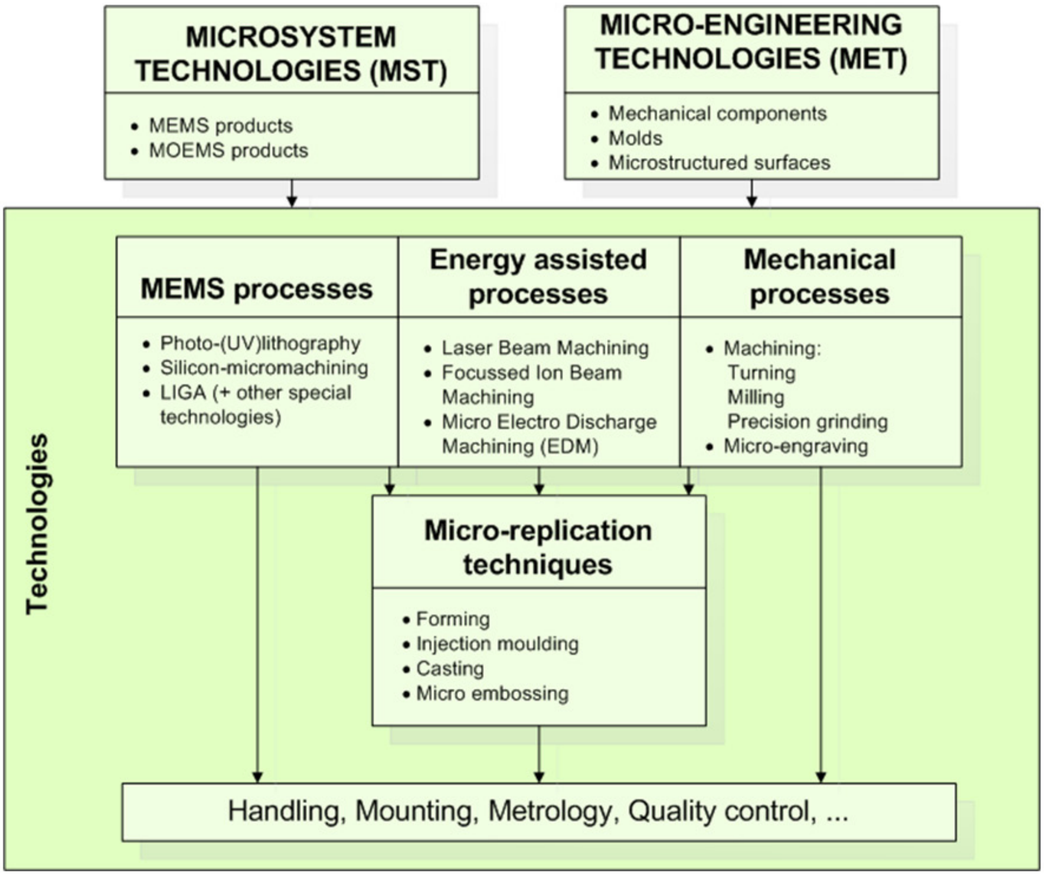

Figure 4.2 - Process technologies for machining of precision parts and microstructures [Brinksmeier, 2001].

The following sections describe the technologies relevant for the case studies of the thesis: mechanical process based on material removal (*Paragraph 4.2.1*), energy assisted process (*Paragraph 4.2.2*), electroforming (*Paragraph 4.2.3*) and micro injection moulding (*Paragraph 4.2.4*).

4.2.1 Mechanical processes based on material removal

Cutting processes - Micro milling

Micro cutting is a process defined by the mechanical interaction of a sharp tool with the material of a workpiece. This interaction causes on the workpiece a breakage along defined paths and, eventually, removes the useless material in form of chips [Alting, 2003]. The process is possible under certain conditions for the tool: the tool has to be harder than the workpiece material and its edge radius must be in the order of the cut thickness or smaller. A major implication is the relatively high machining force which influences the machining accuracy and the practical limit of the machinable size due to deflections of tool and workpiece.

The main advantages of this process are:

- Plastics and metallic materials can be machined as well as composite materials since there is no influence on the process by their electrical properties [Masuzawa, 2000];
- The possibility of machining 3D micro structures characterized by high aspect ratios and high geometric complexity [Adams, 2000], [Adams, 2001] and [Weule, 2001].

The main issues interest,:

- Tool fabrication: the most suitable material for the tool is the mono-crystalline diamond but its affinity with steel causes diffusion and unacceptable wear [Alting, 2003];
- Very hard or brittle materials are difficult to machine [Alting, 2003];
- Brittle chipping of the workpiece cannot be suppressed completely [Schaller, 1999].

Conventional cutting processes are turning, milling and drilling. Milling is probably the most versatile due to its ability to produce almost any shape of component. Micro milling is defined as the downscaling of the conventional milling process, involving the use of tools with diameters in the sub-mm range [Bissacco, 2004].

Micro milling is suitable for machining microstructures characterized by high aspect ratios (maximum aspect ratio equal to 7 - 8) and complex geometries (minimum feature size approximately equal to 50 μm and Ra down to 0.2 μm). It can be used for manufacturing small batches or for producing mould inserts, see Figure 4.3.

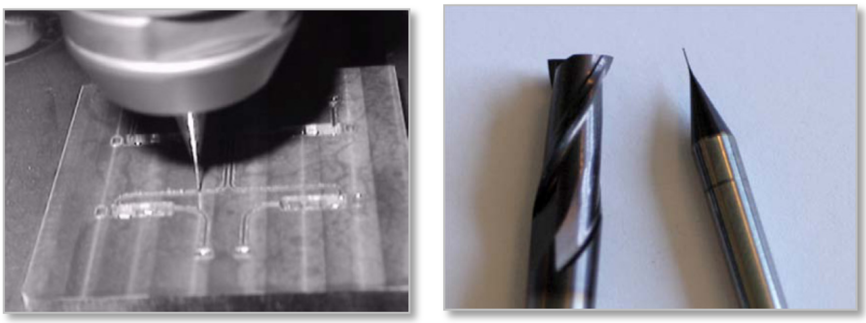

Figure 4.3 – Examples of structures realized by micro milling and tools used for micro milling process [Bissacco, 2004].

The main challenges for this process are [Bissacco, 2004]:

- Process implementation with conventional equipment;
- Surface generation prediction and optimization;
- Surface topography measurements;
- Subsurface integrity measurement and evaluation methods;
- Prediction of cutting forces and machining errors due to tool deflections.

Grinding - Polishing

Micro grinding is another material removal technique which involves mechanical forces used for machining pins and grooves with small dimensions (minimum feature size approximately equal to 5 μm), but also for producing flat surfaces with very fine finishing (Ra down to 0.05 μm). Due to the very small obtainable depth of cut this process is suitable for fine finishing of brittle materials [Alting, 2003]. One limitation is the minimum obtainable tip radius of the tool which is strongly influenced by the grit size [Ohmori, 2001].

Polishing is usually the very last stage of the manufacturing process for industrial tools and components, see Figure 4.4. Even today it is performed by individual craftsmen using simple hand-held tools and motorized equipment. This means that the process is highly dependent on the individual craftsman and his subjective interpretation influences the surface quality evaluation. In other words, all stages and processes in the manufacturing chain of a product can be controlled and monitored, but not the surface polishing process [Hansen, 2011(1)].

Figure 4.4 – Examples of polished surfaces and tool used for polishing [Strecon, 2011].

4.2.2 Energy assisted processes

EDM – Micro EDM, Micro Die sinking EDM, Micro Wire EDM

EDM (Electro Discharge Machining) is an energy assisted process based on two electrodes which are separated by a dielectric fluid. The process is activated by the imposition of a voltage on the electrodes: when the sparks are generated, the electrode materials erode and the material removal is realized. This implies that both electrodes have to be conductive and with no critical hardness [Alting, 2003].

Micro EDM is used for making micro mould, micro valves, micro nozzle etc. Grooves, channels (see Figure 4.5), bore holes, linear profiles, columns and even complex 3D structures can be realized by being burr free [Brinksmeier, 2001].

Some micro EDM processes are micro EDM milling, micro wire EDM and micro die sinking EDM. The respective capabilities are summarized in Table 4.1.

In the micro EDM milling, the material is removed layer by layer along defined paths. It uses cylindrical electrodes with diameter of 20 – 80 μm and permits a higher geometrical flexibility [Uhlmann, 2005].

In the wire EDM process, wires with diameters down to 20 μm are used as electrodes. It is primarily used for producing 2D structures and electrodes as shown in Figure 4.5.

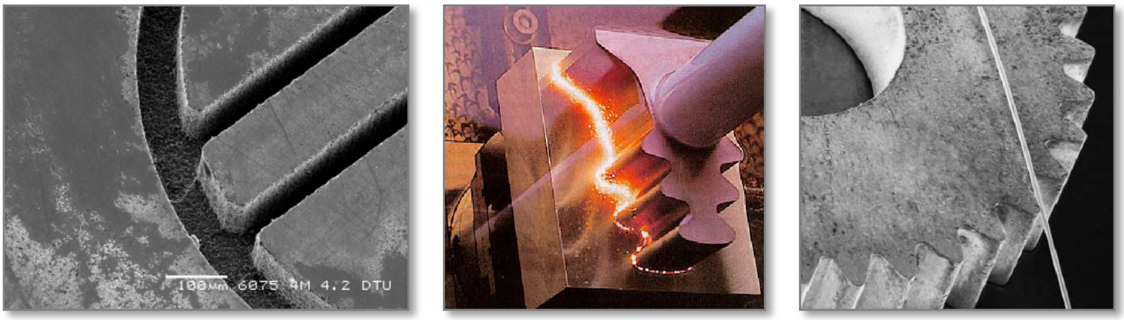

Figure 4.5 - Examples of structures realized by micro EDM milling [Tosello, 2008], die sinking EDM and wire EDM [Uhlmann, 2005].

In the die sinking EDM process, the electrodes are in graphite or copper with micro-structured form, manufactured by mechanical machining, LIGA technology or by wire EDM, see Figure 4.5. This process is mainly used for the manufacture of replication tools for micro-injection moulding or hot embossing [Uhlmann, 2005].

Processes	Micro EDM milling	Micro wire EDM	Micro die sinking EDM
Geometries	• 3D • Free form surfaces	• 2½D • Straight structures without curvature in the direction of the unwinding wire • Tapered structures up to 15°	• 3D • Free form surfaces limited by electrode manufacturing
Structure dimensions	• Minimum inner radii depending on pin electrode diameter • Applicable electrode diameter dmin=0.1mm	• Minimum inner radii, cutting width, maximum workpiece height dependent on wire diameter i.e. at dw,min=0.03mm; hmax=5mm; smin=0.04mm	• Depending on electrode manufacturing and material • Minimum structure width~0.02 mm, aspect ratio~20
Surface quality	• Ra ~ 0.2 µm • Rz ~ 0.8µm	• Ra ~ 0.07 µm[a] • Rz ~ 0.35 µm[a]	• Ra ~ 0.1 µm • Rz ~ 0.5 µm
Application	• Cavities for micro-injection moulding • Embossing or coining tools	• Forming tools (i.e. opto-electronic components, V-grooves) • Stamping tools (i.e. lead-frames) • Micro components (i.e. micro-gears, medical instruments)	• Replication moulds (i.e. micro-injection moulding) • Embossing tools

Table 4.1 - Overview of micro EDM processes ([a] with finishing technology) [Uhlmann, 2005].

4.2.3 Electroforming

The processes described previously are characterized by material removal, whereas electroforming is based on electrochemical material deposition. The metal is first dissolved electrolytically at an anode, see Figure 4.6 left. The resulting metal ions are transported through an electrolyte solution, usually containing a high concentration of the same metallic ions, to be deposited at a cathode [McGeough, 2001].

The advantages of this process are [Sole, 1994]:

- High dimensional precision (< 5 µm);
- Accurate reproduction of surface details (typically 0.01 µm);
- Production of complex-shaped components and thin-walled components;
- Extensive range of size: from a few millimetres to several meters;
- Composite materials of various metals can be built as sandwiches structures;
- Suitable for mass production.

The principal limitations are [Watson, 1989]:

- Long deposition times;
- Material restrictions: due to brittleness, oxidation and internal stresses, usually only copper, nickel and gold are used;
- Electroform/mandrel separation needs a careful procedure to avoid damages;
- Non uniform thickness and internal stresses are present in most of the obtained electroforms.

Its applications are wide [McGeough, 2001]: thin foils, perforated products, record stampers (see Figure 4.6 right), moulds and dies.

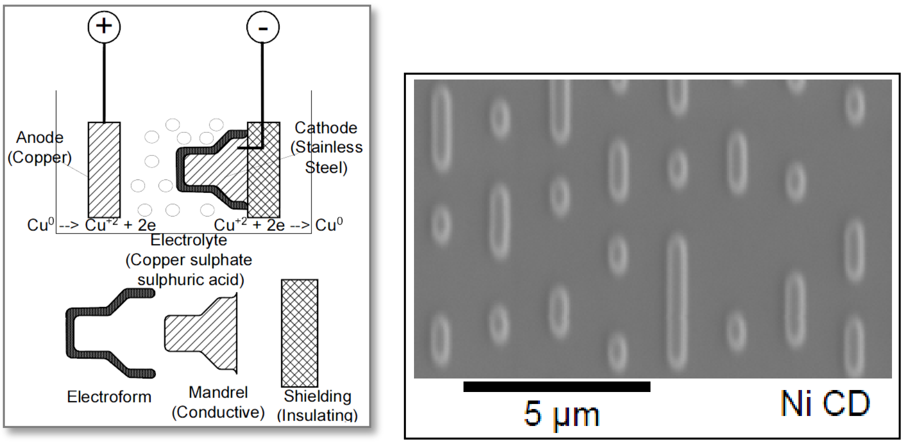

Figure 4.6 – Left: the principles of electroforming [McGeough, 2001]; right: SEM images of nickel stamper (Ni) for compact discs (CD) made by electroforming [Gasparin, 2010].

4.2.4 Replication processes

In a replication process a master geometry is transferred to a substrate material in this way copying the master geometry. This transfer can be induced by means of heat, force, chemical activation or other energy input or activation [Hansen, 2011(2)].

This section describes the injection moulding process since it interests several case studies of the thesis.

Micro injection moulding

In injection moulding the polymer material is first heated and melted and then forced into the tool cavity using high pressure. Finally the material solidifies under a maintained pressure before it is ejected out of the tool [Alting, 2003].

Microstructures with wall thickness of 20 μm, structural details in the range of 0.2 μm and surface roughness Rz < 0.5 μm can be produced, see Figure 4.7. Aspect ratio exceeding 20 are obtainable and 2D, 2½D and 3D micro products are possible to manufacture. Micro products used in biological and medical technology are also achieved from this process.

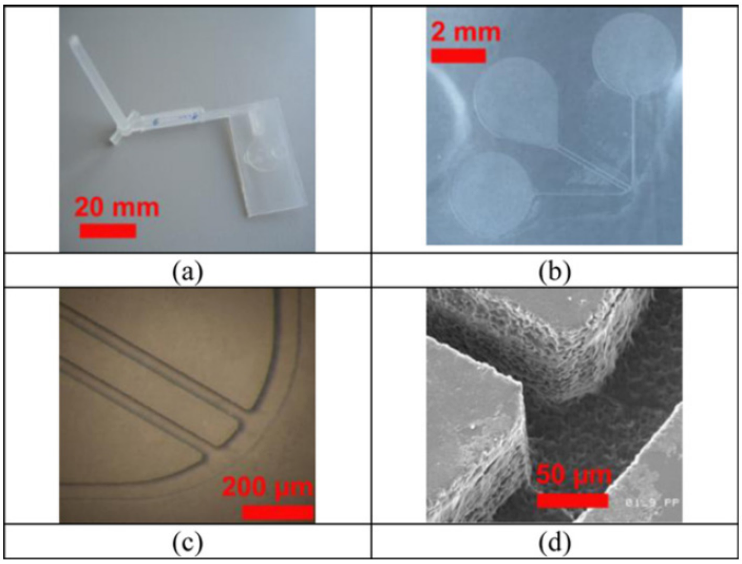

Figure 4.7 - Blood/plasma separation unit for microfluidic system produced by injection moulding: microfluidic platform (a), micro structured area (b), micro channels bend structures (c), detail of the 48 mm wide and 110 mm deep micro channel and 25 mm radius (d) (material = PP) [Hansen, 2011(2)].

In particular micro injection moulding is an innovative technology for the replication on medium-large scale of micro components. The process introduces additional design freedom, new application areas, unique geometrical features, and sustainable economical benefits, as well as material properties and part quality that cannot be accomplished by the conventional injection moulding process. Among the various micro manufacturing processes, micro injection moulding has the advantage of having a wealth of experience available in conventional plastics technology, standardized process sequence, high level of automation and short cycle time. Due to the miniature characteristics of the moulded parts, however, a special moulding machine and auxiliary equipment are required to perform tasks such as shot volume control, process parameters control, injection, ejection, plastification, inspection, handling, packaging of moulded parts, etc. Furthermore, micro machining technologies are needed to produce micro cavity [Tosello, 2008].

4.2.5 Summary

An overview and summary of the discussed processes is given in Table 4.2.

Processes capabilities	Mechanical process		Energy assisted process	Electro-forming	Micro injection moulding
	Micro milling	**Micro grinding/ Polishing**	**Micro EDM milling**		
Geometries	True complex 3D	3D limited by wheel access	True complex 3D	True complex 3D, no undercuts	3D
Accuracy	Vertical: 2 - 5 µm Lateral: 2 - 10 µm	0.5 µm	~ 2 µm	Replicates perfectly the "master" geometry	Few µm
Min feature size	~ 50 µm	~ 5 µm	~ 10 µm	Few nm	Sub µm
Max aspect ratio	7 - 8	Different in 2 orthogonal directions	20 - 50, depending on geometry	10 - 20, depending on geometry	Up to 10
Surface quality	Ra ≥ 0.2 µm on vertical surfaces	Ra ≥ 0.05 µm	Ra ≥ 0.1 µm	As good as the master	Up to optical (Ra<0.05µm)
Material removal rate (*Material addition rate for electroforming*)	High depending on tool dimensions	Low, grit size and process parameters	Low, depends on tool dimensions and desired accuracy and surface quality	Few µm/min	-
Tool material (*Master material for electroforming*)	Micro grain tungsten carbide	-	-	Must be possible to dissolve afterwards	-
Work materials (*Mould material for electroforming*)	Metals and alloys, hardness up to 60 HRC Suitable for brittle materials	Hardened tool steel, tungsten carbides Suitable for brittle materials	Only electrical conductors (metals and alloys) Hardness is not relevant, suitable for brittle materials	Nickel, copper, iron	Thermoplastic polymers, ceramics, metal in a blending polymer matrix (sintering phase must follow)

Table 4.2 - Comparison of the processes capabilities: micro milling, micro grinding/polishing, micro EDM milling, electroforming and injection moulding.

4.3 Tooling fabrication

Mass production of micro parts is mostly based on replication technologies since replication processes allow the manufacturing of large numbers of products at a reasonable price. The quality and performance of a micro part depend mainly on the quality and performance of the corresponding micro mould. Therefore, mould making, and so tool making, is an important phase of the process chain for the production of a micro polymer part [Azcarate, 2006]. This is the reason why, in most of the application cases, a combination of the processes described previously is required. This combination is called hybrid tooling. In [Azcarate, 2006] *hybrid tooling* is defined as "the capability of producing a mould insert combining two or more processes in sequence". Most of the cases are based on a combination of conventional and energy assisted processes like micro milling, micro EDM, micro ECM (micro electrochemical milling) or laser. This combination is considered not an alternative, but a need for the production of tool inserts with real 3D free-form micro features [Azcarate, 2006].

Moreover two tooling fabrication strategies are usually used: direct tooling and indirect tooling. In *direct tooling*, the tool geometry represents the negative geometry. In this way, when the replication process is carried out, the positive geometry represented by the polymer part is produced [Tosello(1), 2007]. When the focus is on micro tooling and especially on micro fluidic production purposes, this strategy is time consuming due to the machining of protruding walls and plateaus which will create channels and reservoir chambers, respectively. *Indirect tooling*, instead, refers to a tooling technology where a master structure produced by machining is the positive geometry, identical in shape to the final product, see Figure 4.8. This strategy reduces enormously the amount of material to be removed: channels and reservoir chambers will be directly machined [Tosello(2), 2007].

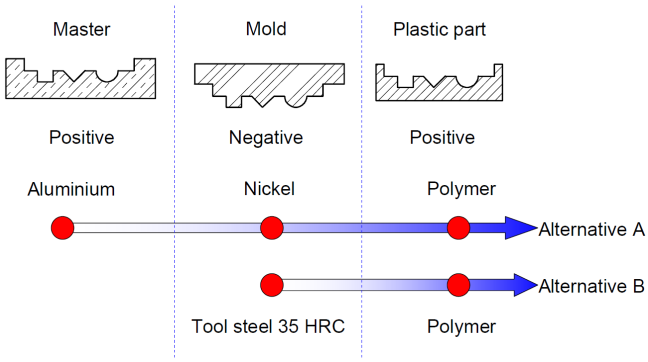

Figure 4.8 – Example of indirect tooling vs direct tooling [Bissacco, 2005].

A better understanding of the indirect tooling is given by the following investigation.
The studied part, described in [Tang, 2006] and [Bissacco, 2005], presented four main chambers with micro features for fluid mixing and a series of channels connecting the chambers with each other and with the areas where the fluids are injected, see Figure 4.9.

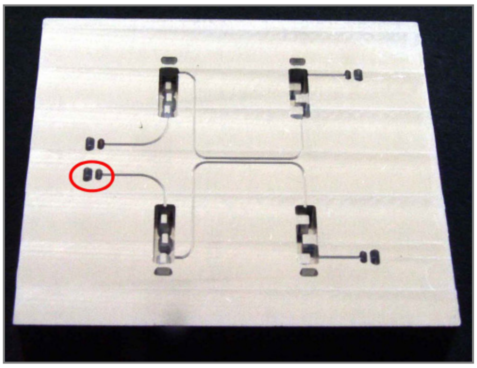

Figure 4.9 - Micro-fluidics system [Tang, 2006].

The process chain for the part is illustrated in Figure 4.10. The master (positive structure) was in aluminium, which means that a minimum tool wear and a good surface quality can be reached using micro milling. Afterwards pre-treatments were applied to the master, including cleaning and deposition of a thin copper layer. During the electroforming process a thick and mechanically durable nickel layer was deposited. When it was thick enough to provide the required mechanical strength, the block constituted by the master and the insert was removed from the electroforming bath. The block was then mechanically machined in order to remove the material in excess and to produce a flat reference surface on the back of the insert. The next step was the selective etching of the master by immersion in a warm alkaline solution. Finally, the copper layer was cleaned and selective etched [Tang, 2006].
The benefits of this method are the ease machining of the master due to the soft aluminium alloy and the ease and fast machining of a “positive” structure than a “negative”.

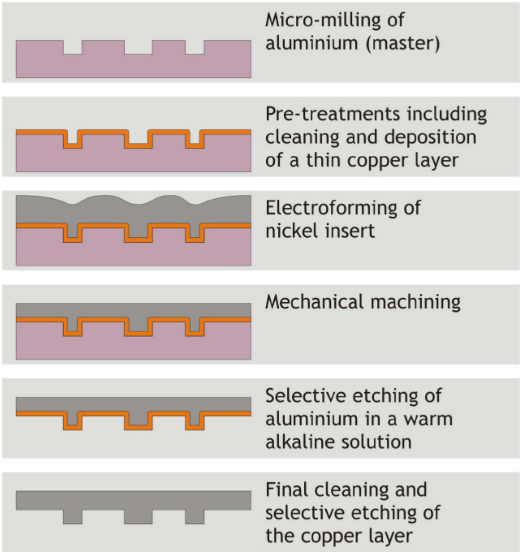

Figure 4.10 - Process chain for the micro-fluidics system [Tang, 2006].

4.4 Mould design for micro injection moulding – an example

The activities involved in the concept development phase comprise investigation of product concept feasibility and experimental prototyping as well as first analysis of production feasibility. In the design stage, choice of materials, definition of part geometry and tolerancing are determined together with production processes, tooling and quality assurance methods [Alting, 2003]. Having this in mind, a study was carried out with the aim of designing and fabricating an insert used in a micro injection process. The investigated part was the volume control of a hearing aid, see Figure 4.11.

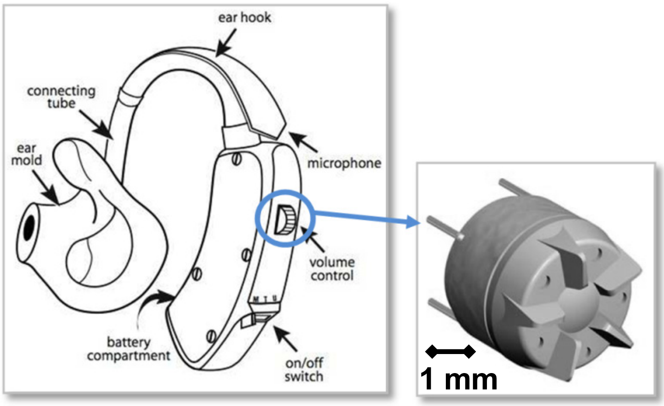

Figure 4.11 - Left: illustration of a hearing aid; right: illustration of a digital volume control of the type DCU 193 [Angel, 2009].

The drawing is illustrated in Figure 4.12 and the technical specifications of the part are given in Appendix 11.2 (the insert has been designed and fabricated in the frame of the collaborative EU project COTECH).

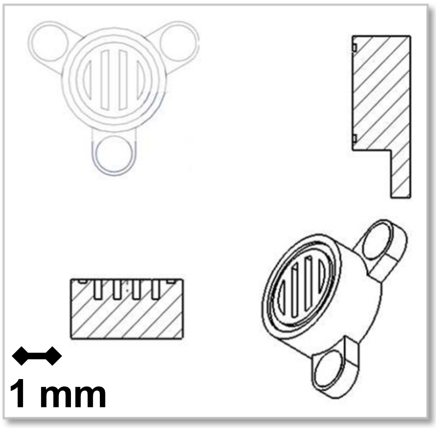

Figure 4.12 - Volume control drawing and its cross sections [Angel, 2009].

The insert fabrication had some crucial requirements to be satisfied and to be taken into account during the design phase:

1. The insert should be easy to produce, easy to replace and interchangeable;
2. Ejectors had to be made in order to push the polymer item out of the mould when it solidified without deformation or breakage;
3. Avoid sharp corners to prevent cracks;
4. Avoid adhesion between the polymer part and the insert;
5. Satisfy typical requirements of the insert manufacturing phase for these components, see Table 4.3.

Processes capabilities for the insert	
Micro structured area [mm]	2 x 2
Maximum valid tool size [mm]	0.1
Minimum feature dimension [μm]	100
Accuracy [μm]	± 10
Aspect ratio	2.5
Roughness, Ra [μm]	0.8
Material removing rate [mm^3/min]	Fast as possible

Table 4.3 - Manufacturing requirements for the insert used in the injection moulding of a volume control for hearing aid [Angel, 2009].

For this reason the design phase was divided into five steps so that the previous requirements could be satisfied:

1. In order to obtain a flexible and interchangeable insert, it was designed with a pin shape. A course design was obtained subtracting the polymer part from the insert design as shown in Figure 4.13(1);
2. Three ejectors were placed on the flanges of the polymer part; therefore the insert was conceived having three holes in the base. These holes were used also to lock the insert to the tool plate, see Figure 4.13(2);
3. To avoid cracks in the tool the sharp corners were filled between the cylinder component and the base as shown in Figure 4.13(3);
4. Ribs were made with a draft angle of 4° to fulfil the fourth requirement: avoid adhesion between polymer part and insert, as shown in Figure 4.13(4);
5. In order to choose the most appropriate machining process, Table 4.3 was compared with the summary of the process capabilities in Table 4.2: the micro milling process was selected as it ensured a relatively short machining time.

Following the previous five steps, the insert design was finalized and the tool was manufactured, see Figure 4.13(5). Finally, an injection moulding process was performed and the polymer specimen was produced. The final part is shown in Figure 4.13(6).

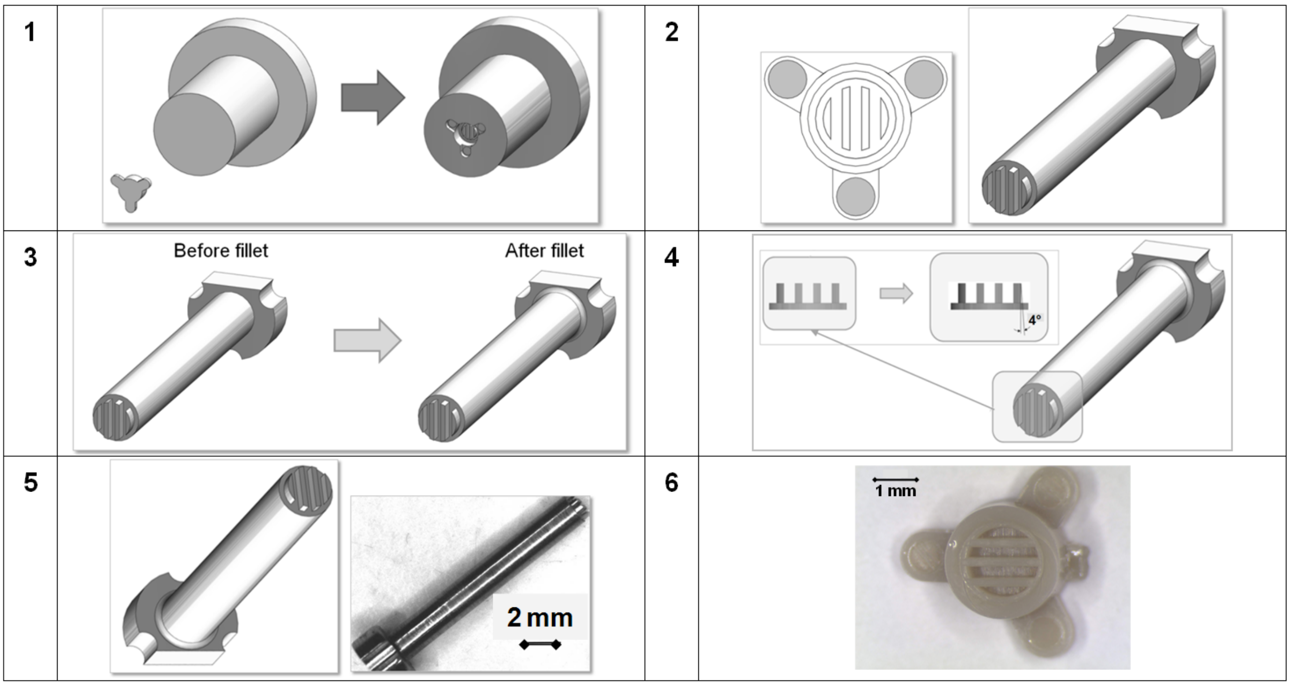

Figure 4.13 – Design phases of an insert used in the injection moulding of a volume control for hearing aid [Angel, 2009].

4.5 Hybrid tooling

In this paragraph, design for micro manufacturing rules is presented and applied. The aim is to improve the re-positioning and workpiece alignment when performing hybrid machining (in this specific case µ-milling and µEDM milling). A series of strategies were implemented according to four different designs. A metrological approach and calibrated measurements were carried out in order to perform a quantitative comparison with the currently employed technology.

When performing single machining process on different machines, the main alignment principle is actually to attach the coordinate reference system to the workpiece itself. After a first machining step, the following process should be able to detect such reference system and therefore re-align its machining chain according to the first one (see Figure 4.14).

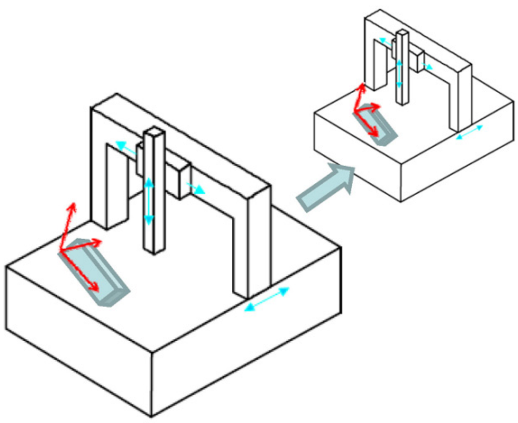

Figure 4.14 - Workpiece coordinate reference system transfer for processing (i.e. machining) on two different machines [Esmoris, 2011].

In the present investigation, a micro-fluidic design was selected for the machining experiments. It was characterized by two grooves in order to investigate the combination of the two machining processes, i.e. µ-milling and µEDM milling, (see Figure 4.15):

1. 600 µm wide, 5 mm long and 110 µm deep channel (i.e. *Mini channel*);
2. 100 µm wide, 5 mm long and 50 µm deep channel arranged on a 90° L-shaped (i.e. *Micro channel*).

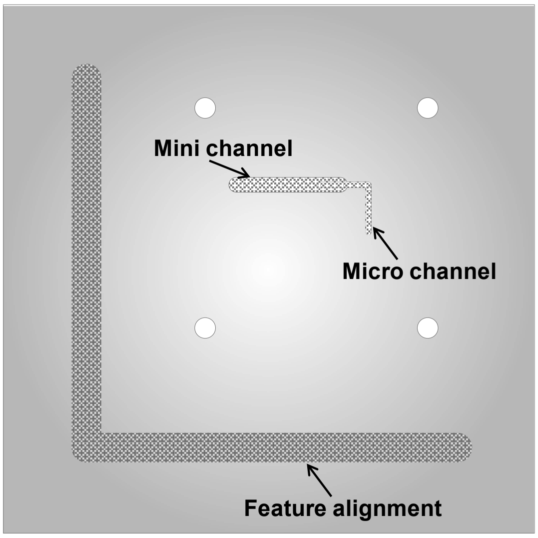

Figure 4.15 – Design of the micro-fluidic channel: "*Mini channel*" is the groove 600 μm wide, 5 mm long and 110 μm deep. "*Micro channel*" is the groove 100 μm wide, 5 mm long and 50 μm deep arranged on a 90° L-shaped.

Four different designs were produced depending on different steps of feature-aided tool transfer strategy in order to improve the alignment accuracy:

- **1A**: without feature alignment + pocketing only by μ-milling + μ-channel by μEDM;
- **2A**: with feature alignment + pocketing only by μ-milling + μ-channel by μEDM;
- **1B**: without feature alignment + pocketing by μ-milling + μ-channel and groove finishing by μEDM;
- **2B**: with feature alignment + pocketing by μ-milling + μ-channel and groove finishing by μEDM.

The feature alignment had a 90° L-shaped and is shown in Figure 4.15

In order to cut the tool insert out of the starting block, all 4 designs were provided with 4 micro holes (500 μm diameter) to be employed in a final micro wire EDM stage, see Figure 4.15. The 4 holes were manufactured using the same precision milling centre and in the same machining chain as the micro milled feature.

Micro milling was performed using a precision 5-axis machining centre. The employed micro milling tool had a diameter of 500 μm, see Figure 4.16 on the left.

Micro EDM milling was performed using a μEDM milling machine. An electrode with an 80 μm diameter was employed during the machining, see Figure 4.16 on the right.

Figure 4.16 – Left: micro milling step; right: μEDM machine employed for the hybrid tooling experiments [Esmoris, 2011].

The results of the four hybrid tooling strategies are illustrated in Figure 4.17: it is clearly visible that the distance between the axes of the two channels in the specimens without the feature alignment (**1A** and **1B**) was larger than the axes distance obtained for the specimens with the feature alignment (**2A** and **2B**).

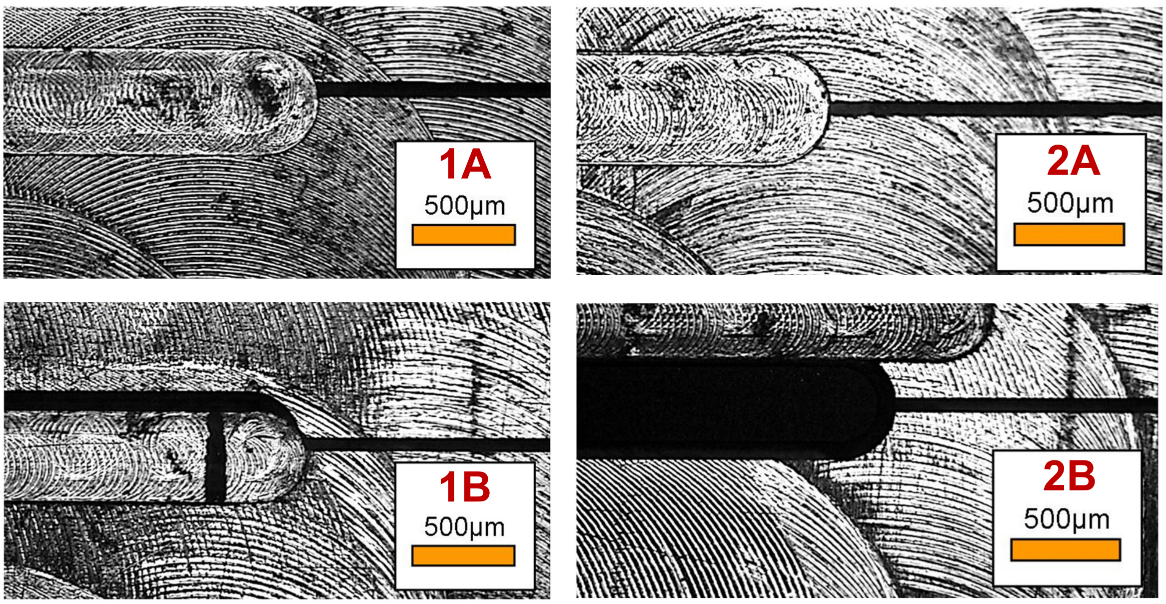

Figure 4.17 – Hybrid tooling results **1A** (without feature alignment + pocketing only by μ-milling + μ-channel by μEDM), **2A** (with feature alignment + pocketing only by μ-milling + μ-channel by μEDM), **1B** (without feature alignment + pocketing by μ-milling + μ-channel and groove finishing by μEDM) and **2B** (with feature alignment + pocketing by μ-milling + μ-channel and groove finishing by μEDM).

After the production of the four tool-transfer approaches, the four machined workpieces were measured using the optical coordinate measuring machine described in appendix 11.1.6. The aim of the measurements was to create the background set of data for the quantitative comparison depending on the employed design (and workpiece/micro features alignment strategy).

The measurands considered to evaluate the effect of the different tool-transfer strategies were width, length, depth of the grooves and errors between the channels (i.e. perpendicularity, straightness and parallelism). The two most important measurands are illustrated in Figure 4.18. They take into account the parallelism between the axis of the mini channel and the micro channel and the distance between the axes of the two channels.

a)
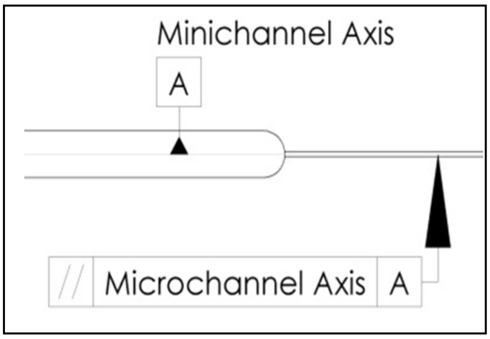

b)
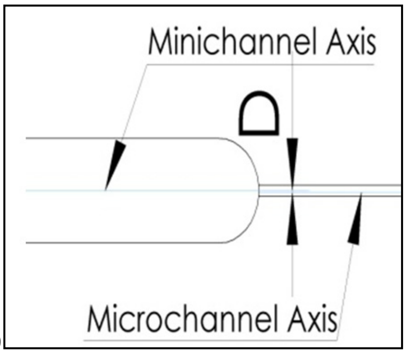

Figure 4.18 – a) Parallelism between the axis of the mini channel and micro channel; b) Distance between the axis of the mini channel and the axis of the micro channel.

Micro-machining strategies based on best practices of operators are not enough in order to prevent inaccuracies on micro-size features (e.g. dimensional, geometrical, alignment/work-piece relocation). Therefore activities focused on minimizing machining errors (e.g. machine thermal compensation, tool length control and repositioning strategies based on previous machined micro-features) are requested.

From the investigation, the micro-milling/micro-EDM process hybridisation (based on strategies supported by alignment features) contributed to a 50% decrease of parallelism error between mini and micro channels and to a 70 - 85% decrease of error on the distance between mini and micro channels axis [Tosello, 2010].

4.6 Process chain characterization - an example

The challenging step in the manufacturing process of a speaker house for a hearing aid component is the production of the mould. For the current case study, the insert fabrication is made by die sinking EDM. The electrodes are made in copper and machined by milling or EDM-based technology. Before die-sinking EDM, their surfaces are finished in order to achieve a roughness average (Ra) of 0.8 – 1.6 µm. Due to the electrode wear, two electrodes are usually made for each process. It is not unusual that their manufacture fails due to broken tools or due to wrong dimensions since it is difficult to maintain a standard guidance every time an order of a prototype arrives [Hedegaard, 2009].

The speaker house of a hearing aid component is shown in Figure 4.19a. The workpiece, its mould (Figure 4.19b) and the electrode (Figure 4.19c) were investigated with the aims of:

1. Defining the size of the sparking gap during a die-sinking EDM process;
2. Characterizing the electrode, the mould and the workpiece through dimensional and roughness measurements.

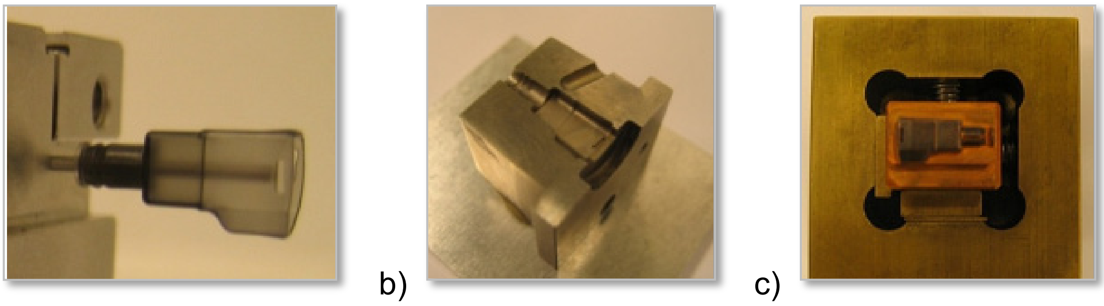

a) b) c)

Figure 4.19 – a) Speaker house of a hearing aid; b) Mould of the speaker house; c) Electrode used for the production of the mould [Hedegaard, 2009].

The workpiece was made by an injection moulding process and the involved mould was produced by die-sinking EDM. During this process the electrode moved in spherical paths of 50 µm radius as it is shown in Figure 4.20. It is, therefore, expected a deviation of 100 µm along *x* and *y* dimensions of the mould and the electrode.

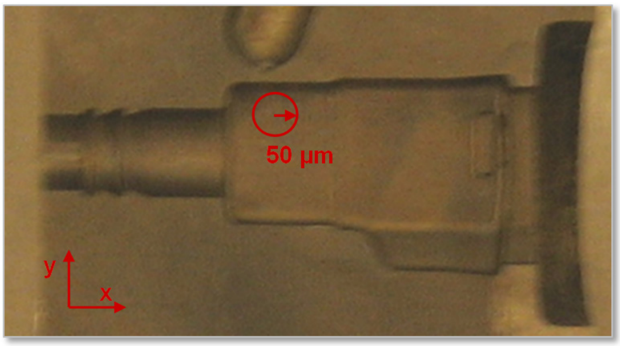

Figure 4.20 - Spherical paths of the electrode during the EDM process.

The electrode was made in copper using a milling centre machine with an accuracy of ± 1 µm. A finishing process was necessary before entering the production line. The black surface visible in Figure 4.19c is leftover from the sparking process made by chips of the electrode (copper) and the workpiece (steel). It was assumed that the surface was changed during the die sinking process. Moreover the process was divided into several electrodes due to limited availability of the machining tools. The division of the electrodes is often done during the machining of ribs and grooves especially when the distance between the features is too small to be accessed by the cutting tool. The division is sketched in Figure 4.21.

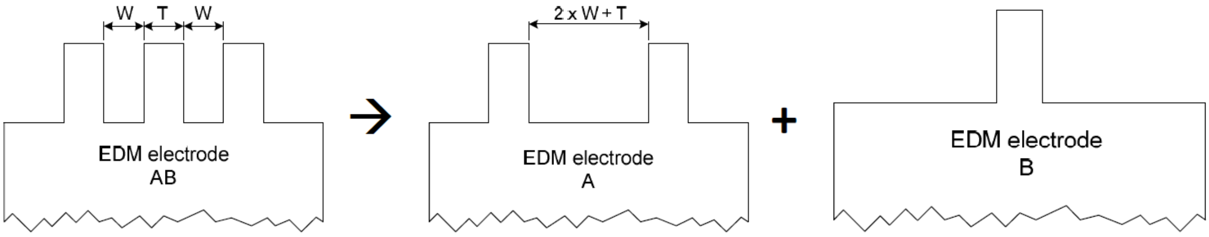

Figure 4.21 - Division of the electrodes used for the mould production of a speaker house [Hedegaard, 2009].

Since the distance *W* between the pins of the electrode *AB* was too small to be accessed by the milling tool, the electrode *AB* was split into electrode *A* and electrode *B*. In this way, the electrode *A* presented a distance between the pins increased of two times *W* plus the thickness *T* of the feature and the electrode *B* got unlimited access for the cutting tool.

In order to characterize the electrode, the mould and the workpiece, some features were defined as critical. These features, sketched in Figure 4.22, were:

- *X1* = distance along the *x* axis from the oblong hole until the middle part;
- *X2* = distance along the *x* axis from the middle part until the second thread;
- *Y1*, *Y2* = distances along the *y* axis across the part;
- *Y3* = diameter of the cylindrical section.
- *R1*, *R2* = areas chosen for the roughness measurements. The nominal roughness was defined to be 0.8 μm.

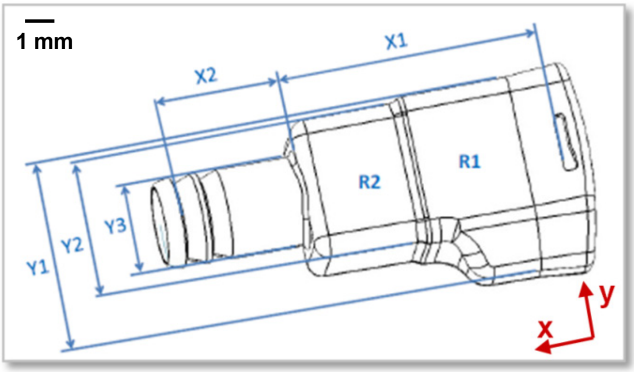

Figure 4.22 – Investigated critical features of a speaker house [Hedegaard, 2009].

Note that only the specifications of the roughness values were given by the manufacturer. For the other dimensions, it was performed only a comparison of the measurements between mould-electrode and between workpiece-mould.

The dimensional measurements were carried out using the InfiniteFocus instrument and the tactile coordinate machine described, respectively, in appendix 11.1.5 and 11.1.6.
Figure 4.23 shows the deviation of the mould results from the electrode ones. The optical measurements revealed to be the most inaccurate as it was proved by the large error bars (standard deviations of the measurements) on the blue columns. The main issue was to identify the exact edge of the part and to understand where the feature was starting and where was ending. On the other hand, the problems with the tactile instrument were of a different nature: it was difficult to know whether the probe was approaching the right measuring point.

According to the principle of the machining process, the expected deviation of the mould from the electrode was 100 µm along both *x* and *y* axis. This means that the mould dimensions should be larger than the electrode ones. Looking at Figure 4.23, it is not possible to give an estimation of the sparking gap due to the deviations completely different from feature to feature. Moreover, for two distances (*X2* and *Y2*) the deviation was even negative. This is not possible according to the process principle.

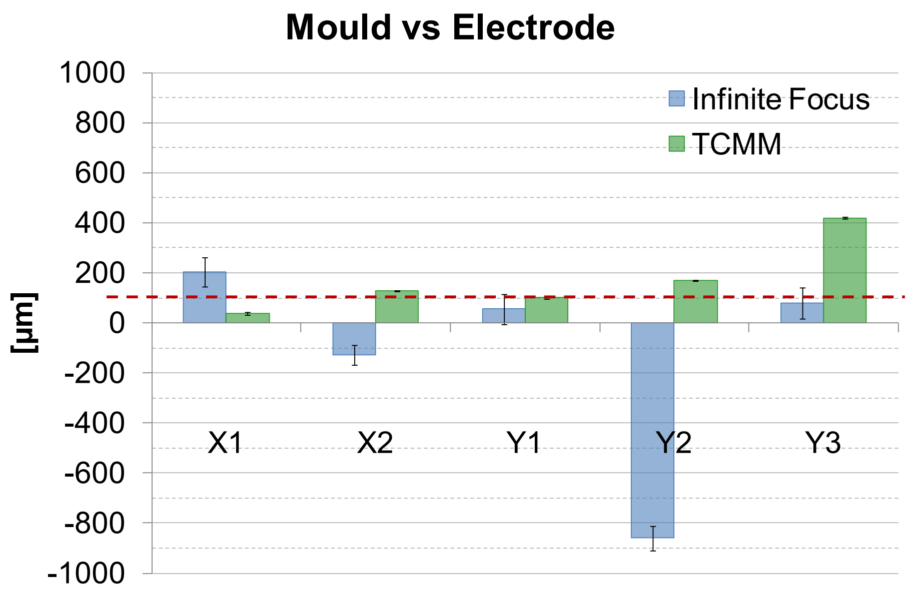

Figure 4.23 - Deviation of the mould dimensional results from the electrode ones for the distance *X1*, *X2*, *Y1*, *Y2* and *Y3*. They were obtained using an optical instrument, *Infinite Focus*, and a tactile coordinate measuring machine, *TCMM*. The red dashed line represents the expected deviation (100 µm) due to the machining process.

Figure 4.24 shows the deviation of the workpiece results from the mould ones. There was no agreement between the results achieved using the two measuring instruments. The reasons were related to the previous discussion.

Therefore, as conclusion, the results could not be seen reliable for the estimation of the sparking gap and, moreover, the characterization of the workpiece, the mould and the electrode was not exhaustive due to the different issues in the measurements analyses.

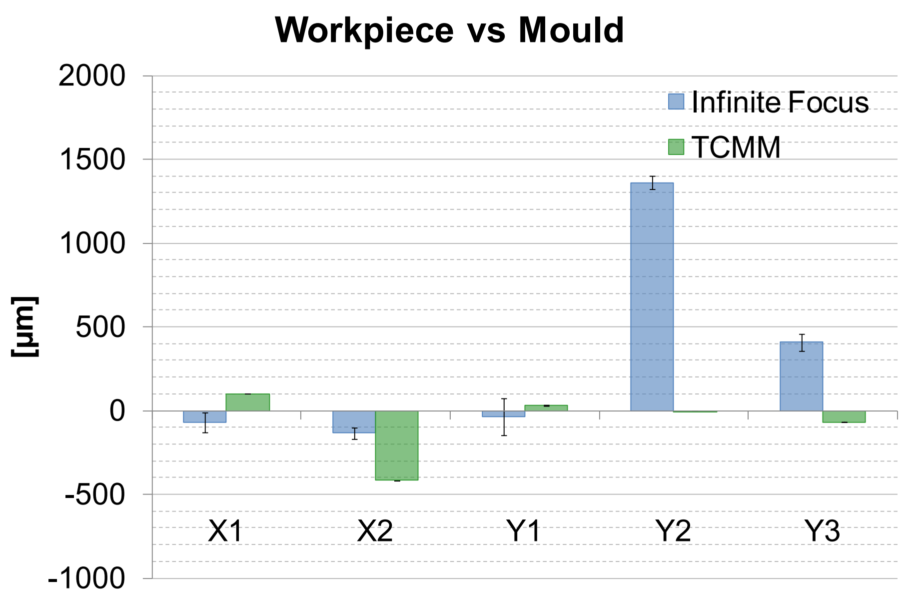

Figure 4.24 - Deviation of the workpiece dimensional results from the mould ones for the distance *X1*, *X2*, *Y1*, *Y2* and *Y3*. They were obtained using an optical instrument, *Infinite Focus*, and a tactile coordinate measuring machine, *TCMM*.

The roughness measurements were performed using the InfiniteFocus instrument and the stylus profilometer described, respectively, in appendix 11.1.5 and 11.1.2.

Figure 4.25 shows the deviation of the mould roughness results from the electrode ones.

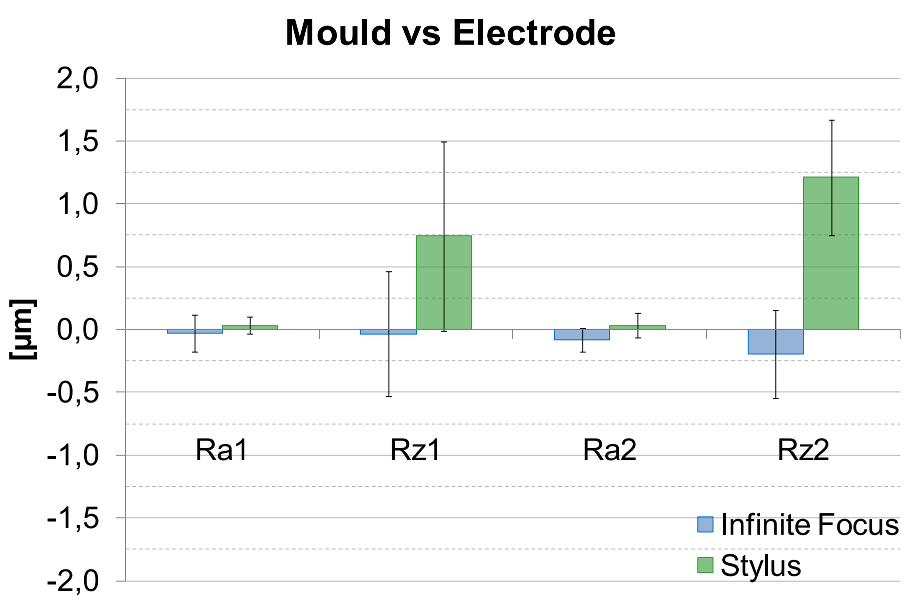

Figure 4.25 - Deviation of the mould roughness results from the electrode ones in the areas R1 (*1*) and R2 (*2*). They were obtained using an optical instrument, *Infinite Focus*, and a stylus profilometer, *Stylus*.

In this case no particular problems were found during the measurement procedure. The nominal roughness (*Ra*) given by the manufacturer was 0.8 µm. This value was both verified by the optical and the contact measurements.
Looking at Figure 4.25, the deviation of the *Rz* values obtained from the roughness profilometer was 50% larger than the optical one. *Rz* represents the maximum height of the traced profile; therefore it is sensitive to the measuring principle of the instrument and to any kind of dust or damage on the surface.

Figure 4.26 shows the deviation of the workpiece roughness results from the mould ones. No challenges were found during the measurement procedures and the two instruments agreed on the results. As it was expected, the roughness of the polymer part is lower than the roughness of the mould.

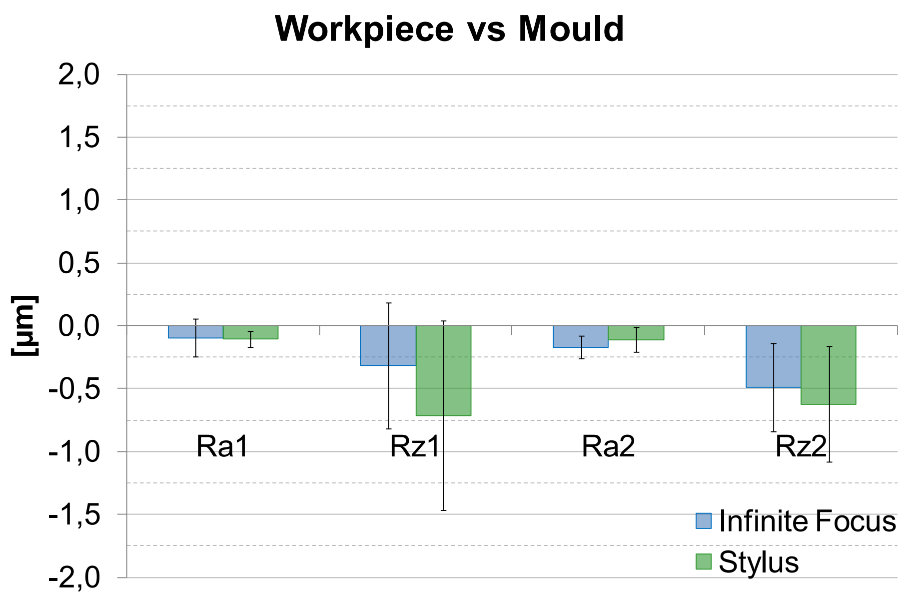

Figure 4.26 - Deviation of the workpiece roughness results from the mould ones in the areas R1 (*1*) and R2 (*2*). They were obtained using an optical instrument, *Infinite Focus*, and a stylus profilometer, *Stylus*.

4.7 Conclusion

The development and manufacture of a product are described by the process chain: a physical flow which starts with the image or concept of the product and ends with its physical realization. One of the main challenges related to the micro manufacturing is to establish a continuous and coherent flow due to the different and diverse required competences.

Firstly, the chapter introduced an overview of the available micro-manufacturing technologies, focusing on the tooling fabrication for injection moulding. Mould making is an important phase of the process chain since mass production of micro parts is mostly based on replication technologies. Process capabilities in terms of precision, geometry realization, material interaction, etc determine which processes should be applied for a given micro product.

The second part of the chapter presented three case studies extracted from three different phases of their process chain (i.e. design, tool fabrication and process control).

During the design study, some design solutions were given as example in order to satisfy specific technical requirements of a micro part.

In the tool fabrication phase, critical steps of tool fabrication were presented, such as the alignment during machining. The best practices of operators are usually not enough to prevent inaccuracies on micro-size features. Experimental results showed that hybrid strategies, e.g. combination of μ-milling and μ-EDM milling, should be applied in order to minimize machining errors.

Finally, for the process control, the process chain of a speaker house was characterized through dimensional and roughness measurements. The measurements were carried out on the electrode, on the mould and on the workpiece to describe the manufacturing process during its different phases. The measurements led to no significant conclusions, however a deeper investigation on the process control approach is presented in chapter 7 and 8.

4.8 References

[Adams, 2000] D.P. Adams, M.J. Vasile, A.S.M. Krishnan, "Microgrooving and microthreading tools for fabricating curvilinear features", Precision Engineering, 2000, Volume 24, pp. 347-356.

[Adams, 2001] D.P. Adams, M.J. Vasile, G. Benavides, A.N. Campbell, "Micromilling of metal alloys with focused ion beam-fabricated tools", Precision Engineering, Volume 25, Issue 2, pp. 107-113

[Alting, 2003] L. Alting, F. Kimura, H.N. Hansen, G. Bissacco, "Micro engineering", Annals of the CIRP, 2003, Volume 52, Issue 2, pp.635-657.

[Angel, 2009] J.A.B. Angel, "Design and fabrication of tool insert for micro injection moulding", Department of Manufacturing Engineering and Management, Technical University of Denmark, 2009.

[Azcarate, 2006] S. Azcarate, L. Uriarte, S. Bigot, P.J. Bolt, L. Staemmler, G. Tosello, S. Roth, A. Schoth, "Hybrid tooling: a review of process chains for tooling microfabrication within 4M", 2nd International Conference on Multi-Material Micro Manufacture (4M), 2006, pp. 305-308.

[Bissacco, 2004] G. Bissacco, "Surface generation and optimization in micromilling", PhD thesis, Department of Manufacturing Engineering and Management, Technical University of Denmark, 2004.

[Bissacco, 2005] G. Bissacco, H.N. Hansen, P.T. Tang, J. Fugl, "Precision manufacturing methods of inserts for injection molding of microfluidic systems", ASPE Spring Topical Meeting on Precision Micro/Nano Scale Polymer Based Component & Device Fabrication, 2005, Volume 35, pp. 57-63.

[Brinksmeier, 2001] E. Brinksmeier, O. Riemer, R. Stern, "Machining of precision parts and microstructures", Proceedings of the 10th ICPE Conference, 2001, pp. 3–11.

[Brousseau, 2010] E.B. Brousseau, S.S. Dimov, D.T. Pham, "Some recent advances in multi-material micro- and nano-manufacturing", Int J Adv Manuf Technol, 2010, Volume 47, Numbers 1-4, pp. 161-180.

[Esmoris, 2011] J.I Esmoris, G. Tosello, G. Bissacco, "Report on design rules of μ-tools for hybrid tooling", EU-project COTECH (COnverging TECHnologies for micro systems manufacturing) report; SP2-Tooling. WP2.2-New tool-making solutions for μ-IM and HE, (Grant Agreement no.: CP-IP 214491-2 COTECH) English, 2011, pp 1-64.

[Gasparin, 2010] S. Gasparin, G. Tosello, H.N. Hansen, “Tolerance verification of micro and nano structures on PC substrates”, 7th International Conference on Multi-Material Micro Manufacture (4M/ICOMM 2010), pp. 387-390.

[Hansen, 2006] H.N. Hansen, K. Carneiro, H. Haitjema, L. De Chiffre, “Dimensional micro and nano metrology”, Annals of CIRP, 2006, Volume 55, Issue 2, pp.721-743.

[Hansen, 2011(1)] H.N. Hansen, S. Gasparin, R. Sobiecki, J. Grønbæk, R. Lazarev, “Characterization of ultra-fine surfaces produced by robot assisted polishing”, 13th International conference on metrology and properties of engineering surfaces, 2011, pp. 244-248.

[Hansen, 2011(2)] H.N. Hansen, R.J. Hocken, G. Tosello, ”Replication of micro and nano surface geometries”, Annals of CIRP, 2011, Volume 60, pp.695-714.

[Hedegaard, 2009] M. Hedegaard, “Process chains for establishing tooling for micro manufacturing”, Department of Manufacturing Engineering and Management, Technical University of Denmark, 2009.

[Masuzawa, 2000] T. Masuzawa, “State of the art in micromachining”, Annals of the CIRP, 2000, Volume 49, Issue 2, pp.473-488.

[McGeough, 2001] J.A. McGeough, M.C. Leu, K.P. Rajurkar, A.K.M. De Silva, Q. Liu, “Electroforming process and application to micro/macro manufacturing”, Annals of CIRP, 2001, Volume 50, Issue 2, pp. 499-515.

[Ohmori, 2001] H. Ohmori, N. Ebizuka, S. Morita, Y. Yamagata, H. Kudo, “Ultraprecision microgrinding of germanium immersion grating element for mild-infrared super dispersion spectrograph”, Annals of CIRP, 2001, Volume 50, Issue 1, pp. 221-224.

[Qin, 2010] Y. Qin, A. Brockett, Y. Ma, A. Razali, J. Zhao, C. Harrison, W. Pan, X. Dai, D. Loziak, “Micro-manufacturing: research, technology outcomes and development issues”, Int J Adv Manuf Technol, 2010, Volume 47, Numbers 9-12, pp. 821-837.

[Schaller, 1999] Th. Schaller, L. Bohn, J. Mayer, K. Schubert, “Microstructure grooves with a width of less than 50 µm cut with ground hard metal micro end mills”, Precision Engineering, 1999, Volume 23, pp. 229-235.

[Sole, 1994] M.J. Sole, "Electroforming: methods, materials and merchandise", Journal of the Minerals Metals and Materials Society, Volume 46, pp. 29-35.

[Strecon, 2011] http://www.strecon.com/, 2001.

[Tang, 2006] P.T. Tang, J. Fugl, L. Uriarte, G. Bissacco, H.N. Hansen, "Indirect tooling based on micromilling, electroforming and selective etching", 2nd International Conference on Multi Material Micro Manufacture (4M), 2006, pp. 183-186.

[Tosello, 2007(1)] G. Tosello, B. Fillon, S. Azcarate, A. Schoth, L. Mattsson, C. Griffiths, L. Staemmler, P.J. Bolt, "Hybrid tooling technologies and standardization for the manufacturing of inserts for micro injection molding", 65th Annual Technical Conference (ANTEC), 2007.

[Tosello, 2007(2)] G. Tosello, G. Bissacco, P.T. Tang, H.N. Hansen, P.C. Nielsen, "High aspect ratio micro tool manufacturing for polymer replication using µEDM of silicon, selective etching and electroforming". Microsystem Technologies, 2007, Volume 14, Issue 9-11, pp. 1757-1764.

[Tosello, 2008] G. Tosello, "Precision moulding of polymer micro components", PhD thesis, Department of Manufacturing Engineering and Management, Technical University of Denmark, 2008.

[Tosello, 2010] G. Tosello, S. Gasparin, A. De Grave, H.N. Hansen, "Report on tool transfer and alignment methods", EU-project COTECH (COnverging TECHnologies for micro systems manufacturing) report; SP2-Tooling. WP2.2-New tool-making solutions for µ-IM and HE, (Grant Agreement no.: CP-IP 214491-2 COTECH) English, 2010, pp 1-42.

[Uhlmann, 2005] E. Uhlmann, S. Piltz, U. Doll, "Machining of micro/miniature dies and moulds by electrical discharge machining - Recent development", Journal of Materials Processing Technology, 2005, Volume 167, Issues 2-3, pp. 488-493.

[Watson, 1989] S.A. Watson, "Modern electroforming", Transactions of the Institute of Metal finishing, 1989, Volume 67, pp. 89-94.

[Weule, 2001] H. Weule, V. Huntrup, H. Tritschler, "Microcutting of steel to meet new requirements in miniaturization", Annals of CIRP, 2001, Volume 50, Issue 1, pp. 61-64.

5. Surface wear of micro structured tools during injection moulding

5.1 Introduction

Injection moulding is an effective replication manufacturing technique for mass production of high value optical components such as high precision lenses [Michaeli, 2007] or micro/nano optics [Kang, 2004], [Yoon, 2006]. Precision moulding of polymer micro structured surfaces with optical quality poses challenges in terms of tooling and replication because of the combination of high geometrical complexity and high accuracy.

The crucial steps of the process chain for manufacturing polymer micro-optics are:

a. Ultra-high accuracy micro machining of the mould cavity with nanometre (i.e. optical) surface finishing;
b. Achievement of an optimized injection moulding process to obtain high geometrical replication fidelity and optical surface finishing of the plastic part;
c. Capability of maintaining a repeatable replication moulding process over a large number of cycles (i.e. mass production capability).

This latter aspect is directly related to the repeatability of the moulding process (including injection moulding machine, process parameters and polymer material). Furthermore the mould cavity capability of maintaining its geometrical characteristics plays an important role for the whole production. This means that the tool wear should not compromise the integrity of the tool and consequently the quality of the moulded optical part (especially on the micro structured area) [Tosello, 2012].

Recent studies have shown challenges in finding a suitable measuring instrument for the characterization of optical components, such as Fresnel lenses. Contact measurements could not be performed without damaging the high surface finishing of the components, while optical measurements could not be accurate due to the high surface slopes. To

overcome these challenges an optical profilometric method that works with transmitted light was proposed in [Antón, 2011] and an opal diffuser in [Chemisana, 2011].
In [Schmitt, 2006], the quality control of the manufacturing process was performed integrating a measurement system into an injection moulding machine. This set-up is quite challenging since it should be immune from machine vibrations, acoustic noise and air turbulences, unavoidable in a machine environment.
Yang proposed a hybrid device having the functionality of grating and Fresnel lenses at the same time. The device was made through a polydimethylsiloxane (PDMS) soft lithography and verified using an optical profilometer [Yang, 2010].

The present chapter deals with the characterization of two moulds used for the injection moulding of Fresnel lenses. In particular, the investigation focuses on the coating wear resistance during production: both moulds were in nickel, and one had a TiN coating on the surface. In order to perform the characterization, the inserts should be dismounted at each quality control step and positioned on the measuring instrument, making the whole procedure lengthy. A solution could be to integrate the measurement system into the manufacturing machine as proposed in [Schmitt, 2006], but the procedure is quite long and difficult to realize. Therefore the characterization was performed using the replica technique described in chapter 3. Afterwards, the replicas of the two moulds were measured using an InfiniteFocus instrument and inspected through SEM (Scanning Electron Microscope) imaging and EDS (Energy Dispersive Spectroscopy) analysis.
The main results of the present case study have been published in [Gasparin, 2012] and [Tosello, 2012].

5.2 Case description

The moulds investigated in the present study are used for the injection moulding of micro Fresnel lenses which were designed for a miniaturized portable lighting device for digital imaging. The production volume of the lenses forecast is in the order of 10^5 specimens/year, therefore a relatively long tool life is of paramount importance.
The two moulds were tested by injection moulding for a large number of cycles (24500) in a production environment. Both moulds were in nickel and one had an additional titanium

nitride (TiN) coating on the surface. TiN coating has been previously found to increase the wear resistance of substrates such as ceramic and hard metal (e.g. WC-Co) cutting tool inserts [Grzesik, 2011], [Settineri, 2005] as well as metal forming dies [Osakada, 2000].

The main investigated factors were:

- Evaluation of the replication fidelity through stability and reproducibility studies;
- Evolution of the wear on the micro structures as a function of the:
    a) Effect of TiN coating;
    b) Number of moulding cycles (surface wear was monitored at different intervals during the production until 24500 cycles);
    c) Distance of the lenses from the injection gate.

The two moulds are illustrated in Figure 5.1. The upper tool is the coated mould. As shown in the picture, the inserts are characterized by six pairs of Fresnel lenses.

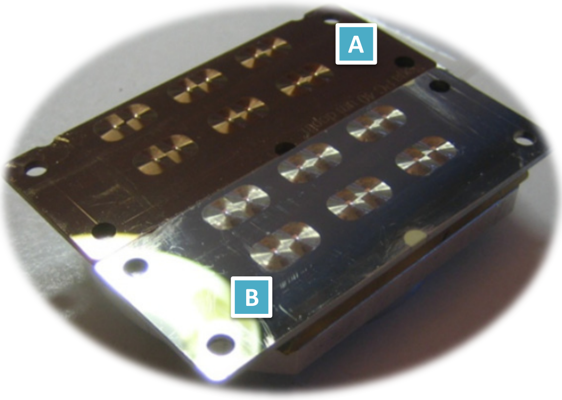

Figure 5.1 - Fresnel lenses moulds used for the micro tool investigation: (A) nickel insert with TiN coating, (B) nickel insert.

5.2.1 Tooling

The mould insert is made of nickel (Ni), obtained using an electroforming deposition process (see paragraph 4.2.3). The primary master geometry used for deposition is made of aluminium and generated by ultra-high-precision diamond cutting technology. It is subsequently replicated by nickel electroforming. The result is a 3D micro Fresnel lens geometry (see Figure 5.2) with an average surface roughness Sa = 3.3 nm measured by atomic force microscopy (AFM) (with an expanded measuring uncertainty of ± 1.3 nm, k = 2 and confidence level of 95%, estimated applying the GUM [GUM, 2008] and the method described in [Tosello, 2010]), suitable for optical applications at the nanometre scale.

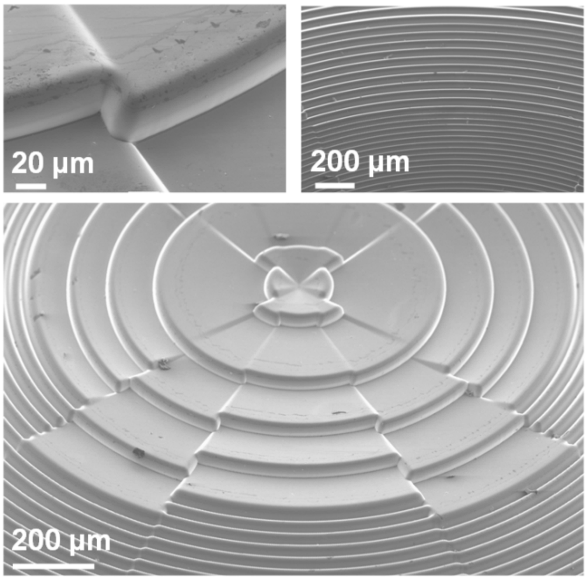

Figure 5.2 - Overview and geometrical details of one Fresnel lens in the mould.

The two nickel-plated plates were manufactured and cut by wire electrical discharge machining on a 30 x 80 mm^2 rectangular shape in order to be mounted on a two-cavity flexible mould capable of accommodating differently structured mould inserts (see Figure 5.3, left). One of the plates was then TiN coated. By mounting both plates in the two-cavity flexible mould, it was possible to mould the polymer Fresnel lenses from both the coated and uncoated insert during the same moulding cycle. Therefore both moulds were subject to analogous moulding processing conditions (Figure 5.3, right).

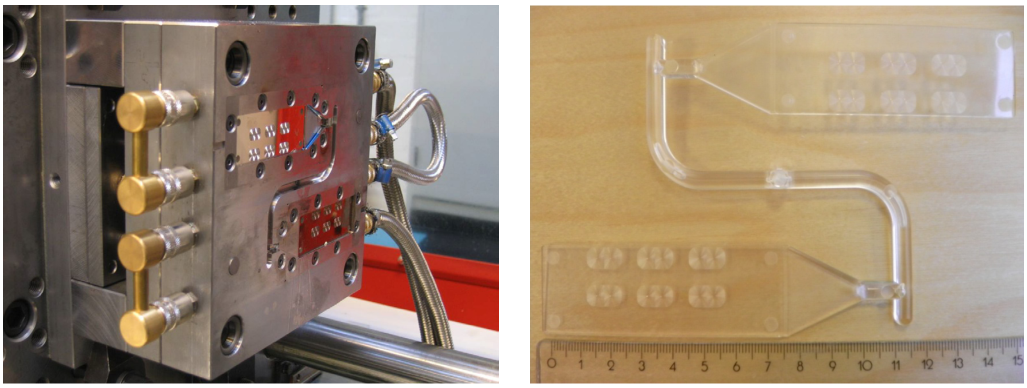

Figure 5.3 - Two-cavity flexible mould with both coated and non-coated micro Fresnel nickel tool inserts mounted (left); two-parts moulded parts: the six pairs of micro Fresnel lenses are visible on the surface of both components (material = polycarbonate) [Riel-Bachmann, 2011].

5.2.2 TiN coating

TiN coatings were prepared on the electroplated nickel substrate using a reactive pulsed magnetron sputtering. Magnetron sputtering is a widely used physical vapour deposition (PVD) technology employed to deposit thin films based on the generation of a magnetically enhanced glow discharge (i.e. the magnetron discharge). When a reactive gas such as nitrogen or oxygen is added to the discharge, it becomes possible to deposit the desired compound materials depending on the target material.

The process was aimed at obtaining a final coating thickness of 2 µm. As a result of the TiN deposition, the surface roughness of the tool insert increased to 13.6 nm (with an expanded measuring uncertainty of ± 4.0 nm, k = 2 and confidence level of 95% [GUM, 2008], [Tosello, 2010]). The newly obtained surface roughness was still suitable for optical application at the nanometre scale. The deposited TiN particles were also visible on the surface of the coated tool as compared with the uncoated Ni surface (see Figure 5.4) [Tosello, 2012].

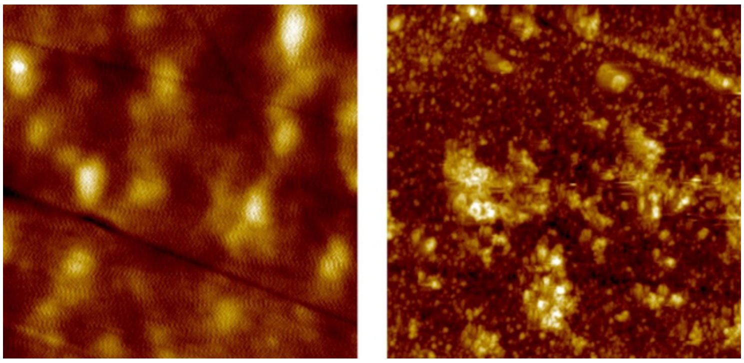

Figure 5.4 - AFM scannings (15 µm × 15 µm) of the nickel surface (left, Sa=3.3±1.3 nm) and the TiN coated surface (right, Sa=13.6±4.0 nm) [Tosello, 2012].

A tribology test and a nanoindentation hardness test were performed to characterize the TiN coated surface characteristics as compared with the uncoated Ni surface.

The tribology test was performed to determine the ability of the coating to resist wear under linear-oscillation motion. Results showed that the TiN coated surface had a slightly higher coefficient of friction (15 - 20%) than the uncoated nickel [Tosello, 2012].

Nanoindentation has established itself in the last decade as the fundamental quasi-non-destructive method for the evaluation of the mechanical response of small material volumes and thin films to applied loading [Lucca, 2010], [Bruzzone, 2008]. As such, nanoindentation tests were performed on both uncoated Ni and TiN coated specimen to evaluate the increase of hardness of the insert surface as consequence of the coating deposition process. Residual indentation depth of 0.238 µm and of 0.073 µm were obtained for the Ni and TiN coated specimens respectively with a repeatability of ± 0.003 µm. Indentation hardness of 3.00 ± 0.15 GPa for the Ni insert and of 12.77 ± 0.18 GPa for the TiN insert were obtained [Tosello, 2012].

5.2.3 Injection moulding

The polymer micro structured optical Fresnel lenses were injection moulded using a commercially available optical grade high-flow polycarbonate (Makrolon 2405 by Bayer MaterialScience). Injection mouldings were executed on a conventional injection moulding machine with a reciprocating screw of diameter of 35 mm and a clamping force of 60 kN. The injection moulding was set in order to provide similar conditions to those encountered during actual processing in order to comply with industrial requirements such as cycle time, optical functionality (i.e. surface replication) and tool wear conditions as experienced in production. For these reasons, a melt temperature of 295°C was selected close the maximum recommended from the material supplier in order to avoid polymer overheating and subsequent material degradation (which could compromise the optical performance of the lens) and to optimize polymer surface replication [Hansen, 2011]. A mould temperature of 90°C was set following the recommendations from the material supplier, in order to allow successful demoulding of the part from the cavity, to perform the injection process within a suitable cycle time (i.e. short cooling time) and maximize surface replication [Hansen, 2011]. An actual injection speed of 200 mm/s was used taking into account the machine capability. A high injection speed allows improving surface replication because reduces cavity injection time avoiding polymer premature freezing. A maximum injection pressure of 900 bar was reached. A total cycle time of 15 s was obtained including packing, cooling and demoulding phases [Tosello, 2012].

5.2.4 Replica set-up

As explained in the introduction, characterization of optical devices is a challenging task using contact instruments (damages could be left on the surface) and optical instruments (measurements could be inaccurate due to the surface high slopes and transparency).

A tactile measurement was attempted on the polymer micro Fresnel lenses using the stylus profilometer described in appendix 11.1.1.

Figure 5.5 illustrates the profile of a Fresnel lens traced by the contact instrument.

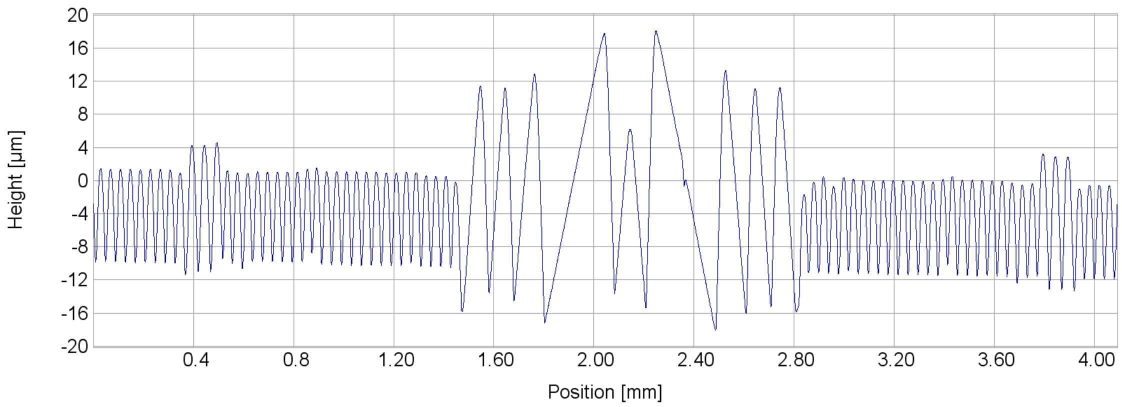

Figure 5.5 – Profile traced by the stylus instrument on a polymer micro Fresnel lenses.

Figure 5.6 shows the SEM pictures made on the measured area of the polymer part. It is evident that the stylus profilometer damaged the ribs of the lens leaving very well defined traces. Note that the force of the contact instrument was 1 mN according to the technical specifications given by the manufacturer.

This experiment demonstrated the usefulness of the replica technique.

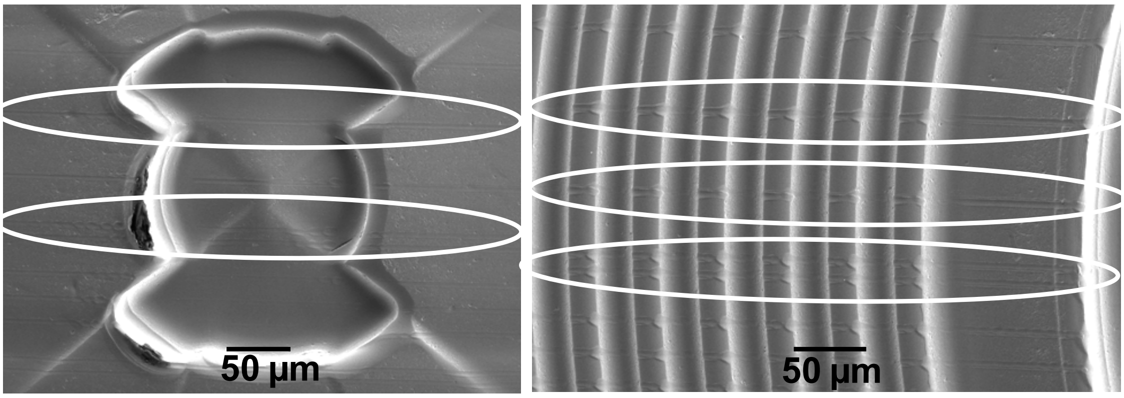

Figure 5.6 – Traces left on the polymer micro Fresnel lenses by the stylus instrument.

A replication mould device that could be easily mounted and removed from the mould was designed and manufactured to solve the issue of disassembling the inserts from the injection moulding tool (Figure 5.7). Both mould inserts were cleaned using acetone prior the soft replication step to avoid that polymer residual could affect the replication fidelity of the surface. The used replica material was the red-soft compound studied in chapter 3.

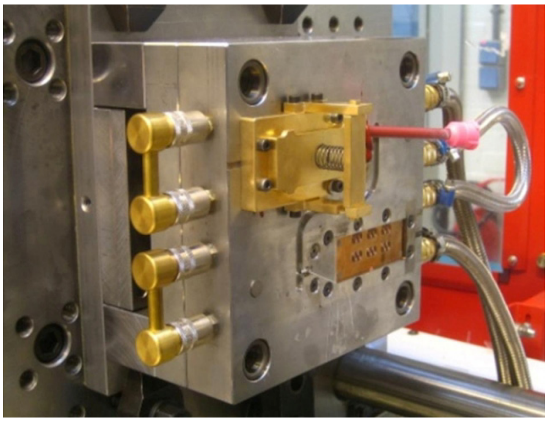
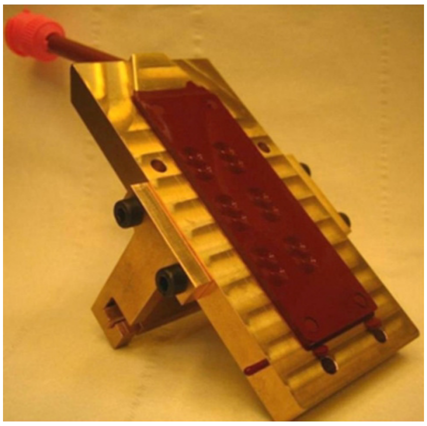

Figure 5.7 - Replication mould device mounted on the injection moulding tool (left); replication mould device disassembled from the injection tool and containing the soft replica of the insert (right) [Riel-Bachmann, 2011].

5.2.5 Micro dimensional geometrical metrology

The dimensions of the micro structures on the tool inserts were investigated at different production stages to evaluate the tool wear progress. A total number of 24500 injection moulding cycles were run. Dimensional measurements were carried out using the replica technique each 1000 - 2000 cycles with the tool inserts mounted on the mould during production. Once the replicas of the tool inserts were produced, they were measured using the InfiniteFocus instrument described in appendix 11.1.5. The measurements were carried out on the moulds replica of two selected lenses (Figure 5.8):

1. CLOSE: close to the injection gate because supposed to suffer the most stresses;
2. FAR: far from the injection gate because supposed to suffer the least stresses.

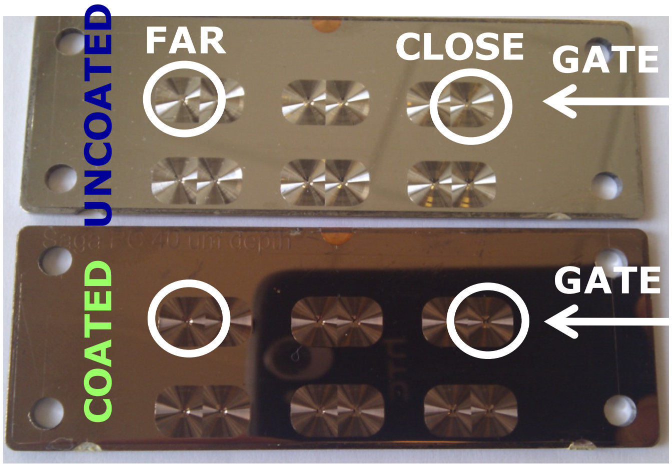

Figure 5.8 - The two selected lenses for the investigation in the uncoated and coated mould: one close to the injection gate (“*CLOSE*”) and one far from the injection gate (“*FAR*”).

For each lens, the measurements were performed in 10 small ribs left from centre, in 3 large ribs left from centre and in the centre feature in order to test both small and large geometries, see Figure 5.9.

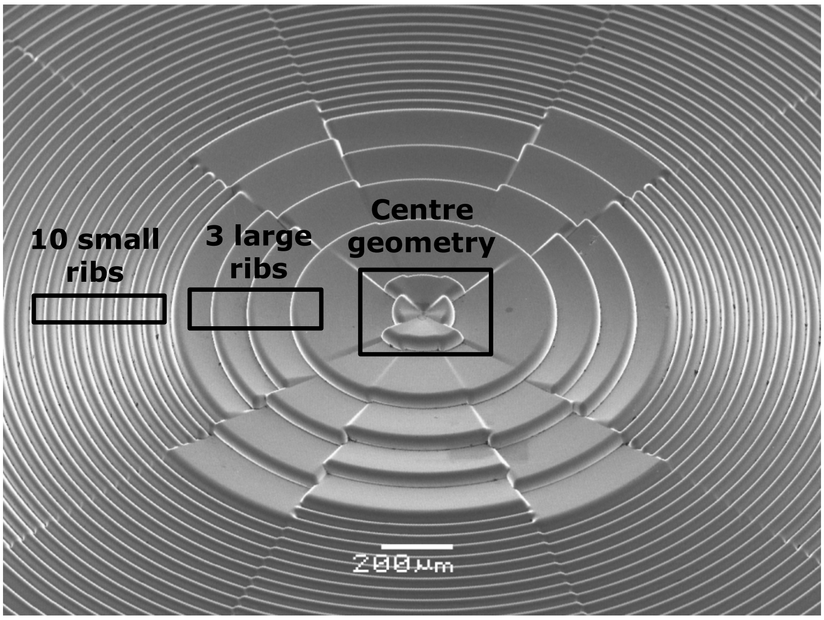

Figure 5.9 - Overview of the three investigated areas in one lens: 10 small ribs left from centre, 3 large ribs left from centre and centre geometry.

Examples of the measurements carried out in the three single areas are shown in Figure 5.10. The red colour of the picture is due to the fact that the InfiniteFocus instrument provides colour information registered together with the 3D data.

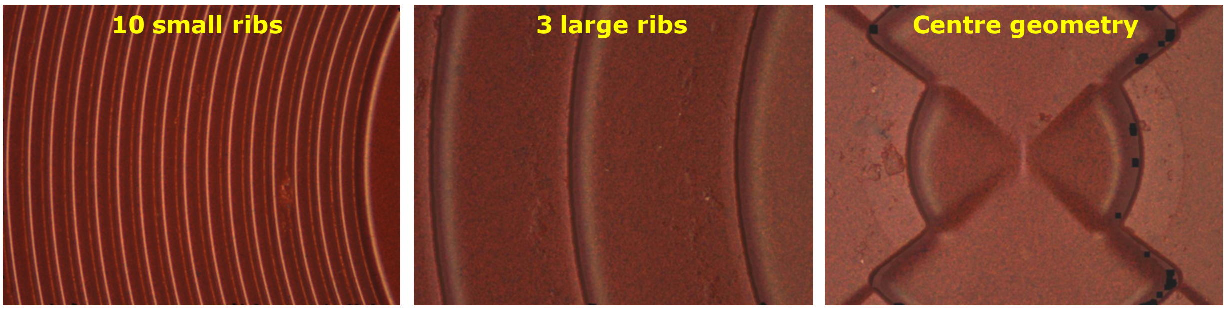

Figure 5.10 - Three measurements performed by the InfiniteFocus instrument in the three selected areas: 10 small ribs left from centre, 3 large ribs left from centre and centre geometry.

The average height of the ribs, as depicted in Figure 5.11, was chosen as the factor to monitor the tool wear progress. To calculate the rib height, a height distribution frequency analysis was performed. Such analysis allowed excluding the influence of ribs sidewalls, measuring the distance between the bottom and the plateau regions.

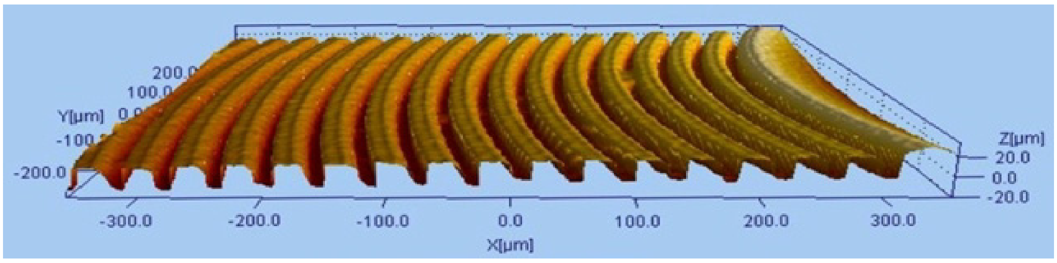

Figure 5.11 - Result of a three-dimensional optical scanning of the Fresnel lens tool soft polymer replica on the area with 23 µm high micro ribs.

The tool wear was also investigated through SEM - EDS technique, described in chapter 2, paragraph 2.2.3.2. This analysis needed the inserts to be dismounted in order to be placed inside the scanning electron microscope described in appendix 11.1.4.

Table 5.1 shows the present research carried out in four time periods between November 2010 and July 2011. The different production stages correspondent to:

- Optical measurements;
- Dismounting/mounting of the moulds from the injection moulding machine for SEM - EDS analysis.

N of cycles																				
0	50	500	1000	2000	3000	3750	5000	6000	7000	9000	11000	13000	14000	15000	16000	17000	19500	22000	23500	24500
SEM EDS				1			SEM EDS		SEM EDS		2			3		SEM EDS		4		SEM EDS
November 2010 - February 2011										May 2011			June 2011				July 2011			

Table 5.1 – Plan of the optical measurements and the inspections carried out between November 2010 and July 2011.

5.3 Replication fidelity results

The replication fidelity results were estimated comparing visually the replicas and the moulds through SEM pictures and evaluating the stability of the replica itself.

SEM pictures were performed in the same area of the lens far and near the gate of the replica and the corresponding insert. Table 5.2 shows that the replica material was able to replicate both the areas affected by tool wear as much as the polymer residuals from the injection moulding process.

	Replica	Mould
Lens close to gate	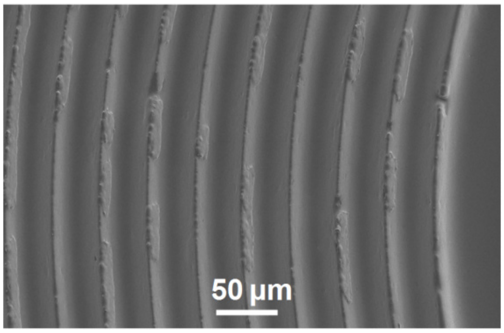	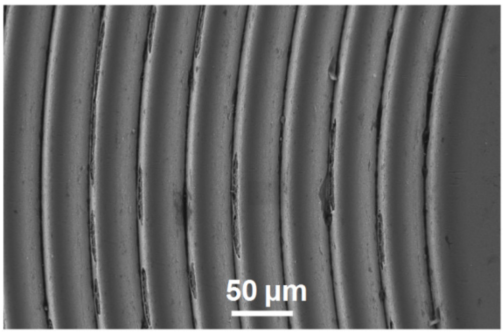
	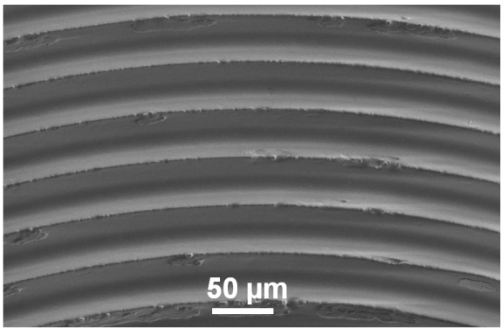	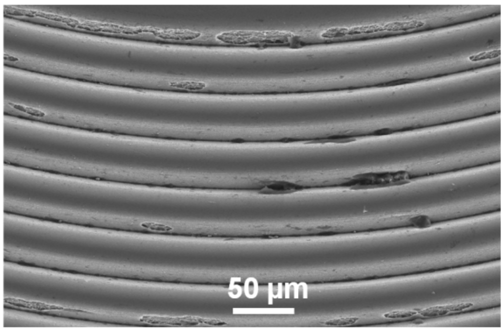
Lens far from gate	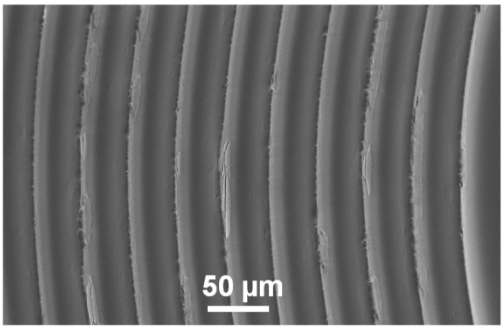	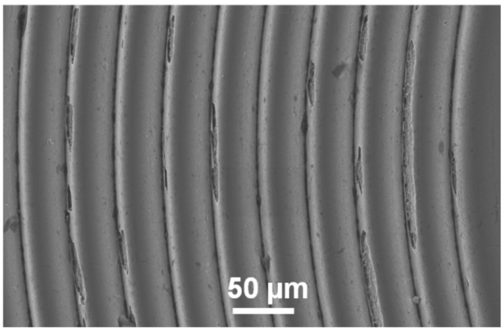
	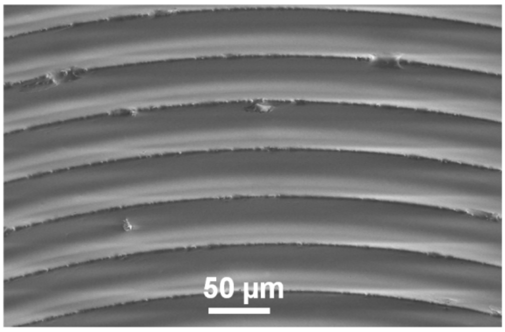	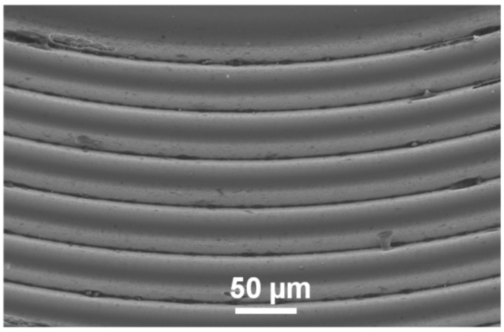

Table 5.2 – Visual comparison of the replica with the correspondent master (mould).

Figure 5.12 underlines the previous visual comparison. The yellow solid circles indicate wear on the coated mould; the white dash-dot circles indicate residuals of polymer material from the injection moulding process.

a) 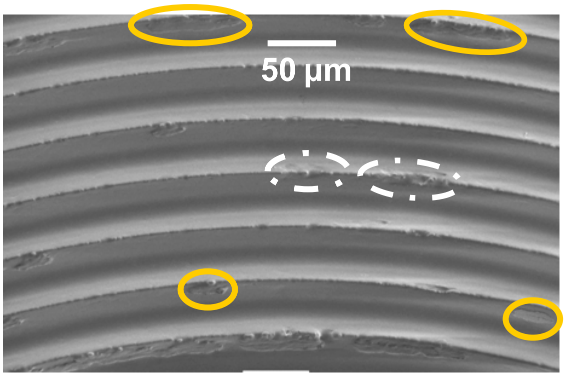

b) 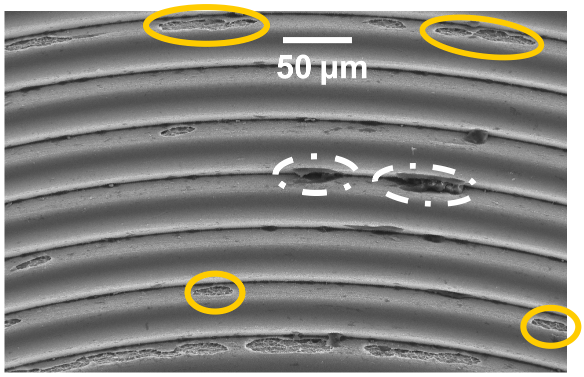

Figure 5.12 - a) SEM picture of the replica obtained from one lens detail of the coated mould after 24500 cycles; b) SEM picture of one lens detail of the coated mould (same spot of the Figure 6.10a) after 24500 cycles. Circles with the yellow solid line indicate the wear of the coated mould; circles with the white dash-dot line indicate residuals of polymer material from the injection moulding process.

Stability and repeatability studies were conducted on the tool replicas in order to ensure the reliability of the measurements over different periods of time. The results were shown in chapter 3, paragraph 3.4.2.1. As conclusion, measurements on replicated micro structures with a height of 23 µm could be reproduced within a range of 0.1 µm, 0.3 µm, and 0.4 µm in a period, respectively, of few minutes, 3 hours and 24 hours for 14 days. The combined standard uncertainty of the measurements was equal to 0.4 µm.

5.4 Dimensional measurements

The optical measurements carried out on the two lenses of the coated and uncoated moulds are illustrated in Figure 5.13, Figure 5.14, Figure 5.15 and Figure 5.16.

In particular, taking into account the three investigated areas:

1. *10 small ribs*: Figure 5.13 shows the average results of the replica measurements carried out on 10 small ribs of the lenses close and far from the gate during a production of 24500 cycles. A decreasing of 1 µm in average was found in both the lenses close and far from the gate and in both the Ni and TiN moulds.
2. *3 large ribs*: Figure 5.14 shows the average results of the replica measurements carried out on 3 large ribs of the lenses close and far from the gate during a production of 24500 cycles. No actual variations were detected.
3. *Centre geometry*: Figure 5.15 and Figure 5.16 shows the average results of the replica measurements carried out, respectively, on the right and on the left side of

the centre geometry of the lenses close and far from the gate during a production of 24500 cycles. Again no actual variations were detected.

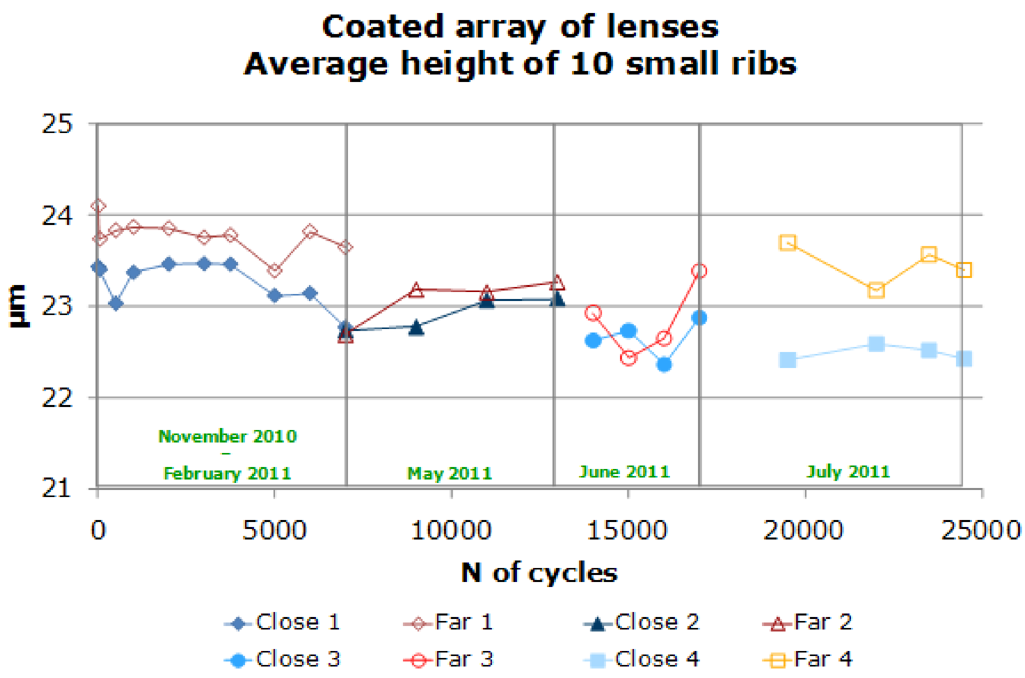

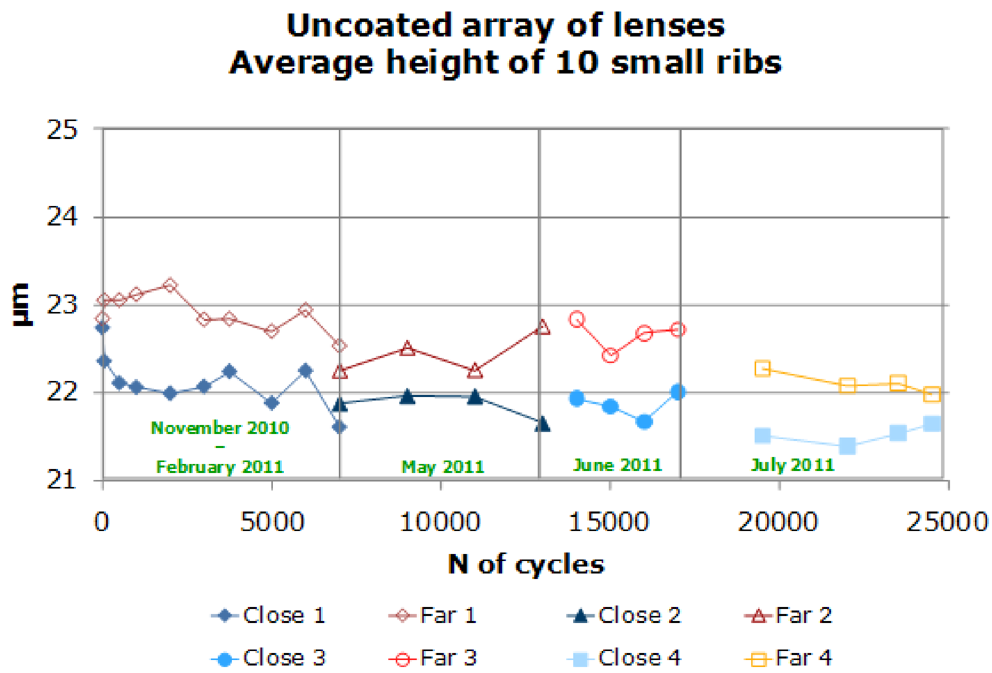

Figure 5.13 - Average height of 10 small ribs measured on two replica lenses close and far from the gate, during a production of 24500 cycles. The upper graph shows the results for the coated mould; the lower graph for the uncoated mould.

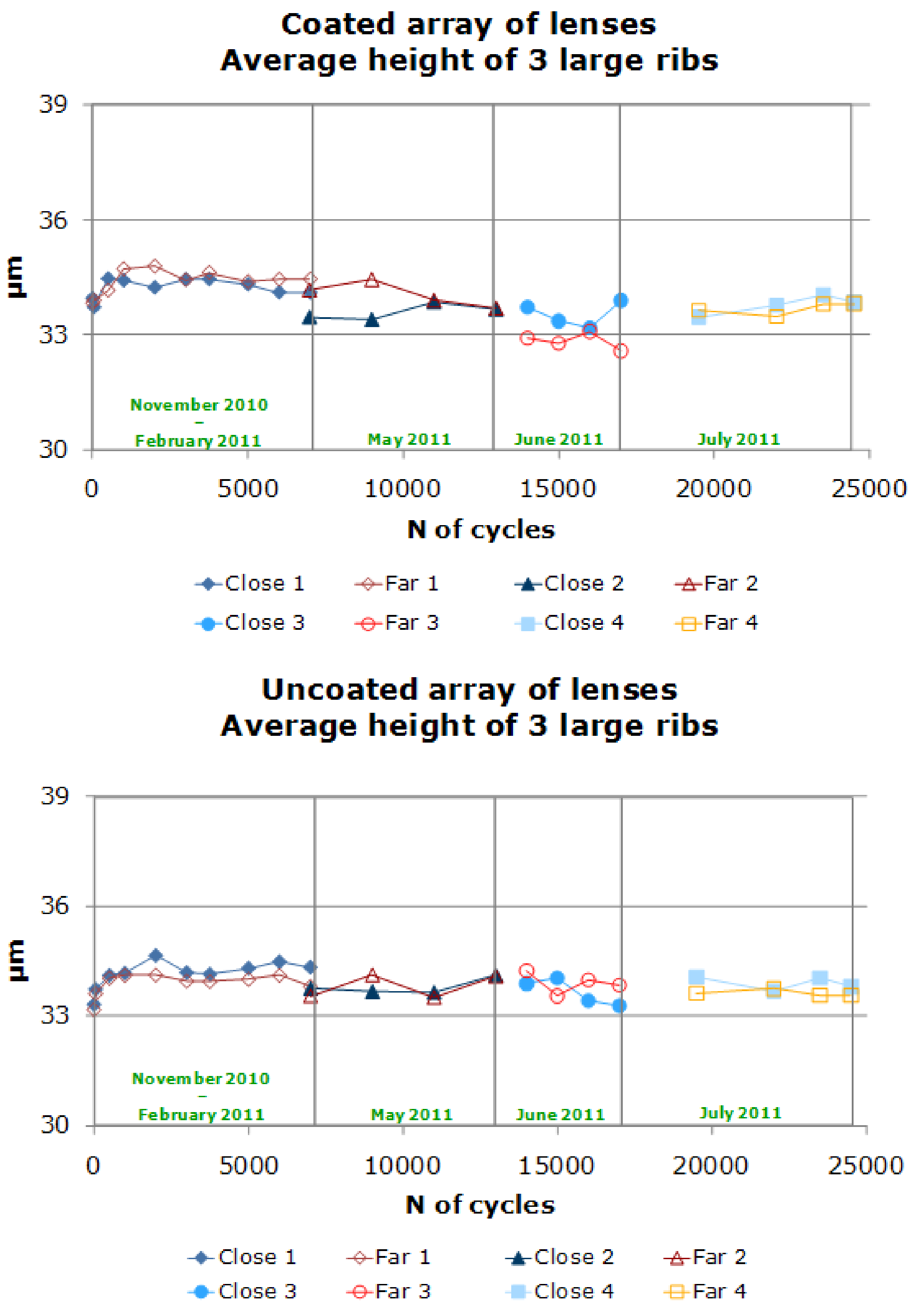

Figure 5.14 - Average height of 3 large ribs measured on two replica lenses close and far from the gate, during a production of 24500 cycles. The upper graph shows the results for the coated mould; the lower graph for the uncoated mould.

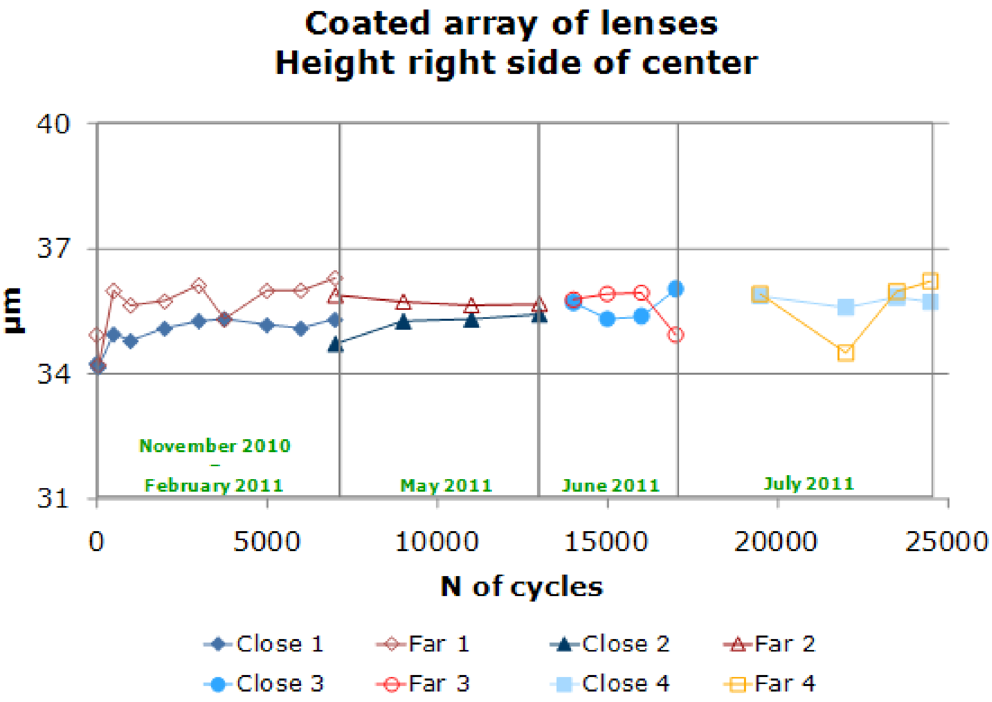

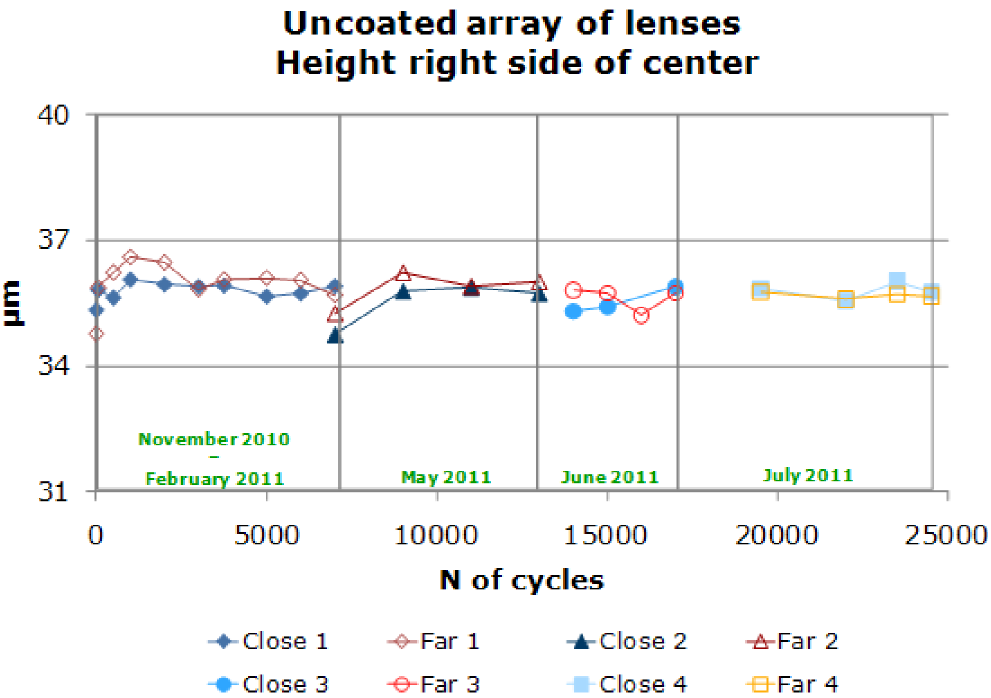

Figure 5.15 - Average height on the right side of the centre geometry measured on two replica lenses close and far from the gate, during a production of 24500 cycles. The upper graph shows the results for the coated mould; the lower graph for the uncoated mould.

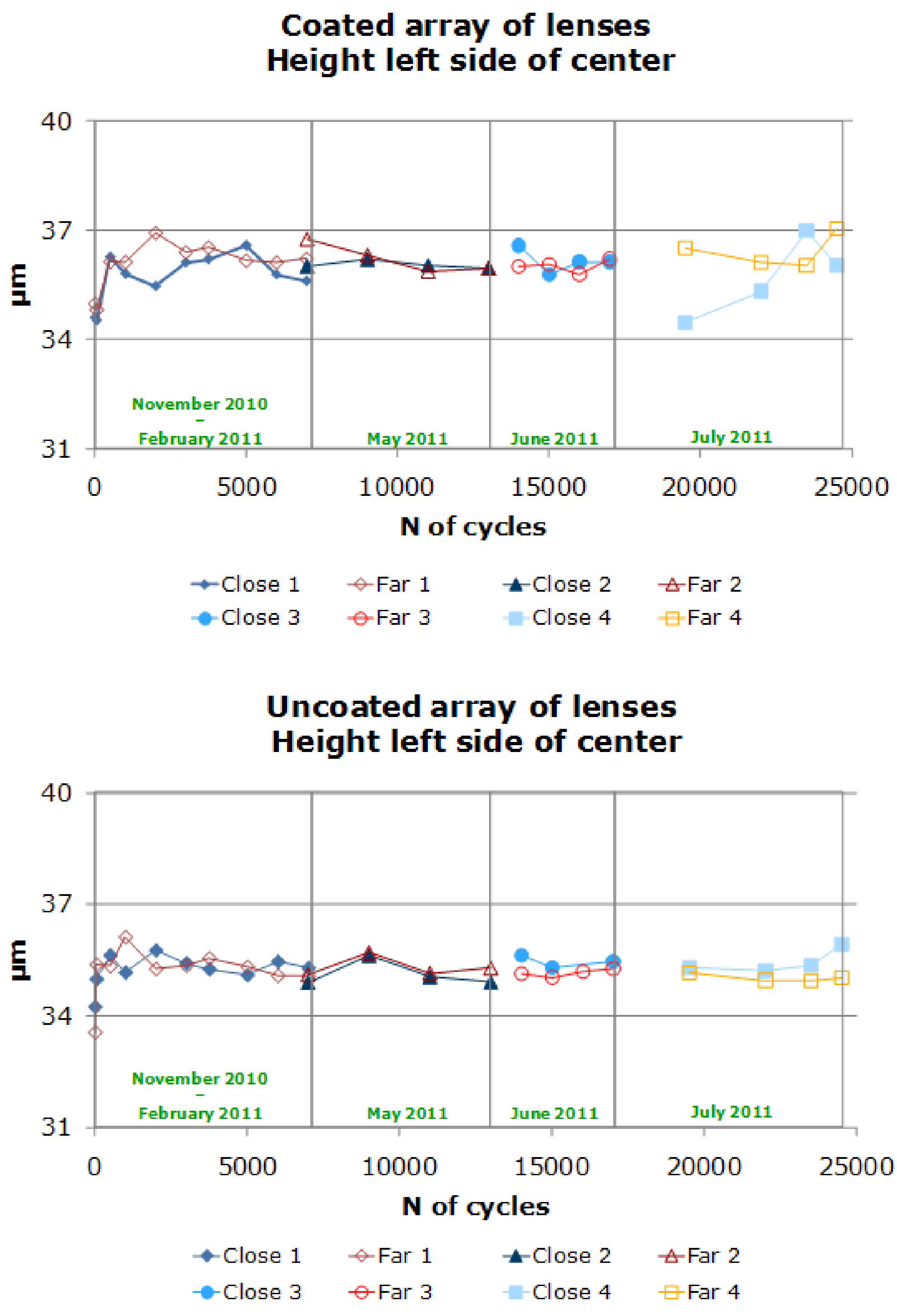

Figure 5.16 - Average height on the left side of the centre geometry measured on two replica lenses close and far from the gate, during a production of 24500 cycles. The upper graph shows the results for the coated mould; the lower graph for the uncoated mould.

Significant variations (average value equal to 1 µm) were detected only in the area correspondent the 10 small ribs. Therefore the single deviations were summarized in a unique graph in order to perform a better comparison between the two lenses (far/close) and the two moulds (coated/uncoated), see Figure 5.17. Results showed a reduction of the average ribs height in the range between 0.7 and 1.1 µm for the uncoated lenses (both near and far from the gate) and the TiN coated lenses near the gate, whereas the TiN coated lenses far from the gate exhibit a height decrease of about 0.4 µm.

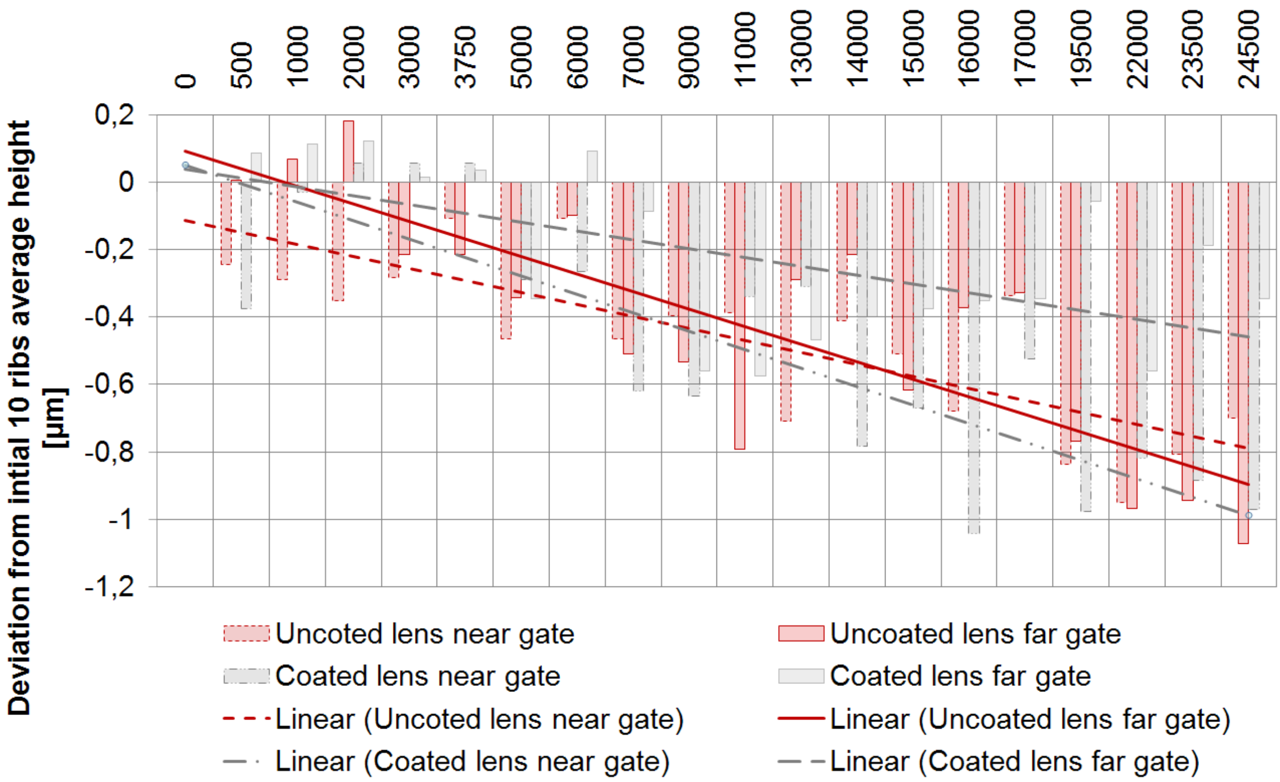

Figure 5.17 - Deviation of the average 10 ribs height from the initial value before production for coated and uncoated lenses as a function of distance from the gate. The lines represent the linear regression of the different data.

5.5 SEM inspection

An SEM inspection was carried out on the coated and uncoated mould after 0, 5000, 7000, 17000 and 24500 cycles in order to have a direct visual characterization of the wear progress. The most important results are summarized in Table 5.3.

SEM		Coated	Uncoated
N of cycles	0	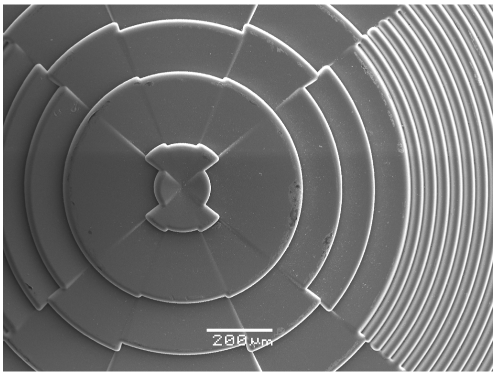	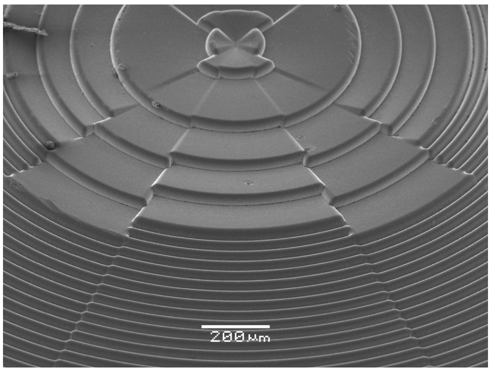
	7000	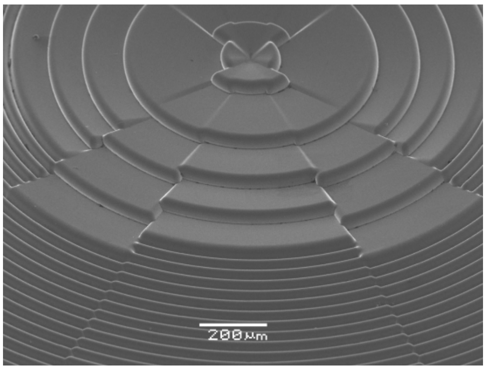	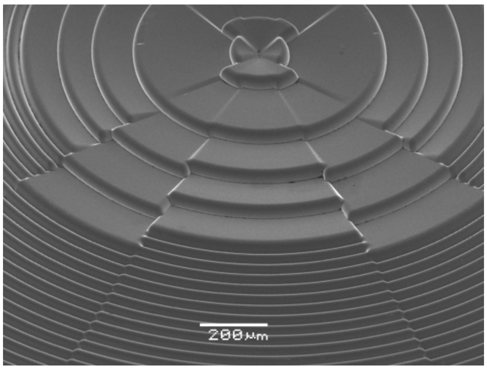
	17000	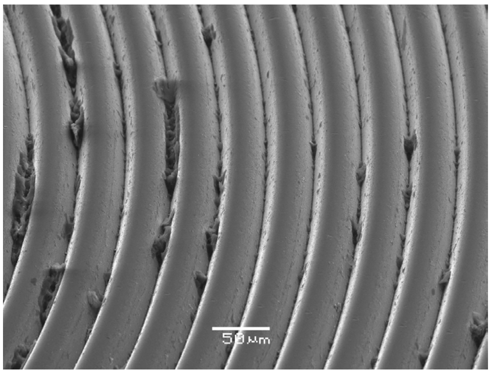	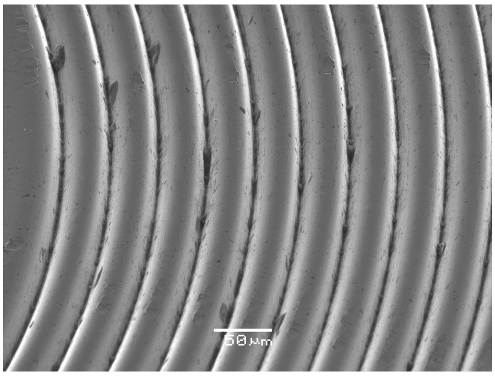
	24500	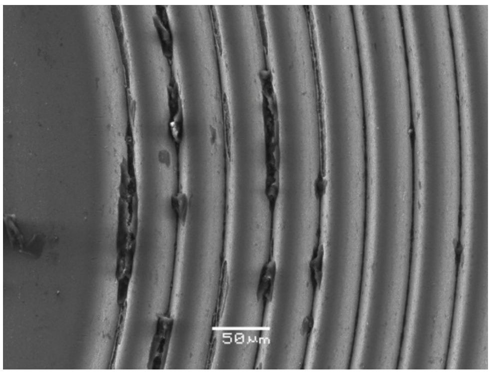	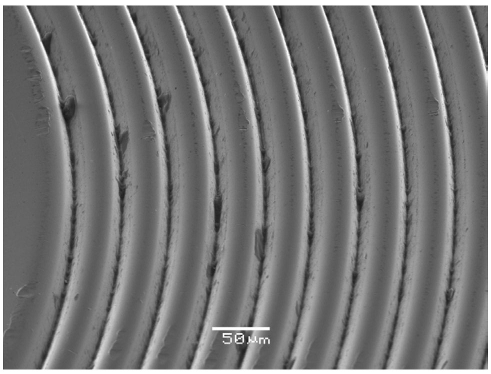

Table 5.3 – SEM inspection on the coated and uncoated moulds at 0, 7000, 17000 and 24500 cycles.

The first observation regards the cleaning of the mould.

After 17000 cycles, particles of polycarbonate were stuck on the surface, especially on the coated mould, see Figure 5.18. The particles were found even if the moulds were cleaned with acetone every time a replica was made.

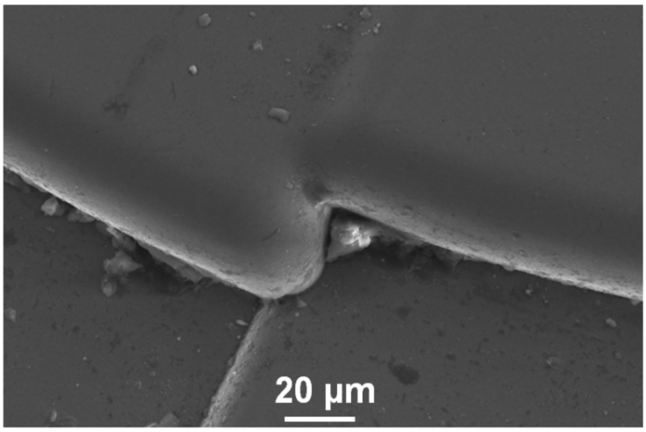

Figure 5.18 - Polycarbonate particles stuck on the coated mould.

The most important result was obtained after 24500 cycles, when actual “craters” started to be visible on the coated mould surface. The uncoated insert, instead, seemed to be still intact. These craters, shown in Table 5.3 and Figure 5.19, were not easy to detect because they appeared only in the lateral walls of the ribs

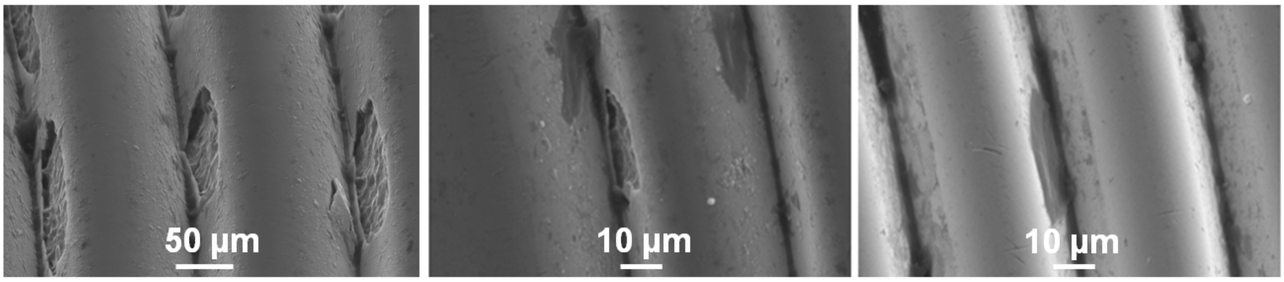

(a) (b) (c)

Figure 5.19 - (a) and (b): cracks and polymer left in the coated mould; (c): only residual polymer and no cracks on the surface of the uncoated mould.

A study on the fracture of the coating has been carried out by means of image processing of high resolution SEM pictures, see Figure 5.20. It was evident that the cracks have been caused by a mechanical fracture of the coating produced by the polymer. These cracks occurred when the polymer separated from the tool surface during cooling (due to shrinkage) and ejection (due to mould opening and the action of the ejectors).

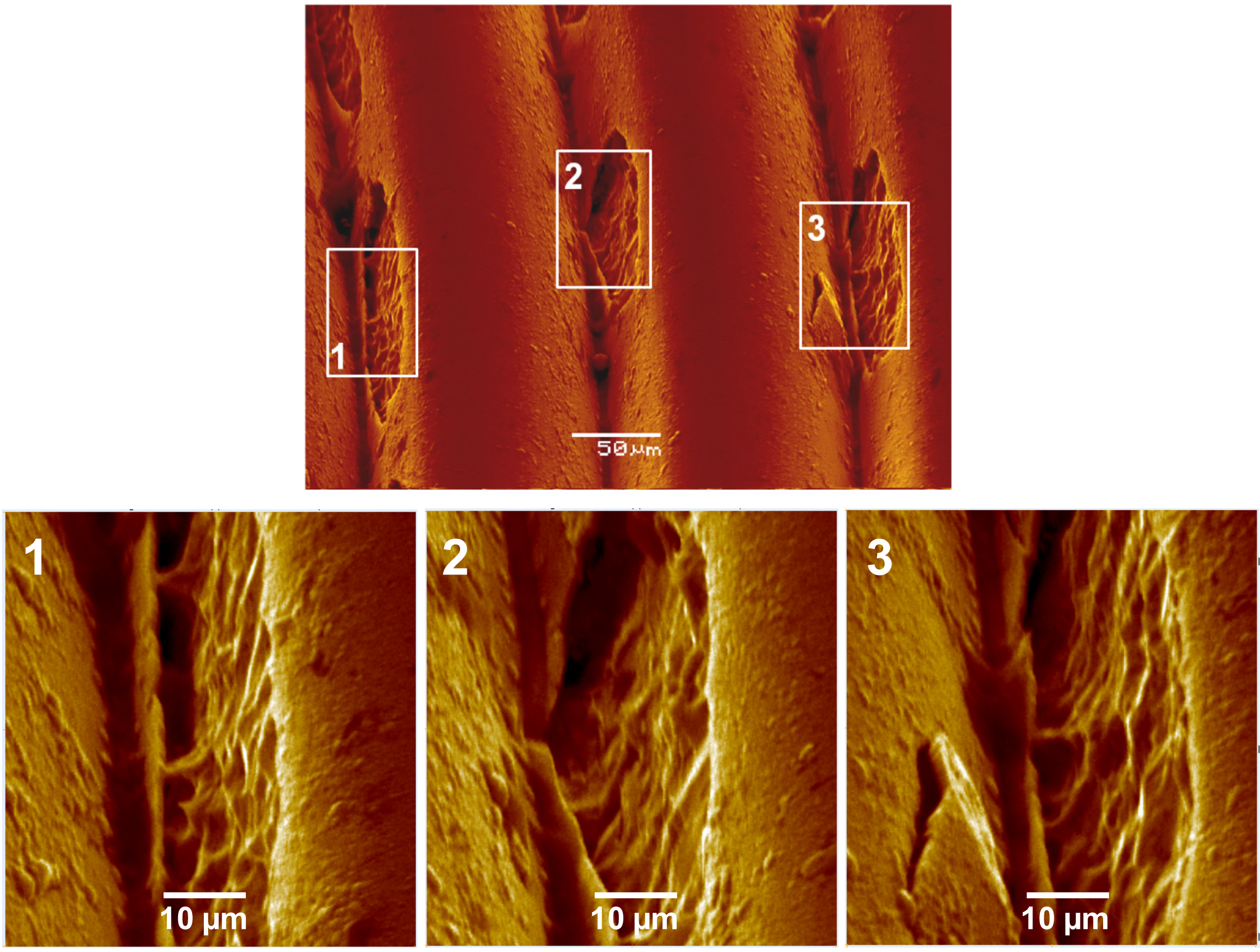

Figure 5.20 – Cracks analysis based on image processing of high resolution SEM pictures.

Additionally, in order to understand if the position of the cracks on the coated mould was correlated to the flow of the polymer material, a deeper SEM investigation was carried out. The study was performed on the lenses near the gate and far from the gate.
The results are shown in Figure 5.21 and Figure 5.22.

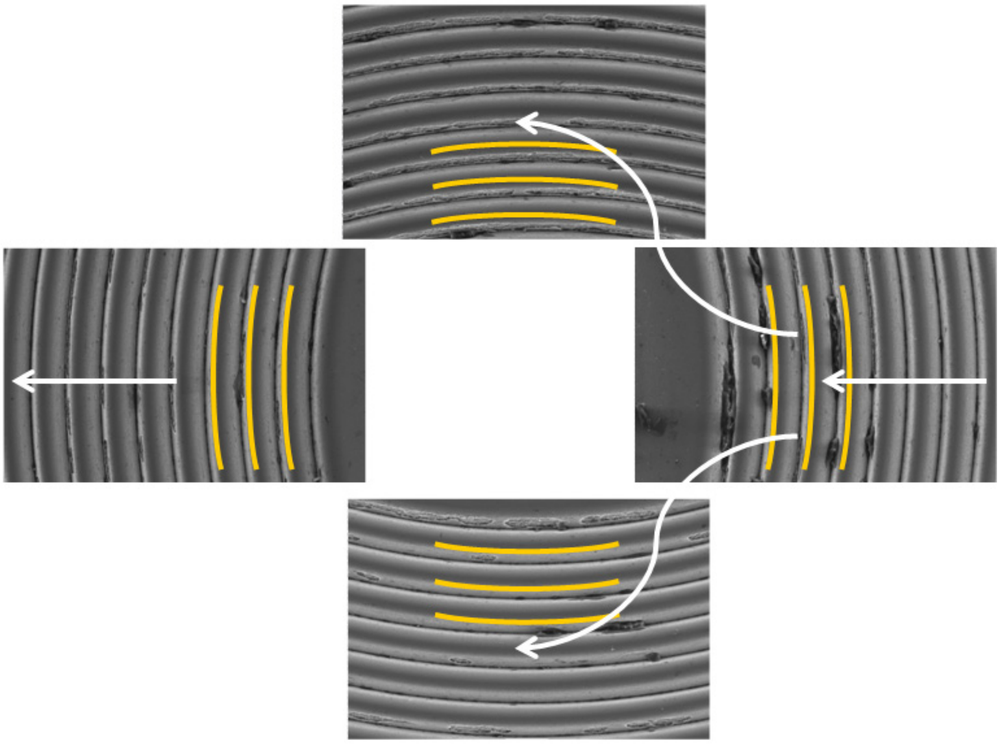

Figure 5.21 - Lens close to the gate of the coated mould. Arrows indicates polymer flow direction, lines indicate where the cracks were present.

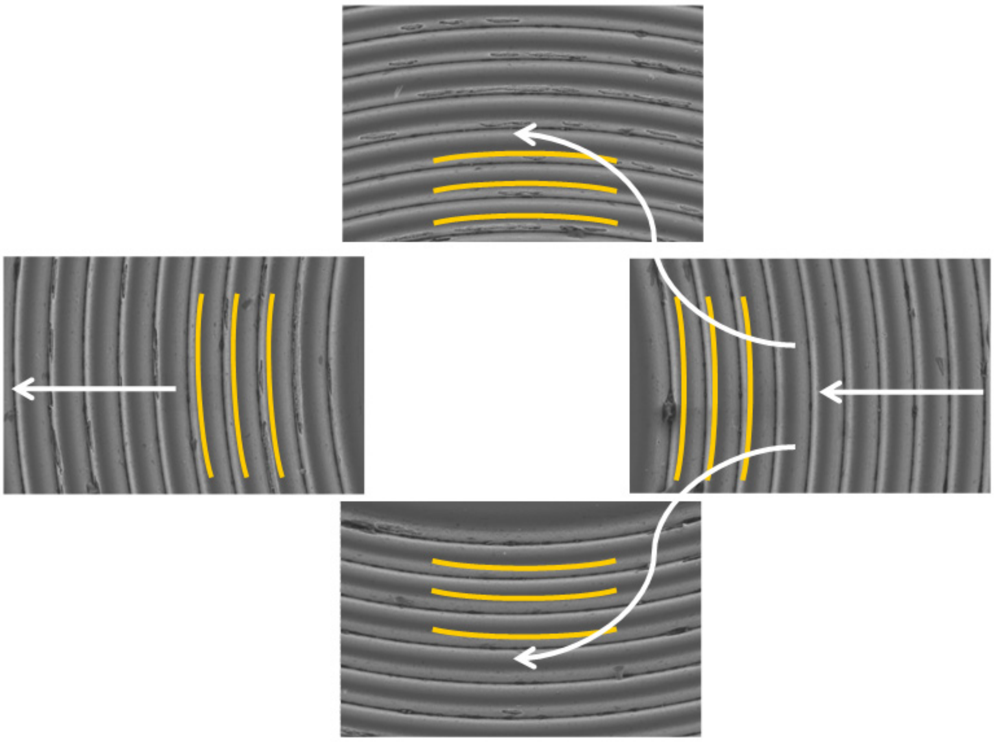

Figure 5.22 - Lens far from the gate of the coated mould. Arrows indicates polymer flow direction, lines indicate where the cracks were present.

The cracks on the coated mould surface appeared on different sides of the grooves independently from the polymer flow direction; in particular:

- Without following a clear symmetrical pattern with respect to the centre of the lens;
- Without following a clear pattern with respect to the advancing of the polymer before and after the centre of the lens.

As a consequence, it is possible to conclude that within a single lens, there was not actual influence of the polymer flow direction on the wear of the coated tools but, rather, the coating resulted to be weaker in some areas than others. However, it was demonstrated that different wear occurred considering different areas within the insert as whole. Indeed, lenses far from the gate exhibited a much lower number of cracks than the lenses close to the gate. This was due to the fact that far from the gate the polymer flow had lower pressure due to a pressure drop along the flow path, and lower temperature due to cooling during filling time. These two phenomena combined made the action of the polymer flow less aggressive far from the gate than close to the gate.

In conclusion, the investigation showed that until 17000 cycles no wear could be observed on the tool surface. However, after this point, at 24500 cycles, craters distributed on several zones of the TiN coated surface appeared as result of the structural deterioration of the coating. In particular, it was observed a delamination failure mode of the coated lenses near the gate and a surface integrity of the coated lens far from the gate and of the uncoated tool.

5.6 EDS inspection

To complete the investigation with the scanning electron microscope, an EDS analysis of the material composition was carried out on both tool inserts (see Table 5.4). A 7.5% decrease of the Ti content on a 2 μm thick section of the surface was observed after 24500 cycles, proving the tool wear progress. This result was verified by performing the EDS analysis inside the craters themselves. The inspection showed a Ti content value of 14.3% and 85.7% of Ni. The substrate at the bottom of the craters was still part of the TiN coating, but a structural failure occurred.

EDS		Coated		Uncoated
		TiN [%]	Ni [%]	Ni [%]
N of cycles	0	99.8	0.2	100
	5000	99.8	0.2	100
	7000	99.9	0.1	100
	17000	93.7	6.3	100
	24500	92.5	7.5	100

Table 5.4 - EDS inspection in the coated and uncoated moulds at 0, 5000, 7000, 17000 and 24500 cycles.

5.7 Conclusion

A study on tool wear of two inserts for polymer optics application was conducted. The two inserts were in Ni, one with TiN as coating. They are both used for injection moulding of Fresnel lenses. The investigation was performed through a quantitative study based on a soft replica technique and 3D optical metrology combined with SEM-EDS analysis.

The obtained replicas revealed high replication fidelity of the actual moulds: the replica material was able to replicate both the areas affected by tool wear as much as the polymer residuals from the injection moulding process.

The tool wear progress showed a surface wear of the coated tool at 24500 moulding cycles. Despite the high hardness of the coating (as shown by the indentation hardness test), the coating showed a structural failure under the cyclic thermo-mechanical load typical of the injection moulding process, where high temperatures and pressures are repeatedly reached during the filling of the cavity and decrease during the packing and cooling phases. The coating wear was also promoted by the higher coefficient of friction as proved by the tribological test.

Finally, the effect of the lens position relatively to the injection gate was highlighted: it had the effect of decreasing the tool wear of the TiN coated insert (i.e. lower deviation from initial dimension and no craters on the surface) on lens far from the gate. This related with the lower pressure at the end of the cavity due to the pressure drop experienced by the polymer far from the injection location. Indeed, even though measurements on the tool micro features still showed a height decrease during the production, a slight better performance of the TiN coating far from the gate (where the thermo-mechanical conditions were less severe) was observed.

5.8 References

[Antón, 2011] J.C.M. Antón, J.A.G. Pedrero, J.A. Fernández, J.A. Quiroga, “Optical method for the surface topographic characterization of Fresnel lenses”, Optical Fabrication, Testing, and Metrology IV, Proc. of SPIE, 2011, Volume 8169, 816910-1, 8 pp.

[Bruzzone, 2008] A.A.G. Bruzzone, H.L. Costa, P.M. Lonardo, D.A. Lucca DA, “Advances in engineered surfaces for functional performance”, Annals of CIRP, 2008, Volume 57, Issue 1, pp. 750-769.

[Chemisana, 2011] D. Chemisana, A. Vossier, L. Pujol, A. Perona, A. Dollet, “Characterization of Fresnel lens optical performances using an opal diffuser”, Energy Conversion and Management, 2011, Volume 52, pp. 658–663.

[Gasparin, 2012] S. Gasparin, G. Tosello, H.N. Hansen, J.A. Albajez, “Replica casting technique for micro Fresnel lenses characterization”, Proceeding of 12th International Euspen Conference 2012, pp. 319-322.

[Grzesik, 2011] W. Grzesik, J. Małecka, “Documentation of tool wear progress in the machining of nodular ductile iron with silicon nitride-based ceramic tools”, Annals of CIRP, 2011, Volume 60, Issue 1, pp. 121-124.

[GUM, 2008] Joint Committee for Guides in Metrology (JCGM). JCGM 100:2008, Guide to the Expression of Uncertainty in Measurement (GUM), 2008, pp. i–viii, 1–132.

[Hansen, 2011] H.N. Hansen, R. Hocken, G. Tosello, “Replication of micro/nano geometries”, Annals of CIRP, 2011, Volume 60, Issue 2, pp. 695-714.

[Kang, 2004] S. Kang, “Replication technology for micro/nano optical components”, Japanese Journal of Applied Physics, Volume 43/8B, pp. 5706-5716.

[Lucca, 2010] D.A. Lucca, K. Herrmann, M.J. Klopfstein, “Nanoindentation: Measuring methods and applications”, Annals of CIRP, 2010, Volume 59, Issue 2, pp. 803-819.

[Michaeli, 2007] W. Michaeli, S. Heßner, F. Klaiber, J. Forster, “Geometrical accuracy and optical performance of injection moulded and injection-compression moulded plastic parts”, Annals of CIRP, 2007, Volume 56, Issue 1, pp. 545-548.

[Osakada, 2000] K. Osakada, R. Matsumoto, “Fundamental study of dry metal forming with coated tools”, Annals of CIRP, 2000, Volume 49, Issue 1, pp. 223–226.

[Riel-Bachmann, 2011] A. Riel, S.G. Bachmann, “Tool life assessment for injection molding of micro optics”, Bsc. thesis, Department of Manufacturing Engineering and Management, Technical University of Denmark, 2011.

[Schmitt, 2006] R. Schmitt, D. Doerner, “Measurement technology for the machine-integrated determination of form deviations in optical surfaces”, Annals of CIRP, 2006, Volume 55, Issue 1, pp. 559–562.

[Settineri, 2005] L. Settineri, R. Levi, “Surface properties and performance of multilayer coated tools in turning inconel”, Annals of CIRP, 2005, Volume 54, Issue 1, pp. 515-518.

[Tosello, 2010] G. Tosello, H.N. Hansen, F. Marinello, S. Gasparin, “Replication and dimensional quality control of industrial nanoscale surfaces using calibrated AFM measurements and SEM image processing”, Annals of CIRP 2010, Volume 59, Issue 1, pp. 563-568.

[Tosello, 2012] G. Tosello, H.N. Hansen, S. Gasparin, J.A. Albajez, J.I. Esmoris, “Surface wear of TiN coated nickel tool during the injection moulding of polymer micro Fresnel lenses”, Annals of the CIRP, 2012, Volume 61, Issue 1, pp. 535-538.

[Yang, 2010] C. Yang, K. Shi, P. Edwards, Z. Liu, “Demonstration of a PDMS based hybrid grating and Fresnel lens (G-Fresnel) device”, Optics Express, 2010, Volume 18, Issue 23, pp. 23529-23534.

[Yoon, 2006] S.H. Yoon, J. Lee, K. Park, J.L. Mead, S. Matsui, C.M.F. Barry, “Critical factors for nanoscale injection molding”, Smart Medical and Biomedical Sensor Technology IV, Proc. of SPIE, 2006, Volume 6380, 63800K1-12, 12 pp.

6. Tolerance chain verification at micro dimensional scale

6.1 Introduction

The characterization of micro injection moulded (μIM) parts brings challenges in terms of measurements because of the integrated multi-scale dimensional range of the features to be controlled: macro and micro scale devices, micro scaled features, details in the sub-μm range. Furthermore, the mass production capability of μIM calls for in-line process control instrumentation. Three-dimensional (3D) measuring capabilities are required, along with sub-μm or even nanometre accuracy. The most suitable measuring techniques are the optical instruments, but they present limitations in terms of capability, speed and accuracy at micro scale. High accuracy quality control of both dimensions and surfaces is still performed off-line [Hansen, 2011]. Moreover one of the major challenges related to performing traceable measurements at micro scale is the tolerance verification: the measurement uncertainty becomes relatively large compared to the tolerance interval, leaving a smaller conformance zone for process variations [Hansen, 2006] and [Hansen, 2008]. According to [Theilade, 2007], when the measurement uncertainty is estimated, three different kinds of variability contributions can be identified: instrument, metrology procedure and process variations, see Figure 6.1.

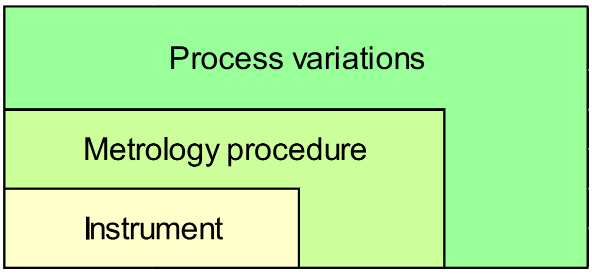

Figure 6.1 - Three contributions which characterize the variability of a measurement: process variations, metrology procedure and instrumentation.

If the measurement procedure is semiautomatic, the most important variation comes from the operators; on the other hand if the measurement procedure is completely automatic the influence of the instrument settings can be well known. In the latter case the influence parameters are variations coming from the instrument (e.g. its specifications) and contributions resulting from the metrology procedure (e.g. instrument settings). Finally, with no regard to the type of approach, the process variability derives from changes that follow process conditions, materials or other process parameters.

This chapter addresses product compliance with specifications, focusing on tolerances of dimensions and position on μIM components selected from an industrial production (*Paragraph 6.2*). Two systems were analysed: a tactile coordinate measuring machine (TCMM) with micrometer uncertainty and an optical coordinate measuring machine (OCMM) allowing relatively fast measurements, suitable for in-line quality control. Product quality control capability, measuring uncertainty and calibration guidelines are discussed for both systems (*Paragraph 6.3* and *6.4*). An investigation of different set-ups of the optical measurements was carried out to evaluate the influence parameters in optical coordinate metrology (*Paragraph 6.5*). A statistical Quality Control (QC) method was implemented for estimating the three variability contributions schematically represented in Figure 6.1 (*Paragraph 6.6*). Finally, the optical system capability was estimated according to the measurement system capability indices Cg and Cgk (*Paragraph 6.7*).
The main results of the present case study have been published in [Gasparin, 2009] and [Tosello, 2009] and submitted in [Gasparin, 2012].

6.2 Case description

The selected product for the present investigation is a component for micro mechanical application, characterized by weight in the range of milligrams as well as functional features and tolerance requirements expressed in terms of micrometers. Particularly, it is a toggle for a hearing aid application made of liquid crystal polymer (LCP) with a part weight of 35 mg (see Figure 6.2). The component is produced in batch sizes of several hundred thousand parts per year using a conventional injection moulding machine having a rather small plasticizing screw (diameter 15 mm) and a mould with micro cavities machined by micro die sinking EDM.

Four different measurands were chosen for the investigation: inner diameter (*d*), outer diameter (*D*), concentricity between the two circles (*C*) and height (*H*) of the pillar placed at the bottom of the component and visible in Figure 6.2.

The employed quality control procedure was performed manually using an optical dial gauge for height measurements and an optical measuring microscope for measurements in *x*-*y* plane. The limitations of this approach concerned issues on the verification and calibration of the instruments, low measurement repeatability and low speed due to manual execution [Fugl, 2004]. It was calculated that the ratio (*U*/*T*) between the measuring uncertainty (*U*) and the tolerance (*T*) to be verified was not suitable for the considered measuring tasks and therefore was leaving a very limited conformance zone available for tolerance verification (from a maximum of 19 μm in case of the inner diameter to a minimum of no conformance zone for the concentricity). On the contrary, it is recommended that the *U*/*T* ratio shall be less than 10% or, at least, lower than 20% [Knapp, 2001]. Moreover, manual measurements are time consuming and have a very low repeatability (which represented 90% of the final measuring uncertainty). The need for automated and more repeatable measuring systems with a lower uncertainty is clear [Tosello, 2009].

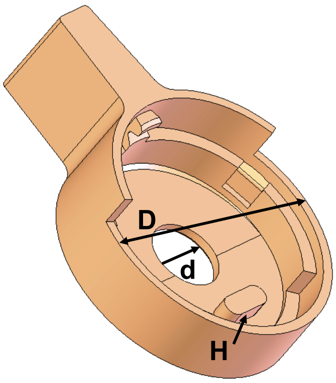

Measurands	*Nominal dimensions ± tolerances [μm]*
Inner diameter (*d*)	1550 ± 20
Outer diameter (*D*)	5400 ± 30
Concentricity (*C*)	20
Pillar height (*H*)	380 ± 30

Figure 6.2 - Micro injection moulded component (toggle for hearing aid application) and the four measurands with the nominal values and tolerances taken into account in the present investigations.

In order to provide an automated and highly accurate measuring system, the low uncertainty tactile coordinate measuring machine described in appendix 11.1.7 was selected. The main goal was to set the baseline of the quality control system capability in terms of uncertainty with respect to tolerance. For this purpose, a sample of 21 micro products was randomly chosen from the actual production, glued to a steel plate and mounted on the TCMM's measuring plane. The four measurands previously introduced were measured. A sub-millimetre probe was employed (ball tip diameter of 500 µm) and a specific set-up of the measuring force suitable for micro application was used (probing force of 50 mN).

Afterwards 3 toggles were randomly selected from the sample of 21 workpieces and measured using the optical coordinate measuring machine described in appendix 11.1.6. Firstly, a comparison between tactile and optical measurements was carried out and secondly an investigation on the optical set-up was performed. The outer and the inner diameter were estimated through an edge detection algorithm based on black-white contrast. The concentricity was calculated from the coordinates of the centre points of the two diameters; the height of the pillar was estimated using an auto-focusing routine applied on the base and on the top of the pillar.

6.3 Measurements using TCMM

The measuring uncertainty of the two diameters was evaluated using the maximum permissible error (MPE = 0.4 + *L*/900 µm, *L* in mm) of the TCMM. This estimation was applied to both *x* and *y* direction and the resulting *u(x)* and *u(y)* were considered as the standard uncertainty associated to the measured points on the circle. These standard uncertainties were treated as independent uncertainty components and were combined following the GUM [GUM, 2008]. Standard combined uncertainties related to points belonging to both circles (outer and inner) were then combined with each other in order to estimate the concentricity measurement uncertainty as well. Those estimations took into account uncertainty sources such as machine calibration, repeatability and resolution. The expanded uncertainty for diameter measurements was 0.8 µm and for concentricity measurements 1.1 µm.

For height measurements an experimental approach was applied: repeated measurements were performed on a calibrated 400 µm step created by mounting two gauge blocks grade 2 [ISO 3650, 1998] on an optical glass (flatness of 0.2 µm). ISO 15530 part 3 [ISO 15530-3, 2004][c] was applied to calculate the measuring uncertainty of the TCMM measurements of step along the *z* direction as follows:

$$U_{TCMM,H} = k\sqrt{u_{cal}^2 + u_p^2 + u_w^2 + u_{glass}^2} + |b| \quad (6.1)$$

Where:

- $U_{TCMM,H}$ = expanded combined uncertainty of step measurements by TCMM;
- k = coverage factor (= 2) for a confidence level of 95.45%;
- u_{cal} = standard calibration uncertainty of the gauge blocks;
- u_p = standard uncertainty of the measurement procedure = standard deviation of 5 repeated measurements of the step height between 2 adjacent gauge blocks;
- u_w = temperature-related standard uncertainty, calculated for a maximum temperature variation of ± 1 °C (measurements were carried out in a controlled environment at standard temperature of 20 ± 0.5 °C);
- u_{glass} = standard uncertainty due to the planarity of the optical glass;
- b = systematic error, calculated as a difference between the value obtained from the gauge blocks calibration certificate and measured values by the TCMM.

The expanded uncertainty for height measurements was 1.2 µm.

In order to take into account the uncertainty due to the actual workpiece being measured (i.e. µIM component), the material (i.e. polymer), the miniaturized probe tip and shaft, the different U_{TCMM} were combined with the standard deviation of repeated measurements on the polymer parts related with the different measurands. The calibration uncertainty of polymer objects using the TCMM was calculated as follows:

$$U_{cal(TCMM),j} = k\sqrt{u_{TCMM,j}^2 + u_{p,j}^2 + u_{w,j}^2} \quad (6.2)$$

Where:

- j = (D, d, C, H) depending on the measurands;
- $U_{TCMM,j}$ = TCMM's standard uncertainty as previously calculated for the jth measurand;
- $u_{p,j}$ = standard deviation of repeated measurements of the jth measurand on the polymer micro-products;

[c] A revised version is available (ISO15530-3:2011), where: $U = k\sqrt{u_{cal}^2 + u_p^2 + u_w^2 + b^2}$

- u_w = temperature-related standard uncertainty, calculated for a maximum temperature variation of ± 1 °C (conservative assumption since measurements were carried out in a controlled environment at standard temperature of 20 ± 0.5°C) and using a coefficient of linear expansion for LCP of a $\alpha = 49 \times 10^{-6}$ °C^{-1}.

Applying the previous equation to the TCMM measurements, the maximum expanded uncertainties for the different measurands were: $U_{OCMM,d}$ = 3.4 µm, $U_{OCMM,D}$ = 1.5 µm, $U_{OCMM,H}$ = 1.7 µm, $U_{OCMM,C}$ = 4.7 µm (see Table 6.1).

With the establishment of the presented metrology framework, the *U/T* ratio was decreased down to 8.5% and the conformance zone to tolerance ratio was increased up to at least 83%, greatly improving the quality control efficiency (see Table 6.1). Therefore, compliance with the specifications of the products in terms of outer diameter can now be proved as well as the non compliance in terms of inner diameter. Moreover, outliers regarding concentricity and step height were highlighted, see Figure 6.3.

However, despite the efficiency of this quality control procedure, the high accuracy TCMM presented a number of drawbacks: measurements are relatively slow (especially if compared with production cycle times), contact measurements are not suitable for relatively soft substrate materials such as polymers (drifts up to 3 – 4 µm were observed on repeated measurements on the same item), a stable fixture of the workpieces is mandatory and in-line implementation is not possible.

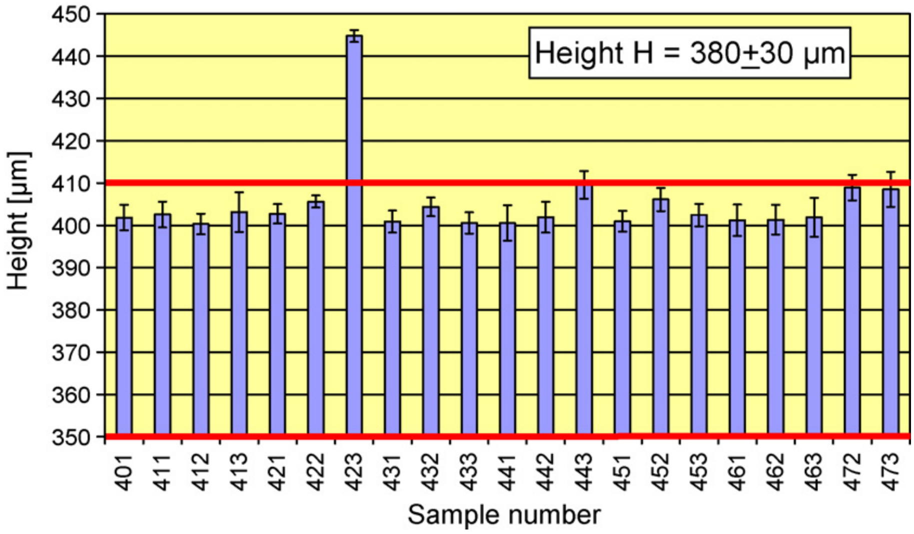

Figure 6.3 - Quality control results of micro injection moulded components using a TCMM. Red lines indicate tolerance range, vertical error bars indicate expanded combined uncertainty (k = 2, confidence level 95%) [Tosello, 2009].

6.4 Measurements using OCMM

The uncertainty assessment procedure described in [ISO 15530-3, 2004][d] was applied to the optical measurements employing as calibrated artefacts the polymer micro components. The measuring results and the uncertainties from the TCMM were used as calibration data.

Repeated measurements with the OCMM were performed on 3 selected polymer components, the measuring uncertainty was calculated and the results compared with the ones obtained with the TCMM, each one taking into account the related uncertainty:

$$U_{OCMM,j} = k\sqrt{u_{cal(TCMM),j}^{2} + u_{p,j}^{2} + u_{w,j}^{2}} + |b| \quad (6.3)$$

Where:

- j = (D, d, C, H) depending on the measurands;
- $U_{OCMM,j}$ = expanded combined uncertainty of optical CMM measurements for the jth measurand;
- k = coverage factor (= 2) for a confidence level of 95.45%;
- $u_{cal(TCMM),j}$ = standard calibration uncertainty from the TCMM for the jth measurand as calculated in equation 6.2;
- u_p = standard uncertainty of the measurement procedure, calculated as standard deviation of five repeated measurements on the polymer micro product;
- u_w = temperature-related standard uncertainty as previously described and considered negligible;
- b = systematic error, calculated as a difference between the value obtained with the TCMM (considered as calibrated value) and measured values by the OCMM.

The maximum expanded uncertainties among the three investigated specimens for the different measurands were: $U_{OCMM,d}$ = 24 µm, $U_{OCMM,D}$ = 12 µm, $U_{OCMM,H}$ = 86 µm, $U_{OCMM,C}$ = 9.7 µm (see Table 6.1).

These uncertainties did not allow an efficient quality control in the considered case because of the unfavourable U/T ratio and the drastic reduction of the available conformance zone. However, it was observed that, regardless the considered workpiece

[d] A revised version is available (ISO15530-3:2011), where: $U = k\sqrt{u_{cal}^{2} + u_{p}^{2} + u_{w}^{2} + b^{2}}$

and measurand, the *b* factor in the uncertainty calculation (i.e. systematic error) always represented 70 – 80% of the combined expanded uncertainty. This means that *b* was repeatable on different workpieces (within 25%) and was the factor to be decreased in order to reduce the final uncertainty. This error was mainly due to an edge detection issue on diameter measurements (the OCMM measures smaller diameters) and on plane detection when focusing on the polymer surface (the OCMM measures smaller depths). The measurements could therefore be compensated; however, a compensation for the systematic error (*b*) introduced a further uncertainty component (u_b) defined as the standard deviation of 5 different *b* factors calculated under the same measuring conditions for the same polymer component. As a consequence, two results were obtained:

1. The expanded uncertainties are reduced: $U_{OCMM,d}$ = 5.4 μm, $U_{OCMM,\mathrm{D}}$ = 8.7 μm, $U_{OCMM,H}$ = 25 μm, $U_{OCMM,C}$ = 3.3 μm;
2. The actual OCMM measurements on the polymer object were compensated using the *b* factor as calculated from the reference object.

The substitution method was applied to all the measurands and the beneficial effect on the quality control capability performance of the OCMM is summarized in Table 6.1. The uncertainties were decreased so that the *U*/*T* ratio for *D* and *d* is only slightly higher than 20% (and lower than 30%) so that could be considered acceptable. The available conformance zone for tolerance verification was also improved. Furthermore, the advantages of optical measurements were obtained: contactless, forceless, fast (less than 1 min for one measuring cycle of one item) and suitable for in-line implementation on the production floor in a micro manufacturing environment.

Measurand	*Nominal dimension [μm]*	*Tolerance [μm]*	*TCMM*		*OCMM*		*OCMM comp*	
			U_{TCMM} [μm]	*U/T [%]*	*U_{OCMM} [μm]*	*U/T [%]*	*U_{OCMM} [μm]*	*U/T [%]*
d	1550	(-20, +20)	3.4	17.0	24	120.0	5.4	27.0
D	5400	(-30, +30)	1.5	5.0	12	40.0	8.7	29.0
C	0	(0, +20)	1.7	8.5	9.7	48.5	3.3	16.5
H	380	(-30, +30)	4.7	15.7	86	286.7	25	83.3

Table 6.1 - Uncertainty *U* to tolerance *T* ratio (*U*/*T*) for different measurand, tolerances, measuring uncertainties and measuring instruments.

6.5 Optical set-up investigation

After performing the quality control on the micro polymer parts, an investigation on different OCMM set-ups was carried out in order to analyze the influence parameters and in order to identify the three main variability contributions: instrument, metrology procedure and process variation, according to Figure 6.1.

The investigated set-ups are summarized in Table 6.2: two lens magnifications (2x and 5x) were used; two types of illumination (coaxial and ring light) were applied; three different illumination intensities were set according to the light used.

Lens	*Illumination type*	*Illumination intensity [%]*		
Leica 2x	Coaxial light	40	43	46
	Ring light	3.7	4.7	5.7
Leica 5x	Coaxial light	40	43	46

Table 6.2 - Set-up parameters of the used OCMM.

Firstly, the three selected toggles (designed as *411*, *413* and *422*) were measured using the optical set-ups summarized in Table 6.2. The measuring uncertainties were calculated according to the compensation method described in paragraph 6.4:

$$U_{OCMM,j} = k \cdot \sqrt{u^2_{cal(TCMM),j} + u^2_{p,j} + u^2_{w,j} + u^2_{b,j}} \quad (6.4)$$

Where:

- $j = (D, d, C, H)$ depending on the measurands;
- $U_{OCMM,j}$ = expanded combined uncertainty of OCMM measurements for the *j*th measurand;
- k = coverage factor (= 2) for a confidence level of 95.45%;
- $u_{cal(TCMM),j}$ = standard calibration uncertainty from the TCMM for the *j*th measurand calculated following equation 6.2;
- u_p = standard uncertainty of the measurement procedure, calculated as standard deviation of five repeated measurements on the polymer micro product;
- $u_{w,j}$ = temperature-related standard uncertainty and considered negligible;

- $u_{b,j}$ = standard deviation of five different b factors calculated under the same measuring conditions (*b* = systematic error, calculated as difference between the calibrated value and the values measured by the OCMM).

Table 6.3 summarizes the expanded uncertainties for the three micro parts. The lowest uncertainties, approximately 4 µm, were obtained using a magnification lens equal to 5x and the highest illumination intensity for the coaxial light. The difficulties derived from the estimation of the outer diameter and the pillar height are represented by the achieved uncertainties in the range of 10 µm - 40 µm. In particular, some problems were encountered for the height measurements when applying different illumination lights. The ring light was not able to produce a sufficient contrast for the auto-focus detection having as output no successful measurements. On the other hand, only the coaxial light was able to focus on the top and on the bottom of the pillar giving repeatable results.

U [µm] (k=2)	*2x*						*5x*		
	Ring light			*Coaxial light*			*Coaxial light*		
	3.7%	*4.7%*	*5.7%*	*40%*	*43%*	*46%*	*40%*	*43%*	*46%*
d	8.0	8.1	8.0	9.2	8.1	8.6	8.4	7.9	8.4
D	5.0	6.0	3.8	24.4	40.6	8.2	10.5	6.0	3.6
C	2.5	1.9	2.4	5.6	7.3	4.5	6.2	3.6	3.8
H				5.2	10.6	13.5	2.8	2.7	3.6

Table 6.3 - Uncertainty values for the optical measurements obtained using different set-ups of the OCMM.

Afterwards in order to identify the three main variability contributions (instrument, metrology procedure and process variation), the deviation of the OCMM results from the TCMM was calculated as:

$$\delta_j = \mu_{TCMM,j} - \mu_{OCMM,j} \qquad (6.5)$$

and the combined standard uncertainty estimated as:

$$\sigma_j = \sqrt{\sigma^2_{TCMM,j} + \sigma^2_{OCMM,j}} \qquad (6.6)$$

Where:

- j = (D, d, C, H) depending on the measurands;
- $\mu_{TCMM,j}$ = average of five calibrated data for the *j*th measurand;

- $\mu_{OCMM,j}$ = average of five optical measurements for the *j*th measurand;
- $\sigma_{TCMM,j}$ = standard deviation of five calibrated data for the *j*th measurand. This parameter differs from $u_{cal(TCMM),j}$ since it does not take into account the contributions derived from the calibration of the TCMM and the temperature-related standard uncertainty of the tactile measurements;
- $\sigma_{OCMM,j}$ = standard deviation of five optical measurements for the *j*th measurand.

The deviation of the optical measurements from the reference values in conjunction with their relative standard deviations are plotted in Figure 6.4.
The graphs on the left represent the absolute deviation from the reference values of the optical results obtained using different lens magnifications (2x - 5x), same illumination type (coaxial light) and different illumination intensity (40% - 43% - 46%) for the three micro parts (411 – 413 - 422) and for the four measurands (inner diameter, outer diameter, concentricity and height). According to the previous conclusions, a brighter light (larger intensity) led to better results and a magnification lens equal to 5x gave optical values closer to the reference ones (deviation average equal to 10 μm). The problems encountered on the outer diameter investigation are underlined by the substantial standard deviations (20 μm), especially for the sample number 422. Regarding the outer diameter, the software had difficulties in finding the edge of the circle. The contrast between white and black areas was not sufficiently evident due to the glue used to fix the workpiece on the steel plate. The fixing method revealed to be a good solution to settle the coordinate system for the measurements of the samples, but it created shadows which made the component contour not well defined. The large deviations (approximately equal to 50 μm - 70 μm) achieved during the height estimation represent the difficulties and the limitations in *z*-axis of this type of optical CMM. Another conclusion that can be drawn by the present investigation regards the variability of the instrument and the metrology procedure. It was possible to estimate the instrument variability in relation to the lens magnification: there was no significant change in results if the measurements were carried out using a 2x or a 5x lens. On the other hand, the metrology procedure variability was related to the illumination intensities: a stronger intensity gave results closer to the reference values.

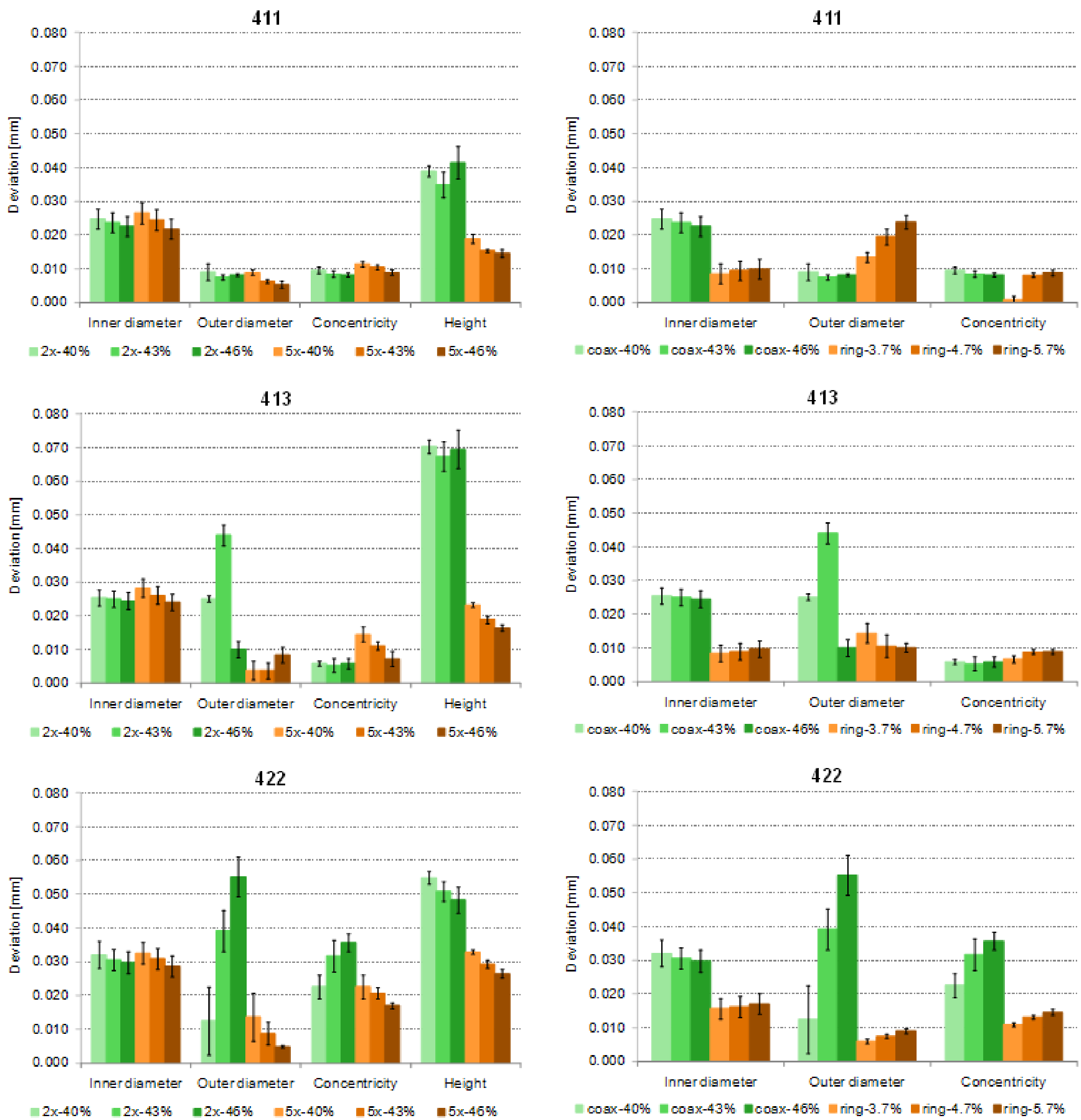

Figure 6.4 - *Left*: Absolute deviation from reference values of the optical measurements obtained using different OCMM set ups. Lenses: 2x and 5x; illumination type: coaxial light with intensities: 40%, 43% and 46%. Samples: 411, 413 and 422. Measurands: inner diameter, outer diameter, concentricity and height. *Right*: Absolute deviation from reference values of the optical measurements obtained using different OCMM set ups. Lens: 2x; illumination types: coaxial light (coax) (with intensities: 40%, 43%, 46%) and ring light (ring) (with intensities: 3.7%, 4.7%, 5.7%). Samples: 411, 413 and 422. Measurands: inner diameter, outer diameter and concentricity.

The graphs on the right of Figure 6.4 represent the absolute deviation from the reference values of the optical results obtained using the same lens magnification (2x), different illumination type (coaxial and ring light) and different illumination intensity (40% - 43% - 46% for the coaxial light; 3.7% - 4.7% - 5.7% for the ring light) for the three micro parts (411 – 413 – 422) and for three measurands (inner diameter, outer diameter and concentricity). A brighter light (larger intensity) for the coaxial light led to better results (deviation average equal to 10 µm). A darker light (lower intensity) for the ring light gave optical results closer to the reference ones (deviation average equal to 5 µm). The problems encountered on the outer diameter investigation are underlined by the substantial standard deviations (20 µm), especially for the samples number 422. Finally, the estimation of the variability coming from the metrology procedure was carried out. A significant change of the results was given both by the used light illumination and by the applied illumination intensity.

6.6 Quality control approach

A Quality Control approach (QC) was implemented for estimating the main variability contributions illustrated in Figure 6.1: instrument, metrology procedure and process variation. The QC approach was applied following the procedure described in [Montgomery, 2005]. According to [Montgomery, 2005], the standard deviation of the total variability of the measuring instrument ($\sigma_{tot,j}$) is the standard deviation of the five performed optical measurements. This variability includes both the variability related to the instrument ($\sigma_{instr,j}$) and the contribution coming from the process ($\sigma_{proc,j}$):

$$\sigma^2_{tot,j} = \sigma^2_{instr,j} + \sigma^2_{proc,j} \qquad (6.7)$$

Moreover the instrument variability ($\sigma_{instr,j}$) contains also the variability derived from the metrology procedure:

$$\sigma^2_{instr,j} = \frac{\overline{\overline{R_j}}}{d_2} \qquad (6.8)$$

Where:

- $\underline{R_j}$ = is the average of the difference between the largest and the smallest observation for the jth measurand;

- d_2 = coefficient related to the sample size given in [Montgomery, 2005].

The results, shown in Figure 6.5, confirm the conclusions drawn for the previous analysis.

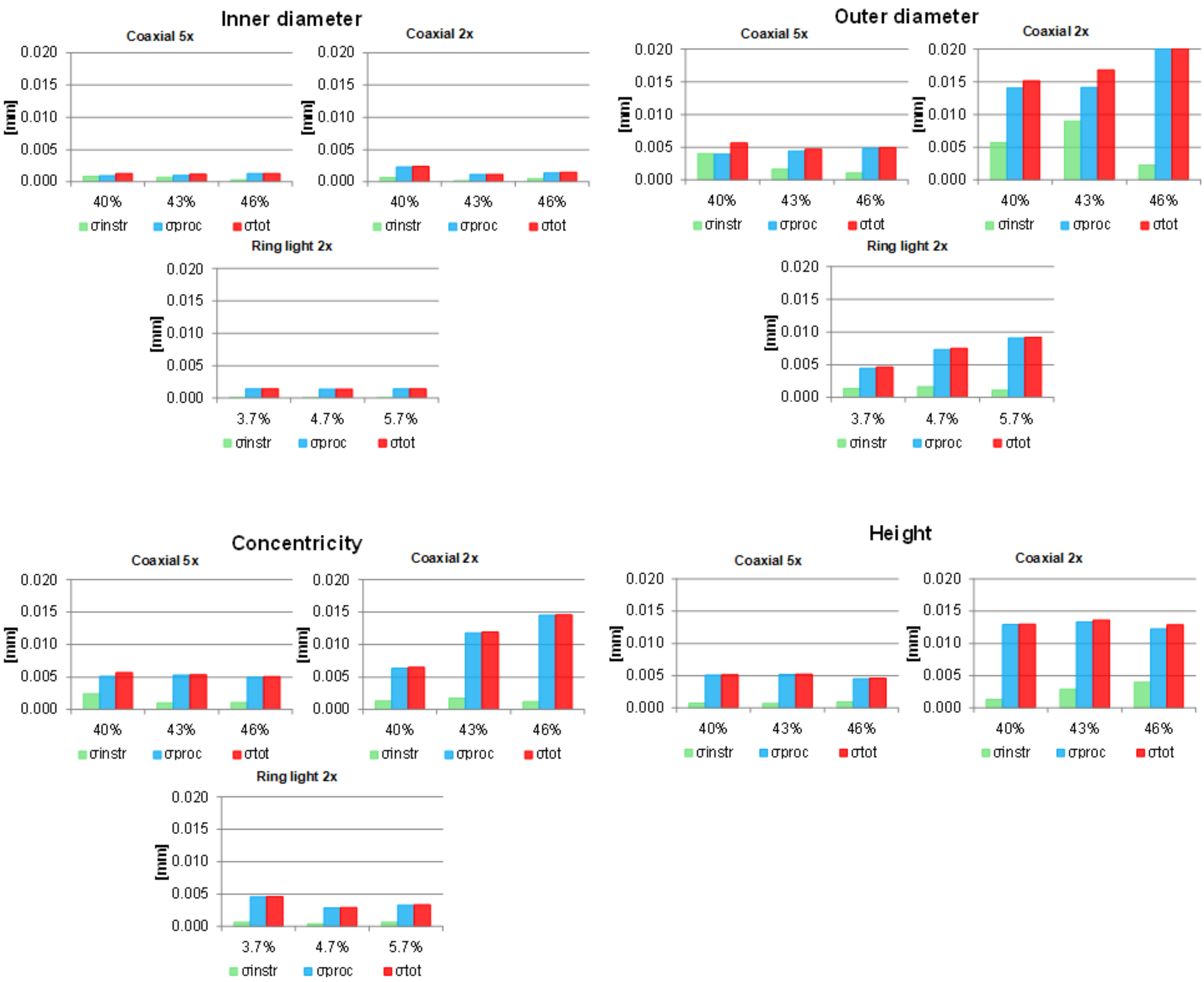

Figure 6.5 - Estimation of the average variability for samples 411, 413 and 422 coming from the total variability (σ_{tot}) which includes the instrument (σ_{instr}) and the process (σ_{proc}) contributions. The measurements were performed using 2x lens, coaxial light (coax) with illumination intensity: 40%, 43% or 46% and ring light (ring) with illumination intensity: 3.7%, 4.7% or 5.7%; using 5x lens, coaxial light (coax) with illumination intensity: 40%, 43% or 46%. Measurands: inner diameter, outer diameter, concentricity and pillar height.

No substantial difference in the optical values was obtained using a 2x or a 5x lens magnification. Furthermore, a larger intensity for the coaxial light or a smaller intensity for the ring light gave a lower variability on the results. The problems coming from the outer

diameter and the height measurements were again pointed out by the instrument variability (5 μm), quite large compared to the variability for the inner diameter (0.5 μm).
New information coming from this analysis concerned the estimation of σ_{instr}. A considerable contribution was given by the process variability, strongly dependent on the process conditions, the samples material or on other process factors. No process variations below σ_{tot} could be identified by this approach.

6.7 Measuring instrument indices approach

The measuring instrument indices approach was implemented in order to evaluate the measuring system capability. This method was previously investigated for metrology studies of components made by LIGA technique [Mäder, 2009], [Meyer, 2009]; for automatic measurement systems [Flynn, 2009]; for comparative analysis of hardness assessment methods [Czarski, 2009] and for measurement systems in a manufacturing company [Cagnazzo, 2010].
In order to evaluate the measuring instrument capability, 20 measurements were performed on one micro part (411) using the different optical set-ups listed in Table 6.2. The measuring instrument indices Cg and Cgk were calculated as:

$$Cg_{ij} = \frac{k/100 \cdot T_j}{6\sigma_{ij}} \tag{6.9}$$

$$Cgk_{ij} = \frac{k/200 \cdot T_j - \left|\mu_{ij} - \mu_{nom,j}\right|}{3\sigma_{ij}} \tag{6.10}$$

Where:

- i = OCMM set-ups used according to Table 6.2;
- j = (D, d, C, H) depending on the measurands;
- k = percent of the tolerance (equal to 20% from literature [Mäder, 2009], [Meyer, 2009], [Czarski, 2009] and [Cagnazzo, 2010]);
- T =tolerance range= USL – LSL (upper specification limit – lower specification limit);
- σ_{ij} = standard deviation of the measurements for the j-measurand;
- μ_{ij} = average of the data for the j-measurand;

- $\mu_{nom,j}$ = nominal value of the *j*-measurand listed in Figure 6.2.

In order to apply the instrument capability analysis, the process must be under control and stable. Output data must be independent and normally distributed [Flynn, 2009].

The index Cg compares the spread of the instrument measurements with a percentage of the tolerance. Values greater than 1.33 indicate that the measurements are acceptable in relation to the tolerance range. The index Cgk takes into account the spread of the measurement, but also the deviation of the results from the nominal value. Values greater than 1.33 are acceptable.

Cg and Cgk were calculated for the four measurands (inner diameter, outer diameter, concentricity and height) of the micro part 411.

Table 6.4 summarizes the results obtained for the index Cg. The coloured cells indicate that Cg is lower than 1.33 and therefore the measurements are not acceptable according to the tolerance range. The results showed that the OCMM was capable of measuring the inner diameter using the different optical set ups. A coaxial light was preferable for measuring the outer diameter; while a lens magnification equal to 5x with a coaxial light were suggested for the verification of the concentricity and the pillar height.

Cg	*Lens*	*2x*			*2x*			*5x*		
	Illumination type	*Coaxial light*			*Ring light*			*Coaxial light*		
	Illumination intensity [%]	*40*	*43*	*46*	*3.7*	*4.7*	*5.7*	*40*	*43*	*46*
Inner diameter		2.44	5.75	3.63	16.15	16.41	17.68	5.16	2.43	5.33
Outer diameter		1.29	8.01	8.43	0.66	0.75	1.23	5.39	4.65	11.24
Concentricity		0.35	1.19	1.14	0.25	0.36	0.17	1.91	1.39	0.74
Height		0.57	0.46	0.55				2.12	1.57	0.93

Table 6.4 – Instrument capability index, *Cg*, calculated for the measurands: inner diameter, outer diameter, concentricity and height of the micro part 411 using the different optical set-ups. The coloured cells indicate that Cg is lower than 1.33: the measurements are not acceptable according to the tolerance range.

Cgk was estimated only for the measurands estimated to be inside the tolerance range. This measurand was the outer diameter, measured using a coaxial light and a lens magnification equal to 2x and 5x.

Cgk indices are summarized in Table 6.5. Again the coloured cells indicate that Cgk is lower than 1.33. As conclusion it was suggested to perform optical measurements using higher lens magnification and stronger light intensity.

Cgk	*Lens*	*2x*			*5x*		
	Illumination type	*Coaxial light*			*Coaxial light*		
	Illumination intensity [%]	*40*	*43*	*46*	*40*	*43*	*46*
Outer diameter		0.55	3.29	2.32	3.42	3.51	9.05

Table 6.5 - Instrument capability index, *Cgk*, calculated for the measurand: outer diameter of the micro part 411 using the different optical set-ups. The coloured cells indicate that Cgk is lower than 1.33: the measurements are not acceptable.

The same indices Cg and Cgk were calculated considering the uncertainties of the optical measurements obtained from equation 6.4 instead of the measurement standard deviations. Therefore the new Cg and Cgk were estimated as:

$$Cg_{ij} = \frac{k/100 \cdot T_j}{6U_{OCMM,j}} \qquad (6.11)$$

$$Cgk_{ij} = \frac{k/200 \cdot T_j - \left|\mu_{ij} - \mu_{nom,j}\right|}{3U_{OCMM,j}} \qquad (6.12)$$

The new values are shown in Table 6.6 and Table 6.7. Looking at the results, the instrument capability indices were subjected to a considerable decrease: the optical instrument was now capable of measuring only the outer diameter. This drastic reduction was related to the three additional contributors which were taken into account in the uncertainty estimation:

1. u_{cal}: calibration uncertainty;
2. u_w: temperature-related uncertainty;
3. u_b: uncertainty of the systematic error.

Cg	*Lens*	*2x*			*2x*			*5x*		
	Illumination type	*Coaxial light*			*Ring light*			*Coaxial light*		
	Illumination intensity [%]	*40*	*43*	*46*	*3.7*	*4.7*	*5.7*	*40*	*43*	*46*
Inner diameter		0.17	0.16	0.17	0.17	0.17	0.17	0.16	0.16	0.17
Outer diameter		0.44	1.71	1.76	0.23	0.26	0.42	1.41	1.31	1.88
Concentricity		0.12	0.37	0.36	0.09	0.12	0.06	0.51	0.41	0.25
Height		0.20	0.16	0.19				0.71	0.55	0.33

Table 6.6 - Instrument capability index, *Cg*, calculated using the uncertainties of the optical measurements instead of the measurement standard deviations. Measurands: inner diameter, outer diameter, concentricity and height of the micro part 411. Different optical set-ups used. The coloured cells indicate that Cg is lower than 1.33: the measurements are not acceptable according to the tolerance range.

Cgk	*Lens*	*2x*			*5x*		
	Illumination type	*Coaxial light*			*Coaxial light*		
	Illumination intensity [%]	*40*	*43*	*46*	*40*	*43*	*46*
Outer diameter		0.19	0.70	0.48	0.89	0.99	1.51

Table 6.7 - Instrument capability index, *Cgk*, calculated using the uncertainties of the optical measurements instead of the standard deviations. Measurand: outer diameter of the micro part 411. Different optical set-ups used. The coloured cells indicate that Cgk is lower than 1.33: the measurements are not acceptable.

6.8 Conclusion

In this chapter the quality control of injection moulded micro mechanical parts was analyzed and investigated. The uncertainty assessment was performed and the analysis of the influence parameters of an Optical Coordinate Measuring Machine (OCMM) was presented. The uncertainties were calculated following a compensation method based on the substitution approach to correct the measuring results and decrease the OCMM's uncertainty. The OCMM influence parameters taken into account were related to the lens magnification, the illumination type and the illumination intensity. These factors were investigated first comparing the optical measurements with the reference values.

If an optical instrument is used to perform the quality control of a part, the crucial step is the applied measuring set-up. In the current investigation, 10 μm of difference between the optical set-ups was observed. If the component is a micro component, as in the present case study, 10 µm represents a huge gap (≈ 33 - 50% of the tolerance range). This wrong conclusion could lead to the rejection of good components from the production. Therefore before measuring, it is suggested to perform a thoughtful analysis of the optical instrument in order to optimize and maximize the repeatability of the results.

A second investigation was based on the statistical quality control approach. It revealed to be a useful method to estimate the contributions coming from the measurements, the process and the instrument. In the case study, the substantial variability was the process, usually influenced by different factors such as process conditions, samples material or other process parameters. This conclusion prompted that a better control on the production phases should be considered for the specific case study.

A third method involved the investigation on the measuring instrument capability indices Cg and Cgk. This analysis is useful to evaluate the capability of the used measuring instrument. Following this approach and assuming a normal distribution of the data, it is possible to know whether the measuring instrument is capable to check the desired component in relation to the tolerance range. Moreover it is important to underline how different conclusions can be drawn when either the measurement standard deviations or the measurement uncertainties are taken into account. In fact, the three factors involved on the uncertainty calculation (i.e. u_{cal}, u_w and u_b) have a substantial influence on the final results.

6.9 References

[Cagnazzo, 2010] L. Cagnazzo, T. Sibalija, V. Majstorovic "The measurement system analysis as a performance improvement catalyst: a case study", Business Performance Measurement and Management, 2010, Volume 7, pp. 269-292.

[Czarski, 2009] A. Czarski, "Comparative analysis of methods of hardness assessment", Archives of materials science and engineering, 2009, Volume 40, pp. 94-97.

[Flynn, 2009] M.J. Flynn, S. Sarkani, T.A. Mazzuchi "Regression analysis of automatic measurement systems", IEEE Instrumentation and measurement society, 2009, Volume 58, pp. 3373-3379.

[Fugl, 2004] J. Fugl, "In-line measurement and quality control of micro objects", Department of Manufacturing Engineering and Management, Technical University of Denmark, 2004.

[Gasparin, 2009] S. Gasparin, G. Tosello, H.N. Hansen, M.B. Jørgensen, "Quality control of injection moulded micro mechanical parts", 5th International Conference on Multi-Material Micro Manufacture (4M) and 4th International Conference on Micro Manufacturing (ICOMM) 2009, pp.175-178.

[Gasparin, 2012] S. Gasparin, G. Tosello, H.N. Hansen, A. Islam, "Quality control and process capability assessment for injection moulded micro mechanical parts", Submitted for The International Journal of Advanced Manufacturing Technology, 2012.

[GUM, 2008] Joint Committee for Guides in Metrology (JCGM). JCGM 100:2008, Guide to the Expression of Uncertainty in Measurement (GUM), 2008, pp. i–viii, 1–132.

[Hansen, 2006] H.N. Hansen, K. Carneiro, H. Haitjema, L. De Chiffre, "Dimensional micro and nano metrology", Annals of CIRP, 2006, Volume 55, Issue 2, pp.721-743.

[Hansen, 2008] H.N. Hansen, L. De Chiffre, J. Fugl, "Tolerancing issues in micro manufacturing", Proceedings of the Euspen International Conference, 2008, Volume 2, pp. 317-320.

[Hansen, 2011] H.N. Hansen, G. Tosello, S. Gasparin, L. De Chiffre, "Dimensional metrology for process and part quality control in micro manufacturing", Int. J. Precision Technology, 2011, Volume 2, Issue 2/3, pp.118–135.

[ISO 15530-3, 2004] ISO 15530 part 3: 2004 - Geometrical Product Specifications (GPS) - Coordinate Measuring Machine (CMM): techniques for determining the uncertainty of measurement – Part 3: Use of calibrated workpieces or standards.

[ISO 3650, 1998] ISO 3650:1998 - Geometrical Product Specifications (GPS) – Length Standards – Gauge Blocks, International Organization for Standardization.

[Knapp, 2001] W. Knapp, "Tolerance and Uncertainty", 5th International Conference on Laser Metrology, Machine Tool, CMM and Robot Performance, LAMDAMAP, 2001, pp. 357–366.

[Mader, 2009] O. Mader, P. Meyer, V. Saile, J. Schulz, "Metrology study of high precision mm parts made by the deep x-ray lithography (LIGA) technique", Measurement science and technology, 2009, Volume 20.

[Meyer, 2009] P. Meyer, O. Mäder, V. Saile, J. Schulz, "Comparison of measurement methods for micro system components: application to microstructures made by the deep x-ray lithography process (x-ray LIGA)", Measurement science and technology, 2009, Volume 20.

[Montgomery, 2005] D.C. Montgomery, "Introduction to statistical quality control", 5th edition, John Wiley & Sons, 2005.

[Theilade, 2007] U.A. Theilade, "Surface micro topography replication in injection moulding", Department of Manufacturing Engineering and Management, Technical University of Denmark, 2007.

[Tosello, 2009] G. Tosello, H.N. Hansen, S. Gasparin, "Applications of dimensional micro metrology to the product and process quality control in manufacturing of precision polymer micro components", Annals of CIRP, 2009, pp. 467-472.

7. Tolerance chain verification at sub-micro dimensional scale

7.1 Introduction

In the field of media support for both data storage and entertainment, polymer-based substrates composed of thin polycarbonate discs having a sub-micro structured surface (so called optical discs) are nowadays the established format for a variety of different uses. Since the beginning of its introduction, first at research and development level and then at the market place in 1982, the compact disc (CD) format attained a successful market position, reaching its peak of 15 billion CDs produced worldwide in 2001 [Jones, 1986], [Binkowska, 2007].

The need for higher data content in both the entertainment sector (to achieve the shift from digital audio to audio/video content) and the electronic/information technology sector (increased data storage) created the motivations to enhance the capacity of CD support and to develop the digital versatile disc (DVD) format, introduced in 1996. Different strategies were adopted to increase the capacity of the media, ranging from drives and drive precision to multi-layer technology, encoding/decoding electronics and optics design. The latter dealt with the use of shorter laser wavelength and larger numerical aperture, which reduced the CD spot diameter from 780 nm to 650 nm. This has enabled to miniaturize the surface structures and therefore to increase data density [S-Immink, 1996]. The result was that a single-layer DVD has a storage capacity 7 times higher than the one of a CD and a double-layer DVD up to 14 times, equivalent to 135 min of wide-screen high quality video including multiple audio and subtitle channels [Yamada, 1997]. DVD production worldwide has grown since the format introduction into the market in 1998 with a peak in 2006 of about 10 billion discs and a market worth $100 billion [Binkowska, 2007], [Yamada, 2004].

Lately, starting from 2004, new formats appeared on the market in order to satisfy a renovated demand for increased capacity; for example, the high definition DVD (HD-DVD), capable of storing 15 – 30 GB on a single- and double-layer disc respectively. The drive for such increased capacity has been mainly the spreading of the High Definition Television (HD-TV) service which promoted the diffusion of high definition flat screens larger than 30 in. (in order to take advantage of the new TV format) with a market size of 7.6 million and 10.5 million units in Japan and USA respectively in 2006. As a consequence, high definition flat displays larger than 30 in. have shown the limitations of the current DVD format in terms of image quality and therefore the need for a new optical disc support, creating a technology gap to be addressed [Yamada, 2004]. For the same reasons, also the Blue-ray Disc (BD-ROM) format, with a storage capacity of 25 GB, has been introduced. Both HD-DVD and BD-ROM present features with characteristic dimensions in the order of about 100 nm – 400 nm. This increase of data storage density caused the decrease of surface structure dimensions, leading the product quality control to a crucial step in order to validate process, processing condition and production batch.

This chapter introduces new procedures for quality control of nickel stampers and polymer moulded discs for CD, DVD and HD-DVD manufacture: quantitative application of AFM to calibrate height, depth and pitch of sub-micrometer features and SEM image processing to verify length and width. Surface replication is analyzed using a metrological approach:

- Nano-features on nickel stampers and injection–compression moulded polycarbonate substrates are measured;
- Measurement uncertainty calculated;
- Replication fidelity assessed quantitatively;
- Dimensional tolerances at the nanometre scale verified.

The main results of the present case study have been published in [Gasparin, 2010] and [Tosello, 2010].

7.2 Optical discs manufacturing process chain

Despite the different capacities of the three formats (CD, DVD, HD-DVD), the optical disc layout and process chain are basically the same. In particular, there is a first phase devoted to the manufacture of a master made of metal (typically nickel) and a second phase dealing with the production of polymer optical discs (typically made of polycarbonate).

7.2.1 Stamper making

After a pre-mastering phase (where a source material such as an audio/video recording or a computer software is converted into a digital format), the digital content is encoded by a mastering system and transferred to a glass master, inspected and then transferred to an electroformed nickel stamper under the form of sub-micrometer pillars (i.e. peak pits) ordered on a spiral pattern at determined distances from each other (i.e. lands), see Figure 7.1. These features are fundamental for the functionality of an optical disc because on their quality depends the ability of the user to listen to stored music or watch a movie.
A stamper is defined as the particular mould employed to replicate optical discs such as CD, DVD or HD-DVD [Greener, 2006]. Typically, stampers have a diameter of 138 mm, a thickness of 300 µm with a 20 mm – 40 mm central hole. This first electroformed stamper (father) can be either used directly for polymer disc manufacturing, to shorten production times, or can be used for a galvanic process to produce other impressions (mothers). Such impressions are subsequently employed to manufacture nickel moulding matrices by electroforming (i.e. new stampers), obviously increasing the throughput of the production line [McGeough, 2001]. In fact, the number of polymer discs made from the same stamper is mostly determined by the batch size rather than the stamper tool life, time-to-market being the crucial aspect on optical disc manufacturing industry [Bifano, 1997].

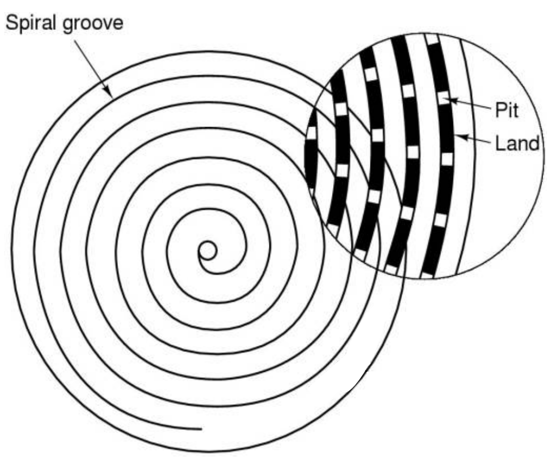

Figure 7.1 - Pit and land regions in an optical disc.

7.2.2 Polymer replication

Nickel stampers are then fitted into an injection mould cavity formed between a mirror block and the stamper itself. By either a high-pressure/thin-wall injection moulding processes (CD) or an injection–compression moulding process (DVD, HD-DVD) the nickel stamper pattern is transferred into a polycarbonate disc (1.2 mm thick for CD, 0.6 mm thick for DVD and HD-DVD) in the form of shallow grooves of variable lengths (i.e. valley pits) positioned at certain distances (i.e. lands) along the spiral pattern. Therefore the nickel stamper has pit regions characterized by peaks; while the polymer substrate has pit regions characterized by valleys, see Figure 7.2. A high-grade polycarbonate resin is selected due to its excellent characteristics such as high transparency, dimensional stability, high flowability for accurate mould surface reproduction, minimum water absorption, good impact resistance, easy processing characteristics and absence of impurities [Pohlmann, 1992].

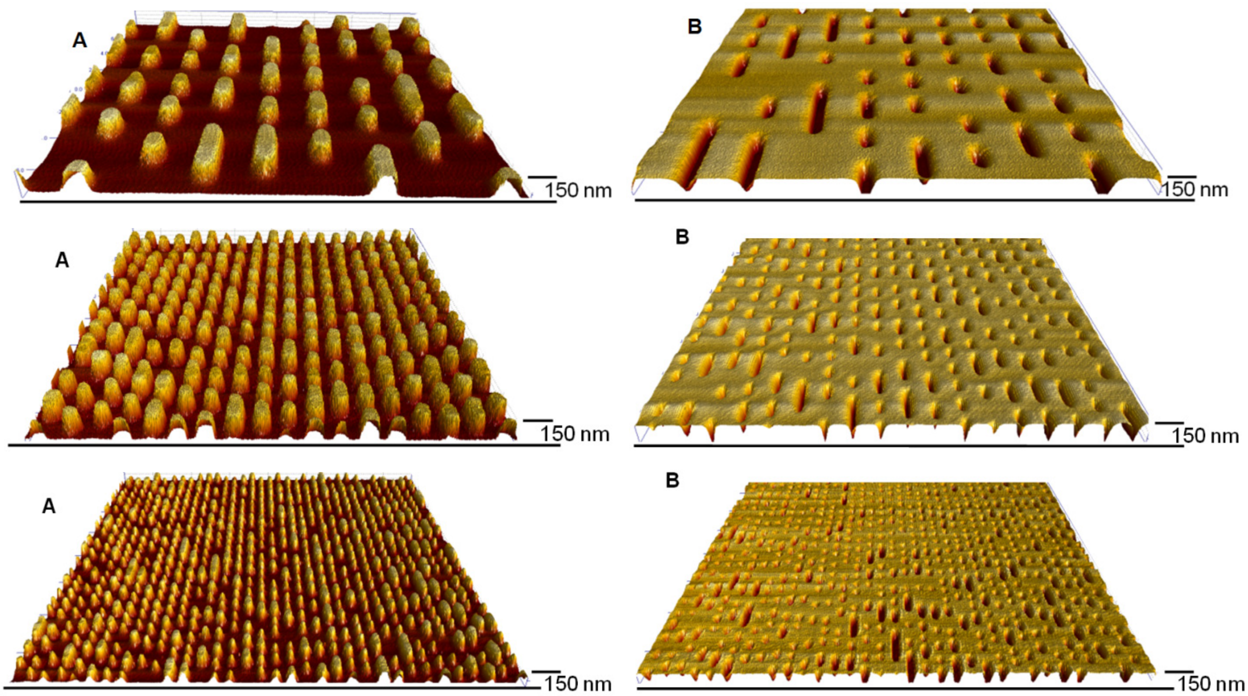

Figure 7.2 – A) Peaks pit regions in the nickel stamper (Ni). B) Valleys pit regions in the polycarbonate substrate (PC). Scanning area: 15 x 15 μm^2. Top: CD; middle: DVD; bottom: HD-DVD.

7.3 Nano-features dimensional quality control

The increased data storage density from CD, DVD to HD-DVD formats causes the decrease of the surface structure dimensions (see Figure 7.2), challenging not only the tooling phase (i.e. stamper making process), but also the moulding process (i.e. replication fidelity within a very short moulding cycle time of 2 – 3 s). As a consequence, the product quality control (dimensional compliance to specifications) is a crucial step in order to validate process, processing conditions and production batch. Additionally, due to the extremely short cycle time, online measurement of disc properties is desirable; therefore high measuring speed and data processing rate are of high importance. Research and applications ([Binkowska, 2007], [Losner, 1990], [Kang, 2000], [Kim, 2002]) have dealt mostly with functional check of written tracks onto the disc surface at the production line end (e.g. quality control performed by playing a disc on a fast simulator employing a reading laser beam); digital image processing to detect opaque inclusions, holes, scratches; birefringence distribution measurements to ensure that internal stresses induced by the moulding process into the polymer do not prevent the disc to play correctly. Additionally, dimensional approaches to quality control of polymer optical disc structured surfaces were also investigated showing the capability of replicating features with height and track pitch respectively of 50 nm and 680 nm [Kim, 2002], 25 – 40 – 60 nm and 160 – 200 nm [Schift, 2000], 100 nm and 130 nm [Heidari, 2000]. Atomic force microscopy (AFM) was in particular employed to measure the nanometre-sized features; however, the establishment of measurement traceability, the definition of replication fidelity parameters, the effect of downscaling from CD, DVD to HD-DVD both in the stamper and in the polymer replicas, as well as nano-structures dimensional compliance with specifications still need to be addressed.

7.3.1 Nano-tolerances of optical disc features

The specification of a micro/nano mechanical component is usually defined on the basis of the desired function of the part. For the optical disc features, the fundamental feature dimensions (pit/land lengths, track pitch, pit width, pit height, see Figure 7.3) are defined along with their tolerances in order to ensure a correct data transfer (i.e. accurate pit/land scanning by the diode reading panel).

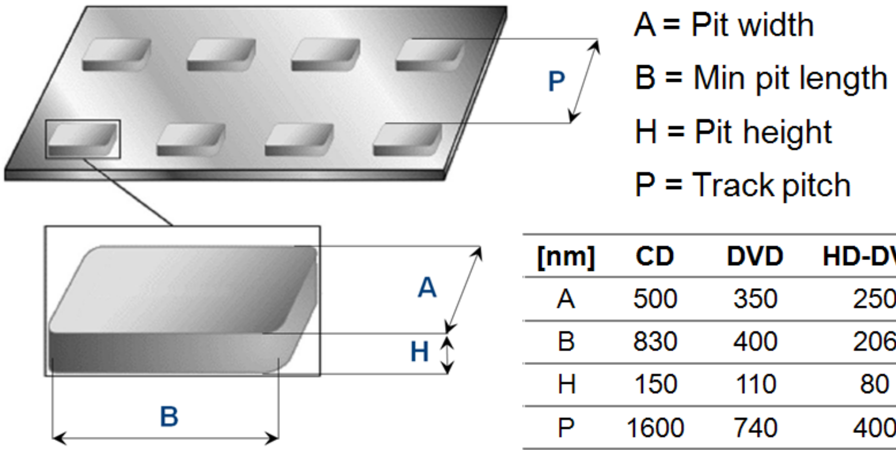

[nm]	CD	DVD	HD-DVD
A	500	350	250
B	830	400	206
H	150	110	80
P	1600	740	400

Figure 7.3 - Nano-features which characterize optical discs and their nominal values.

The specifications are usually given in terms of maximum deviations from an ideal geometric form, but a downscaling below the defined lower borders of ISO GPS standards may prove to be problematic. According to the definition given in [Weckenmann, 2000], an optical disc for data storage can be considered as a product made by a ‘monolithic integration’ process, where all the process steps are on substrate.
This research investigates and presents dimensional compliance of the polymer substrate features in terms of track pitch, pit height and pit/land length. In particular:

- *Track pitch tolerance (CD, DVD, HD-DVD)*: includes the specified upper and lower limits of the distance between two consecutive lines of features, see Table 7.1;
- *Pit height tolerance (CD, DVD, HD-DVD)*: is defined as the allowed variation of groove depth in the polymer disc in order to ensure a proper signal level while reading (i.e. equivalent to a flatness tolerance), see Table 7.1;
- *Pit/land length tolerance (CD)*: is defined in order to satisfy the correct data transfer. For this reason the data encoding is the crucial phase. Therefore the controlled process parameters are ‘time’ and ‘scanning velocity’. CD pit and land lengths in terms of ‘time’ are clustered according to the runlength (3T, ..., 11T) and given in Table 7.2, left. The scanning velocity during encoding is 1.2 - 1.4 m/s with a maximum variation through the whole disc of ± 0.01 m/s. The features lengths in ‘ns’ have to be multiplied by the scanning velocity in order to obtain the features lengths in ‘nm’ and therefore it permits the tolerance verification from a metrological

point of view. The scanning velocity given by the manufacturer is 1.2 m/s, so it is possible to calculate the CD pit and land length tolerances listed in Table 7.2, right.

Characteristic (dimension ± tolerance)	Disc format		
	CD	DVD	HD-DVD
Track pitch [nm]	1600 ± 100	740 ± 46	400 ± 25
Pit height [nm]	150 ± 15	110 ± 15	80 ± 9

Table 7.1 - CD, DVD, and HD-DVD track pitch and pit height specifications (dimensions and tolerances).

Runlength	CD Nominal Length ± Tolerance [ns]	
	PIT	LAND
3T	660 ± 40	675 ± 40
4T	910 ± 42.5	925 ± 42.5
5T	1165 ± 45	1165 ± 45
6T	1400 ± 47.5	1400 ± 47.5
7T	1635 ± 50	1635 ± 50
8T	1875 ± 52.5	1875 ± 52.5
9T	2110 ± 55	2105 ± 55
10T	2340 ± 57.5	2335 ± 57.5
11T	2570 ± 60	2560 ± 60

Runlength	CD Nominal Length ± Tolerance [nm]	
	PIT	LAND
3T	792 ± 48	810 ± 48
4T	1092 ± 51	1110 ± 51
5T	1398 ± 54	1398 ± 54
6T	1680 ± 57	1680 ± 57
7T	1962 ± 60	1962 ± 60
8T	2250 ± 63	2250 ± 63
9T	2532 ± 66	2526 ± 66
10T	2808 ± 69	2802 ± 69
11T	3084 ± 72	3072 ± 72

Table 7.2 – Left: pit and land length specifications for CD in terms of 'time'; right: pit and land length specifications for CD.

For these reasons, a metrological approach was investigated to control the replication quality of the stamper pattern into the polymer substrate as well as to the tolerance verification at nanometre dimensional scale, in particular:

- *Pit height* and *track pitch* (i.e. "*H*" and "*P*" in Figure 7.2) for *CD, DVD, HD-DVD* were investigated and verified applying AFM measurements (*Paragraph 7.4*);
- *Pit width* (i.e. "*A*" in Figure 7.2) for *CD, DVD, HD-DVD* was investigated by SEM image processing (*Paragraph 7.5.1*);
- *Pit/land length* (i.e. "*B*" in Figure 7.2) for *CD* was investigated and verified by SEM image processing (*Paragraph 7.5.2*).

7.4 AFM measurements of pit height and track pitch

For the present study a compact stand-alone instrument, which can be easily implemented in industrial manufacturing environment, was chosen. It was employed first in connection with the experimental session on calibrated gratings, and then used for the measurement campaign on the industrial specimens (nickel stampers and polycarbonate replicas of CD, DVD, HD-DVD). The employed AFM is described in appendix 11.1.3.

The idea underlying this study is to implement metrological laboratory calibration practices into a production environment in order to ensure an accurate assessment of the measurement uncertainty.

A pilot study was performed in order to achieve the optimal instrument set up. The metrological approach, including instruments calibration, uncertainty assessment and tolerance verification, was executed in particular considering the two most influencing factors, scan speed and force (eventually set at 20 µm/s and 10 nN respectively). These values were found to be a convenient trade-off between accuracy, precision of measuring results and scanning time [Tosello, 2009(1)]. The calibrated instrument with optimized settings was then implemented to take 5 measurements on each surface of the nickel stampers and the polycarbonate discs, with a scan range of 15 µm x 15 µm and a sampling strategy of 2048 x 512 points (i.e. a higher resolution on fast scan direction of about 7 nm). The instrument was actuated in contact mode, with the probe parallel to features and fast scan direction orthogonal to the cantilever. The same measuring conditions were applied for the calibration session.

Each AFM scan covered an area with a number of features between 50 for CDs and 750 for HD-DVD. To calculate the pit height, ISO 5436 part 2 [ISO 5436-2, 2001] was applied coupled with a height distribution frequency analysis. Such analysis allowed excluding the influence of pits sidewalls, including only the substrate and pits plateau regions. Pitch measurements were carried out by calculating the average profile aligned along the slow scanning direction (i.e. *Y* direction) and then identifying the main peak position in the Fast Fourier Transform of the profile.

7.4.1 Uncertainty assessment and traceability of measurements

The uncertainties of both horizontal (i.e. track pitch) and vertical (i.e. pit height) measurements were calculated following the GUM [GUM, 2008] and by adapting to AFM measurements recommendations given for CMM measurements in [ISO 15530-3, 2004][e]. A number of error contributors typical of AFM instruments [Marinello, 2009] was considered in the uncertainty budget; for each uncertainty contributor a standard uncertainty *u* was assigned [Tosello, 2010].

The standard uncertainties were treated as independent and were combined following the law of propagation of uncertainty:

$$U_i = k\sqrt{u_{res,i}^2 + u_{c(i)}^2 + u_{cal,i}^2 + u_{rep,i}^2 + u_{noise}^2} \quad (7.1)$$

with:

$$u_{rep,i} = \max(u_{AFM,i}; u_{features,i}; u_{DISC,i}) \quad (7.2)$$

Where:

- U = expanded combined uncertainty;
- $i = x, z$ depending on the measurand (track pitch or pit height respectively);
- k = 2 in order to obtain a confidence level of approximately 95%;
- $u_{res,i}$ = instrument resolution depending on the number of pixels and the scanning length along the fast scanning direction (horizontal measurements) and scanning probe characteristics (vertical measurements);
- $u_{c(i)}$ = variability of the calibration factor (calculated as the standard deviation of 5 different calibration factors c(*i*) obtained from 5 repeated independent calibrations);
- $u_{cal,i}$ = calibration of reference artefacts employed for scanner calibration: a 100 nm calibrated *Z* step height for vertical calibration and a 2121 nm pitch *XY* grid (see Figure 7.4). For both artefacts, expanded calibration uncertainty *U* = 1 nm;
- $u_{rep,i}$ = repeatability;
- $u_{AFM,i}$ = standard deviation of 5 repeated measurement on the same feature (see e.g. Figure 7.2) (to estimate the instruments repeatability);

[e] A revised version is available (ISO15530-3:2011).

- $u_{features,i}$ = standard deviation of repeated measurements on 5 different features on the same scanning area (to estimate the feature repeatability in terms of master making and polymer replication);
- $u_{DISC,i}$ = standard deviation of repeated measurements on 5 different features on 5 different scanning area (to estimate the disc manufacturing repeatability);
- u_{noise} = instrument background noise estimated by applying the "standstill measurement" method [Danzebrink, 2006] on a flat silicon plane as Root Mean Square roughness (Rq_{Si} < 0.25 nm).

It is interesting to notice that relocated measurements on the same scanning area as well as on different areas of the disc were also affected by the instrument repeatability. Therefore, the maximum value among the uncertainty contributors related to instrument repeatability (u_{AFM}, $u_{features}$, u_{DISC}) was selected; otherwise, the influence of instrument repeatability and re-location on the final uncertainty would have been overestimated. This observation was also confirmed by the experiments, which showed u_{AFM} in average was lower than the other repeatability contributors of at least 20% and up to 70%. This behaviour was also observed on white light interferometer measurements [Tosello, 2009(2)] and appeared to be a suitable procedure to treat repeatability of measurements.

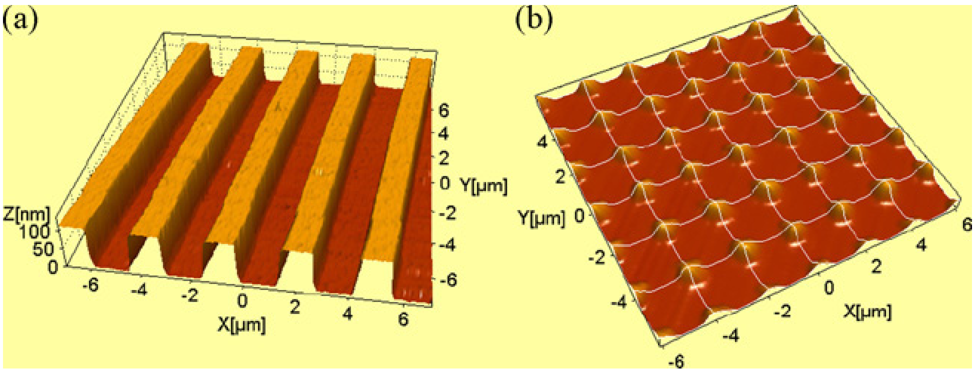

Figure 7.4 - AFM scanning of silicon calibrated objects: (a) 100 nm step height (TGZ02) for scanner vertical calibration and (b) 2121 nm grid (TGT) for *XY* scanner calibration (axis magnifications: *X* = 1x, *Y* = 1x, *Z* = 20x) [Tosello, 2010].

7.4.2 Measurements results

Results in terms of measurements, uncertainties, tolerances for both nickel stampers and polymer discs are reported in Figure 7.5 and Figure 7.6.

Physical replication of feature height depends on the disc format and it is directly influenced by the employed process. In CD manufacture, the high-pressure/thin-wall speed injection moulding process was not capable of providing full replication, due to the missing compression phase: with an optimized injection moulding, average groove depth was 80% of the average pillar height. In DVD manufacture, it could be seen that the compression moulding process improved the replication quality (average groove depth was 88% of the average pillar height). Finally, as far as HD-DVD was concerned, the compression phase was further optimized in order to comply with stricter dimensional tolerance and a 100% replication of pit height was realised.

The advantages obtained by employing an injection–compression moulding process was also observed in the track pitch replication, when comparing results obtained on CD manufacture with DVD and HD-DVD measurements. In fact, track pitch ratio from stamper to disc increased from 94% (CD) to 100% for both DVD and HD-DVD. This was due to the fact that polymer shrinkage during cooling was higher when the injection moulding process was employed (which leaved higher internal stresses in the polymer matrix due to higher cooling rates) than when injection–compression was used. The compression phase contributed to release internal stresses of the polymer material reducing shrinkage and increasing dimensional stability.

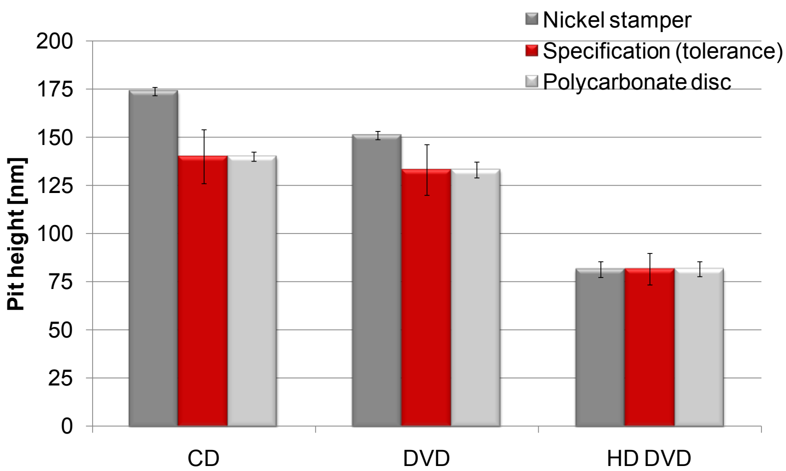

Figure 7.5 - Replication assessment and tolerance verification at the nanometre scale of pit height on CD, DVD, HD-DVD stampers and discs.

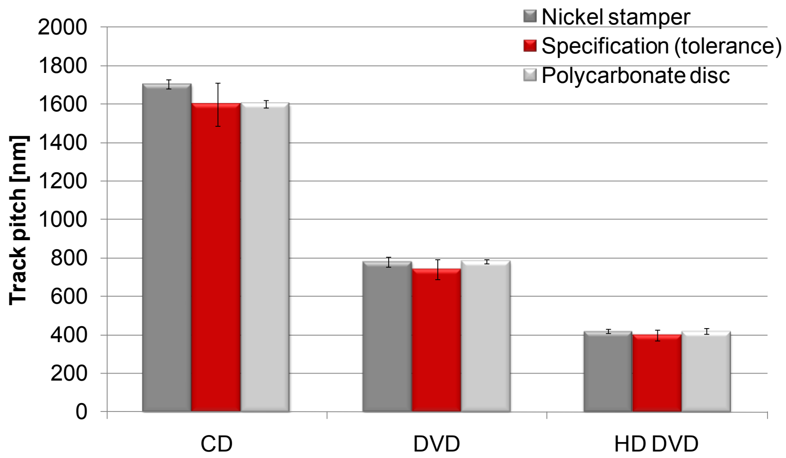

Figure 7.6 - Replication assessment and tolerance verification at the nanometre scale of track pitch on CD, DVD, HD-DVD stampers and discs.

Features miniaturization due to increased data storage capacity of optical discs caused the reduction of the tolerance (i.e. highly demanding specification requirements). Therefore, the ratio between the measuring uncertainties and related tolerances (*U/T*) worsen going from CD, DVD, to HD-DVD disc formats. In particular, as far as pit height was concerned, *U/T* increased from 16% (CD), to 27% (DVD), to 44% (HD-DVD), see Table 7.3. A similar trend was observed when considering the track pitch, with the *U/T* ratio increasing from 19% (CD), to 24% (DVD), to 58% (HD-DVD) , see Table 7.3. These *U/T* values were, especially for HD-DVD, much higher than the recommended ratio of 10 – 20% [Knapp, 2001] and clearly showed the challenge of performing an effective dimensional quality control and a reliable manufacturing process when nanometre tolerances are specified. Indeed, when further miniaturization is required (to achieve higher data density storage, i.e. BD-ROM) lower tolerances are specified, increasing the challenge of manufacturing products within specifications and carrying out the related quality control.

	Pit Height			*Track Pitch*		
	CD	*DVD*	*HD-DVD*	*CD*	*DVD*	*HD-DVD*
Tolerance [nm]	± 15	± 15	± 9	± 100	± 46	± 25
Uncertainty [nm]	2.4	4.0	4	19.1	11	15
U/T [%]	16	27	44	19	24	58

Table 7.3 – Uncertainty *U* to tolerance *T* ratio (*U/T*) for pit height and track pitch of CD, DVD and HD-DVD.

7.5 SEM measurements of pit width and pit/land length

SEM image processing was carried out using the SEM described in appendix 11.1.4, see Figure 7.7. The purposes were:

- Assessment of the replication quality for the pit width of CD, DVD and HD-DVD;
- Verification of the tolerances of pit/land length on CD nickel stampers and on CD polycarbonate substrates.

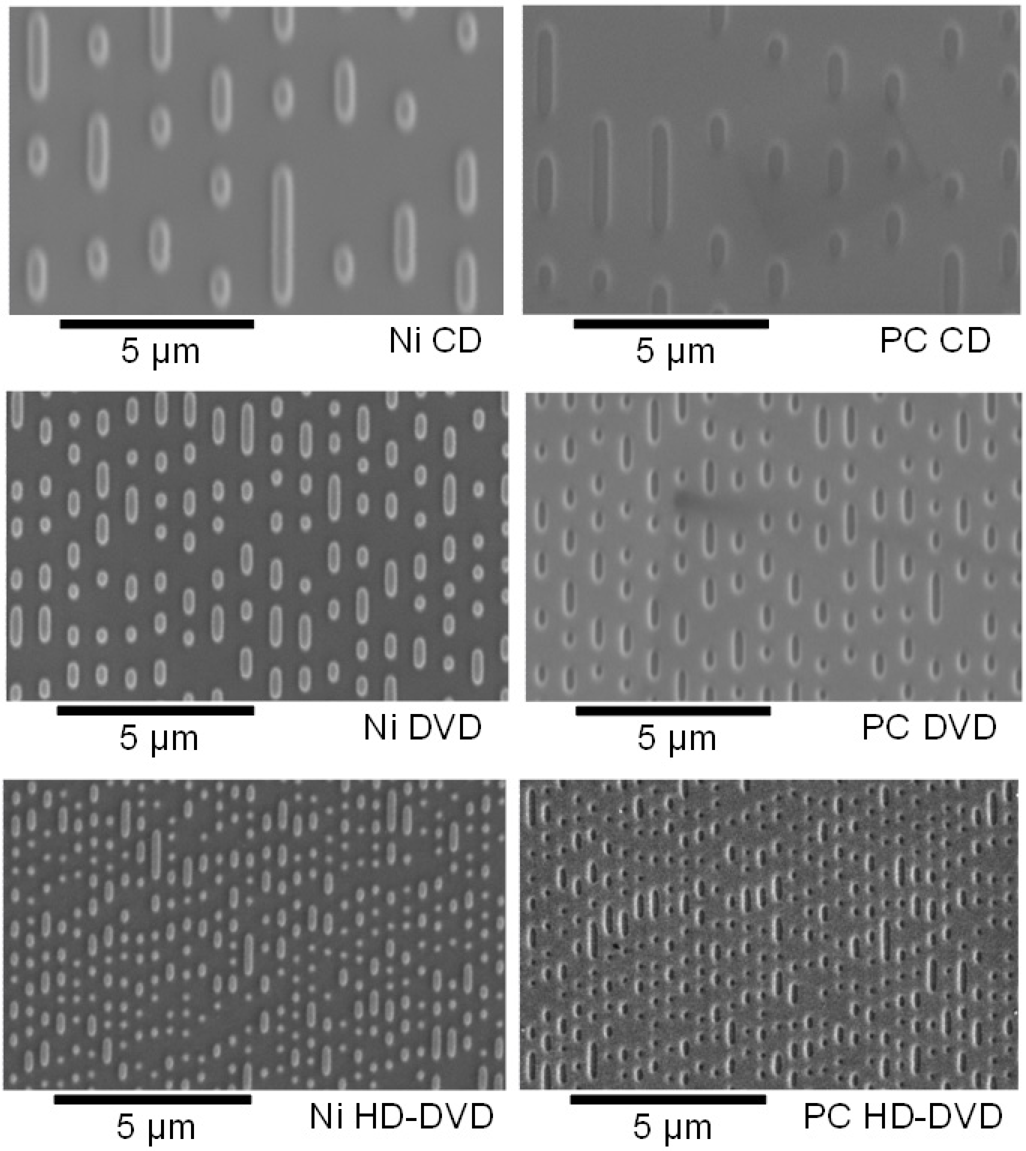

Figure 7.7 - Left: SEM images of nickel stamper (Ni) for optical discs moulding. Right: SEM images of polycarbonate moulded optical discs (PC). Top: CD; middle: DVD; bottom: HD-DVD.

For the SEM analyses, the uncertainty budget was calculated following [GUM, 2008]:

$$U_i = k \cdot \sqrt{u_{res,i}^2 + u_{cal,i}^2 + u_{rep,i}^2} \tag{7.3}$$

with:

$$u_{rep,i} = \max(u_{SEM,i}, u_{feat,i}) \tag{7.4}$$

Where:

- U = expanded combined uncertainty;
- $i = x$, y depending on the measurand (width or length respectively);
- k = 2 in order to obtain a confidence level of approximately 95%;
- $u_{res,i}$ = instrument resolution depending on the number of pixels;
- $u_{cal,i}$ = deviation between the nominal pixel size and the measured one according to [Bariani, 2005] and appendix 11.1.4;
- $u_{rep,i}$ = repeatability;
- $u_{SEM,i}$ = standard deviation of 3 repeated measurements on the same feature;
- $u_{feat,i}$ = standard deviation of different features on 3 SEM images.

Measurements on the same feature as well as on different features of the disc were affected by instrument repeatability. Therefore, the maximum value among the uncertainty contributors (u_{SEM}, u_{feat}) was selected to not overestimate the repeatability.

7.5.1 Replication quality

The pit width of CD, DVD and HD-DVD was measured in the SEM calibrated images of Figure 7.7 using an image processor. The obtained results were compared with the nominal value (“*A*”) of Figure 7.3 and the uncertainty budget estimated.

The results are summarized in Figure 7.8.

From the obtained values, the pit width was 40 - 50% larger on the nickel stamper than on the polymer disc. Especially this amount decreased from CD to DVD and from DVD to HD-DVD. As explained in the previous paragraph, this was due to the injection moulding process which presented a further compression phase for DVD and HD-DVD.

Moreover comparing the nominal values with the results of the polycarbonate disc, the difference was about 30 - 50%. This was probably due to a no controlled process for the pit width. Pit height, length and track pitch were, instead, the functional features which had to fulfil the specifications and had to guarantee a proper CD, DVD and HD-DVD usage.

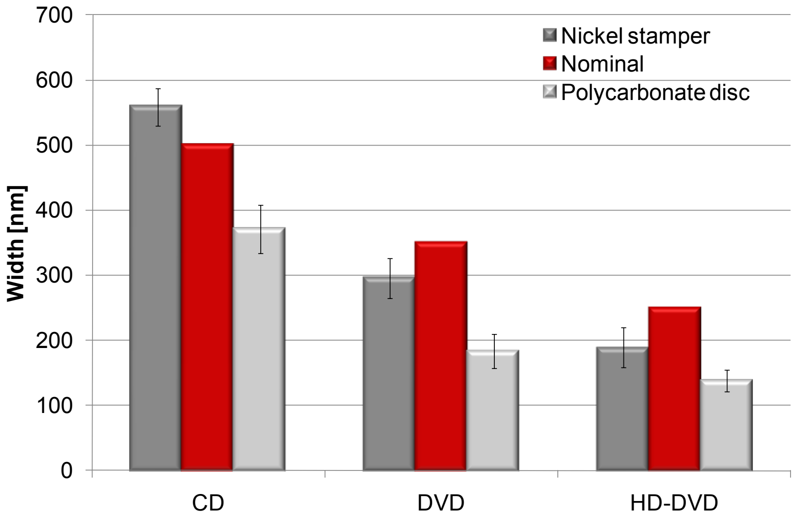

Figure 7.8 - Comparison between CD, DVD, HD-DVD pit width of nickel stamper and polycarbonate disc.

7.5.2 Tolerance verification

The SEM calibrated images were analyzed using an image processing software in order to evaluate, also, the pit/land length on the CD nickel stamper and on the polycarbonate CD.

Pit and land length values obtained from the analysis were grouped according to the clusters in Table 7.2 and compared to the nominal dimensions.

Figure 7.9 and Figure 7.10 illustrates respectively the average of pit/land lengths on the Nickel stamper (Ni CD) and on the polycarbonate CD (PC CD) inside the clusters: 3T, ..., 11T runlengths. Comparing the length values obtained from the stamper and the polycarbonate substrate, it was possible to notice that the mould was manufactured 13 - 20% larger than the polymer part. This was due to the polymer shrinkage occurred during the injection moulding process. From a statistical point of view it was possible to state that the measured values for the polycarbonate moulded optical discs were in tolerance compared to the nominal values.

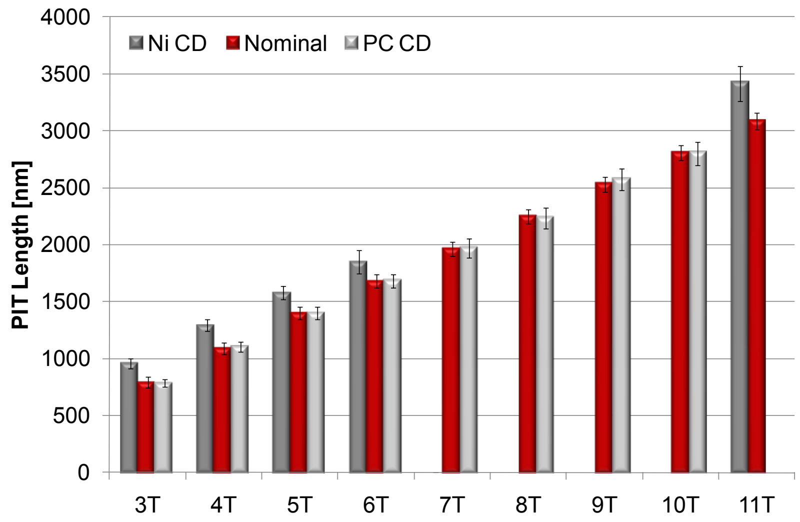

Figure 7.9 - Comparison between CD pit length of stamper (Ni), specifications (Nominal) and polycarbonate part (PC) for the different runlegth (3T, ..., 11T).

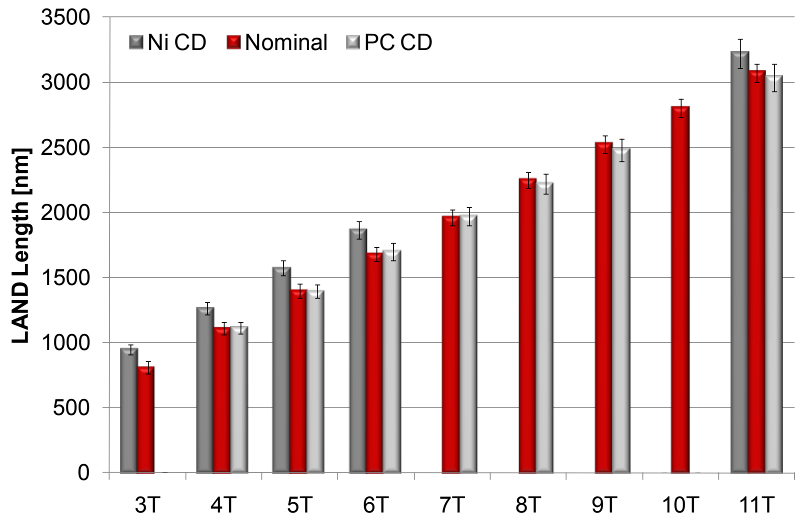

Figure 7.10 - Comparison between CD land length of stamper (Ni), specifications (Nominal) and polycarbonate part (PC) for the different runlegth (3T, ..., 11T).

From a metrological point of view the measured values in Figure 7.9 and Figure 7.10 for the polycarbonate substrates were not in tolerance compared to the nominal values. The resultant uncertainty was larger than the tolerance range. The uncertainty amount is mainly due to the contributors: u_{feat} (standard deviation of different features on 3 SEM images) and u_{SEM} (standard deviation of 3 repeated measurements on the same feature).

Figure 7.11 and Figure 7.12 illustrates the PC CD pit length and land length respectively which were measured inside the 4T runlength. The graphs show how the measured values were spread along the tolerance zone which led to a remarkable u_{feat}. Moreover the uncertainty shown in the two graphs verified the considerable contribution derived from u_{SEM}. The repeated measurements on the same feature led to different results for the same measurand. This was due to the not well defined edge on the single pattern of a SEM image. The reason was the material of the CD: it is evident from Figure 7.7 that the edges were better defined for the stamper than for the polymer optical disc.

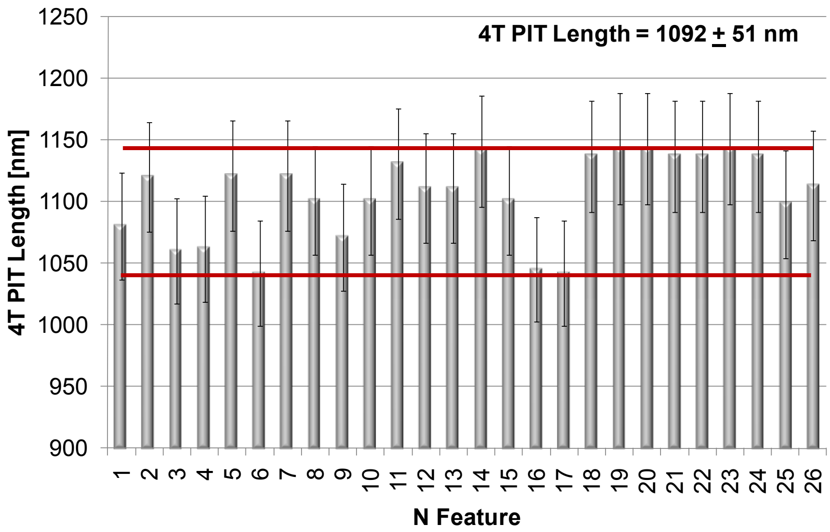

Figure 7.11 - 4T pit length of the polycarbonate CD (PC CD) features. Red lines indicate the tolerance range.

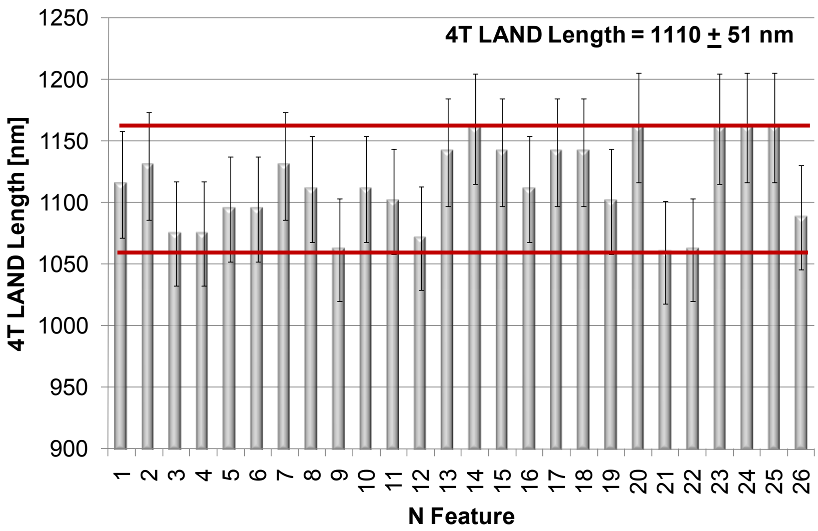

Figure 7.12 - 4T land length of the polycarbonate CD (PC CD) features. Red lines indicate the tolerance range.

7.6 Conclusion

Tolerance verification and replication quality evaluation were performed on nickel stampers and polycarbonate optical moulded discs for data storage application. Three different disc formats such as CD, DVD, and HD-DVD were investigated. A quantitative evaluation of the replication quality was performed using both scanning electron microscopy (SEM) and atomic force microscopy (AFM).

Dimensional tolerance verification at nanometre scale and replication accuracy investigation were carried out using a metrological approach. Track pitch and pit height of sub-micrometer sized features on the discs surfaces were measured and calibrated using AFM; while pit width replication and pit/land length were evaluated using SEM calibrated images. Comprehensive uncertainty budgets were created in order to calculate the measuring uncertainty and establish traceability.

The replication fidelity study showed the advantages obtained when an injection-compression moulding process (i.e. DVD and HD-DVD) is employed respect to an injection moulding process (i.e. CD). The replication ratio (i.e. stamper to disc) for CD was 6% – 50% lower to the replication ratio for DVD and HD-DVD (according to the measured feature). This result was due to the fact that the polymer shrinkage during cooling was lower in the injection-compression process than in the injection moulding process in order to comply with the stricter dimensional tolerance of DVD and HD-DVD. Moreover, the tolerance verification study showed that an increased feature miniaturization challenge both the replication process and the quality control technology. In fact, less favourable uncertainty to tolerance ratios (*U/T*) were observed on smaller features typical of HD-DVD discs when compared to DVD and CD discs showing the challenge of performing an effective quality control at nanometre dimensional scale.

7.7 References

[Bariani, 2005] P. Bariani, "Dimensional metrology for microtechnology", PhD thesis, Department of Manufacturing Engineering and Management, Technical University of Denmark, 2005.

[Bifano, 1997] T.G. Bifano, H.E. Fawcett, P.A. Bierdent, “Precision manufacture of optical disc master stampers”, Precision Engineering, 1997, Volume 20, pp. 53–62.

[Binkowska, 2007] P. Binkowska, B. Cord, P. Wohlfart, “Mass Production of DVDs: Faster, More Complex but Cheaper and Simpler”, Microsystem Technologies, 2007, Volume 13, pp. 139–144.

[Danzebrink, 2006] H.U. Danzebrink, L. Koenders, G. Wilkening, A. Yacoot, H. Kunzmann, “Advances in scanning force microscopy for dimensional metrology”, Annals of CIRP, Volume 55, Issue 2, pp. 841–878.

[Gasparin, 2010] S. Gasparin, G. Tosello, H.N. Hansen, “Tolerance Verification of Micro and Nano Structures on Polycarbonate Substrates”, 7th International Conference on Multi-Material Micro Manufacture (4M/ICOMM 2010), 2010, pp. 287-290.

[Greener, 2006] J. Greener, R. Wimberger-Friedl, “Precision Injection Moulding” Hanser, 2006, ISBN: 3-446-21670-7, pp. 192–201.

[GUM, 2008] Joint Committee for Guides in Metrology (JCGM). JCGM 100:2008, Guide to the Expression of Uncertainty in Measurement (GUM), 2008, pp. i–viii, 1–132.

[Heidari, 2000] B. Heidari, I. Maximov, L. Montelius, “Nanoimprint lithography at the 6 in. wafer scale”, Journal of Vacuum Science and Technology B Microelectronics and Nanometer Structures, 2000, Volume 18, Issue 6, pp. 3557–3560.

[ISO 15530-3, 2004] ISO 15530 part 3: 2004 - Geometrical Product Specifications (GPS) - Coordinate Measuring Machine (CMM): techniques for determining the uncertainty of measurement – Part 3: Use of calibrated workpieces or standards.

[ISO 5436-2, 2001] ISO 5436 part 2: 2001 Geometrical Product Specification (GPS) - Surface texture: Profile method - Measurements standards - Part 2: Software measurement standards.

[Jones, 1986] R. Jones, “Compact Disc Technology”, Data Processing, 1986, Volume 28, Issue 6, pp. 295–298.

[Kang, 2000] S. Kang, J.S. Kim, H. Kim, “Birefringence distribution in magneto-optical disk substrate fabricated by injection–compression molding”, Optical Engineering, 2000, Volume 39, Issue 3, pp. 689–694.

[Kim, 2002] Y. Kim, K. Seong, S. Kang, "Effect of insulation layer on transcribability and birefringence distribution in optical disk substrate", Optical Engineering, 2002, Volume 4, Issue 9, pp. 2276–2281.

[Knapp, 2001] W. Knapp, "Tolerance and uncertainty", 5th LAMDAMAP, 2001, pp. 357–366.

[Losner, 1990] L. Losner, A.S. Voloshin, "Compact disc quality control using digital image processing", NDT&E (Non-Destructive Testing and Evaluation) International, 1990, Volume 23, Issue 3, pp. 147–151.

[Marinello, 2009] F. Marinello, P. Bariani, S. Carmignato, E. Savio, "Geometrical modelling of scanning probe microscopes and characterization of errors", Measurement Science and Technology, 2009, Volume 20, Issue 8, pp. 084002.

[McGeough, 2001] J.A. McGeough, M.C. Leu, K.P. Rajurkar, A.K.M. De Silva, Q. Liu, "Electroforming process and application to micro/macro manufacturing", Annals of CIRP, 2001, Volume 50, Issue 2, pp. 499-515.

[Pohlmann, 1992] K.C. Pohlmann, "The Compact Disc Handbook", 2nd ed. A-R Editions, ISBN-13:978-0895793003.

[Schift, 2000] H. Schift, C. David, M. Gabriel, J. Gobrecht, L.J. Heyderman, W. Kaiser, S. Köppel, L. Scandella, "Nanoreplication in polymers using hot embossing and injection moulding", Microelectronic Engineering, 200, Volume 53, Issue 1–4, pp.171–174.

[S-Immink, 1996] K.A. Schouhamer Immink, "The Digital Versatile Disc (DVD): System Requirements and Channel Coding", SMPTE Journal, 1996, Volume 105, Issue 8, pp. 483–489.

[Tosello, 2009(1)] G. Tosello, A. Antico, H.N. Hansen, F. Marinello, G. Lucchetta, "Influence of measuring parameters on the accuracy of atomic force microscope in industrial applications", 5th 4M/ICOMM Conference, 2009, pp. 401–406.

[Tosello, 2009(2)] G. Tosello, F. Marinello, H.N. Hansen, "Characterization and analysis of micro channels and sub-micron surface roughness of injection moulded microfluidic systems using optical metrology", PPE'09 (Polymer Process Engineering), 2009.

[Tosello, 2010] G. Tosello, H.N. Hansen, F. Marinello, S. Gasparin, "Replication and dimensional quality control of industrial nanoscale surfaces using calibrated AFM measurements and SEM image processing”, Annals of CIRP 2010, Volume 59, Issue 1, pp. 563-568.

[Weckenmann, 2000] A. Weckenmann, R. Ernst, “Studies on new tolerancing rules for micro- and nanotechnology”, 1st EUSPEN Conference, 2000, Volume 1, pp. 214-221.

[Yamada, 1997] H. Yamada, “DVD overview”, Compcon Proceedings, IEEE, 1997.

[Yamada, 2004] H. Yamada, “HD DVD optical technology overview”, Proceedings of EPCOS (European Phase Change and Ovonics Science) Symposium 2004.

8. Process chain validation of 3D micro structured optical surfaces

8.1 Introduction

The relationship between required functionality, specifications and final tolerancing of a micro component is a key step in a micro product development which has also large consequences related to design principles. In any micro manufacturing technology, the production phases affect the technical performances and the quality of a product. Therefore, several constraints due to incompatibilities of materials, processes and geometries have to be considered while defining a manufacturing sequence. Since each process step influences, in principle, the results of both the previous and the following process steps, the process sequence has to be checked for consistency, and incompatibilities must be identified. Eventually this will influence the design parameters [Alting, 2003].

In particular, in many application areas like optics, optoelectronics and biomedical industry, the realisation of complex multiple three dimensional (3D) structures at micro and nano scales is a crucial issue that poses further constraints in designing and implementing successful manufacturing solutions. Such applications usually require structures such as lenses and pyramids, having micron and/or nanometre dimensions to be produced as large arrays rather than as single features, i.e. structured surfaces containing numerous 3D features. Usually, there are strict technical requirements in regard to such arrays of 3D features, e.g. geometrical accuracy, aspect ratio, positional and alignment accuracy and field stitching, which make the design and implementation of cost effective solutions for their manufacture even more difficult [Velkova, 2011].

This chapter deals with the characterization of an optical component and its mould through dimensional measurements of critical features, such as pitches, heights and angles. The measurements results obtained from the optical part are compared with the mould results

in order to perform a quality control of the manufacturing process through a control of the product.
Some results of the present case study have been published in [Gasparin, 2011].

8.2 Case description

The investigated micro-structured optical component and its correspondent mould are characterized by an array of triangular micro-pyramidal structures as shown in Figure 8.1.
The quality control of the manufacturing process was performed comparing the dimensional measurement of the component and the mould.
The measurements were carried out:

- Through SEM image processing on pitches (*Paragraph 8.3*);
- Through 3D-SEM reconstruction on pitches, heights and angles (*Paragraph 8.4*);
- Through an optical instrument using a replica casting technique on pitches, heights and angles (*Paragraph 8.5*).

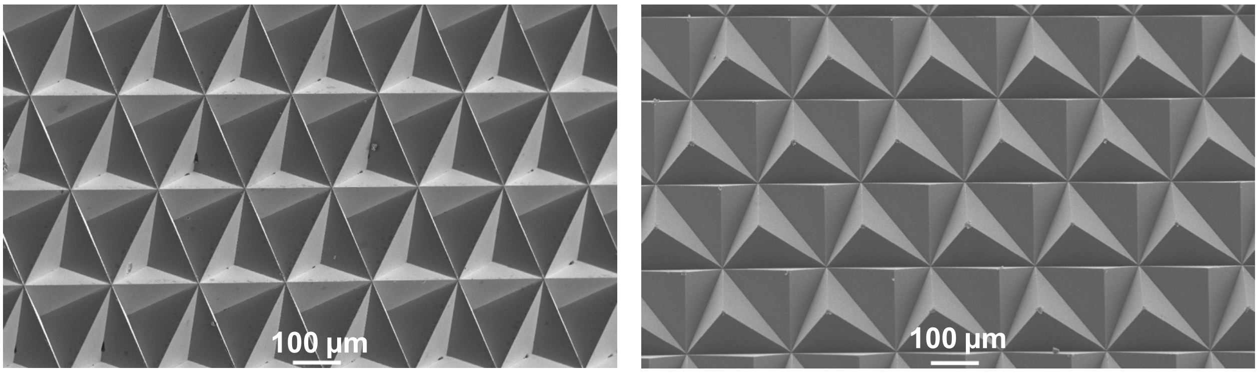

(a) (b)

Figure 8.1 - SEM images of the nickel mould (a) and the PMMA polymer part (b).

8.2.1 Tooling

The mould is in nickel (Ni) made through an electroforming process. The used master is in aluminium realized using diamond cutting technology and subsequently replicated by nickel electroforming (see Figure 8.2). Special machining is requested in order to obtain ultra-high accuracy cavities. Very low surface roughness suitable for optical applications

(Ra = 2 - 5 nm) and very high form accuracy (form error < 20 nm) can be achieved using diamond cutting [Taniguchi, 1983], [Corbett, 2000], [Byrne, 2003] and [Brinksmeier, 2006].

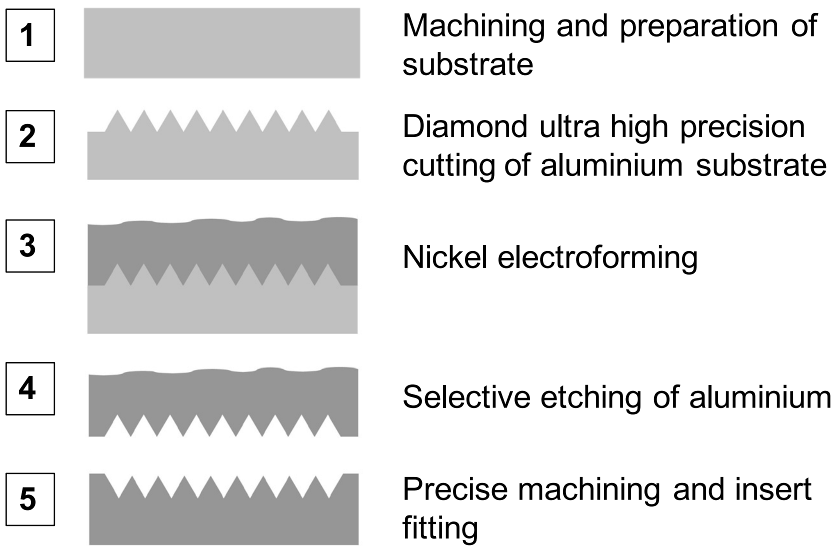

Figure 8.2 - Tooling process chain for the manufacturing of micro structured mould for optical applications: diamond ultra high precision cutting of aluminium substrate, nickel electroforming, selective etching of aluminium, precise machining and insert fitting.

8.2.2 Injection compression moulding

The optical parts are produced through an injection compression moulding process using polymethyl-methacrylate (PMMA, ALTUGLASS V 825 T grade) as polymer material. The injection compression moulding process leads to high accuracy replication of micro structures and a surface finishing suitable for optical applications [Chen, 2008], [Ito, 2008]. The injection compression technology can be considered a natural extension of the traditional injection moulding process for thermoplastic materials and it is characterized by two phases, see Figure 8.3:

1. *Injection*: during this phase the mould cavity is kept partially open to facilitate the flow of plastic inside the cavity. Mechanical solutions are designed for the closure of the cavity in order to prevent the spillage of the polymer outside the mould;
2. *Compression*: during the injection phase or at the end of the injection phase, the machine closing force reduces the thickness of the mould cavity to the actual thickness of the component and the polymer is driven inside the empty region of the

cavity. This phase produces a uniform distribution of the pressure into the mould cavity, unlike traditional injection moulding where a gradient of pressure occurs.

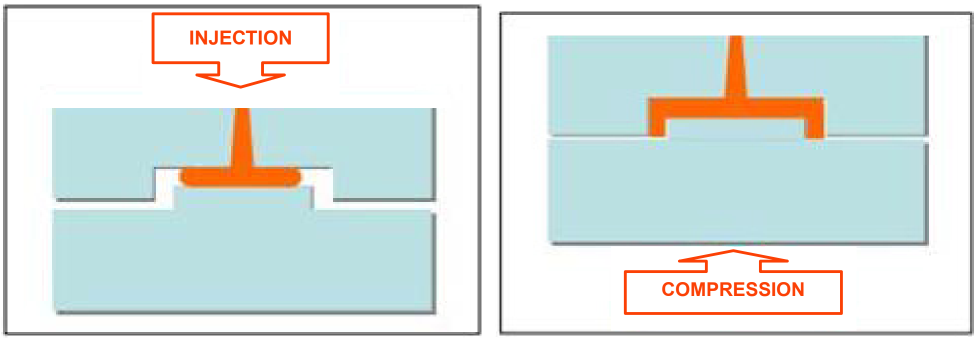

Figure 8.3 - Two stages of the injection compression moulding process: injection and compression.

The main advantages and the main applications of the injection-compression moulding are reported in Table 8.1. It is a process that guarantees: decreasing of moulding pressure, reducing of residual stress, packing evenly, reducing of shrinkage and increasing dimensional accuracy [Wu, 2006]. It is especially employed for optical components, such as lenses, DVD and Blue-Ray disc.

Advantages respect to conventional injection moulding	*Applications*
• Homogeneous physical properties • Dimensional stability • Good control on the residual stresses • Low volumetric shrinkage • Improved mould cavity replication	• High thickness lenses • Components with small cavity to be filled (e.g. Fresnel lenses) • Elements with micro-structures (e.g. CD, DVD, Blue-Ray disc) • Thin wall components • Components with both thin and thick parts

Table 8.1 - Advantages and main applications of injection compression moulding.

8.3 SEM measurements

The pitches of the micro-pyramidal structures were characterized through analyses of SEM images taken on the mould and on the polymer part using the scanning electron microscope described in appendix 11.1.4.

The measurements were carried out in ten different areas (A, B, … , L), shown in Figure 8.4. On each area three different features were measured and analyzed using an image processor software called Scanning Probe Image Processor [SPIP, 2011].

Referring to Figure 8.4, the three investigated pitches were:

a) Vertical pitch (1-2): 21 vertical pitches were measured for each area and the average was calculated;

b) Diagonal pitch (2-3): 24 diagonal pitches were measured for each area and the average was calculated;

c) Horizontal pitch (3-4): 42 horizontal pitches were measured for each area and the average was calculated.

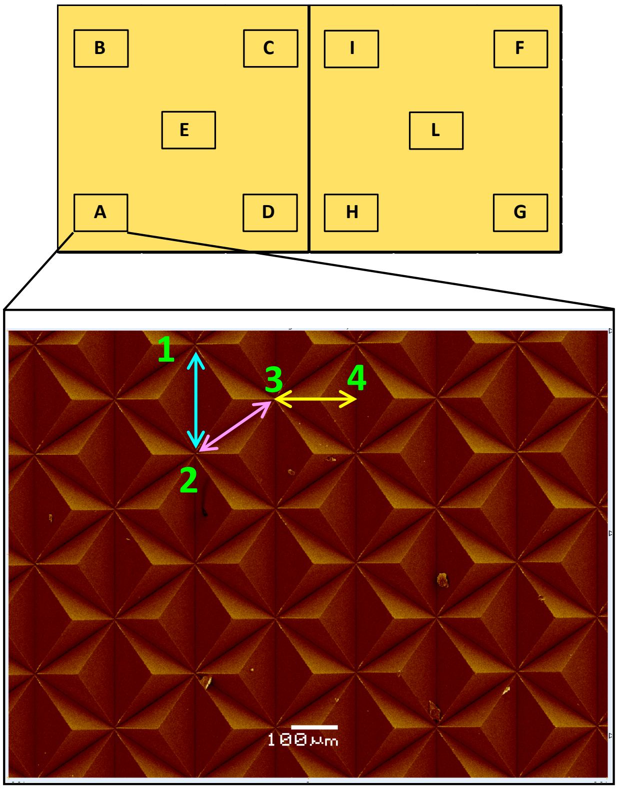

Figure 8.4 - Ten areas (A, B, ..., L) investigated on the parts and the three measured pitches: vertical (1-2), diagonal (2-3) and horizontal (3-4).

Finally, the uncertainty of the measurements was assessed following the Guide to the Expression of Uncertainty in Measurements (GUM) [GUM, 2008] and the substitution method applied to CMMs (i.e. ISO 15530-3:2004) [ISO 15530-3, 2004][f], see equation 8.1:

[f] A revised version is available (ISO15530-3:2011).

$$U_i = k \cdot \sqrt{u_{res}^2 + u_{cal}^2 + u_{SEM,i}^2 + u_{magn}^2} \qquad (8.1)$$

With:

$$u_{SEM,i} = \max(u_{rep}; u_{area}) \qquad (8.2)$$

Where:

- U = expanded combined uncertainty;
- $i = x$, y depending on the measurand (x for horizontal pitch; y for vertical pitch; xy for diagonal pitch);
- k = 2 in order to obtain a confidence level of approximately 95%;
- u_{res} = instrument resolution;
- u_{cal} = calibration uncertainty;
- u_{rep} = repeatability = standard deviation of three measurements carried out on the same five pitches (equation 8.2);
- u_{area} = standard deviation of all the pitches measured in the same area (equation 8.2);
- u_{magn} = deviation between the nominal pixel size and the measured one according to [Bariani, 2005] and appendix 11.1.4.

Measurements on the same pitches as well as on different pitches of the components are affected by instrument repeatability. Therefore, the maximum value among the uncertainty contributors (u_{rep}, u_{area}) was selected to not overestimate the repeatability.

8.3.1 Results of the SEM measurement on the pitches

The quality control of the manufacturing process was performed through a control of the product. For this reason the achieved measurements on the mould were compared to the measurements obtained on the polymer part.

The results are graphically represented in Figure 8.5.

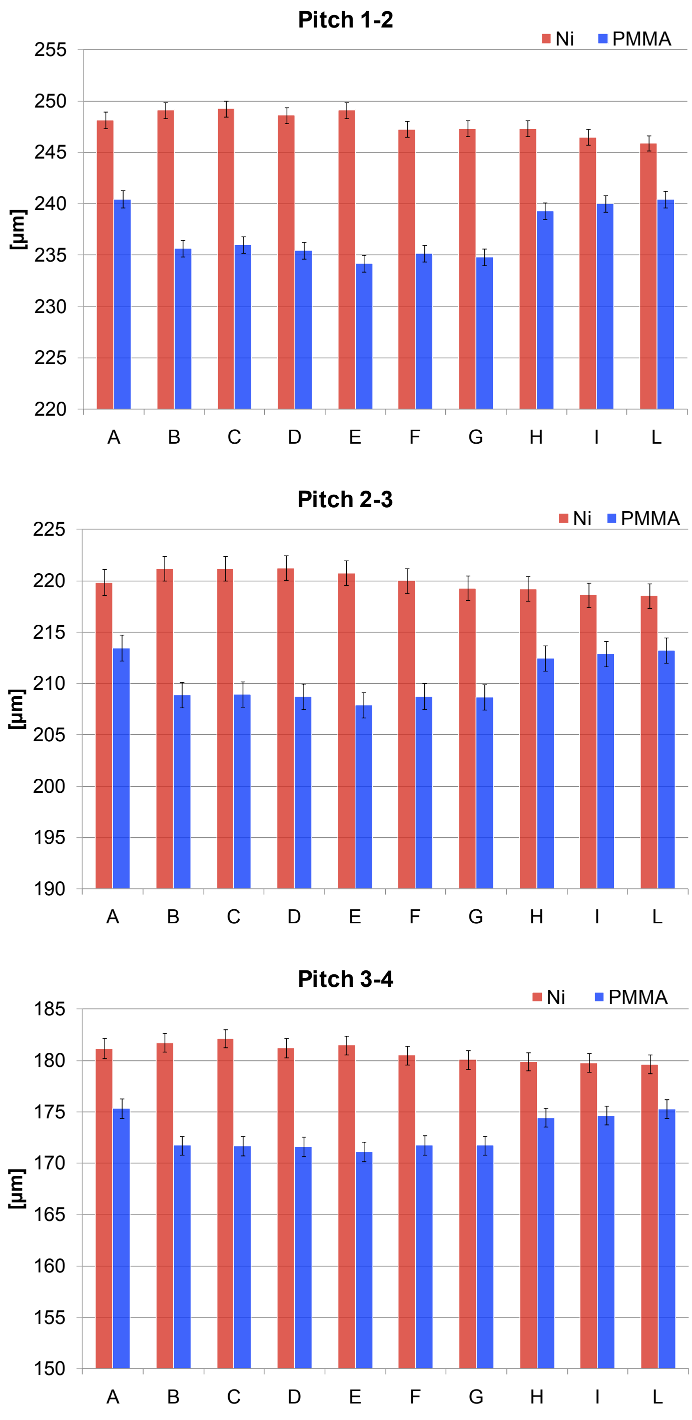

Figure 8.5 - Comparison between the measured pitches on the mould (red columns) and on the polymer part (blue columns): vertical pitch (1-2); diagonal pitch (2-3) and horizontal pitch (3-4). The measurements were obtained from SEM images analysis.

Taking into account the values obtained from the mould measurements (red columns on Figure 8.5), the pitch lengths of every area appeared to be in the same range. This is the reason why in the following investigations, the measurements are concentrated only in specific areas. The different pitch lengths were in average equal to:

a) 250 µm for the vertical pitch 1-2;
b) 220 µm for the diagonal pitch 2-3;
c) 181 µm for the horizontal pitch 3-4.

The vertical pitch had larger dispersions of the values due to the machining process: the reason is that the vertical pitches were the result of the intersections between the vertical and the diagonal passes as it is visible in Figure 8.4. The results obtained from the measurements on the polymer component (blue columns on Figure 8.5) showed that the deviation from the mould values was approximately 3 - 5% and equal to 6 - 11 µm. This deviation was due to the polymer shrinkage occurring during the cooling phase after the mould filling. Moreover, looking at Figure 8.5 and Figure 8.6, the same trend was found on the same area of the different pitches. This proved that the shrinkage was correlated to the different location inside the mould. If there is a non-uniform temperature and pressure distribution in the cavity, the shrinkage will be unbalanced due to polymer compressibility (i.e. specific volume depends on both pressure and temperature).

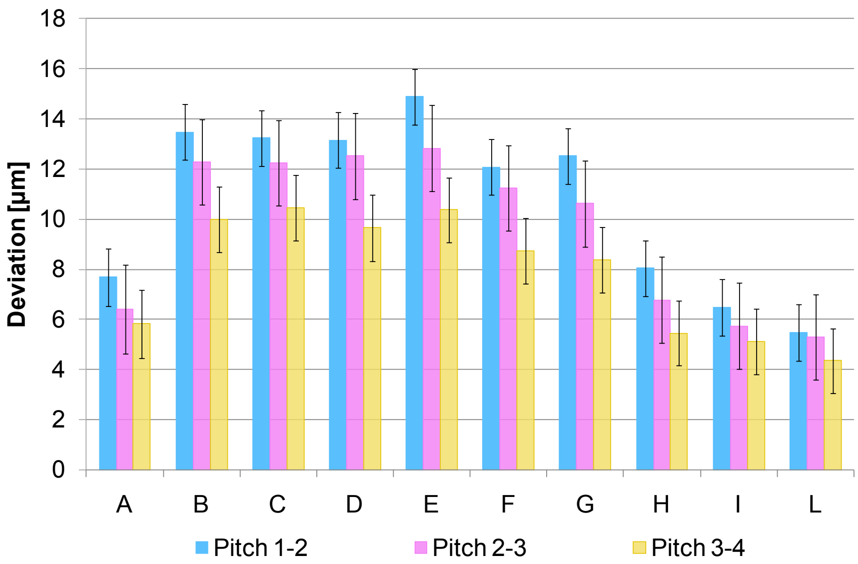

Figure 8.6 - Deviation of the measured pitches on the polymer part respect to the measured pitches on the mould: vertical (1-2); diagonal (2-3) and horizontal (3-4). The measurements were obtained from SEM images analysis.

For each measurement performed on the mould and on the optical component the uncertainty budget was calculated according to equation 8.1. The average of the different uncertainties is listed in Table 8.2. The calculated uncertainties for the mould and the part measurements appeared to be 0.5% of the measured pitches.

U [µm]	Pitch 1-2	Pitch 2-3	Pitch 3-4
Mould	0.8	1.2	0.9
Part	0.8	1.2	0.9

Table 8.2 - Average of the uncertainty budgets calculated for the different pitches measured on the ten areas of the corresponding component. The measurements were obtained from SEM images analysis.

8.4 3D-SEM measurements

As described in chapter 2, the information achieved from SEM is inherently 2D and no height information can be extracted. However, reconstruction from stereo pairs or triplets of SEM images can be used for creating 3D information of the sample, as described in e.g. [Bariani, 2005] and [Carli, 2010].

Since the aim of the study was to perform a manufacturing process control through dimensional measurements on the mould and on the optical part, a 3D-SEM analysis was carried out. Triplets of SEM images were taken in E, H and L area (shown in Figure 8.4). The three images were combined together in order to create a 3D overview of the desired area. The employed software was MeX^{TM} from Alicona Imaging GmbH [MeX].

An example of a 3D image obtained in E area of the mould is illustrated in Figure 8.7.

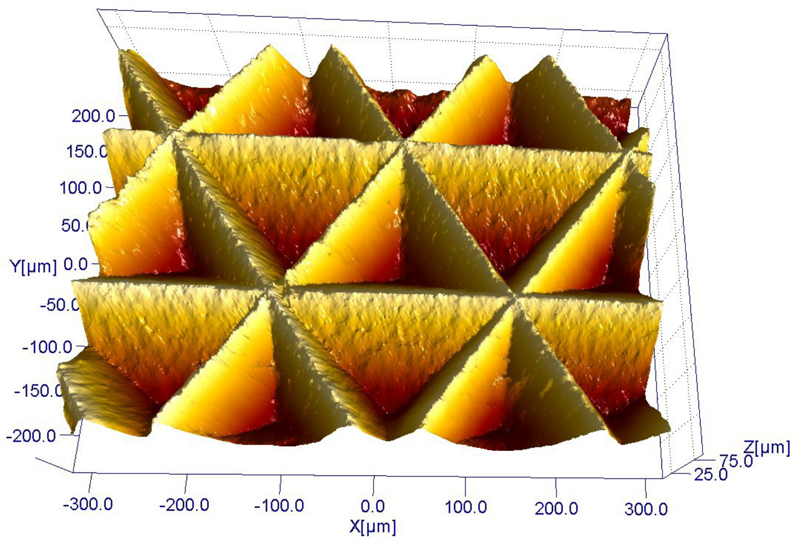

Figure 8.7 – 3D-SEM reconstruction of the area E in the mould.

No successful results were achieved for the polymer part, probably due to not enough texture on the surface. As shown in Figure 8.8, the micro-pyramids appeared to have a deformed shape. Therefore the measurement results for the 3D-SEM analysis refer only to the Ni mould.

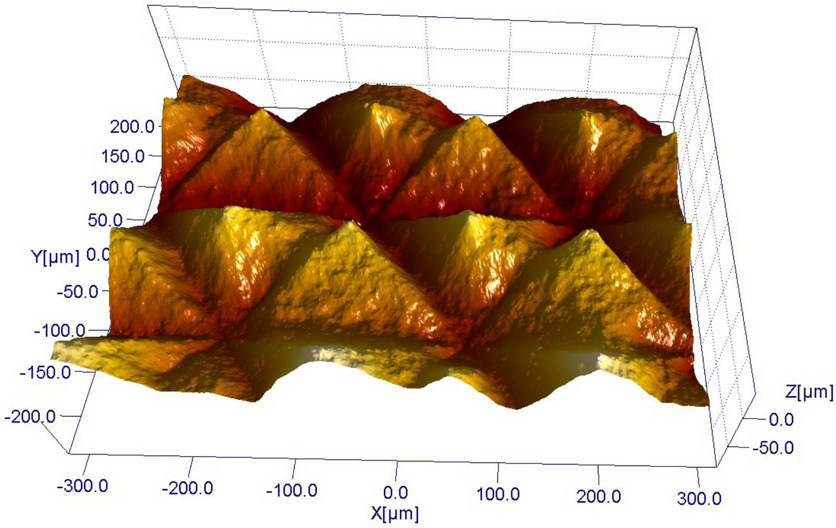

Figure 8.8 – Unsuccessful 3D reconstruction for the optical component in the area E.

Through this analysis the measured features were:

1. *Pitches*: vertical, diagonal and horizontal (illustrated in Figure 8.4);
2. *Heights* of the micro-pyramids in the intersection between the pitches (*H1*) and in the pyramid edges (*H2*), see Figure 8.9;
3. *Angles* of the micro-pyramids according to the three edges direction. An example is shown in Figure 8.10.

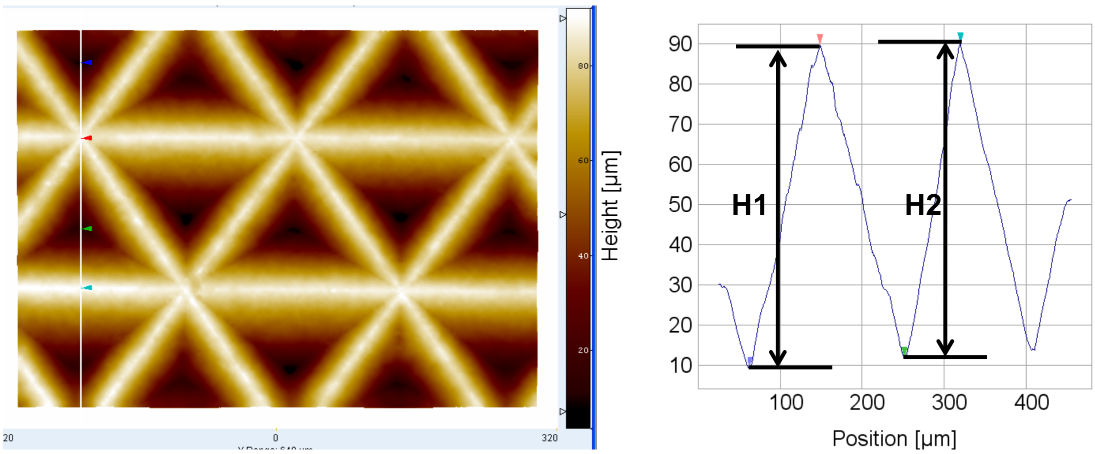

Figure 8.9 – Measured heights of the micro-pyramids in the intersection between the pitches (*H1*) and in the pyramid edges (*H2*).

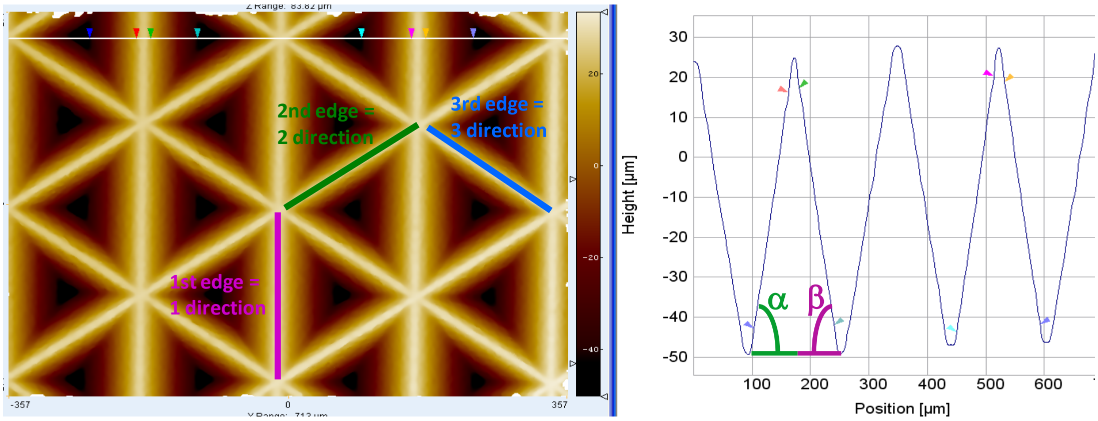

Figure 8.10 – Measured angles (α and β) of the micro-pyramids according to first edge direction.

Finally, the uncertainty of the measurements was assessed following the GUM [GUM, 2008] and the substitution method [ISO 15530-3, 2004][9], see equation 8.3:

$$U_i = k \cdot \sqrt{u_{res}^2 + u_{cal}^2 + u_{rep}^2 + u_{magn}^2 + u_{3D-SEM}^2} \quad (8.3)$$

Where:

- U = expanded combined uncertainty;
- i = x, y, z depending on the measurand (x for horizontal pitch; y for vertical pitch; xy for diagonal pitch; z for height);
- k = 2 in order to obtain a confidence level of approximately 95%;
- u_{res} = instrument resolution;
- u_{cal} = calibration uncertainty;
- u_{rep} = repeatability = standard deviation of the measurements carried out in the 3D-SEM image;
- u_{magn} = deviation between the nominal pixel size and the measured one according to [Bariani, 2005] and appendix 11.1.4.
- u_{3D-SEM} = uncertainty derived from the 3D-SEM reconstruction. The uncertainty value was estimated according to the experimental work of [Carli, 2010]: a combined uncertainty of 2.0 µm was obtained for a hypodermic needle with a calibrated diameter of 259.7 µm; while a combined standard uncertainty of 0.5 µm was obtained for a step height of 56.3 µm.

[9] A revised version is available (ISO15530-3:2011).

The combined standard uncertainty for the angle measurements was calculated following the GUM [GUM, 2008]. Looking at Figure 8.11, *z* is the height length and *x* is the base length of a right triangle; therefore the angle α is calculated as:

$$\alpha = arctg\frac{z}{x} \tag{8.4}$$

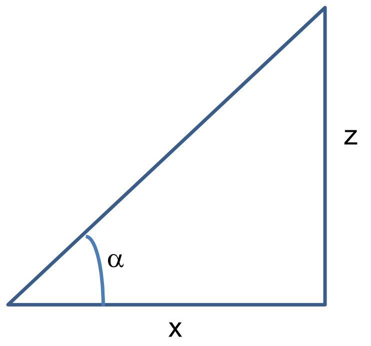

Figure 8.11 – Right triangle with z height length and x base length.

Considering *z* and *x* independent quantities and following the law of propagation of uncertainty (based on a first-order Taylor series approximation of *f*), the combined standard uncertainty of the angle α is given by:

$$u_{\alpha}^{2}(y) = \sum_{i=1}^{N}\left[\frac{\partial f}{\partial x_i}\right]^2 \cdot u^2(x_i) = \left[\frac{\partial f}{\partial x}\right]^2 \cdot u_x^2 + \left[\frac{\partial f}{\partial z}\right] \cdot u_z^2 \tag{8.5}$$

Where *f* is the function given in equation 8.4; u_x and u_z are respectively the combined standard uncertainty of the measured lengths *x* and *z*. According to GUM [GUM, 2008], if *f* presents a significant non-linearity, higher-order terms in the Taylor series expansion must be included in equation 8.5. Since the function *f* was taken in a small interval, it was considered being locally linear. Therefore the combined standard uncertainty of the angle α was approximated to a first-order Taylor series, see equation 8.6.

$$u_{\alpha}^{2} = \left[\frac{\partial}{\partial x}(arctg\frac{z}{x})\right]^2 \cdot u_x^2 + \left[\frac{\partial}{\partial z}(arctg\frac{z}{x})\right]^2 \cdot u_z^2$$

$$= \left[\frac{-z}{z^2 + x^2}\right]^2 \cdot u_x^2 + \left[\frac{x}{x^2 + z^2}\right]^2 \cdot u_z^2 \tag{8.6}$$

8.4.1 Results of the 3D-SEM measurement on the pitches

The results of the 3D-SEM measurements carried out on the vertical, diagonal and horizontal pitches of the Ni mould are shown in Figure 8.12.

The different pitch lengths obtained from the 3D-SEM analysis were in average equal to:

a) 245 μm for the vertical pitch 1-2: 5 μm of difference from the SEM images;
b) 212 μm for the diagonal pitch 2-3: 8 μm of difference from the SEM images;
c) 174 μm for the horizontal pitch 3-4: 7 μm of difference from the SEM images.

The difference between the two techniques was in average 3.7% of the measured feature. Moreover it seems that the 3D reconstruction results presented a systematic error of 5 μm - 10 μm.

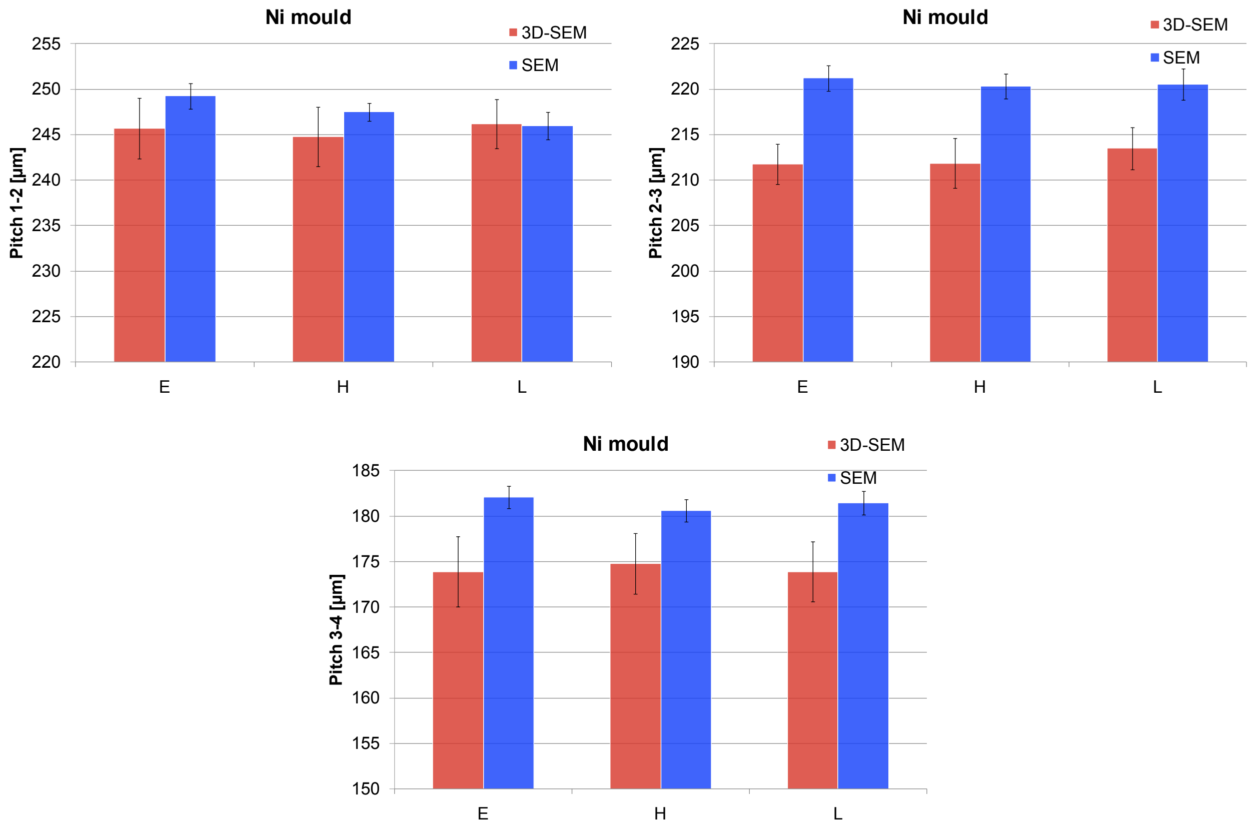

Figure 8.12 - Comparison between the measured pitches on the Ni mould using 3D-SEM analysis (red columns) and using SEM pictures (blue columns): vertical pitch (1-2); diagonal pitch (2-3) and horizontal pitch (3-4).

For each performed measurement the uncertainty budget was calculated according to equation 8.3. The average of the different uncertainties is listed in Table 8.3. The calculated uncertainties appeared to be 1.5% of the measured pitches.

U [µm]	Pitch 1-2	Pitch 2-3	Pitch 3-4
Mould	3.1	2.4	3.5

Table 8.3 - Average of the uncertainty budgets calculated for the different pitches measured on three areas of the corresponding component. The measurements were obtained from 3D-SEM images analysis.

8.4.2 Results of the 3D-SEM measurement on the heights

The results of the 3D-SEM measurements carried out on the heights of the Ni mould are summarized in Table 8.4.

Height ± U [µm]	*E*	*H*	*L*
H1	78.1 ± 7.3	81.2 ± 18.3	77.8 ± 6.4
H2	76.4 ± 7.1	77.2 ± 12.3	76.7 ± 4.4

Table 8.4 – Results of the micro-pyramids heights with the combined uncertainties obtained from the 3D-SEM analysis on the Ni mould.

The obtained combined uncertainties appeared to be 10% of the measured feature. The larger contributor was given by u_{rep} (standard deviation of the measurements carried out in the 3D-SEM image) which represented 50% of the total uncertainty. In fact for both heights, H1 and H2, the results were spread between 76 µm and 81 µm.

Two causes were identified to understand the nature of these results:

1. Wrong procedure of the 3D reconstruction which led to have deformed micro-pyramids with different heights. In this case, an improvement of the 3D reconstruction analysis is required;
2. The spread of the heights really characterizes the micro-pyramids of the mould. More than 5 µm of difference for 80 µm features is quite important; therefore an improvement of the manufacturing process should be performed.

In order to investigate more deeply the two problems, a replica casting technique was carried out in both the mould and the optical component. The results are discussed in paragraph 8.5.

8.4.3 Results of the 3D-SEM measurement on the angles

Four different angles were measured for each micro-pyramid:

1. α according to the first edge direction, see Figure 8.13;
2. β according to the first edge direction, see Figure 8.13;
3. φ according to the second and third edge directions, see Figure 8.14;
4. γ according to the second and third edge directions, see Figure 8.14.

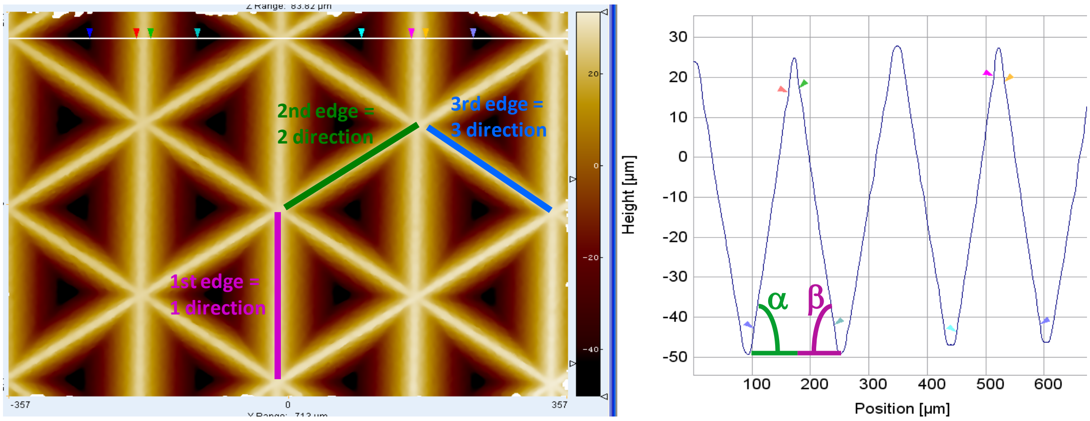

Figure 8.13 – Measured angles (α and β) of the micro-pyramids according to first edge direction.

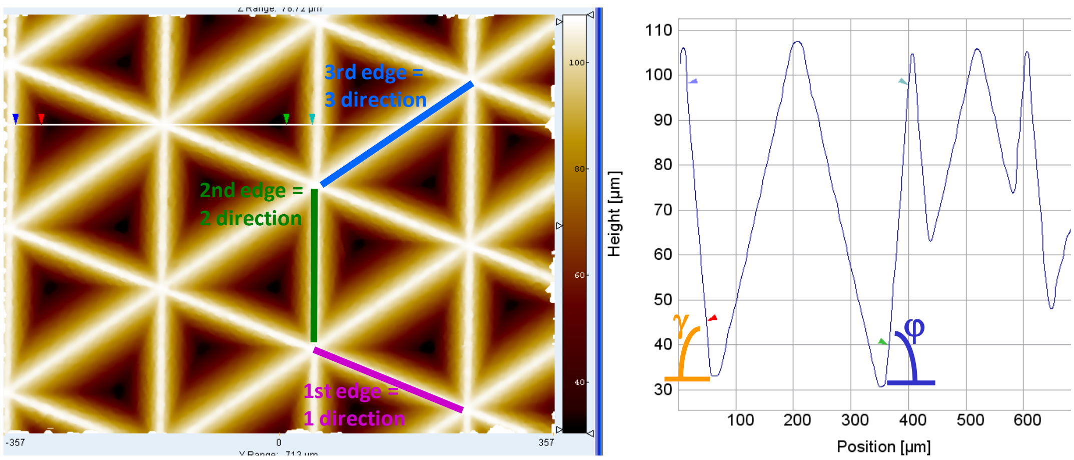

Figure 8.14 – Measured angles (φ and γ) of the micro-pyramids according to second and third edge directions.

It was supposed that the two angles calculated according to the second and third edge directions were the same (φ/γ along 2nd direction equal to φ/γ along the 3rd direction) since the base of the micro-pyramids had two congruent sides (the two congruent sides along the second and third edge), see Figure 8.13 and Figure 8.14.

The results are shown in Figure 8.15. They confirmed the previous assumption: φ and γ had the same value (55° and 62° respectively) for both the second and the third direction.

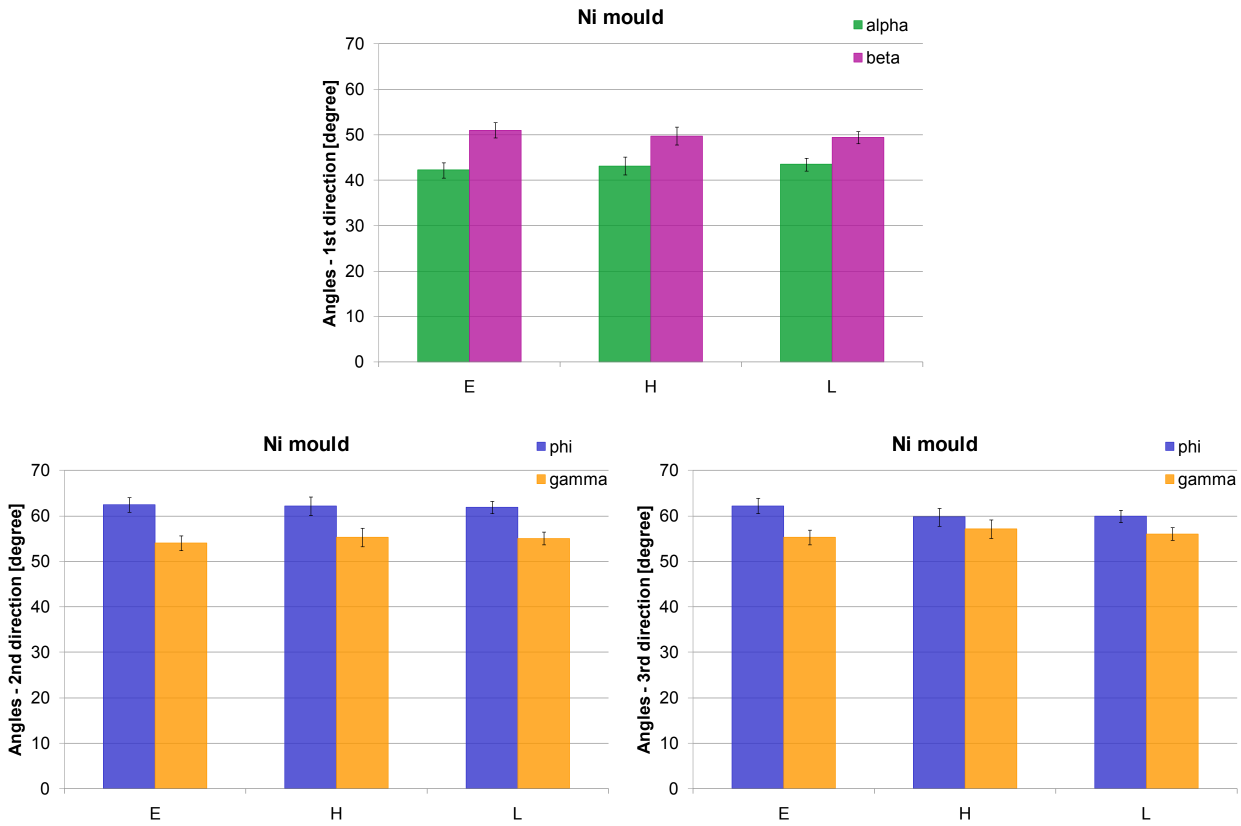

Figure 8.15- Measured angles (α and β), (φ and γ) of the micro-pyramids according respectively to first edge direction, to second and third edge directions. The measurements were obtained from a 3D-SEM analysis.

8.5 Optical measurements

The mould and the optical component were replicated using the red-soft compound of the replica casting technique investigated in chapter 3. Both replicas were measured using the InfiniteFocus instrument described in appendix 11.1.5, see a measurement example in Figure 8.16. The measured area was the centre E area (see Figure 8.4) in order to make a straightforward comparison between the different techniques.

The measured features were:

1. *Pitches*: vertical, diagonal and horizontal (illustrated in Figure 8.4);

2. *Heights* of the micro-pyramids in the intersection between the pitches (*H1*) and in the pyramid edges (*H2*), see Figure 8.9;
3. *Angles* of the micro-pyramids according to the three edges direction. An example is shown in Figure 8.10.

Please note that the replica measurements were inverted before starting the analyses.

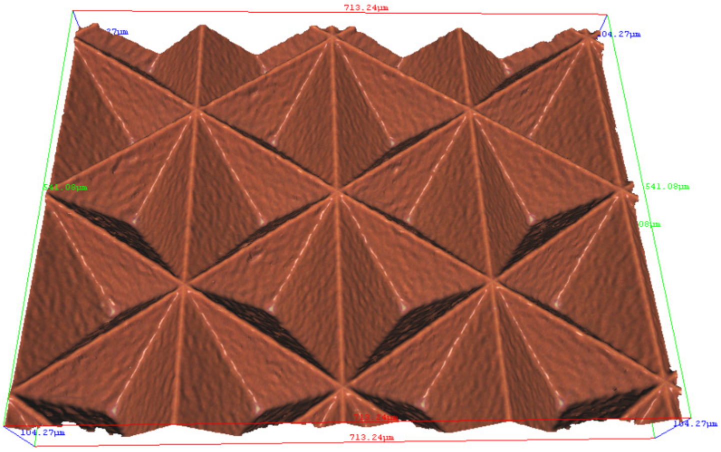

Figure 8.16 – Example of an optical measurement in E area of the polymer part replica.

For each measurand (pitches and heights) the uncertainty budget was calculated following the GUM [GUM, 2008] and the substitution method applied to the CMMs [ISO 15530-3, 2004][h], see equation 8.7:

$$U_{optical,i} = k \cdot \sqrt{u^2_{cal,i} + u^2_{res,i} + u^2_{rep,i}} \tag{8.7}$$

Where:

- $U_{optical}$ = expanded combined uncertainty;
- $i = x, y, z$ depending on the measurand (x for horizontal pitch; y for vertical pitch; xy for diagonal pitch; z for height);
- $k = 2$ in order to obtain a confidence level of approximately 95%;
- u_{cal} = calibration uncertainty which is:
  - for pitches: equal to the combined standard uncertainty given by equation 8.1 since the SEM pictures were calibrated pictures;
  - for height: equal to the combined standard uncertainty given by equation 3.5 in paragraph 3.4.1.1;

[h] A revised version is available (ISO15530-3:2011).

- u_{res} = resolution uncertainty equal to the lateral/vertical resolution used during the optical measurements;
- u_{rep} = repeatability of the measuring process equal to the standard deviation of the measurements performed on the selected area.

The combined uncertainty for the angles was assessed following equation 8.6.

8.5.1 Results of the optical measurement on the pitches

The results in Figure 8.17 summarize the pitch investigations of the E area on:

- Ni mould using:
    a) SEM calibrated pictures;
    b) 3D-SEM reconstruction;
    c) InfiniteFocus instrument on a replica of the mould;
- PMMA part (optical component) using:
    a) SEM calibrated pictures;
    b) InfiniteFocus instrument on a replica of the part.

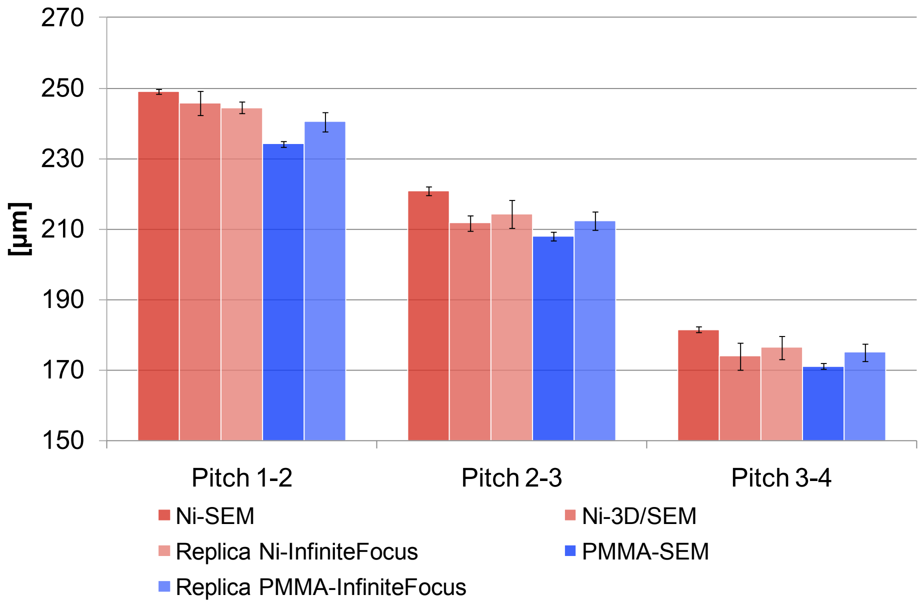

Figure 8.17 – Vertical pitch (1-2), diagonal pitch (2-3) and horizontal pitch (3-4) measured on the E area of the Ni mould using SEM calibrated images and 3D-SEM; of the replica of the Ni mould using an InfiniteFocus instrument; of the PMMA optical component using SEM calibrated images; of the replica of the polymer part using an InfiniteFocus instrument.

Considering the optical measurements, the measured pitches on the replica of the optical component differed 3 µm from the results achieved on the replica of the Ni mould. It confirmed the explanation given in the paragraph 8.3.1: the deviation was due to the polymer shrinkage occurring during the cooling phase after the mould filling.
Comparing the different measuring technique, they agreed in the results of the pitch values for the Ni mould. A larger deviation (approximately 4 µm) was obtained between the SEM calibrated pictures on the PMMA part and the optical measurements on the replica of the polymer part.

8.5.2 Results of the optical measurement on the heights

The results in Figure 8.18 summarize the height investigations of the E area on:

- Ni mould using:
    a) 3D-SEM reconstruction;
    b) InfiniteFocus instrument on a replica of the mould;
- PMMA part (optical component) using:
    a) InfiniteFocus instrument on a replica of the part.

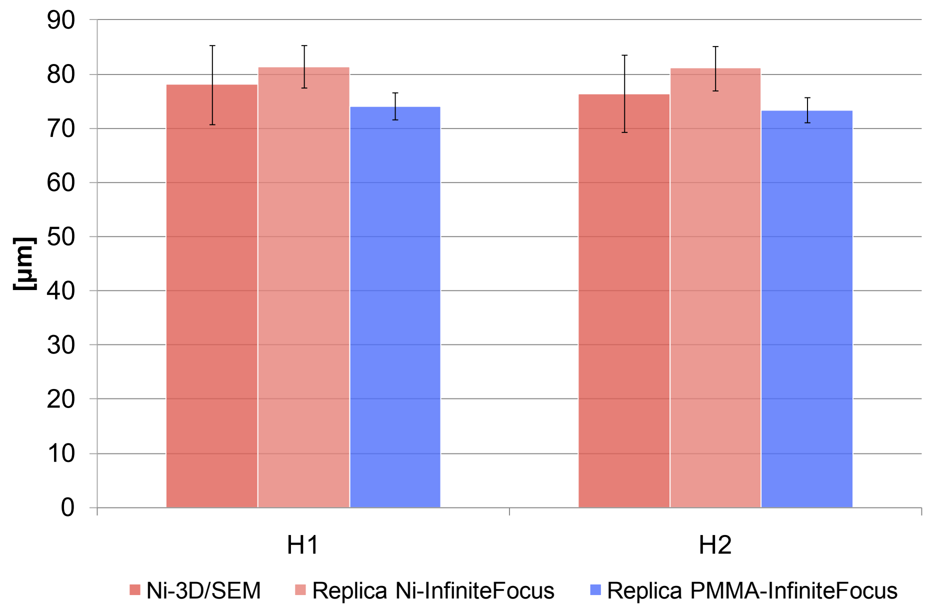

Figure 8.18 – Heights H1 and H2 of the micro-pyramids measured on the E area of the Ni mould using 3D-SEM; of the replica of the Ni mould using an InfiniteFocus instrument; of the replica of the polymer part using an InfiniteFocus instrument.

Using the 3D-SEM reconstruction, a spread of 5 μm was found for the two heights H1 and H2. The problem could be related to a wrong 3D reconstruction or a not satisfactory manufacture of the mould. Therefore, the replica casting technique was carried out in order to have a better understanding of the problem.

Results showed the same distribution for the measured values even using the replica approach, as it is illustrated in Figure 8.18. The second hypothesis was confirmed: the micro-pyramids of the mould, and therefore, of the optical component had variations in the height values.

Moreover, the difference in height between the replica mould and the replica part was equal to 7 μm: 10% of the measured value. This might be due to:

1. Misalignment of the three cutting lines shown in Figure 8.19;
2. Wrong apex replication.

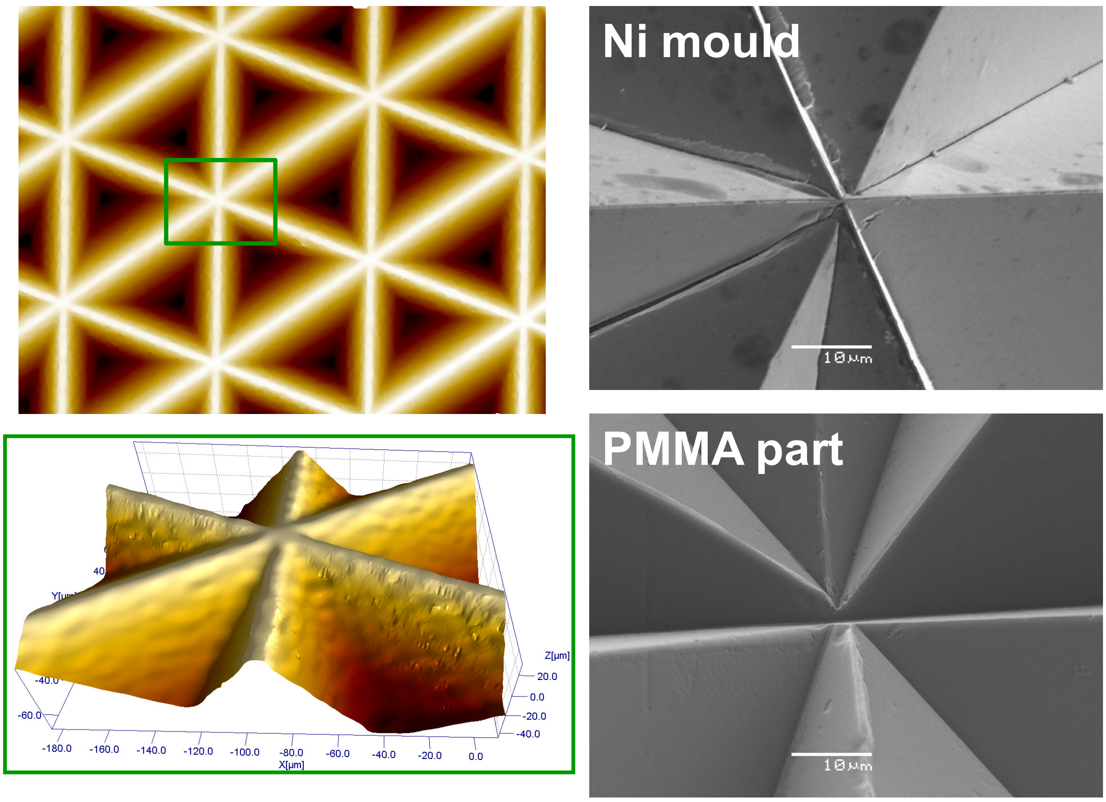

Figure 8.19 – 3 cutting lines of the Ni mould and the PMMA optical component.

The causes of the misalignment could be related to an error made at the first machining phase which was transferred afterwards to the end of the process chain:

Error in z at the top of the valleys on Al master

↓

Error in z at the bottom of the flanks on Ni tool

↓

Error in z at the top of the valleys on PMMA part

The other reason is linked to the apex replication of the micro-pyramids. As it is shown in the SEM pictures of Figure 8.20, the apex of the Ni mould is sharp while it is round on the optical part. This explains the difference in the height values of the mould and the polymer part.

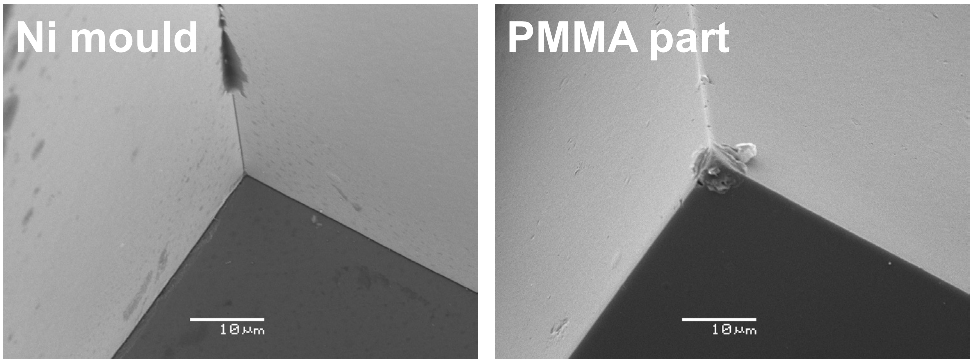

Figure 8.20 – Apex of the micro-pyramids on the Ni mould (bottom) and on the PMMA optical component (top).

8.5.3 Results of the optical measurement on the angles

Figure 8.21 summarizes the results achieved in the height investigations of the E area on:

- Ni mould using:
    - c) 3D-SEM reconstruction;
    - d) InfiniteFocus instrument on a replica of the mould;
- PMMA part (optical component) using:
    - b) InfiniteFocus instrument on a replica of the part.

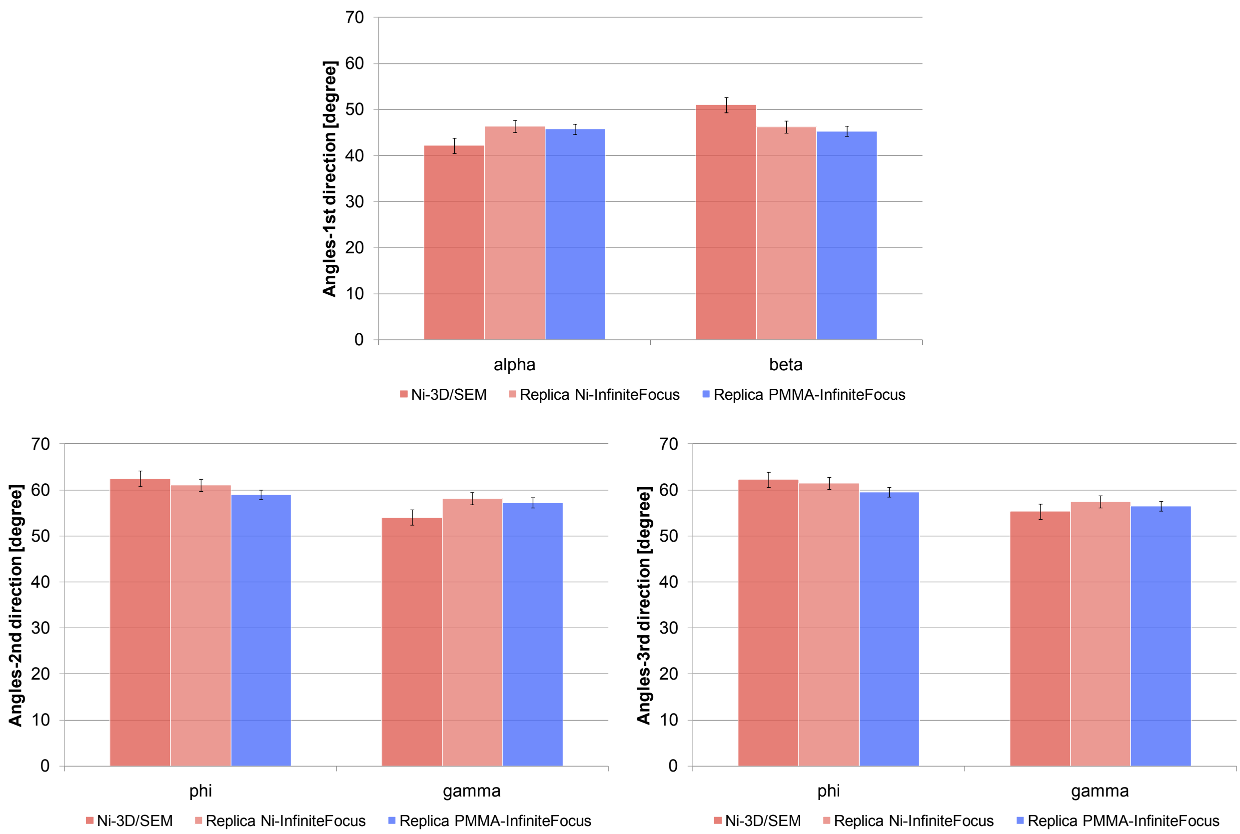

Figure 8.21 - Angles (α and β), (φ and γ) of the micro-pyramids according respectively to first edge direction, to second and third edge directions. They were measured on the E area of the Ni mould using 3D-SEM; of the replica of the Ni mould using an InfiniteFocus instrument; of the replica of the polymer part using an InfiniteFocus instrument.

From the results, it is possible to conclude that:

– φ/γ along 2nd direction is equal to equal to φ/γ along the 3rd direction;

– α is equal to β.

Moreover there is a matching between the achieved results from the different measuring techniques.

8.6 Conclusion

The purpose of the current investigation was to develop and test a quality control method of the manufacturing process through a control of the product.

The selected case study was an optical component and its mould, characterized by micro-pyramidal features, replicated afterwards using a soft polymer casting. For the investigation three critical dimensions (i.e. pitches, heights and angles) were chosen and measured using different techniques: SEM images processing, 3D-SEM reconstruction and optical measurements.

Results showed the manufacture accuracy of the mould and the replication fidelity of the optical component, obtained through injection compression moulding. A deviation of approximately 6 μm was achieved between the pitches measured on the mould and on the polymer part. This deviation was due to the polymer shrinkage occurring during the cooling after the mould filling, but also to the different flow conditions of the polymer inside the mould during filling, packing and cooling phases. However, the most important results were obtained for the heights of the micro-pyramidal structures which varied inside a range of 5 μm. Through SEM pictures and the replica technique, it was possible to detect a misalignment on the machining direction which was probably transferred from the first phase of the machining process until the last phase of the process chain. Moreover it was observed sharp apexes on the mould, but round apexes on the polymer component.

The investigation showed also a comparison between the different measuring techniques and proved the feasibility of the replication methods for the evaluation and characterization of surfaces difficult to measure.

Finally, in all the analyses the uncertainty of the measurements was assessed following the GUM and the substitution method. The uncertainty assessment can be a challenging task for measurements in the sub-mm down to sub-μm dimensional ranges. Therefore the aims of the analyses were to propose a useful guideline to identify the uncertainty contributors to be taken into account during the uncertainty budget and to provide a viable method for the uncertainty calculation for measurements in the 100 μm - 200 μm range.

8.7 References

[Alting, 2003] L. Alting, F. Kimura, H.N. Hansen, G. Bissacco, “Micro engineering”, Annals of the CIRP, 2003, Volume 52, Issue 2, pp.635-657.

[Bariani, 2005] P. Bariani, “Dimensional metrology for microtechnology”, PhD thesis, Department of Manufacturing Engineering and Management, Technical University of Denmark, 2005.

[Brinksmeier, 2006] E. Brinksmeier, R. Gläbe, J. Osmer, "Ultra-precision diamond cutting of steel molds", Annals of CIRP, 2006, Volume 55, Issue 1, pp. 551-554.

[Byrne, 2003] G. Byrne, D. Dornfeld, B. Denkena, "Advancing cutting technology", Annals of CIRP, 2003, Volume 52, Issue 2, pp. 483-507.

[Carli, 2010] L. Carli, "3D-SEM metrology for coordinate measurements at the nanometer scale", PhD thesis, Department of Manufacturing Engineering and Management, Technical University of Denmark, 2010.

[Chen, 2008] S.-C. Chen, W.-Y. Hsu, S.-W. Huang, Y.-C. Wang, "Study of process characteristics on the optical performance of the LGP with three-side micro feature design", Society of Plastic Engineers (SPE)-66th Annual Technical Conference (ANTEC), 2008, pp. 2138- 2142.

[Corbett, 2000] J. Corbett, P. A. McKeown, G. N. Peggs, R. Whatmore, "Nanotechnology: international developments and emerging products", Annals of CIRP, 2000, Volume 49, Issue 2, pp. 523-545.

[Gasparin, 2011] S. Gasparin, G. Tosello, H.N. Hansen, I. Di Vora, S. Priante, S. Sinesi, "Replication quality control of metal and polymer micro structured optical surfaces", 4th Swedish Symposium, 2011, pp.533-539.

[GUM, 2008] Joint Committee for Guides in Metrology (JCGM). JCGM 100:2008, Guide to the Expression of Uncertainty in Measurement (GUM), 2008, pp. i–viii, 1–132.

[ISO 15530-3, 2004] ISO 15530 part 3: 2004 - Geometrical Product Specifications (GPS) - Coordinate Measuring Machine (CMM): techniques for determining the uncertainty of measurement – Part 3: Use of calibrated workpieces or standards.

[Ito, 2008] H. Ito, H. Suzuki, K. Kazama, T. Kikutami, "Structural development and replication properties of micro-molded parts in injection compression molding", Society of Plastic Engineers (SPE)-66th Annual Technical Conference (ANTEC), 2008, pp. 2519- 2523.

[MeX] http://www.alicona.com/home/products/Mex/MeX.en.php.

[SPIP, 2011] SPIP (Scanning Probe Image Processor) from Image Metrology A/S, version 5.0.5.

[Taniguchi, 1983] N. Taniguchi “Current status in, and future trends of, ultraprecision machining and ultrafine materials processing”, Annals of CIRP, 1983, Volume 32, Issue 2, pp. 573- 582.

[Velkova, 2011] V. Velkova, G. Lalev, H. Hirshy, F. Omar, S. Scholz, E. Minev, S. Dimov, “Process chain for serial manufacture of 3D micro- and nano-scale structures”, CIRP Journal of Manufacturing Science and Technology, 2011, Volume 4, Issue 4, pp. 340–346.

[Wu, 2006] C.-H. Wu, W.-S. Chen, “Injection molding and injection compression molding of three-beam grating of DVD pickup lens”, Sensors and Actuators A, 2005, Volume 125, Issue 2, pp. 367–375.

9. Conclusion

9.1 Summary

The overall objective of the present PhD project was to develop methodologies for ensuring the tolerance verification in micro manufacturing. Special attention was paid to the process chain characteristics in relation to micro injection moulding processes.
The main results achieved can be summarized as follows:

- State of the art for dimensional and nano metrology
  The available measuring technique for micro and nano metrology were described, focusing on the available ISO standards for calibration, traceability and uncertainty budget estimation. A comparison between literature and industrial practise (COTECH) led to two main conclusions: (1) lack of calibration standards to ensure the traceability for micro and nano parts; (2) challenges in the tolerance verification of components having downscaled dimensions. The measurement uncertainty should be sufficiently small respect to the tolerance interval in order to leave enough conformance zone for process variation.
- Calibration and traceability
  A polymer casting technique is a useful method to use when dealing with components difficult to characterize. The procedure consists in replicating the part and measuring the replica instead of the part. Several studies were carried out using different specimens and different replica materials in order to define the replication degree, to estimate the replica stability and to ensure a traceable procedure. Two types of specimens were used: (1) artefacts typically described in terms of surface roughness parameters, the so-called roughness specimens: artefacts having Ra between 200 nm and 500 nm were studied. (2) artefacts typically characterized by well-defined geometries, the so-called geometry specimens: specimens with step heights in the range of 0.2 μm and 1000 μm were

investigated. As conclusion of the studies, geometries below 0.5 μm are difficult to replicate due to possible macro deformation. If the replica is kept in a clean environment with constant temperature, its stability is 1.7 - 4% of the measured feature during a period of 15 - 30 days.

For the different investigations, the uncertainty budget was estimated following the GUM [GUM, 2008] and, finally, a replica traceability approach was proposed since the measuring instrument needs to be calibrated on the same replica surface. The new procedure includes the preparation of a replica from a standard artefact and its subsequent calibration. In this way a traceable procedure can be ensured.

- State of the art for process chains in micro manufacturing

  Available process chains for micro-manufacturing were described in relation to the micro-injection moulding process. A critical phase for the process chain of a micro part is the tooling fabrication. The insert is usually the outcome of different process combinations, hence the link with the tolerance chain during production. The repeatability of the inserts fabrication must be enough to produce inserts which satisfy the required geometric tolerance and ensure parts of acceptable quality. Moreover an increased feature miniaturization challenges both the replication process and the quality control technology.

- Tolerancing in micro and nano manufacturing

  A systematic approach based on dimensional and geometrical metrology was applied in order to verify tolerances for micro and nano structured components. A successful verification of tolerances requires the establishment of traceability including the estimation of measurement uncertainty.

  The first issue is related to the instrument capabilities. It is necessary to perform a thoughtful analysis on the instrument set-up in order to optimize and maximize the repeatability of the results and, consequently, decrease the measurement uncertainty. Different methods are available, such as the quality control and the measuring indices approaches.

  The second and more important issue is the uncertainty budget estimation. As previously explained, the measuring uncertainty is a key point in the tolerance verification: too large uncertainties mean no conformance zone available for process variation. Moreover the ratio (U/T) between the measuring uncertainty (U)

and the tolerance (*T*) shall be less than 10% or, at least, lower than 20%; as it is recommended in [Knapp, 2001]. Therefore the available conformance zone for tolerance verification should be improved. During the work, the uncertainty budget was estimated according to GUM [GUM, 2008] and ISO 15530 part 3 [ISO 15530-3, 2004][i]. Results showed the importance of calculating all the uncertainty contributions: a substantial difference in the final results can be achieved if only the measurements standard repeatability is taken into account. Contributions, such as calibration uncertainty, temperature-related uncertainty and systematic errors, could increase considerably the uncertainty budget.

- Development of approaches for validation of micro manufacturing process chains

  During the last case study, the quality control of a manufacturing process for an optical component was performed through a control of the product. Usually different measuring techniques can be used for verifying a part. However in this case, a complete characterization of both the mould and the optical component was possible only through a replica casting technique and an optical measuring instrument. Moreover comparing the measuring results obtained from the mould with the one achieved from the polymer part, it was possible to detect the consistency and incompatibilities of the manufacturing sequence and to find out the critical features and relative dimensions.

  Concluding, this approach reveals to be useful when it is requested to understand, for example, if the detected-critical features are the outcome of the mould fabrication and therefore are linked to the machining process, or if they are the result of the polymer part production and hence are due to the replication process. Furthermore this quality control method can be used to find out the causes related to a not satisfactory functionality of the product. In this way the process parameters could be tuned in order to obtain the aimed micro-polymer part with the requested dimensions and functionality.

[i] A revised version is available (ISO15530-3:2011).

9.2 Discussion and outlook

The work carried out during these three years has originated further discussions which are focused mainly on the crucial question: “*Is it necessary to define so narrow tolerances in micro-product design and manufacture?*”. The so-called ‘golden rule’ of metrology states that the measurement uncertainty should be less than 10% of the tolerance to be verified. However, as tolerances become smaller, the ‘golden rule’ cannot be fulfilled anymore because the lowest level of available uncertainty is reached. The percentage ratio between the uncertainty and the tolerance can be changed to a margin of 20%, but it does not solve the problem [Knapp, 2001]. In case of high accuracy processes, as in the in the field of micro manufacturing, the above mentioned uncertainty limit is reached. Therefore two critical points appear: the tolerance and the measurement uncertainty, see Figure 9.1.

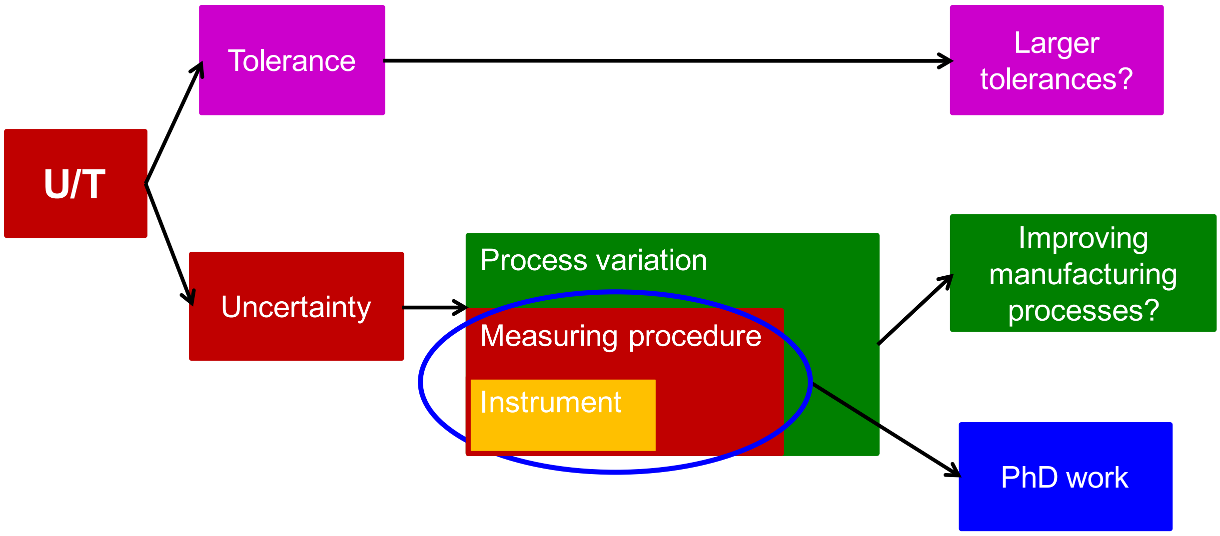

Figure 9.1 – Perspective of tolerance verification in micro manufacturing.

The tolerances are usually defined in relation to three main aspects (see Figure 9.2):

1. *Functionality of the micro parts*: the tolerances have to reflect the functional requirements of the components as well as the functionality coming from the assembly;
2. *Manufacturing processes*: the tolerances have to be “realized” through the manufacturing process which are usually quite accurate for micro components and therefore the specifications can be rather small;

3. *Quality control*: the tolerances have to be verified and therefore they have not to be too narrow, otherwise there are no available measuring instruments for the validation.

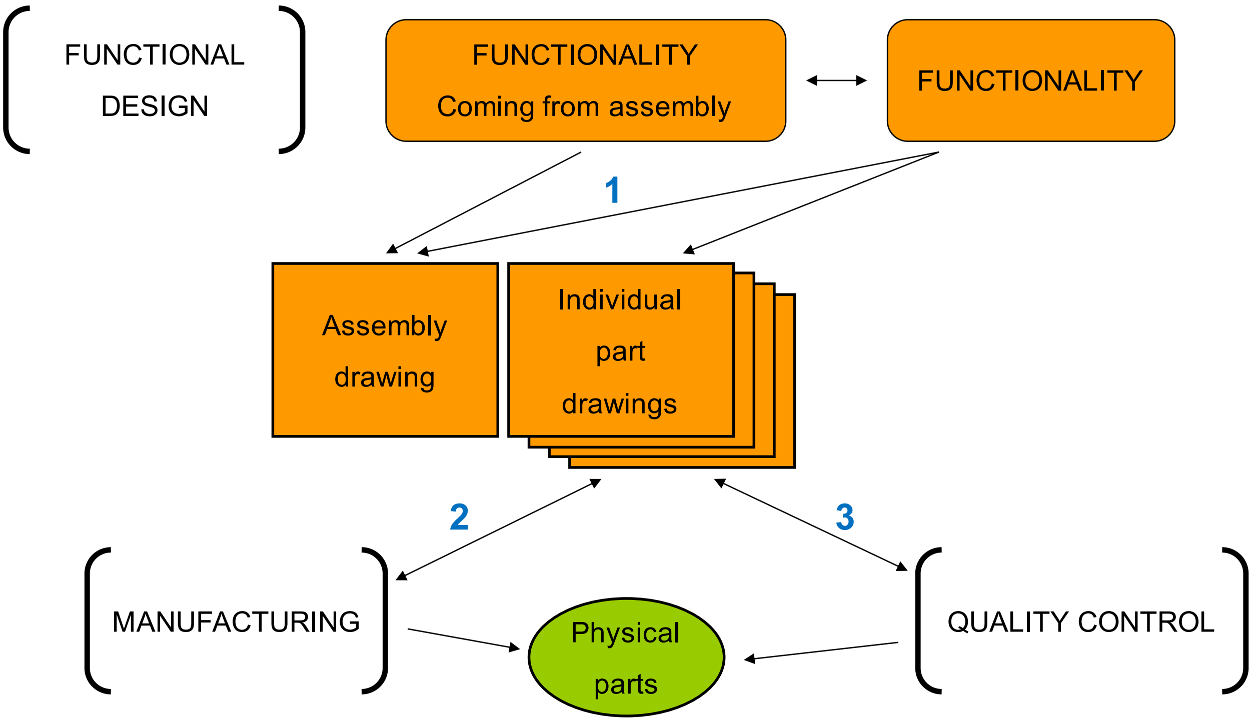

Figure 9.2 – Tolerances in relation to functionality (1), manufacturing process (2) and quality control (3).

On the other hand the measurement uncertainty takes into account three different types of variability: the instrument, the metrology procedure and the process variation (see Figure 9.1). In the present project work the attention was focused on minimizing the measurement uncertainty. The uncertainty should be accurately estimated in order to verify that the instrument being used is suitable for sub-millimetre dimensional ranges. In the case studies considered in this research, the aim was to decrease the uncertainty of the measuring instrument, i.e. to decrease the variability coming from the instrument and the metrology procedure.

The obtained results were:

– *Micro dimensional case study*: the part was verified applying a substitution approach to the uncertainty budget. However the part was made in polymer which could be subject to plastic deformation especially during its assembly in the hearing aid product; therefore: were the tolerances of 20 μm and 30 μm really necessary?

- *Sub-micro dimensional case study*: the required functionality was satisfied even if the pit lengths were out of tolerance and, moreover, one of the largest contributors was coming from the variability of different features within the part: had the manufacturing process to be improved or were the tolerances too tight but not justified by the functionality?
- *3D micro-structured surfaces*: according to industrial application the functional requirement for the optical part is a tolerance of 0.1° on the pyramids faces angle. The calculated measurement uncertainty was in the range of 0.5° and again the major contribution was coming from the standard deviation of the features: had the manufacturing process to be improved or were the tolerances too tight?

It is not easy to give an exhaustive answer to the previous questions, but a fixed point is that the manufacturing process as well as the measuring instrument presents their own variability and uncertainties which have to be considered together with functionality when defining the tolerances for micro products.

Furthermore, the work has originated suggestions for further activities which should be aimed at:

- Studying more deeply the limits of the replica casting technique. For example, the aspect ratio of structures, i.e. ratio between width and height of a feature, should be investigated since high aspect ratios are usually difficult to replicate and complicate to identify [Hansen, 2011].
- Developing a new calibration artefact that could be used as reference when the replica casting technique is applied. The standard should present different types of features, such as roughness surfaces and well-defined geometries, in order to have characteristics similar to the workpiece to be replicated. This artefact could also improve the traceability of the measurements on the replica.
- Understanding the opportunity of producing low cost and reliable reference artefacts through the replica technique. Polymer-based surface roughness calibration standards are not still commercially available, even if this possibility was investigated during the 1990s [Hansen, 2011].

9.3 References

[GUM, 2008] Joint Committee for Guides in Metrology (JCGM). JCGM 100:2008, Guide to the Expression of Uncertainty in Measurement (GUM), 2008, pp. i–viii, 1–132.

[Hansen, 2011] H.N. Hansen, R.J. Hocken, G. Tosello, “Replication of micro and nano surface geometries”, Annals of the CIRP, 2011, Volume 60, pp.695-714.

[ISO 15530-3, 2004] ISO 15530 part 3: 2004 - Geometrical Product Specifications (GPS) - Coordinate Measuring Machine (CMM): techniques for determining the uncertainty of measurement – Part 3: Use of calibrated workpieces or standards.

[Knapp, 2001] W. Knapp, “Tolerance and Uncertainty”, 5th International Conference on Laser Metrology, Machine Tool, CMM and Robot Performance, LAMDAMAP, 2001, pp. 357–366.

10. List of publications

10.1 International ISI journal papers

1. G. Tosello, H.N. Hansen, S. Gasparin, J.A. Albajez, J.I. Esmoris, “Surface wear of micro structured TiN coated nickel tool during the injection moulding of polymer micro Fresnel lenses”, Annals of the CIRP, 2012, Volume 61, Issue 1, pp. 535-538.
2. S. Gasparin, G. Tosello, H.N. Hansen, A. Islam, “Quality control and process capability assessment for injection moulded micro mechanical parts”, Submitted for The International Journal of Advanced Manufacturing Technology, 2012.
3. H.N. Hansen, G. Tosello, S. Gasparin, L. De Chiffre, “Dimensional metrology for process and part quality control in micro manufacturing”, International Journal of Precision Technology 2011, Volume 2, Issue 2-3, pp. 118-135.
4. G. Tosello, H.N. Hansen, F. Marinello, S. Gasparin, “Replication and dimensional quality control of industrial nanoscale surfaces using calibrated AFM measurements and SEM image processing”, Annals of CIRP 2010, Volume 59, Issue 1, pp. 563-568.
5. G. Tosello, H.N. Hansen, S. Gasparin, “Applications of Dimensional Micro Metrology to the Product and Process Quality Control in Manufacturing of Precision Polymer Micro Components”, Annals of CIRP 2009, Volume 58, Issue 1, pp. 467-472.

10.2 Peer reviewed international conference papers

1. S. Gasparin, G. Tosello, H.N. Hansen, J.A. Albajez, “Replica casting technique for micro Fresnel lenses characterization”, Proceeding of 12th International Euspen Conference 2012, pp. 319-322.
2. I. Mizushima, P.T. Tang, K.S. Hansen, S. Gasparin, H. Madsen, "Replication of an aluminum master for large scale optics”, Accepted for 4M conference 2012.

3. S. Gasparin, G. Tosello, H.N. Hansen, I. Di Vora, S. Priante, S. Sinesi, “Replication quality control of metal and polymer micro structured optical surfaces”, 4th Swedish Production Symposium 2011, pp. 533-539.
4. J.A. Yagüe, G. Tosello, S. Carmignato, S. Ontiveros, R. Jiménez, S. Gasparin, H.N. Hansen, A. Pierobon, “Measurement of micro moulded parts by Computer Tomography and comparison to optical and tactile techniques”, Proceeding of 11th International Euspen Conference 2011, pp. 76-79.
5. S. Gasparin, H.N. Hansen, G. Tosello, “Traceable surface characterization using replica moulding technology”, 13th International Conference on Metrology and Properties of Engineering Surfaces 2011, pp. 310-315.
6. H.N. Hansen, S. Gasparin, R. Sobiecki, J. Grønbæk, R. Lazarev, “Characterization of ultra-fine surfaces produced by robot assisted polishing”, 13th International Conference on Metrology and Properties of Engineering Surfaces 2011, pp. 244-248.
7. A. Islam, H.N. Hansen, S. Gasparin, M. Bondo, “Effects of glass fibers on the properties of micro molded plastic parts”, ANTEC Conference 2011.
8. S. Gasparin, G. Tosello, H.N. Hansen, “Tolerance Verification of Micro and Nano Structures on Polycarbonate Substrates”, 7th International Conference on Multi-Material Micro Manufacture (4M/ICOMM 2010), pp.287-290.
9. G. Tosello, H.N. Hansen, S. Gasparin, “Integrating measuring uncertainty of tactile and optical coordinate measuring machines in the process capability assessment of micro injection moulding”, Proceeding of 10th International Euspen Conference 2010, pp. 168-171.
10. H.N. Hansen, S. Gasparin, G. Tosello, “Surface Texture Metrology for High Precision Surfaces”, ICMC 2010 Sustainable Production for Resource Efficiency and EcoMobility, pp. 427-434.
11. S. Gasparin, G. Tosello, H.N. Hansen, M.B. Jørgensen, “Quality control of injection moulded micro mechanical parts”, 5th International Conference on Multi-Material Micro Manufacture (4M) and 4th International Conference on Micro Manufacturing (ICOMM) 2009, pp.175-178.

10.3 Research and technical reports

1. S. Gasparin, G. Tosello, H.N. Hansen, M. Prantl, “Report on reference micro-objects and procedures to establish traceability in micro metrology”, EU-project COTECH (COnverging TECHnologies for micro systems manufacturing) report; SP4–Material Optimization, Simulation, Quality Control and Reliability; WP4.3–Development and standardization of new quality control technology (Grant Agreement no.: CP-IP 214491-2 COTECH) English, 2011, pp. 1-44.
2. S. Gasparin, G. Tosello, H.N. Hansen, “Report on tolerancing guidelines for micro manufacturing”, EU-project COTECH (COnverging TECHnologies for micro systems manufacturing) report; SP4–Material Optimization, Simulation, Quality Control and Reliability; WP4.3–Development and standardization of new quality control technology (Grant Agreement no.: CP-IP 214491-2 COTECH) English, 2011, pp. 1-50.
3. S. Gasparin, G. Tosello, H.N. Hansen, M. Prantl, B. Whiteside, “Report on material optimisation, simulation, quality control and reliability”, EU-project COTECH (COnverging TECHnologies for micro systems manufacturing) report; SP4-Material optimisation, simulation, quality control and reliability. WP4.3-Development and standardization of new quality control technology, (Grant Agreement no.: CP-IP 214491-2 COTECH) English, 2010, pp. 1-151.
4. G. Tosello, S. Gasparin, A. De Grave, H.N. Hansen, “Report on tool transfer and alignment methods”, EU-project COTECH (COnverging TECHnologies for micro systems manufacturing) report; SP2-Tooling. WP2.2-New tool-making solutions for μ-IM and HE, (Grant Agreement no.: CP-IP 214491-2 COTECH) English, 2010, pp. 1-42.

11. Appendix

11.1 Appendix 1: Measuring instruments at MEK-DTU

This section introduces the measuring instruments employed for the investigations on the different case studies of the thesis. The instruments are described together with their technical specifications and calibration data:

- Stylus profilometer (FTS) in *paragraph 11.1.1*;
- Workshop stylus profilometer (Hommel) in *paragraph 11.1.2*;
- Atomic force microscope in *paragraph 11.1.3*;
- Scanning electron microscope in *paragraph 11.1.4*;
- Infinite Focus instrument in *paragraph 11.1.5*;
- Coordinate measuring machine in *paragraph 11.1.6*;
- Tactile coordinate measuring machine in *paragraph 11.1.7*.

11.1.1 Stylus profilometer (FTS)

FTS is a stylus instrument (see Figure 11.1), Taylor Hobson: series 2, 50, equipment of the Accredited Laboratory of the Center for Geometrical Metrology (CGM), which has been established to provide testing and calibration services under accreditation. Its declared uncertainty is 2% from Taylor Hobson specification manual. It is located in building 427S, room 311. The laboratory environment where the measurements are carried out is described in Table 11.1; while the technical specifications are listed in Figure 11.1.

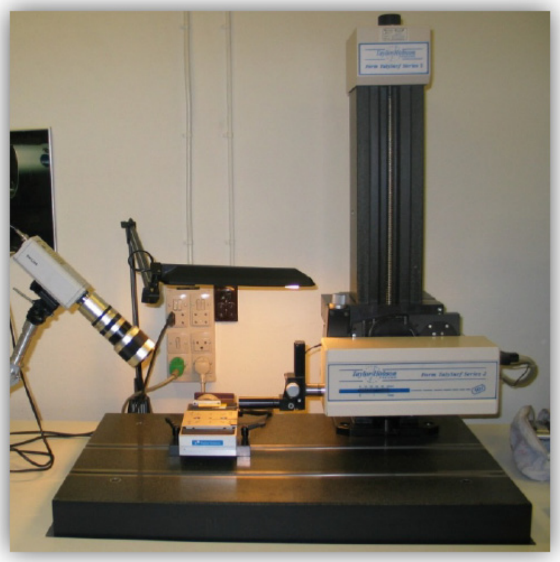

Technical specifications	
TIP RADIUS [µm]	2
TIP SHAPE PROFILE	Conical
TIP ANGLE [°]	90
CONTACT FORCE [N]	0.00075
MEASUREMENT RANGE X x Y x Z [mm]	50 x 50 x 1
MEASUREMENT SPEED RANGE [mm/s]	0.5 – 1
X - RESOLUTION [µm]	0.25
Y - RESOLUTION [µm]	0.5
Z - RESOLUTION [nm]	0.3

Figure 11.1 – Stylus instrument in building 427S, room 311 and its technical specifications.

Environment	
CLEAN ROOM CLASS	NO
VACUUM REQUIRED	NO
TEMPERATURE CONTROL RANGE [°C]	20 ± 1
HUMIDITY CONTROL RANGE [%]	60

Table 11.1 – Laboratory environment in building 427S, room 311.

The verification and calibration of the instrument are performed every 6 months or when they are required, e.g. when changing of the probe or moving of the instrument. They consist in measuring calibrated artefacts, such as roughness standards or step height artefacts, and in checking the background noise on a glass plate. The last verification was carried out in December 2011 and the results are listed in the certificate n^{o} “*Rum11011*”, reported here in the following.

CGM CENTER FOR GEOMETRISK METROLOGI

ilac-MRA

DANAK CAL Reg.Nr. 273

Kalibreringscertifikat
Calibration Certificate

Side 1 af 6
Page 1 of 6
Antal Bilag **2**
No of Enclosures **2**
Rum11011

Certifikat nr. Certificate No.	**Rum11011**
Objekt Object	**Ruhedsmåler / Roughness measuring instrument**
Fabrikant Manufacturer	**Taylor Hobson**
Type Type	**Form Talysurf Series 2 50 i**
Serienummer Serial number	**2593S3C-09 /Stylus 2 µm standard 112/2564-1209**
Rekvirent Customer	**DTU Mekanik** **Produktionstorvet** **2800 Kgs. Lyngby**

Kalibreringscertifikatet må kun gengives i uddrag hvis det enten er offentligt tilgængeligt, eller hvis CGM har godkendt uddraget.

The calibration certificate may not be reproduced other than in full except with the permission of CGM.

Dato for modtagelse Date of reciept	**13.12.11**	Dato for certifikatets udstedelse Date of issue of certificate	**31.12.11**
Dato for kalibrering Date of calibration	**13.12.11**		

Underskrift
Signature

Jan L. Andreasen

Jan L. Andreasen
Fagligt ansvarlig
Signatory, Surface Roughness Calibration

Center for Geometrisk Metrologi, Bygning 425
DTU Mekanik, Danmarks Tekniske Universitet
2800 Kgs. Lyngby, CVR-nr. 30 06 09 46
Telefon 45 25 47 60 – Telefax 45 93 01 90 – Email cgm@cgm.dk

Kalibreringens omfang.

Inden kalibreringen er tastspidserne undersøgt for skader og slid og tasttrykket er evalueret. Baggrundsstøjen på ruhedsmåleren er bestemt ud fra 10 aftastninger på et planglas udtrykt som Ra med cut-off 0.8 mm. I hvert kalibreret forstærkningstrin e er der foretaget 5 aftastninger på relevante forstærkningsnormaler til kalibrering af forstærkning. I det størstforstærkningstrin er der foretaget 12 aftastninger på relevante parameternormaler til kalibrering af Ra.

Extent of calibration.

Before the calibration the stylus tips have been checked for damage and wear and the measuring force has been evaluated. The background noise of the roughness measuring instrument has been determined from 10 traces on an optical flat expressed as Ra using cut-off 0.8 mm. In each calibrated magnification range 5 traces has been made on relevant magnification standards for calibration of magnification. In the highest magnification range 12 traces has been made on relevant roughness standards for calibration of Ra.

Kalibreringsresultater og –usikkerheder.

Nedenfor er baggrundsstøjen på ruhedsmåleren og kalibreringsfaktorerne for de kalibrerede forstærkningstrin angivet. Kalibreringsfaktorerne er kun gyldige for den kombination af forstærkning og tast, som er anvendt ved kalibreringen. For forstærkningstrin, hvor kalibreringen er foretaget med flere normaler er der ligeledes givet en kalibreringstabel, som dækker hele måleområdet. Usikkerheden er angivet med faktor k=2 ≈ 95 % konfidensniveau.

Calibration results and uncertainties.

Below the background noise and the calibration factors for the calibrated magnification ranges are given. The calibration factors are only valid for the combination of magnification range and stylus used during the calibration. In measuring ranges where the calibration has been carried with more than one standard a calibration table covering the whole measuring range is also given. The uncertainties refer to the factor k=2 ≈ 95 % confidence level.

Forstærkningstrin Magnification range	Filter cut-off mm Filtre cut-off mm	Baggrundsstøj Ra µm Background noise Ra µm
210 µm, Ultra software	0.80	0.008
210 µm, Sursam74 software	0.80	0.008

Kalibreret Forstærkning / Calibrated Magnification				
Forstærkningstrin Magnification	Referenceværdi Reference value	Filter cut-off mm Filtre cut-off mm	Kalibreringsfaktor Calibration factor	Usikkerhed µm Uncertainty µm
210 µm, Sursam74 software	d = 9.292 µm	Ufiltreret/unfiltered	1.002	0.112

Kalibreret Ra-beregning / Calibrated Ra calculation				
Forstærkningstrin Magnification	Referenceværdi Reference value	Filter cut-off mm Filtre cut-off mm	Kalibreringsfaktor Calibration factor	Usikkerhed µm Uncertainty µm
210 µm, Ultra software	Ra=0.229 µm	0.80	1.009	0.010
210 µm,Ultra software	Ra=0.604 µm	0.80	1.008	0.024
210 µm, Ultra software	Ra=1.706 µm	0.80	1.016	0.068
210 µm, Sursam74 software	Ra=0.229 µm	0.80	0.996	0.009
210 µm, Sursam74 software	Ra=0.604 µm	0.80	1.002	0.024
210 µm, Sursam74 software	Ra=1.706 µm	0.80	1.006	0.068

Måledata.
Parameternormalerne er aftastet i 12 snit fordelt over målefladen. Den følgende tabel giver de beregnede Ra-værdier. Ruhedsmåleren er ikke blevet justeret.

Measuring data.
The parameter standards have been measured in 12 traces distributed over the measuring surface. The table below gives the calculated Ra values. No adjustment has been performed.

Referenceværdi Ra, cut-off 0.80 mm Reference value Ra, cut-off 0.80 mm	0.229 µm	0.604 µm	1.706 µm	0.229 µm	0.604 µm	1.706 µm
Software	Ultra			Sursam74		
Måling nummer Measurement number						
1	0.2279	0.5670	1.6831	0.229	0.601	1.689
2	0.2340	0.6077	1.6733	0.233	0.600	1.692
3	0.2166	0.6181	1.6733	0.231	0.599	1.683
4	0.2288	0.6187	1.6750	0.232	0.601	1.678
5	0.2264	0.5997	1.7008	0.232	0.600	1.694
6	0.2260	0.5882	1.6532	0.227	0.601	1.697
7	0.2272	0.5785	1.6651	0.228	0.604	1.689
8	0.2271	0.5870	1.6682	0.231	0.606	1.691
9	0.2261	0.6145	1.6701	0.229	0.602	1.715
10	0.2343	0.6153	1.6753	0.231	0.606	1.708
11	0.2316	0.5898	1.6990	0.230	0.609	1.709
12	0.2186	0.6053	1.7177	0.226	0.602	1.702

Måledata.
Forstærknings normalen er aftastet i 5 snit fordelt over målefladen. Den følgende tabel giver de målte rilledybder i form af d. Ingen justering er foretaget.

Measuring data.
The magnification standard has been measured in 5 traces distributed over the measuring surface. The table below gives the measured groove depths in term of d. No adjustment has been performed.

Reference rilledybde / Reference groove depth	9.292 µm		
Forstærkning / Magnification Måling nummer Measurement number	210 µm [µm]		
1	9.262		
2	9.285		
3	9.280		
4	9.262		
5	9.293		

Målebetingelser.

Målingerne er udført ifølge procedurerne RU-522 og RU-541. Kalibreringen af profil diagram er foretaget mod ISO type A2 normal med nominelle rille dybde på 9.3 µm. Kalibreringen af parameterberegningen er foretaget mod ISO type D parameternormaler med nominelle Ra-værdier på 0.2 µm, 0.5 µm og 1.7 µm. Målingerne er foretaget med cut-off 0.8 mm (fasekorrekt filter). Ingen kort bølge Ls filter er anvendt. Målingerne er foretaget ved en temperatur på 20 ± 2°C.

Measuring conditions.

The measurements were carried out in accordance with procedures RU-522 and RU-541. The calibration of the profile diagram has been performed using ISO type A 2 roughness standard with nominal groove depth of 9.3 µm. The calibration of the parameter calculation has been performed using ISO type D roughness standards with nominal Ra values of 0.2 µm, 0.5 µm and 1.7 µm. The measurements have been carried out using cut-off 0.8 mm (Gaussian filter). No short wave Ls cut-off was used. The measurements have been carried out at a temperature of 20 ± 2°C.

Kalibreringen er sporbar via normalen:
The calibration is traceable through the standard: **PTB/Halle RN1171 (ISO type D)**

Med certifikatet:
With the certificate: **Rou11004**

Certifikatet er dateret:
The certificate is dated: **02.03.11**

Og
And

Kalibreringen er sporbar via normalen:
The calibration is traceable through the standard: **PTB/Halle RN1261 (ISO type D)**

Med certifikatet:
With the certificate: **Rou11003**

Certifikatet er dateret:
The certificate is dated: **28.02.11**

Målebetingelser.

Målingerne er udført ifølge procedurerne RU-522 og RU-541. Kalibreringen af profil diagram er foretaget mod ISO type A2 normal med nominelle rille dybde på 9.3 µm. Kalibreringen af parameterberegningen er foretaget mod ISO type D parameternormaler med nominelle Ra-værdier på 0.2 µm, 0.5 µm og 1.7 µm. Målingerne er foretaget med cut-off 0.8 mm (fasekorrekt filter). Ingen kort bølge Ls filter er anvendt. Målingerne er foretaget ved en temperatur på 20 ± 2°C.

Measuring conditions.

The measurements were carried out in accordance with procedures RU-522 and RU-541. The calibration of the profile diagram has been performed using ISO type A 2 roughness standard with nominal groove depth of 9.3 µm. The calibration of the parameter calculation has been performed using ISO type D roughness standards with nominal Ra values of 0.2 µm, 0.5 µm and 1.7 µm. The measurements have been carried out using cut-off 0.8 mm (Gaussian filter). No short wave Ls cut-off was used. The measurements have been carried out at a temperature of 20 ± 2°C.

Kalibreringen er sporbar via normalen:
The calibration is traceable through the standard: **PTB/Halle RN1171 (ISO type D)**

Med certifikatet:
With the certificate: **Rou11004**

Certifikatet er dateret:
The certificate is dated: **02.03.11**

Og
And

Kalibreringen er sporbar via normalen:
The calibration is traceable through the standard: **PTB/Halle RN1261 (ISO type D)**

Med certifikatet:
With the certificate: **Rou11003**

Certifikatet er dateret:
The certificate is dated: **28.02.11**

Og
And

Kalibreringen er sporbar via normalen: The calibration is traceable through the standard:	**PTB/Halle RN1246 (ISO type D)**
Med certifikatet: With the certificate:	**Rou11002**
Certifikatet er dateret: The certificate is dated:	**28.02.11**

Og
And

Kalibreringen er sporbar til: The calibration is traceable to:	**PTB**
Kalibreringen er sporbar via normalen: The calibration is traceable through the standard:	**HALLE no. 826**
Med certifikatet: With the certificate:	**091 PTB 08**
Certifikatet er dateret: The certificate is dated:	**07.11.08**

11.1.2 Workshop stylus profilometer (Hommel)

The workshop stylus instrument is a Hommel Tester T1000, located in building 427, room 122, see Figure 11.2. Its technical specifications are listed in Table 11.2.

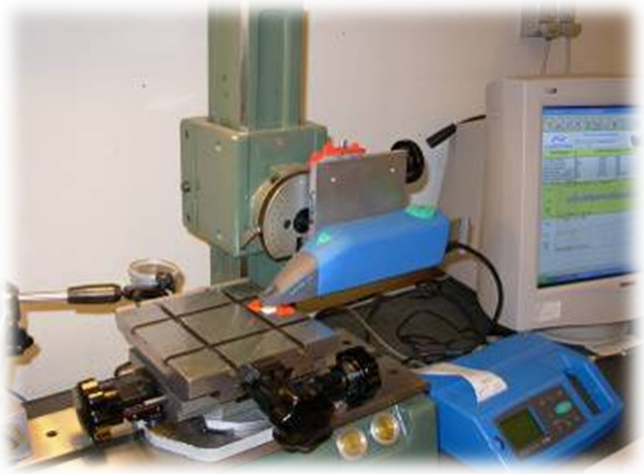

Figure 11.2 – Workshop stylus located in building 427, room 122.

Technical specifications	
TIP RADIUS [µm]	2
TIP SHAPE PROFILE	Conical
TIP ANGLE [°]	90
MEASUREMENT RANGE X x Z [mm]	20 x 0.08/0.320
Z - RESOLUTION [µm]	0.01/0.04

Table 11.2 – Technical specification of the workshop stylus.

The verification and calibration of the instrument are performed every 6 months or when they are required, e.g. when changing of the probe or moving of the instruments. They consist in measuring calibrated artefact and in checking the background noise on a glass plate. The last verification was carried out in September 2011 and the results are listed in the certificate n° “*Rum11008*”, reported here in the following.

CGM
CENTER FOR GEOMETRISK METROLOGI

ilac-MRA

DANAK
CAL Reg.Nr. 273

Kalibreringscertifikat
Calibration Certificate

Side 1 af **4**
Page 1 of **4**
Antal Bilag **2**
No of Enclosures **2**
Rum11008

Certifikat nr. Certificate No.	**Rum11008**
Objekt Object	**Ruhedsmåler / Roughness measuring instrument**
Fabrikant Manufacturer	**Hommel**
Type Type	**T1000**
Serienummer Serial number	**67390 / Stylus: 95112**
Rekvirent Customer	**DTU Mekanik** **Produktionstorvet** **2800 Kgs. Lyngby**

Kalibreringscertifikatet må kun gengives i uddrag hvis det enten er offentligt tilgængeligt, eller hvis CGM har godkendt uddraget.

The calibration certificate may not be reproduced other than in full except with the permission of CGM.

Dato for modtagelse Date of reciept	**19.09.11**	Dato for certifikatets udstedelse Date of issue of certificate	**22.09.11**
Dato for kalibrering Date of calibration	**19.09.11**		

Underskrift
Signature

Jan L. Andreasen
Fagligt ansvarlig
Signatory, Surface Roughness Calibration

Center for Geometrisk Metrologi, Bygning 425
DTU Mekanik, Danmarks Tekniske Universitet
2800 Kgs. Lyngby, CVR-nr. 30 06 09 46
Telefon 45 25 47 60 – Telefax 45 93 01 90 – Email cgm@cgm.dk

Kalibreringens omfang.

Inden kalibreringen er tastspidserne undersøgt for skader og slid og tasttrykket er evalueret. Baggrundsstøjen på ruhedsmåleren er bestemt ud fra 10 aftastninger på et planglas udtrykt som Ra med cut-off 0.8 mm. I hvert kalibreret forstærkningstrin er der foretaget 12 aftastninger på relevante parameternormaler til kalibrering af Ra.

Extent of calibration.

Before the calibration the stylus tips have been checked for damage and wear and the measuring force has been evaluated. The background noise of the roughness measuring instrument has been determined from 10 traces on an optical flat expressed as Ra using cut-off 0.8 mm. In each calibrated magnification range 12 traces have been made on relevant roughness standards for calibration of Ra.

Kalibreringsresultater og –usikkerheder.

Nedenfor er baggrundsstøjen på ruhedsmåleren og kalibreringsfaktorerne for de kalibrerede forstærkningstrin angivet. Kalibreringsfaktorerne er kun gyldige for den kombination af forstærkning og tast, som er anvendt ved kalibreringen. For forstærkningstrin, hvor kalibreringen er foretaget med flere normaler er der ligeledes givet en kalibreringstabel, som dækker hele måleområdet. Usikkerheden er angivet med faktor k=2 ≈ 95 % konfidensniveau.

Calibration results and uncertainties.

Below the background noise and the calibration factors for the calibrated magnification ranges are given. The calibration factors are only valid for the combination of magnification range and stylus used during the calibration. In measuring ranges where the calibration has been carried with more than one standard a calibration table covering the whole measuring range is also given. The uncertainties refer to the factor k=2 ≈ 95 % confidence level.

Forstærkningstrin Magnification range	Filter cut-off mm Filtre cut-off mm	Baggrundsstøj Ra µm Background noise Ra µm
Ra (80 µm range / Sursam 7.4)	0.80	0.011

Kalibreret Ra-beregning / Calibrated Ra calculation				
Forstærkningstrin Magnification	Referenceværdi Reference value	Filter cut-off mm Filtre cut-off mm	Kalibreringsfaktor Calibration factor	Usikkerhed µm Uncertainty µm
Ra (80 µm range / Sursam 7.4)	Ra=0.229 µm	0.80	1.051	0.010
Ra (80 µm range / Sursam 7.4)	Ra=0.604 µm	0.80	1.030	0.024
Ra (80 µm range / Sursam 7.4)	Ra=1.706 µm	0.80	1.010	0.068

Måledata.
Parameternormalerne er aftastet i 12 snit fordelt over målefladen. Den følgende tabel giver de beregnede Ra-værdier. Ruhedsmåleren er ikke blevet justeret.

Measuring data.
The parameter standards have been measured in 12 traces distributed over the measuring surface. The table below gives the calculated Ra values. No adjustment has been performed.

Referenceværdi Ra, cut-off 0.80 mm Reference value Ra, cut-off 0.80 mm	0.229 µm	0.604 µm	1.706 µm
Måling nummer Measurement number			
1	0.220	0.588	1.707
2	0.219	0.583	1.698
3	0.220	0.592	1.695
4	0.217	0.592	1.693
5	0.217	0.587	1.684
6	0.216	0.581	1.679
7	0.216	0.588	1.675
8	0.219	0.579	1.685
9	0.218	0.586	1.666
10	0.216	0.586	1.709
11	0.219	0.587	1.706
12	0.218	0.586	1.668

Målebetingelser.

Målingerne er udført ifølge procedure RU-541. Kalibreringen af parameterberegningen er foretaget mod ISO type D parameternormaler med nominelle Ra-værdier på 0.2 µm, 0.5 µm og 1.7 µm. Målingerne er foretaget med cut-off 0.8 mm. Målingerne er foretaget ved en temperatur på 20 ± 2°C.

Measuring conditions.

The measurements were carried out in accordance with procedure RU-541. The calibration of the parameter calculation has been performed using ISO type D roughness standards with nominal Ra values of 0.2 µm, 0.5 µm and 1.7 µm. The measurements have been carried out using cut-off 0.8 mm. The measurements have been carried out at a temperature of 20 ± 2°C.

Kalibreringen er sporbar via normalen:
The calibration is traceable through the standard: **PTB/Halle RN1171 (ISO type D)**

Med certifikatet:
With the certificate: **Rou11004**

Certifikatet er dateret:
The certificate is dated: **02.03.11**

Og
And

Kalibreringen er sporbar via normalen:
The calibration is traceable through the standard: **PTB/Halle RN1261 (ISO type D)**

Med certifikatet:
With the certificate: **Rou11003**

Certifikatet er dateret:
The certificate is dated: **28.02.11**

Og
And

Kalibreringen er sporbar via normalen:
The calibration is traceable through the standard: **PTB/Halle RN1246 (ISO type D)**

Med certifikatet:
With the certificate: **Rou11002**

Certifikatet er dateret:
The certificate is dated: **28.02.11**

11.1.3 Atomic force microscope

The atomic force microscope located in building 427S-room 311 is mounted in a probe holder on mounted a Coordinate Measuring Machine (CMM). The CMM is a three-coordinate measuring machine in which both movement and detection of axis positions are performed manually. This manual CMM presents guide ways supported by slide ways, which can be used in three different ways:

1. The CMM positions the AFM probe and a measurement is performed covering max 40 µm x 40 µm (corresponding to the maximum scan area of the AFM);
2. The CMM positions the AFM probe at different places for spot wise investigation of larger areas within the CMM working volume (X x Y x Z max: 400 x 100 x 75 mm^3);
3. The CMM is used to reposition the AFM probe in between surface roughness measurements to cover continuous areas larger than 40 µm x 40 µm.

The environment where the measurements are carried out is described in Table 11.1; while the technical specifications are listed in Figure 11.3.

Technical specifications	
TIP RADIUS [nm]	10
TIP SHAPE PROFILE	Pyramid
TIP ANGLE [°]	40
MEASUREMENT RANGE X x Y x Z [µm]	200 x 200 x 15
X - RESOLUTION [nm]	< 1
Y - RESOLUTION [nm]	< 1
Z - RESOLUTION [nm]	< 0.5
Stage	
TYPE	Moving
SIZE [mm]	400 x 100 x 75
MAX WORKPIECE HEIGHT [mm]	100

Figure 11.3 – Atomic force microscope in building 427S, room 311.

The verification and calibration of the instrument are performed every 6 months or when they are required, e.g. when changing of the tip or moving of the instruments. They consist in measuring calibrated artefacts, such as gratings, and in checking the background noise on a glass plate. The last verification was carried out in March 2009 and the results are listed in the certificate n° “*TN2370SN104001*”, reported here in the following. Between March 2009 and December 2011, several measurements on calibrated gratings, such as TGS1, TGZ1, TGZ2 and TGZ3, were performed in order to verify the instrument.

DME - Danish Micro Engineering A/S • Transformervej 12 • DK 2730 Herlev • Denmark
Tel: +45 44 84 92 11 • Fax: +45 44 84 91 97 • www.dme-spm.dk

Certificate of Compliance (DME SPM CoC)

TN2370SN104001 Date:31-03-2009

Scanner type DME2370, DS95-200-15

X-Y plane

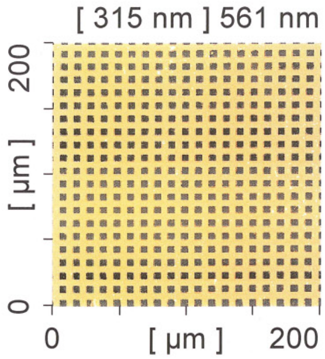

Grating Measurement	Horizontal	Vertical
Area	200µm x 200µm	
Period	10,1µm	9,93µm
Rising edge std. dev.	108nm	134nm
Falling edge std. dev.	155nm	109nm

Note. The standard deviation of the gratings pitch is 30 nm

10Micron 3D 181nm VLSI (Z-lin off)

Noise factor

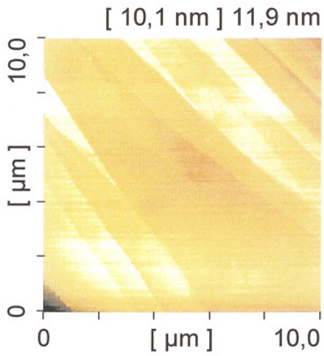

Roughness	Value
Area	10µm x10µm nm
Sz	8,65nm
Sa	1,04nm

NOTE.
Sz is the ten point height
Sa is the Arithmetic mean deviation

HOPG

X:1,245 Y:1,283 Z:0,482 (z-linearization off)
Repeated measurement after repair

Conducted by : Glenn Nielsen

Accepted by : Curt Sander

Delivered to:________________

Date:31-03-2009

Packing list: ________________

11.1.4 Scanning electron microscope

The Scanning electron microscope located in building 425 is a Jeol 5900, see Figure 11.4.

Figure 11.4 – SEM located in building 425.

The pixel size of the SEM images was calibrated for nominal magnification levels in the range 100x – 10000x at a fixed working distance of d = 20 mm. The used magnification calibration artefacts were: one dimensional steel ruler for calibrating low magnifications, and a 2D SPM calibration grating for high magnifications. Traceability of the 1D ruler had been ensured by calibration with laser displacement interferometry. For the 2D grating, calculations were based on the pitch claimed by the manufacturer. The experimental procedure is described in the work of [P. Bariani, "Dimensional metrology for microtechnology", PhD thesis, Department of Manufacturing Engineering and Management, Technical University of Denmark, 2005] and the results are listed in Table 11.3.

Magnification	1D scale *x* direction *s* [µm]	U* [µm]	*y* direction *s* [µm]	U* [µm]	2D grating [µm]
100x	-	-	0.988	0.019	-
200x	0.491	0.003	0.493	0.005	-
400x	0.245	0.002	-	-	0.247
500x	0.199	0.003	0.198	0.003	0.200
1000x	0.099	0.005	0.100	0.005	0.100
2000x	-	-	-	-	0.050
5000x	-	-	-	-	0.020
10000x	-	-	-	-	0.010

Table 11.3 - Magnification calibration results (* Expanded uncertainty calculated with a coverage factor 2; *s* = pixel size).

11.1.5 Infinite Focus – Focus Variation

The instrument based on the Focus-Variation principle is an InfiniteFocus-Standard by Alicona Imaging GmbH, see Figure 11.5. It is located in building 427S, room 311; the laboratory environment is described in Table 11.1.

The instrument technical specifications are listed in Table 11.4.

Figure 11.5 – Optical instrument based on the Focus Variation principle, located in building 427S, room 311.

Technical specifications	
MEASUREMENT RANGE X x Y x Z [mm]	Depending on objective (0.14 x 0.1 mm to 5.7 x 4.3 mm)
X - RESOLUTION [µm]	Depending on objective (0.4 µm to 2.2 µm)
Y - RESOLUTION [µm]	Depending on objective (0.4 µm to 2.2 µm)
Z - RESOLUTION [µm]	Depending on objective (0.001 µm to 0.5 µm)
X - ACCURACY [µm]	Depend on surface structure
Y - ACCURACY [µm]	Depend on surface structure
Z - ACCURACY [µm]	Depend on surface structure
NOTE	Measurement speed: depending on objective 1400 µm/s to 1.4 µm/s; vertical resolution is also dependent on measurement speed
Stage	
TYPE	Moving
SIZE [mm]	100 x 100 x 100
MAX WORKPIECE LOAD [N]	200
MAX WORKPIECE HEIGHT [mm]	240
MAX TRAVEL DISTANCE X [mm]	100
MAX TRAVEL DISTANCE Y [mm]	100

Table 11.4 – Technical specifications of the InfiniteFocus instrument located in building 427S, room 311.

The calibration is performed every 6 months on a calibration artefact made specifically for this instrument. The following calibration data are referred to height calibration, lenses calibration (5x - 10x – 20x - 50x using the coaxial light) and lateral calibration. The calibration was performed in April 2011. The data are reported here in the following.

Alicona Imaging GmbH
Teslastraße 8
A-8074 Grambach

Measurement Report

Calibration Report

IFM Version 3.5 2009-12-03
Hardware ID: H101208089
IFM Serial Number: 002110407208
Date: 2011-04-06T16:23:16
User: user
Optic: IFM G4 10x
Hardware:
  Measurement Device: IFM G4e Measurement Device
  Sensor: IFM G4 High Resolution Sensor Version B
  XY-Controller: IFM G4 XY Controller
  Z-Controller: IFM G4 Z Controller
  Lightsource: Alicona Imaging IFM G4 Lightsource Version 2

Vertical Calibration

Step Height Calibrated Value: 1.0019mm
Step Height Measured Value: 1.0021mm
Step Height Deviation: 278nm

Please note that all values are rounded for display purpose.

Alicona Imaging GmbH
Teslastraße 8
A-8074 Grambach

alicona

Measurement Report

Calibration Report

IFM Version 3.5 2009-12-03
Hardware ID: H101208089
IFM Serial Number: 002110407208
Date: 2011-04-06T16:56:53
User: user
Optic: IFM G4 5x
Hardware:
Measurement Device: IFM G4e Measurement Device
Sensor: IFM G4 High Resolution Sensor Version B
XY-Controller: IFM G4 XY Controller
Z-Controller: IFM G4 Z Controller
Lightsource: Alicona Imaging IFM G4 Lightsource Version 2

Field Of Curvature

Flatness: 369nm
Required Flatness: 410nm
Pan of Calibration Tool: %2
Tilt of Calibration Tool: %2

Please note that all values are rounded for display purpose.

Measurement performed by Alicona InfiniteFocus

Alicona Imaging GmbH
Teslastraße 8
A-8074 Grambach

Measurement Report

Calibration Report

IFM Version 3.5 2009-12-03
Hardware ID: H101208089
IFM Serial Number: 002110407208
Date: 2011-04-06T17:03:21
User: user
Optic: IFM G4 10x
Hardware:
  Measurement Device: IFM G4e Measurement Device
  Sensor: IFM G4 High Resolution Sensor Version B
  XY-Controller: IFM G4 XY Controller
  Z-Controller: IFM G4 Z Controller
  Lightsource: Alicona Imaging IFM G4 Lightsource Version 2

Field Of Curvature

Flatness: 153nm
Required Flatness: 100nm
Pan of Calibration Tool: %2
Tilt of Calibration Tool: %2

Please note that all values are rounded for display purpose.

Measurement performed by Alicona InfiniteFocus

Alicona Imaging GmbH
Teslastraße 8
A-8074 Grambach

alicona

Measurement Report

Calibration Report

IFM Version 3.5 2009-12-03
Hardware ID: H101208089
IFM Serial Number: 002110407208
Date: 2011-04-06T17:09:41
User: user
Optic: IFM G4 20x
Hardware:
  Measurement Device: IFM G4e Measurement Device
  Sensor: IFM G4 High Resolution Sensor Version B
  XY-Controller: IFM G4 XY Controller
  Z-Controller: IFM G4 Z Controller
  Lightsource: Alicona Imaging IFM G4 Lightsource Version 2

Field Of Curvature

Flatness: 55nm
Required Flatness: 50nm
Pan of Calibration Tool: %2
Tilt of Calibration Tool: %2

Please note that all values are rounded for display purpose.

Measurement performed by Alicona InfiniteFocus

Alicona Imaging GmbH
Teslastraße 8
A-8074 Grambach

Measurement Report

Calibration Report

IFM Version 3.5 2009-12-03
Hardware ID: H101208089
IFM Serial Number: 002110407208
Date: 2011-04-06T17:16:42
User: user
Optic: IFM G4 50x
Hardware:
- Measurement Device: IFM G4e Measurement Device
- Sensor: IFM G4 High Resolution Sensor Version B
- XY-Controller: IFM G4 XY Controller
- Z-Controller: IFM G4 Z Controller
- Lightsource: Alicona Imaging IFM G4 Lightsource Version 2

Field Of Curvature

Flatness: 40nm
Required Flatness: 20nm
Pan of Calibration Tool: %2
Tilt of Calibration Tool: %2

Please note that all values are rounded for display purpose.

Measurement performed by Alicona InfiniteFocus

Alicona Imaging GmbH
Teslastraße 8
A-8074 Grambach

Measurement Report

Calibration Report

IFM Version 3.5 2009-12-03
Hardware ID: H101208089
IFM Serial Number: 002110407208
Date: 2011-04-06T16:50:21
User: user
Optic: IFM G4 5x
Hardware:
  Measurement Device: IFM G4e Measurement Device
  Sensor: IFM G4 High Resolution Sensor Version B
  XY-Controller: IFM G4 XY Controller
  Z-Controller: IFM G4 Z Controller
  Lightsource: Alicona Imaging IFM G4 Lightsource Version 2

Lateral Calibration

Grid Distance Calibrated Value: 49.94µm
Grid Distance Measured Value: 49.959µm
Grid Distance Deviation: 20nm

Please note that all values are rounded for display purpose.

Measurement performed by Alicona InfiniteFocus

Alicona Imaging GmbH
Teslastraße 8
A-8074 Grambach

Measurement Report

Calibration Report

IFM Version 3.5 2009-12-03
Hardware ID: H101208089
IFM Serial Number: 002110407208
Date: 2011-04-06T17:59:15
User: user
Optic: IFM G4 10x
Hardware:
  Measurement Device: IFM G4e Measurement Device
  Sensor: IFM G4 High Resolution Sensor Version B
  XY-Controller: IFM G4 XY Controller
  Z-Controller: IFM G4 Z Controller
  Lightsource: Alicona Imaging IFM G4 Lightsource Version 2

Lateral Calibration

Grid Distance Calibrated Value: 23.963µm
Grid Distance Measured Value: 23.988µm
Grid Distance Deviation: 26nm

Please note that all values are rounded for display purpose.

Measurement performed by Alicona InfiniteFocus

Alicona Imaging GmbH
Teslastraße 8
A-8074 Grambach

alicona

Measurement Report

Calibration Report

IFM Version 3.5 2009-12-03
Hardware ID: H101208089
IFM Serial Number: 002110407208
Date: 2011-04-06T18:04:22
User: user
Optic: IFM G4 20x
Hardware:
Measurement Device: IFM G4e Measurement Device
Sensor: IFM G4 High Resolution Sensor Version B
XY-Controller: IFM G4 XY Controller
Z-Controller: IFM G4 Z Controller
Lightsource: Alicona Imaging IFM G4 Lightsource Version 2

Lateral Calibration

Grid Distance Calibrated Value: 23.963µm
Grid Distance Measured Value: 23.991µm
Grid Distance Deviation: 27nm

Please note that all values are rounded for display purpose.

Measurement performed by Alicona InfiniteFocus

Alicona Imaging GmbH
Teslastraße 8
A-8074 Grambach

Measurement Report

Calibration Report

IFM Version 3.5 2009-12-03
Hardware ID: H101208089
IFM Serial Number: 002110407208
Date: 2011-04-06T18:01:46
User: user
Optic: IFM G4 50x
Hardware:
 Measurement Device: IFM G4e Measurement Device
 Sensor: IFM G4 High Resolution Sensor Version B
 XY-Controller: IFM G4 XY Controller
 Z-Controller: IFM G4 Z Controller
 Lightsource: Alicona Imaging IFM G4 Lightsource Version 2

Lateral Calibration

Grid Distance Calibrated Value: 23.963µm
Grid Distance Measured Value: 23.977µm
Grid Distance Deviation: 13nm

Please note that all values are rounded for display purpose.

Measurement performed by Alicona InfiniteFocus

11.1.6 Coordinate measuring machine

The Coordinate measuring machine in building 427S-room 311 is a De Meet 220, see Figure 11.6. It can be used as a contact instrument using two different touch probes or as an optical instrument using three different lens magnifications. Its technical specifications are listed in Table 11.5.

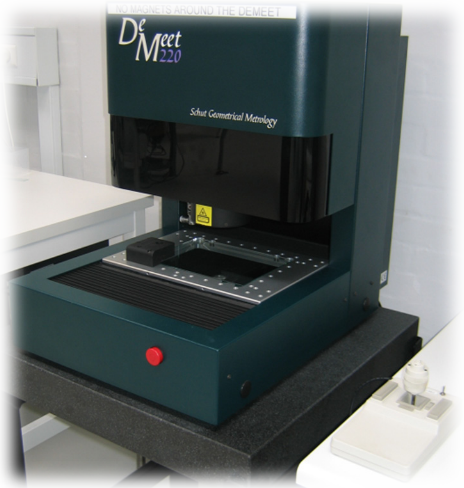

Figure 11.6 – Coordinate measuring machine in building 427S, room 311.

Technical specifications	
SPOT SOURCE	Ringlight, backlight and coaxial light
MEASUREMENT RANGE X x Y x Z [mm]	220 x 150 x 100
X - RESOLUTION [µm]	0.5
Y - RESOLUTION [µm]	0.5
Z - RESOLUTION [µm]	0.5
X - ACCURACY [µm]	4 [µm] + L [mm] /150
Y - ACCURACY [µm]	4 [µm] + L [mm] /150
Z - ACCURACY [µm]	4 [µm] + L [mm] /150
NOTE	Ringlight: 3 rings, 16 segments and 48 cells Backlight and coaxial light: adjustable 3 Leica-Design telecentric lenses are available: 2.0x, 5.0x, 20.0x Probes: ø 2 mm; ø 0.5 mm

Table 11.5 – Technical specifications of the coordinate measuring machine in building 427S, room 311.

The calibration is performed every 6 months using:

- Position offset qualifier to determine the machine offsets to the machine coordinate system for video and touch probe measurements;
- Qualification sphere to determine the probe offset and the accuracy of the styli;
- Field of view qualifier to determine the video image positions and to enable highly accurate optical measurements.

The calibration data of the two probes (2 mm in diameter and 0.5 mm in diameter) and the two lenses (2x and 5x) are listed below.

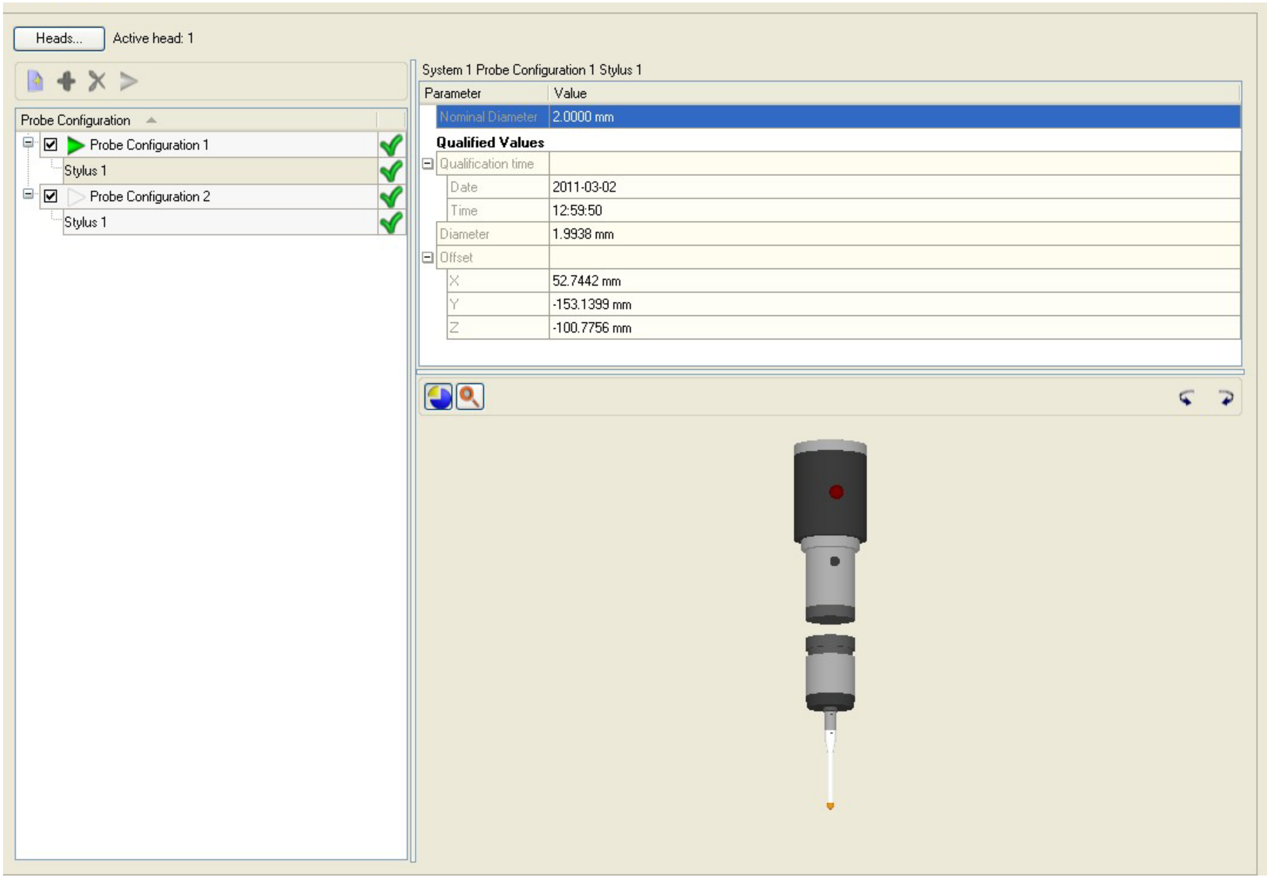

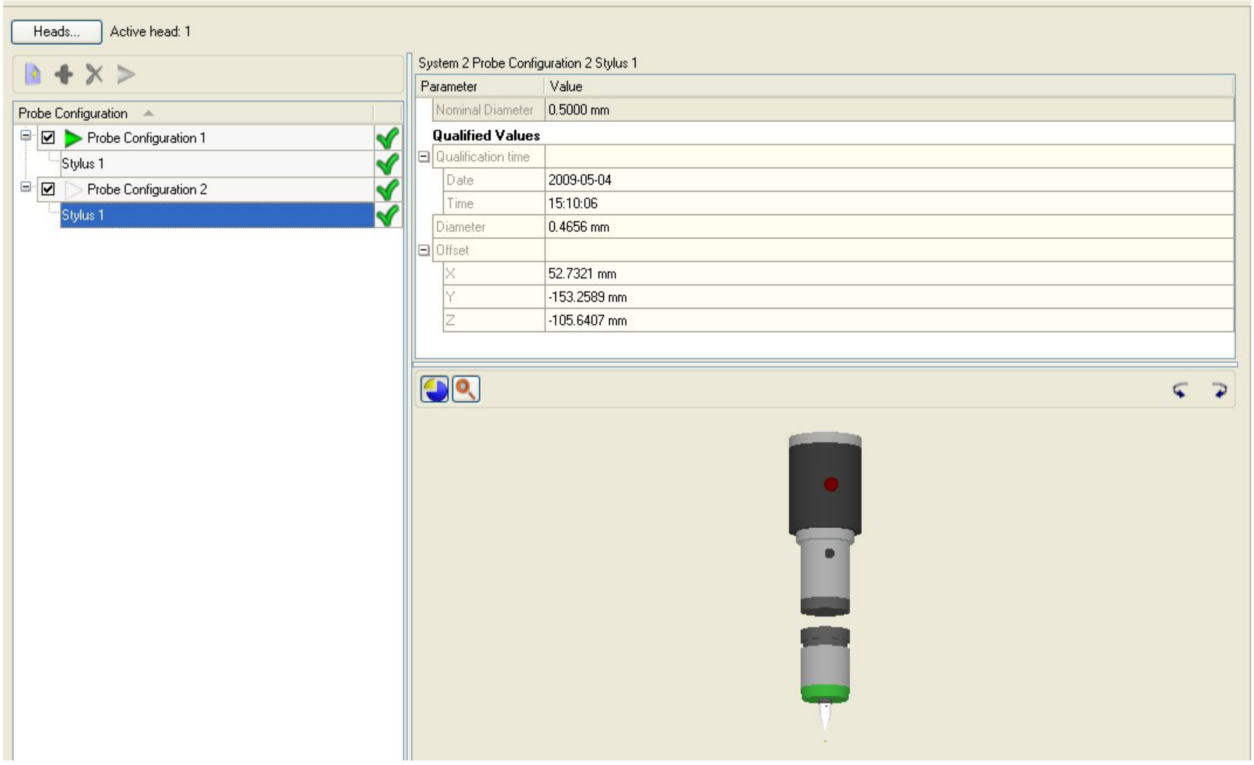
Heads...
Active head: 1
Probe Configuration
Probe Configuration 1
Stylus 1
Probe Configuration 2
Stylus 1
System 2 Probe Configuration 2 Stylus 1
Parameter
Value
Nominal Diameter
0.5000 mm
Qualified Values
Qualification time
Date
2009-05-04
Time
15:10:06
Diameter
0.4656 mm
Offset
X
52.7321 mm
Y
-153.2589 mm
Z
-105.6407 mm

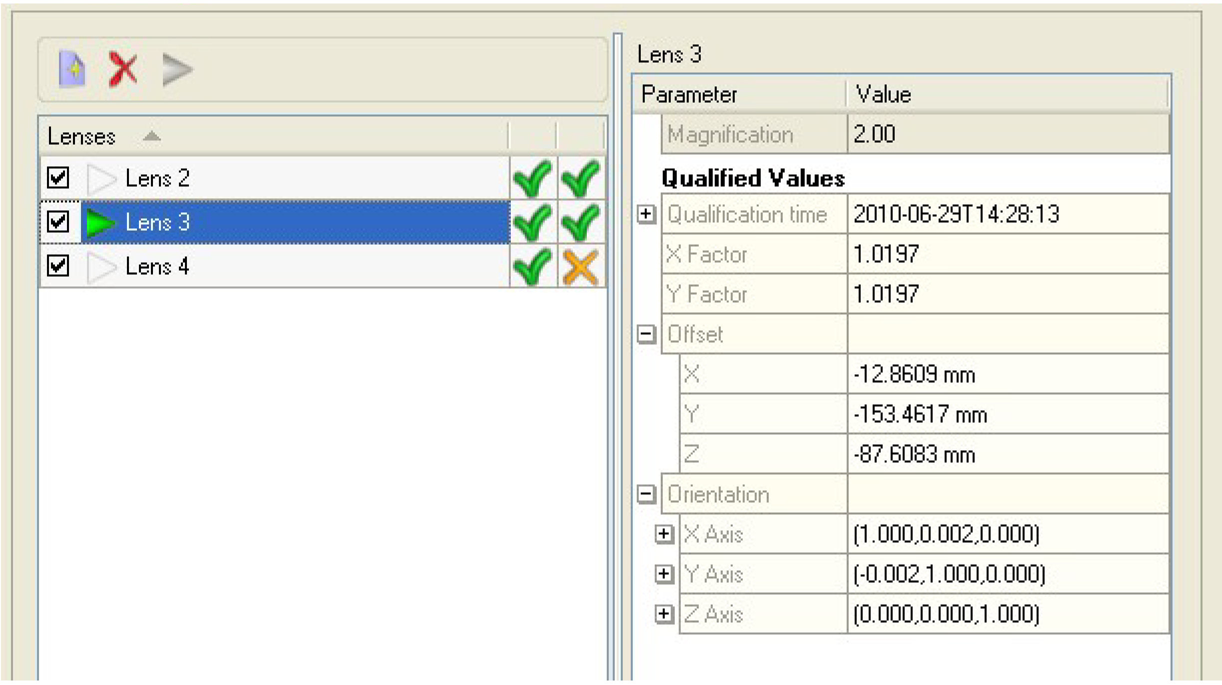
Lenses
Lens 2
Lens 3
Lens 4
Lens 3
Parameter
Value
Magnification
2.00
Qualified Values
Qualification time
2010-06-29T14:28:13
X Factor
1.0197
Y Factor
1.0197
Offset
X
-12.8609 mm
Y
-153.4617 mm
Z
-87.6083 mm
Orientation
X Axis
(1.000,0.002,0.000)
Y Axis
(-0.002,1.000,0.000)
Z Axis
(0.000,0.000,1.000)

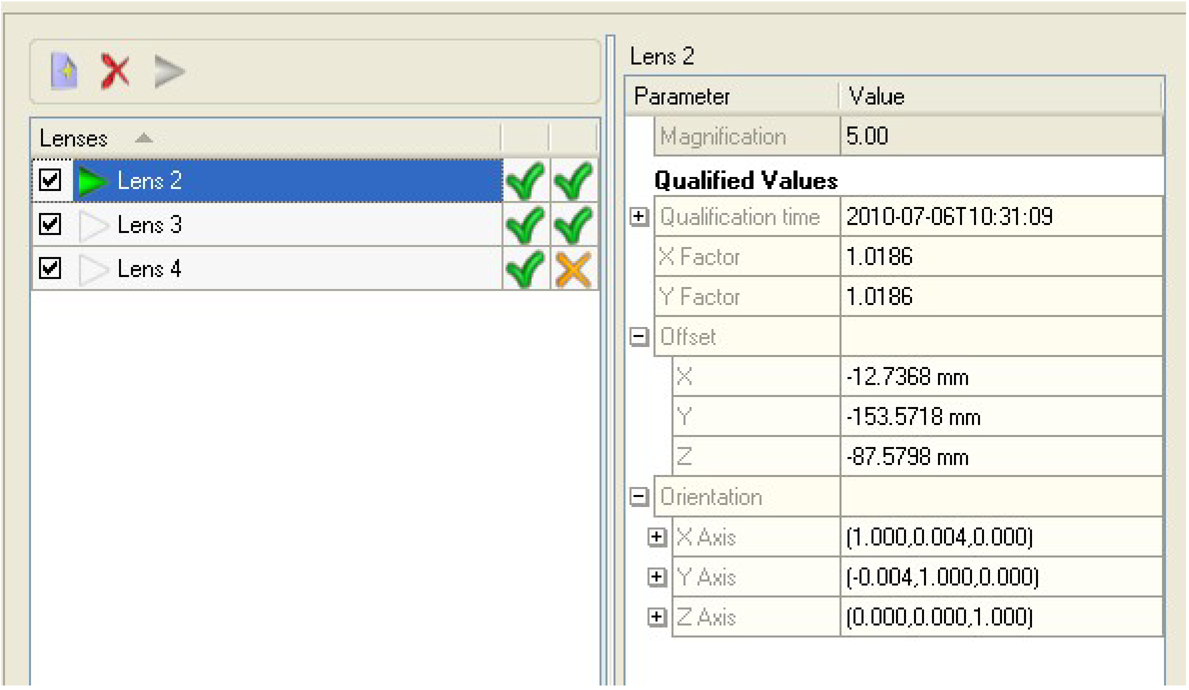

In Table 11.6 the uncertainty of the OCMM using a 5x lens magnification was calculated along the *x* and *y* direction using a line scale characterized by nominal pitch of 80 µm. The measurements were performed in January 2012.

Nominal [µm]	$U_{x,OCMM}$ [µm]	$U_{y,OCMM}$ [µm]
Distance 80	2.5	2.4
Distance 160	2.3	4.4
Distance 240	2.0	5.0
Distance 320	2.5	3.1
Distance 400	3.2	2.3
Distance 480	2.9	3.7
Distance 560	2.4	4.8
Distance 640	2.3	4.9
Distance 720	2.7	3.0

Table 11.6 - Uncertainty of the OCMM using a 5x lens magnification along *x* and *y* direction.

11.1.7 Tactile coordinate measuring machine

A tactile coordinate measuring machine is located in building 425 and it provides testing and calibration services under accreditation. It is a Zeiss UPMC Carat 850, see Figure 11.7. Its technical specifications are listed in Table 11.7.

Figure 11.7 – Accredited tactile coordinate measuring machine in building 425.

Technical specifications	
PROBE RADIUS [mm]	Down to 0.15 mm
NUMBER OF PROBES AND THEIR POSITION	5
FORCE [N]	0.1– 10
MEASUREMENT RANGE X x Y x Z [mm]	820 x 700 x 600
X - RESOLUTION [µm]	0.1
Y - RESOLUTION [µm]	0.1
Z - RESOLUTION [µm]	0.1
X - ACCURACY [µm]	0,4 [µm] + L [mm] / 900
Y - ACCURACY [µm]	0,4 [µm] + L [mm] / 900
Z - ACCURACY [µm]	0,4 [µm] + L [mm] / 900
Stage	
SIZE [mm]	820 x 700 x 600
MAX WORKPIECE LOAD [N]	10000

Table 11.7 – Technical specification of the accreditated tactile coordinate measuring machine in building 425.

The calibration is usually performed every 6 months using a zerodur plate or a holeplate and a reference sphere. The last calibration was carried out in October 2011 in order to prove the traceability in an area of 80 x 80 mm^2, see the certificate n^o "*DP11005*", reported here in the following.

CGM
CENTER FOR GEOMETRISK METROLOGI

ilac-MRA

DANAK
Reg. nr. 273

Kalibreringscertifikat (efter DKD retningslinier)
Calibration certificate (according to DKD guidelines)

Side 1 af **3**
Page 1 of **3**
Antal Appendiks **2**
No of Appendices **2**
DP11005

Certifikat nr.
Certificate No. **DP11005**

Objekt
Object **Optomekanisk hulplade / Optomechanical holeplate**

Fabrikant
Manufacturer **CGM**

Type
Type **25 huller/holes, 80 mm x 80 mm**

Serienummer
Serial number **DP135**

Rekvirent
Customer **NN**
NN

Målerapporten må ikke gengives undtagen i sin helhed, uden skriftlig tilladelse fra CGM.

The measuring report may not be reproduced other than in full except with the permission of CGM.

Dato for modtagelse
Date of receipt **2011-10-21**

Dato for målingen
Date of measuring **2011-10-31-(11-01)**

Dato for udstedelse af rapport
Date of issue of report **2011-11-09**

Underskrift
Signature

Erik Larsen
Fagligt ansvarlig
Signatory, Coordinate Metrology

Center for Geometrisk Metrologi, Bygning 425
DTU Mekanik, Danmarks Tekniske Universitet
2800 Kgs. Lyngby, CVR-nr. 30 06 09 46
Telefon 45 25 47 60 – Telefax 45 93 01 90 – Email cgm@cgm.dk

Måleresultater.

Centerkoordinaterne af hullerne er gengivet i appendiks 1 til dette certifikat. Kun X- og Y-koordinaterne af hullernes centerpunkter er kalibrerede. Z-koordinaten er ikke kalibreret. Værdierne er gældende ved 20°C. Koordinaterne er defineret i henhold til koordinatsystemet beskrevet i appendiks 2 til dette certifikat. Som længdeudvidelseskoefficient α er værdien $11{,}25 \cdot 10^{-6}$ K^{-1} brugt.

Measuring results.

The centre coordinates of the holes are listed in appendix 1 to this certificate. Only the X- and Y-coordinates of the centres of the holes have been calibrated. The Z-coordinate has not been calibrated. The values are valid at 20°C. The coordinates are defined according to the cordinate system described in appendix 2 to this certificate. As thermal expansion coefficient α of the hole plate the value $11{,}25 \cdot 10^{-6}$ K^{-1} has been used.

Måleusikkerhed.

Usikkerheden på afstanden L imellem to vilkårlige hulcentre i hulpladens XY-plan er bestemt til:

0,9 µm

Der er ingen usikkerhedsangivelse for centerpunkternes Z-koordinat (ikke kalibreret).

Måleusikkerheden er angivet med faktor k=2.

Measuring uncertainty.

The uncertainty of a distance L between any two hole centres of the XY-plane of the hole plate has been determined to:

0,9 µm

There is no uncertainty estimation of the Z-coordinate of the centre points (not calibrated).

The measuring uncertainty refers to the factor k=2.

Målebetingelser.

Målingerne er udført i henhold til procedure KO-402 og KO-403. Målingerne er udført på Zeiss UPMC 850 CARAT koordinatmålemaskine med en 3 mm tast med længden 30 mm. Målingerne blev gennemført som fire omslagsmålinger med efterfølgende måloverførsel ved komparator-måling mod Zerodur hulplade. Målingerne blev foretaget ved temperaturforhold som specificeret i procedure KO-402. Den anvendte evaluerings-software er PKAL ver. 2.0.

Measuring conditions.

The measurements were performed according to procedure KO-402 and KO-403. The measurements were performed on a Zeiss UPMC 850 CARAT coordinate measuring machine using a 3 mm probe with the length 30 mm. The measurements were carried out as four swing-round measurements followed by a comparison of length using a Zerodur holeplate. The measurements were carried out at temperature conditions as specified in procedure KO-402. The software used for data evaluation is PKAL ver. 2.0.

Sporbarhed.

Kalibreringen er sporbar til PTB, Tyskland.

Kalibreringen er sporbar via normalen Zeiss Zerodur hulplade, ID: ZERO-01.

Certifikat: 4758 PTB 05.

Certifikatet er dateret: 2005-09-16.

Traceability.

The calibration is traceable to PTB, Germany.

The calibration is traceable through the standard Zeiss Zerodur holeplate, ID: ZERO-01.

Certificate: 4758 PTB 05.

The certificate is dated: 2005-09-16.

Vilkår for certifikatet
Conditions for the certificate

DANAK

Den Danske Akkrediterings- og Metrologifond -DANAK- administrerer den danske akkrediteringsordning på grundlag af en aftale med Sikkerhedsstyrelsen under Økonomi- og Erhvervsministeriet, som er ansvarlig for lovgivningen om akkreditering i Danmark.

De grundlæggende akkrediteringskriterier er beskrevet i henholdsvis DS/EN ISO/IEC 17025 "Generelle krav til prøvnings- og kalibreringslaboratoners kompetence" og i DS/EN ISO 15189 "Medicinske laboratorier- Særlige krav til kvalitet og kompetence". DANAK anvender fortolkningsdokumenter til de enkelte krav i standarderne, hvor det skønnes nødvendigt. Disse vil hovedsageligt være udarbejdet af "European co-operation for Accreditation (EA)" eller "International Laboratory Accreditation Co-operation (ILAC)" med det formål at opnå ensartede kriterier for akkreditering på verdensplan. Sikkerhedsstyrelsen udsteder desuden tekniske forskrifter udarbejdet af DANAK vedr. specifikke krav til akkreditering, som ikke er indeholdt i standarderne.

For at et laboratorium kan være akkrediteret kræves blandt andet:

- at laboratoriet og dets personale skal være fri for enhver kommerciel, økonomisk eller anden form for pression, som kan påvirke deres uvildighed,
- at laboratoriet har et dokumenteret ledelsessystem og en ledelse, der kan sikre, at dette følges og vedligeholdes,
- at laboratoriet råder over teknisk udstyr og lokaler af en tilstrækkelig standard til at kunne udføre den ydelse, som laboratoriet er akkrediteret til,
- at laboratoriet råder over personale med såvel faglig kompetence som praktisk erfaring i udførelsen af de ydelser, som laboratoriet er akkrediteret til,
- at der er indarbejdet faste rutiner for sporbarhed og usikkerhedsbestemmelse,
- at akkrediteret prøvning, kalibrering eller medicinsk undersøgelse udføres efter fuldt validerede og dokumenterede metoder,
- at akkrediterede ydelser udføres og rapporteres i fortrolighed med rekvirenten og i overensstemmelse med dennes behov,
- at laboratoriet skal registrere forløbet af akkrediteret prøvning, kalibrering eller medicinsk undersøgelse således, at dette kan rekonstrueres,
- at laboratoriet er underkastet regelmæssigt tilsyn af DANAK,
- at laboratoriet skal have en forsikring, som kan dække laboratoriets ansvar i forbindelse med udførelsen af akkrediterede ydelser.

Rapporter, der bærer DANAK's akkrediteringsmærke, anvendes ved rapportering af akkrediterede ydelser og viser, at disse er foretaget i henhold til akkrediteringsreglerne.

DANAK

The Danish Accreditation and Metrology Fund -DANAK -is managing the Danish accreditation scheme based on a contract with the Danish Safety Technology Authority under the Danish Ministry of Economics and Business Affairs who is responsible for the legislation on accreditation in Denmark.

The fundamental criteria for accreditation are described in DS/EN ISO/IEC 17025: "General requirements for the competence of testing and calibration laboratories", and in DS/EN ISO/IEC 15189 "Medical laboratories -Particular requirements for quality and competence" respectively. DANAK uses guidance documents to clarify the requirements in the standards, where this is considered to be necessary.. These will mainly be drawn up by the "European co-operation for Accreditation (EA)" or the "International Laboratory Accreditation Co-operation (ILAC)" with a view to obtaining uniform criteria for accreditation worldwide. In addition, the Danish Safety Technology Authority issues Technical Regulations prepared by DANAK with specific requirements for accreditation that are not contained in the standards.

In order for a laboratory to be accredited it is, among other things, required:

- that the laboratory and its personnel are free from any commercial, financial or other pressures, which might influence their impartiality;
- that the laboratory operates a documented management system, and has a management that ensures that the system is followed and maintained;
- that the laboratory has at its disposal all items of equipment, facilities and premises required for correct performance of the service that it is accredited to perform;
- that the laboratory has at its disposal personnel with technical competence and practical experience in performing the services that they are accredited to perform;
- that the laboratory has procedures for traceability and uncertainty calculations;
- that accredited testing, calibration or medical examination are performed in accordance with fully validated and documented methods;
- that accredited services are performed and reported in confidentiality with the customer and in compliance with the customer's request;
- that the laboratory keeps records which contain sufficient information to permit repetition of the accredited test, calibration or medical examination;
- that the laboratory is subject to surveillance by DANAK on a regular basis;
- that the laboratory shall take out an insurance, which covers liability in connection with the performance of accredited services.

Reports carrying DANAK' s accreditation mark are used when reporting accredited services and show that these have been performed in accordance with the rules for accreditation.

Side 1 af **1**
Page 1 of **1**
DP11005

Appendiks 1 til Rapport DP11005
Appendix 1 to Report DP11005

Kalibreringsresultater for Optomekanisk hulplade:
Calibration results for Optomechanical holeplate: **DP135**

Element	X-Coord.[mm]	Y-Coord.[mm]
1	0,0000	0,0000
2	19,9974	-0,0003
3	39,9966	-0,0006
4	59,9952	-0,0005
5	79,9948	0,0000
6	-0,0033	20,0007
7	19,9954	20,0012
8	39,9946	20,0012
9	59,9935	20,0007
10	79,9941	20,0008
11	-0,0026	40,0004
12	19,9951	40,0001
13	39,9947	39,9994
14	59,9938	39,9992
15	79,9936	39,9987
16	-0,0034	59,9988
17	19,9952	59,9988
18	39,9947	59,9979
19	59,9941	59,9974
20	79,9941	59,9973
21	-0,0035	79,9982
22	19,9948	79,9970
23	39,9949	79,9964
24	59,9942	79,9961
25	79,9945	79,9961

* Z-koordinaten er ikke kalibreret /The Z-coordinate has not been calibrated.

CGM, Kgs. Lyngby, 2011-11-09

Side 1 af **1**
Page 1 of **1**
DP11005

Appendiks 2 til Rapport DP11005
Appendix 2 to Report DP11005

Definition af koordinatsystem for hulplade.

I dette appendiks beskrives det koordinatsystem, der er anvendt på hulpladen i forbindelse med kalibreringen. Rumlig opretning er defineret ved planet igennem hulcentrene 1 og , 5. Nulpunktet (X,Y)=(0,0) er placeret i centrum af hul nr 1 (se skitse herunder). Centrene af hullerne 1 og 5 udgør X-aksen i koordinatsystemet. Y-aksen er placeret 90° drejet imod uret i forhold til X-aksen.

Definition of coordinate system of holeplate.

In this appendix the cordinate system of the holeplate is described which has been used during the calibration. Spatial alignment is defined using the centres of the holes 1 and 5. The zero point (X,Y)=(0,0) is placed in the centre of hole no 1 (see sketch below). The centres of hole 1 and hole 5 are defined as the direction of the X-axis of the coordinate system. The Y-axis is defined at 90°rotation counterclockwise with respect to the X-axis.

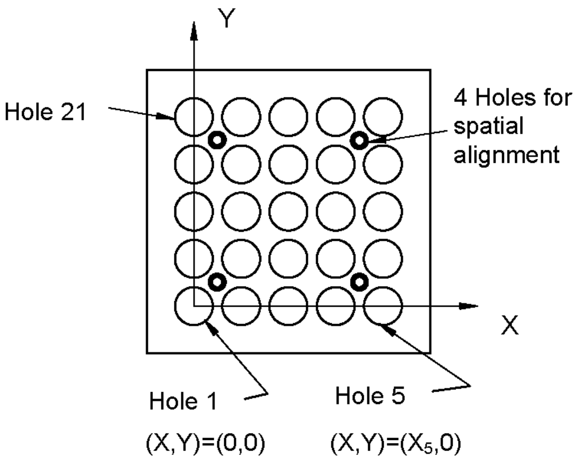

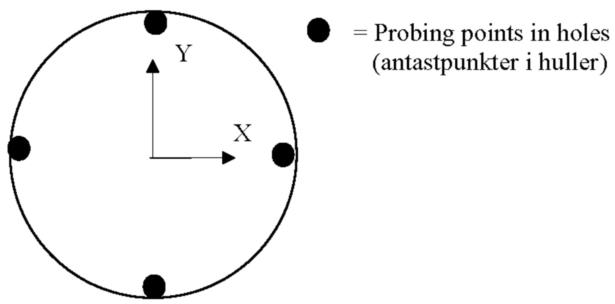

11.2 Appendix 2: Technical drawing for the volume control of a hearing aid

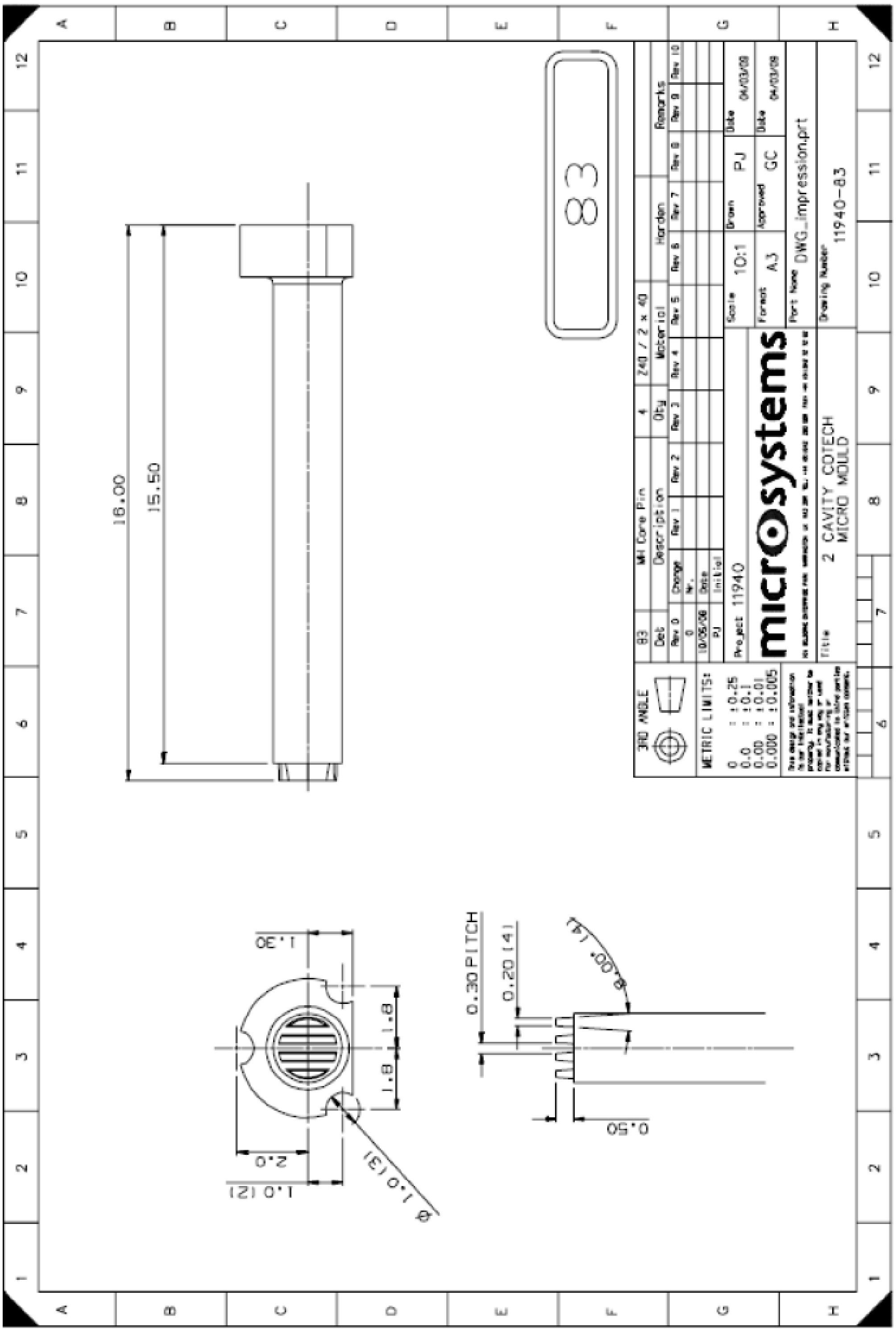

11.3 Glossary

μCMM	micro coordinate measuring machine
μEDM	micro electro discharge machining
μIM	micro injection moulding
μ-milling	micro milling
AFM	atomic force microscope
CMM	coordinate measuring machine
COTECH	COnverging TECHnologies for micro systems manufacturing
CT	computer tomography
EDM	electro discharge machining
EDS	energy dispersive spectroscopy
GPS	geometrical product specifications
GUM	guide to the expression of uncertainty in measurement
ISO	international organization for standardization
NPL	National Physical Laboratory
OCMM	optical coordinate measuring machine
PTB	Physikalisch-Technische Bundesanstalt
SEM	scanning electron microscope
TCMM	tactile coordinate measuring machine